UNIVERSIDADE DE LISBOA

INSTITUTO SUPERIOR TECNICO

Deciphering Mechanisms of Pathogenesis in *Candida glabrata*: in the Crossroad Between Drug Resistance and Virulence

Mafalda Banazol de Santa Rita Cavalheiro

Supervisor: Doctor Miguel Nobre Parreira Cacho Teixeira

Thesis approved in public session to obtain the PhD Degree in Biotechnology and Biosciences

Jury final classification: Pass with Distinction and Honour

2020

UNIVERSIDADE DE LISBOA
INSTITUTO SUPERIOR TECNICO

Deciphering Mechanisms of Pathogenesis in *Candida glabrata*: in the Crossroad Between Drug Resistance and Virulence

Mafalda Banazol de Santa Rita Cavalheiro

Supervisor: Doctor Miguel Nobre Parreira Cacho Teixeira

Thesis approved in public session to obtain the PhD Degree in Biotechnology and Biosciences

Jury final classification: Pass with Distinction and Honour

Jury

Chairperson: Doctor Isabel Maria de Sá Correia Leite de Almeida, Instituto Superior Técnico, Universidade de Lisboa

Members of the Committee:

Doctor Isabel Maria de Sá Correia Leite de Almeida, Instituto Superior Técnico, Universidade de Lisboa

Doctor Etienne Dague, Laboratoire d'Analyse et d'Architecture des Système, France

Doctor Miguel Nobre Parreira Cacho Teixeira, Instituto Superior Técnico, Universidade de Lisboa

Doctor Nuno Gonçalo Pereira Mira, Instituto Superior Técnico, Universidade de Lisboa

Doctor Isabel Alexandra Marcos Miranda, Faculdade de Medicina, Universidade do Porto

Funding Institutions

Fundação para a Ciência e Tecnologia

Fundo Europeu de Desenvolvimento Regional

2020

Acknowledgements

First of all, I would like to acknowledge my supervisor Professor Miguel Teixeira for his guidance, motivation, ideas and infinite support during the development of this thesis, which was imperative for the success of the work and that very much contributed for my personal and professional growth.

Secondly, I have to acknowledge Professor Isabel Sá-Correia as the head of the Biological Sciences Research Group (BSRG) and the director of BIOTECnico program, for the opportunity to work with such an incredible team and have the chance to enroll in such a prestigious doctoral program.

I would also like to take the opportunity to acknowledge all the co-authors of the papers presented in this thesis, particularly to Dr. Etienne Dague, and all his team in LAAS-CNRS, whom have received me so well upon my abroad experience, allowing me an unique opportunity to expand my scientific knowledge. I would also like to thank Dr. Hiroji Chibana, for kindly providing the *Candida glabrata* mutant strains, Professor Geraldine Butler for the collaboration in the transcriptomic analysis, Professor Acácio G. Rodrigues for the collaboration work performed at Centro Hospitalar of S. João, Porto, and Professor Arsénio Fialho for the collaboration in works with *G. mellonella* model of infection.

I acknowledge "Fundação para a Ciência e a Tecnologia" (FCT) PhD grant PD/BD/116946/2016 attributed to the candidate under the framework of the Instituto Superior Técnico BIOTECnico PhD program in Biotechnology and Biosciences. The work carried out during this PhD was financed by FEDER and FCT (Contracts PTDC/BBB-BIO/4004/2014, PTDC/BII-BIO/28216/2017), as well as by Programa Operacional Regional de Lisboa 2020 [LISBOA-01-0145-FEDER-022231 – the BioData.pt Research Infrastructure]. Funding received by iBB from FCT (UID/BIO/04565/2013 and UIDB/04565/2020), and from Programa Operacional Regional de Lisboa 2020 (Project N. 007312) is also acknowledged.

My gratitude must also be express towards all members of the great "MCT group" and to all BSRG colleagues which have somehow collaborated with my work and accompanied me throughout this journey. My appreciation goes also to Mónica Rato, whose work is crucial for our success.

For all the help, friendship and patience for hearing me out, a big thanks to Dr. Catarina Costa, Mónica Galocha, Diana Pereira, Sara Salazar, Andreia Pimenta, Ana Vila-Santa, Maria João Tavares and Ana Luísa Miranda. Thank you, girls, for being with me all the way!

Lastly, I would like to thank my better half, Pierre, for his infinite love, support, patience and faith in me. Thank you for being such a good listener, advisor and my safe harbor. I will never forget your part in all of this. To my family I would like to give a big thank you, specially my parents, whose love and support I could always count on throughout the course of my life.

Deciphering Mechanisms of Pathogenesis in *Candida glabrata*: in the Crossroad Between Drug Resistance and Virulence

Abstract

In this thesis, the study of molecular mechanisms simultaneously involved in at least two of the three main processes for the survival of *C. glabrata* in the human host: biofilm formation, virulence and antifungal resistance; was pursued. This work presents two new regulators of biofilm formation, CgEfg1 and CgTec1, which together control 40% of all the transcriptomic changes happening in this complex process. In addition, biofilm formation was found to depend on unexpected players, like CgDtr1 and CgTpo4, which are key effectors of virulence in this pathogenic yeast, CgDtr1 as an acetate exporter whose action fights oxidative and acetic acid stress, while CgTpo4 is essential to resist the action of antimicrobial peptides and polyamines. Biofilm formation was also found to rely on the expression of two cell peripheral proteins, CgEpa3 and CgPil2, an adhesin and an eisosome component unraveled during the study of *in vitro* evolution towards azole resistance of a *C. glabrata* susceptible clinical isolate. CgEpa3 and CgPil2 are thus two effectors in azole resistance, the first believed to contribute to increased yeast aggregation, decreasing *C. glabrata* exposure to azole drugs, while CgPil2 contributes for lipid homeostasis at the plasma membrane, influencing the presence of MDR transporters involved in both antifungal resistance and biofilm formation.

Altogether, this thesis gives evidence of new molecular mechanisms with intricate functions in biofilm formation, virulence and antifungal resistance, indicating that new therapeutic targets should be chosen according to their importance in as many fundamental roles in *C. glabrata* as possible.

Keywords: *Candida glabrata,* biofilm formation, virulence, antifungal resistance, new effectors

Descodificando mecanismos de patogénese em *Candida glabrata*: no cruzamento entre resistência a drogas e virulência

Mafalda Banazol de Santa Rita Cavalheiro

Doutoramento em Biotecnologia e Biociências

Orientador: Professor Doutor Miguel Nobre Parreira Cacho Teixeira

Resumo

Nesta tese, o estudo dos mecanismos moleculares simultaneamente envolvidos em pelo menos dois dos três principais processos de sobrevivência de *C. glabrata* no hospedeiro humano: formação de biofilme, virulência e resistência a antifúngicos; foi perseguido. Este trabalho apresenta dois novos reguladores de formação de biofilme, CgEfg1 e CgTec1, que juntos controlam 40% de todas as alterações transcriptómicas que acontecem neste processo complexo. Adicionalmente, descobriu-se que a formação de biofilme é dependente de jogadores inesperados, como CgDtr1 e CgTpo4, que são efectores-chave de virulência nesta levedura patogénica, CgDtr1 como um exportador de acetato cuja acção combate o stress oxidativo e o derivado do ácido acético, enquanto o CgTpo4 é essencial para resistir à acção de péptidos antimicrobianos e poliaminas. A formação de biofilme foi descoberta estar dependente da expressão de duas proteínas celulares periféricas, CgEpa3 e CgPil2, uma adesina e um componente de eisossomas desvendados durante o estudo da evolução *in vitro* direccionada à resistência a azóis de um isolado clínico susceptível de *C. glabrata*. CgEpa3 e CgPil2 são assim dois efectores na resistência a azóis, o primeiro acredita-se contribuir para o aumento de agregação entre células de levedura, diminuindo a exposição de *C. glabrata* às drogas azóis, enquanto CgPil2 contribui para a homeostase lipídica na membrana plasmática, influenciando a presença de transportadores MDR envolvidos na resistência a antifúngicos e na formação de biofilme.

De um modo geral, esta tese dá evidências de novos mecanismos moleculares com funções intricadas na formação de biofilme, virulência e resistência a antifúngicos, indicando que novos alvos terapêuticos devem ser escolhidos de acordo com a sua importância no maior número possível de papéis fundamentais em *C. glabrata*.

Palavras-chave: *Candida glabrata*, formação de biofilme, virulência, resistência a antifúngicos, novos efectores

Contents

List of Figures

List of Tables

List of Acronyms

ABC, ATP Binding Cassette

Aed1, Adherence to endothelial cells-1

AFM, Atomic Force Microscopy

Als, Agglutinin-like Sequence

AMP, Antimicrobial Peptide

Awp, Adhesion-Like Wall Protein

BAR, Bin/Amphiphysin/Rvs

BM, Minimal Growth

CFU, Colony Forming Units

CGD, *Candida* Genome Database

ChIP, Chromatin Immunoprecipitation

CLSI, Clinical and Laboratory Standards Institute

conA, Concanavalin A

DHA, Drug:H^+ Antiporter

DHA1, Drug:H+ Antiporter-1

DHA2, Drug:H+ Antiporter-2

DiOC6(3), 3,3'-Dihexyloxacarbocyanine Iodide

ECM, Extracellular Matrix

EGF, Epidermal Growth Factor

EPA, Epithelial Adhesion

EPS, Extracellular Polymeric Substances

ER, Endoplasmic Reticulum

EUCAST, European Committee on Antimicrobial Susceptibility Testing

FC, Fold-Change

FDA, Food and Drug Administration

GAL1, Galactose Inducible Promoter

GFP, Green Fluorescent Protein

GIM, Grace Insect Medium,

GO, Gene Ontology

GOF, Gain-of-function

GPI-CWPs, Glycosyl-phosphatidylinositol-cell wall proteins

HPLC, High-pressure Liquid Chromatography

Hwp, Hyphal Wall Protein

IMPI, Inducible Metalloproteinase Inhibitor

IMUL, Institute of Microbiology, University Hospital of Lausanne

KSF, Keratinocyte Serum Free

LDH, Lactate Dehydrogenase

MAPK, Mitogen-activated Protein Kinase

MCC, Membrane Compartment of Can1

MFS, Major Facilitator Superfamily

MG, Minimal Growth

MICs, Minimal Inhibitory Concentrations

MOI, Multiplicity of Infection

MOPS, Morpholinepropanesulfonic acid

NAD+, Nicotinamide Adenine Dinucleotide

NBD-DHS, C6 NBD-dihydrosphingosine

NBD, Nucleotide-binding Domain

NCCLS, National Committee for Clinical Laboratory Standards

NK, Natural Killer

OD, Optical Density

ORF, Open Reading Frame

PA14, Anthrax protective antigen

PBS, Phosphate-buffered Saline

PCR, Polymerase Chain Reaction

PDR, Pleiotropic Drug Resistance

$PI_{4,5}P_2$, Phosphatidylinositol 4,5-bisphosphate

PKC, Protein Kinase C

Pwp, PA14 domain containing cell wall protein

QI™, Quantitative Imaging™ mode

R, Resistance

RHOE, Reconstituted Human Oral Epithelia

RNA-seq, RNA-sequencing

ROS, Reactive Oxygen Species

RPMI, Roswell Park Memorial Institute

RT-PCR, quantitative Real Time Polymerase Chain Reaction

SCFS, Single-cell Force Spectroscopy

SDB, Sabouraud's Dextrose Broth

S-DD, Susceptible-Dose-Dependent

SGD, *Saccharomyces* Genome Database

SpSyj1, Synaptojanin-like lipid phosphatase

TFs, Transcription Factors

TMDs, Transmembrane Domains

TMS, Transmembrane Spanning Segments

TORC2, Rapamycin kinase complex 2

UPR, Unfolded Protein Response

YNB, Yeast Nitrogen Base

YEPD, Yeast Extract Peptone Dextrose

YPD, Yeast extract Peptone Dextrose

I. Introduction

1. *Candida glabrata*: a human opportunistic pathogen

Fungal infections are a worldwide health problem that affects human health, particularly since there is lack of effective therapeutic options and, often, delayed diagnosis [1]. It has been estimated that fungal pathogens are responsible for over 1.6 million deaths annually [2]. Besides threating human health, fungal pathogens are also known to affect animals and plants, constituting the main cause for host loss [2]. Although not being easily transmitted among humans, and only affecting mainly immunocompromised patients, fungal pathogens should be considered dangerous threats due to the dramatic increase of immune impaired human populations, a consequence of the recent advances in medicine and HIV spreading [1], [3]. In addition, fungal diseases tend to become chronic, gradually killing the host [1]. To increase the problematic, global warming is expected to lead to the upsurge of new fungal pathogens able to grow at 37 ºC by selective pressure imposed by increased levels of temperature [4].

Among all known fungal pathogens, *Candida* species represent the most common causal agents of fungemia encountered in the world [5], and the fifth most common pathogen [6]. The genus *Candida* englobes approximately 200 species, from which only a few are able to infect humans [7]. *Candida* species are responsible for superficial candidiasis, a mucosal infection that might be developed in different human body niches, being designated accordingly as oral, esophageal or vulvovaginal candidiasis [8]–[11]. Additionally, *Candida* species are also able to cause invasive candidiasis, a systemic infection that results in high mortality rates (mainly between 40-60%) [12]. Candidiasis is the most frequent fungal disease in the world, being estimated that 50-75% of women at childbearing years have at least one episode of vulvovaginal candidiasis, while 5-8% of women have recurrent vulvovaginal candidiasis, with at least four episodes per year [5]. *Candida* species are accountable for 12.7% of all catheter-associated urinary infections and 14.6% of central line–associated bloodstream infections [6], corresponding to the major cause of systemic fungal infections [2].

Although *Candida albicans* is still the most isolated *Candida* species from healthy and diseased humans [13], increased isolation of non-*albicans Candida* species has been observed in recent years [14]–[16], *Candida glabrata* being the second most common cause of candidiasis [15], [17]–[19]. Certain reports show that *C. glabrata* has even supplanted *C. albicans*, by being the most common *Candida* species isolated from diabetic patients and abdominal sources [20], from medical wards in a tertiary teaching hospital in Southwest China [21], or from Lebanese pregnant women with 35-37 weeks of gestation [22]. Over the last 20 years, an increased isolation of *C. glabrata* in the United States was registered, clearly indicating the worldwide tendency for its increased significance as a human pathogen. Interestingly, *C. glabrata* affects more adults than children and 75% of the patients was found to carry a single strain type of *C. glabrata* over time, with little diversity of strain in each patient [13]. Its high prevalence is also observed in bloodstream infections, *C. glabrata* being responsible for 15% of all those caused by *Candida* species [23].

Candida glabrata was classified, in 1978, as belonging to the *Torulopsis* genus given its incapacity for polymorphic growth. Later, *C. glabrata* was included in the genus *Candida,* after the observation that it is able to form pseudohyphae and to cause human infections [13]. Although included

in this genus, *C. glabrata* has several differences from other *Candida* species. First of all, *C. glabrata* blastoconidia size is smaller (1-4 μm) than that of other *Candida* species (2.5-8 μm), having a haploid genome, different from the diploid genomes of *C. albicans* and others [13]. *C. glabrata* is much closer, phylogenetically, to *Saccharomyces cerevisiae*, than to other *Candida* species. In fact, *C. glabrata* genome comprises 13 chromosomes, with 38.8% of G+C content, similar to what is found for *S. cerevisiae* (38.3%) [24]. Nonetheless, some metabolic characteristics distinguish these two species. *C. glabrata* seems to have lost genes related to thiamine, pyridoxine and nicotinic acid biosynthesis, galactose and sucrose assimilation, and phosphate, nitrogen and sulfur metabolism [24]. This pathogenic yeast is considered an asexual organism, but has a putative mating-type locus, a pheromone gene, and at least 31 orthologs of *S. cerevisiae* genes whose only known roles are related to mating and meiosis [25].

C. glabrata is considered extremely fit to resist antifungal drugs [15], [26]–[28]. It's ability to acquire drug resistance is reflected in the number of resistant clinical isolates that have been found through the years in different reports. From the study of Pfaller and colleagues focused on 20 788 *Candida* invasive isolates collected over 20 years, from 39 countries, *Candida glabrata* was identified as the species with highest number of isolates resistant to fluconazole and echinocandins [15]. Similar results have also been described in two studies of the same authors, indicating the prevalence of *Candida glabrata* as the number one *Candida* species resisting several antifungal drugs, even the most recently used class, echinocandins [27], [28]. In another study focused on 146 *C. glabrata* isolates recovered from cancer patients suffering from fungemia, 19.8% of them were identified as multiazole resistant, 16.4% as intermediate and 10.3% as resistant to caspofungin, and 6.8% as multidrug resistant (resistance towards fluconazole, caspofungin and amphotericin B) [29]. The clear incidence of multidrug resistance in *C. glabrata* isolates is a very concerning aspect of *Candida* infections that should be surveilled and addressed so that patients are not left without any therapeutic options.

Similarly to all pathogenic *Candida* species, *C. glabrata* is able to form biofilms, not only in the host mucosa but also on indwelling devices applied on patients [30]–[33]. This ability is closely linked to the pathogenesis and virulence of *Candida* species. In fact, a recent study shows how higher fatality is linked with *Candida* biofilms with high metabolic activity by analyzing the ability to form biofilms of *Candida* isolates recovered from different candidemia cases [34]. *C. glabrata* has a very unique way to form biofilms, architecting a very different structure from other *Candida* species, based on a dense and compact structure of yeast cells wrapped in an extracellular matrix (ECM), composed mainly by proteins and carbohydrates [35]. The biofilm has the capacity to protect *C. glabrata* cells from environmental stress, ensuring its prevalence and survival in the human host and resistance to antifungal drugs [13], [36], [37]. Besides biofilm formation, different molecular mechanisms of virulence are known to improve the ability of this yeast to infect the human host, as its adherence capacity and enzyme production and secretion that help degrade host tissues [13], [38].

To better resist the environmental stress found in the human host, *C. glabrata* has a set of different mechanisms which allow this pathogenic yeast to cope with oxidative and osmotic stress, as well as stresses directed to the cell wall and endoplasmic reticulum (ER) [35]. The environmental stress response is regulated by CgMsn2 and CgMsn4 transcription factors, orthologs of the regulators found

with the same function in *S. cerevisiae* [39]. *C. glabrata* relies as well on a single catalase, CgCta1, to fight oxidative stress, regulated by CgMsn2, CgMsn4, CgSkn7 and CgYap1 [40], as well as two superoxide dismutases, CgSod1 and CgSod2 [41], and the glutathione biosynthetic enzymes CgGsh1 and CgGsh2 [42]. The cell wall is safely guarded by the protein kinase C (PKC)-mediated signaling pathway [35]. ER stress is sensed by the CgIre1 endoribonuclease, which functions as a stress sensor that together with PKC-mediated cell wall integrity and calcineurin signaling regulates the ER stress response [43], [44].

Due to all the mechanisms *C. glabrata* is able to trigger, this yeast is well prepared to face our immune response and proliferate causing persistent infections. It is essential that further research is undertaken to better understand how to correctly tackle *C. glabrata* infections.

The following Subchapter I.2, which was published as a review paper, highlights in detail the main molecular mechanisms *C. glabrata* uses to form biofilms and prevail in the human host, resisting to antifungal therapy and evading the host immune response. Subchapter I.3 highlights the complexity of antifungal resistance and virulence mechanisms in this yeast, reviewing the known examples of interconnectivity between drug resistance and virulence factors.

2. *Candida* Biofilms: Threats, Challenges, and Promising Strategies

Published as a review paper, with the following citation reference:

Mafalda Cavalheiro and Miguel C. Teixeira, *Candida* Biofilms: Threats, Challenges, and Promising Strategies, *Frontiers in Medicine,* 5(28), 2018.

2.1. Abstract

Candida species are fungal pathogens known for their ability to cause superficial and systemic infections in the human host. These pathogens are able to persist inside the host due to the development of pathogenicity and multidrug resistance traits, often leading to the failure of therapeutic strategies. One specific feature of *Candida* species pathogenicity is their ability to form biofilms, which protects them from external factors such as host immune system defenses and antifungal drugs.

This review focuses on the current threats and challenges when dealing with biofilms formed by *Candida albicans, Candida glabrata, Candida tropicalis* and *Candida parapsilosis*, highlighting the differences between the four species. Biofilm characteristics depend on the ability of each species to produce extracellular polymeric substances (EPS) and display dimorphic growth, but also on the biofilm substratum, carbon source availability and other factors. Additionally, the transcriptional control over processes like adhesion, biofilm formation, filamentation and EPS production displays great complexity and diversity within pathogenic yeasts of the *Candida* genus. These differences not only have implications in the persistence of colonization and infections, but also on antifungal resistance typically found in *Candida* biofilm cells, potentiated by EPS, that functions as a barrier to drug diffusion, and by the overexpression of drug resistance transporters. The ability to interact with different species in *in vivo Candida* biofilms is also a key factor to consider when dealing with this problem.

Despite many challenges, the most promising strategies that are currently available or under development to limit biofilm formation or to eradicate mature biofilms are discussed.

2.2. The Threats

A biofilm consists in a community of microorganisms that are irreversibly attached to a given surface, inert material, or living tissue, producing extracellular polymers that provide a structural matrix [45], [46]. The microorganisms in this type of community exhibit lower growth rates and higher resistance to antimicrobial treatment, behaving very differently from planktonic cells [46]. The ability to adhere to different types of surfaces enables microorganisms to form biofilm on medical devices, such as intravascular catheters, prosthetic heart valves and joint replacements, or in different tissues in the host [47], linking biofilms to persistent colonization and infections [48]. A single microbial species is able to form biofilm although a mixture of bacterial and fungal species usually underlies biofilm formation *in vivo* [47], [49]. Given that 80% of all microorganisms live in this form, biofilm formation becomes an irrevocable field to explore [50].

Due to these general characteristics, biofilms potentiate the establishment of unyielding infections in the human host. This is the case of biofilms formed by *Candida* species, causing superficial and systemic fungal infections in immunocompromised patients [51]. These infections are very difficult to treat due to the characteristics of these species: resistance to antifungal drugs, expression of virulence factors and the ability to form biofilm. Indeed, mucosal infections involve biofilm formation [52], usually including the interaction with commensal bacterial flora and host components [53]. *Candida* species are the fourth most common cause of nosocomial bloodstream infection in the United States. These infections are associated with a high mortality rate of approximately 50% [54], [55]. Biofilms are an additional problem since they are usually found in medical devices, such as prostheses, cardioverter defibrillators, urinary and vascular catheters, and cardiac devices [56], [57], hindering the eradication of *Candida* infections.

These challenging infections may be caused by different *Candida* species. *Candida albicans* is the most frequent pathogen responsible for *Candida* infections, followed by *Candida glabrata* [58]. *Candida tropicalis* is particularly relevant in urinary tract infections [59] while *Candida parapsilosis* is frequently found in the skin of healthy hosts, being the causative agent of catheter-related infections [60], [61]. Each *Candida* species exhibits differences in terms of biofilm formation, namely at the level of their morphology, characteristics of the extracellular matrix and ability to confer antifungal resistance [62]. This variability increases the challenge of finding an effective solution to tackle the threats of *Candida* biofilms as a unique problem. In fact, due to the emergence of these fungal infections, there is an urgent need to find adequate therapeutics that might be able to treat patients more efficiently. The path to find these therapeutics certainly involves the study of the different pathogenic features of these species such as biofilm formation.

Biofilm formation, although being a process present in all the *Candida* species focused above, differs significantly from species to species, and in the dependency of surface, host niche and other factors. For example, *C. albicans* mature biofilms exhibit a more heterogenous structure, composed by blastophores and hyphae surrounded by an ECM of polysaccharide material [63]. The ECM provides structural scaffold for adhesion between cells and with different surfaces, and a barrier between the cells in the biofilm and the neighbouring environment [64]. Within the structure of these biofilms there is usually water channels surrounding the microcolonies [65]. In the case of *C. glabrata*, the biofilm is exclusively composed by yeast form cells in a multilayer structure intimately packed or in clusters of cells [66]. In turn, *C. tropicalis* biofilm corresponds to a network of yeast, pseudohyphae and hyphae, with intense hyphal budding [67], while *C. parapsilosis* exhibits a biofilm formed by clusters of yeast cells adhered to the surface, with minimal ECM [68]. These differences highlight the complexity of the processes underlying biofilm formation and the difficulty to find a unique way to eradicate all *Candida* biofilms. *Candida* biofilms occur mostly in the mucosa or endothelium being involved in the development of common candidiasis, such as vaginal and oral candidiasis, but also associated with medical devices, such as vascular and urinary catheters and dentures [69]. Interestingly, however, in all cases, biofilm formation compromises antifungal treatment and, when occurring in implanted medical devices, such as central venous catheters, implant replacement is often required [50], [70].

This review highlights the main challenges found in the process of developing effective therapy against *Candida* biofilms, considering differences found in biofilm formation and its regulation, as well as antifungal resistance found in biofilms and the establishment of mixed-species biofilm. Currently proposed promising strategies are also discussed herein.

2.3. The Challenges

2.3.1. The Complex Process of Biofilm Formation in *Candida* species

Biofilm formation is a multifaceted process well described for *C. albicans*. In this case, the early phase of biofilm formation starts with adhesion of yeast cells to a given surface, followed by the formation of a discrete colony. Afterwards, in the intermediate phase, cells become organized and start producing and secreting extracellular polymeric substances (EPS). These components allow the maturation of a three-dimensional structure, forming the biofilm as we know it, in the maturation phase. Once the mature biofilm is formed, there is still the possibility of dissemination of progeny biofilm cells that become detached migrating to other niches to form more biofilm [62], [71].

For *C. albicans in vitro* biofilm formation, the early phase takes approximately 11 h, leading to the formation of distinct microcolonies. The intermediate phase of biofilm formation may last for 12–30 h, being characterized by the production of EPS and the formation of a bilayer usually composed by yeast, germ tubes and/or young hyphae. After this phase, *C. albicans* biofilm maturation includes the development of a thick layer of EPS where yeasts, and hyphae are present, forming a dense network. The maturation process usually takes approximately 38–72 h [62], [63], [71]. Following maturation comes the dispersal phase, where mature biofilms release budding daughter cells as non-adherent yeast cells to propagate the colonization/infection [72].

It is important to highlight that most studies on biofilm formation have been conducted *in vitro*. A good example of an *in vivo* study was that conducted by Andes *et al.* that have followed the development of *C. albicans* biofilm in a rat central venous catheter [73]. This study reported important differences in biofilm formation between *in vivo* and *in vitro* experiments. For instance, the duration of the early phase of biofilm formation *in vivo* was found to be smaller than that observed *in vitro*, several layers of yeast cells and hyphae being already present after 8 h of *in vivo* biofilm formation [73]. Furthermore, maturation of the *C. albicans* biofilm *in vivo* was observed at 24 h in the rat central venous catheter and in an avascular implantation of small catheter in rats, contrary to the 38 to 72 h observed *in vitro* [73], [74]. In the case of *C. glabrata, in vivo* maturation of the biofilm was only observed after 48 h in serum-coated triple-lumen catheters in a rat subcutaneous model. Although the early phase was similar between *in vivo* and *in vitro* conditions, after 24 h *in vitro* biofilms presented a confluent layer of yeast cells while *in vivo* biofilms only exhibited patches of aggregated yeast cells. Moreover, *in vivo C. glabrata* biofilm development is dependent of the number of cells attached to the catheter, while *in vitro* it is not. The thickness of *C. glabrata* biofilm, 75–90 + 5 μm, is approximately half of the thickness of *C. albicans* biofilm [75].

The first crucial step of biofilm formation is adhesion. This process relies on several cell wall proteins, called adhesins, that promote the attachment to other cells, both to epithelial and to other

microbial cells, or abiotic surfaces by binding to specific amino acid or sugar residues. Generally, adhesins are glycosyl-phosphatidylinositol-cell wall proteins (GPI-CWPs), comprising a GPI anchor, a serine/threonine domain and a carbohydrate or peptide binding domain [76]. In *C. albicans*, several adhesins belong to the Als (agglutinin-like sequence) family, which is part of the GPI_CWP family. Such adhesins are known to bind to several proteins through its C-terminal region. Among the 8 members of the Als family, Als3 has the most prominent role in biofilm formation, as its deletion leads to severe biofilm defects when compared to the wild-type parental strain [77]. *ALS*-like proteins have also been described to be present in other *Candida* species, such as *C. parapsilosis, C. tropicalis, C. dubliniensis, C. lusitaniae* and *C. guilliermondii* [78], although still very little is known about the role of these adhesins in each species. Another important family of adhesins in *C. albicans* is the hyphal wall protein (Hwp) family, including the Hwp1. Hwp1 is a mannoprotein of the cell wall of germ-tubes and hyphal cells, with a role in biofilm formation [33], [79]. Besides Hwp1, also four other proteins in the Hwp family are required for biofilm development: Hwp2, Rbt1, Eap1 and Ywp1 [78]. In *C. glabrata*, the EPA (epithelial adhesion) family of adhesins is the main responsible for adhesion. Most of these are encoded by genes localized in subtelomeric regions, including the *EPA1*, *EPA2*, *EPA3* and *HYR1* cluster, and the *EPA4* and *EPA5* cluster [80]. Although the EPA family in *C. glabrata* is predicted to comprise 17 to 23 genes, *EPA1*, *EPA6* and *EPA7* genes are described as the most important in adhesion [79].

After adhesion, biofilm development continues through morphologic modifications, increase in cell number and production of EPS, influencing the final biofilm architecture. Analysis of the development of biofilm and production of ECM in *Candida albicans*, *C. parapsilosis, C. tropicalis*, and *C. glabrata* isolates of different origins have highlighted the differences in biofilm formation between species. Biofilms of *C. albicans* are more confluent than other *Candida* species biofilms [62], exhibiting different morphologic forms: oval budding, continuous septate hyphae and pseudohyphae, in infected tissues [47]. On the surface of plastic coverslips, *C. albicans* biofilms exhibit a dense network of yeasts and filamentous cells embedded in a matrix of exopolymeric material [81]. *C. albicans* is also considered to be the biggest biofilm producer among the *Candida* species focused herein [82]. *C. glabrata* biofilms exhibit an ECM with high levels of carbohydrates and proteins [66], while isolates from the same species were observed to exhibit a scant population of blastospores, in silicone elastomer sheets [82]. On the other hand, *C. parapsilosis* biofilm structure may vary according to the strain in study but usually comprises yeast and pseudohyphae morphologies, producing a compact multilayer or non-contiguous cell aggregates. The ECM of *C. parapsilosis* biofilms has been shown to be mainly composed by carbohydrates with low levels of proteins [66]. Nevertheless, other evidences show that *C. parapsilosis* biofilms are the ones with less ECM produced when compared to *C. albicans, C. glabrata* and *C. tropicalis* biofilms [82]. Regarding *C. tropicalis*, a biofilm formation analysis revealed a structure composed mainly by yeast shaped cells, although some strains have exhibited filamentous forms in thick biofilms of coaggregated cells or in a discontinuous monolayer of yeasts anchored to the surface [66], [67]. One specific isolate was shown to produce biofilm with a thin layer of matrix-encased hyphae [82]. Although *C. tropicalis* biofilms have an extracellular matrix with a low content of carbohydrates and proteins [66], they are more resistant to detachment of the surface than those formed by *C. albicans* [83]. When comparing the biofilm production by *C. albicans*, *C. parapsilosis* and *C. tropicalis* invasive

isolates and *C. glabrata* blood isolates with non-invasive isolates, a significant higher production is observed in first isolates for all species, except for *C. tropicalis* [82].

Formed biofilms are also dependent on the EPS that are produced, which give a gel-like hydrated three-dimensional structure to the biofilm where the cells become partially immobilized [84]. EPS plays different roles such as defense against phagocytosis, scaffold for biofilm integrity and prevention of drug diffusion. The production of EPS is dependent on the species and strain the carbon source and the rate of medium flow. For instance, it is known that *C. tropicalis* has a higher production of EPS matrix than *C. glabrata*. On the other hand, the increase of flow rate of the medium has shown to increase significantly the formation of the matrix [83]. Usually, the major component of *Candida* biofilm EPS are polysaccharides (nearly 40%), although some differences are observed according to each *Candida* species [63], [83]. In *Candida albicans* and *C. tropicalis*, the major carbohydrates present in the biofilm are glucose and hexosamine (39.6% and 27.4%, respectively). Proteins, phosphorus, and uronic acid may also be present but in small amounts [83]. A biochemical analysis of *C. albicans* biofilm matrix in *in vitro* and *in vivo* models led to the identification of the following distribution of macromolecular components: 55% of proteins and their glycosylated counterparts, 25% of carbohydrates, 15% of lipids, and 5% of noncoding DNA. α-1,2-Branched α-1,6-mannans were the more abundant polysaccharides found associated with unbranched α-1,6-glucans, forming a mannan–glucan complex on the matrix [85]. Although being relatively minor components of the ECM of *C. albicans*, β-1,3-glucan and β-1,6-glucan are also important components of this structure. Together with mannan, an interdependency between the synthesis or incorporation of these compounds seems to take place in the ECM since the inhibition of one of these three components leads to the decrease of the concentration of the others. Moreover, mannan and β-1,6-glucan, seem to be essential for ECM formation since the single deletion of genes encoding proteins involved in their production (*ALG11, MNN9, MNN11, VAN1, MNN4-4, PMR1*, and *VRG4* for mannan production and *BIG1* and *KRE5* for β-1,6-glucan production) nearly led to the complete elimination of the biofilm matrix [86]. The majority of the identified lipids were neutral glycerolipids, polar glycerolipids and, in a smaller percentage, sphingolipids [85].

Candida biofilms have thus a variety of possible architectures, adhesion properties, cellular morphologies and EPS composition, as illustrated in Figure I.1, which are, not only species-, but in some cases strain-dependent, that turn the process of fighting these structures clinically very difficult. To increase the complexity of the problem, several other external factors related to the environment surrounding the biofilm also influence the final biofilm produced.

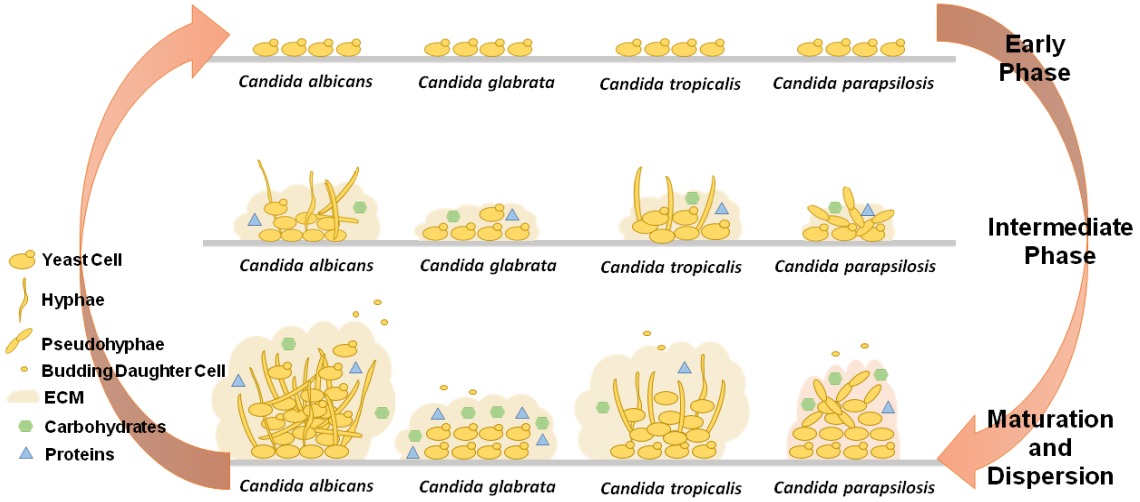

Figure I.1. Comparative schematic of the three stages of biofilm formation by *Candida albicans*, *Candida glabrata, Candida tropicalis* and *Candida parapsilosis*, highlighting the different capacities to produce extracellular matrix (ECM), the varying components present in the ECM, and the ability to exhibit different cell morphologies.

2.3.2. External Factors Influencing Biofilm Development

Each step of biofilm formation depends on the environmental conditions experienced by *Candida* species (Table I.1).

One important factor is the substratum to which the biofilm is attached. There are several options of substratum used to study *Candida* biofilms *in vitro*: polystyrene [87], polymethylmethacrylate [63], polyvinyl chloride [88], cellulose cylindrical filters [88], acrylic [89] and denture base materials [90] have been described for *C. albicans* biofilm formation, while silicone elastomer catheter disks have been tested for different *Candida* species [31], [63]. Among these, hydrophobic surfaces lead to the formation of two phases in *C. albicans* biofilm. The first phase corresponds to the adhesion of blastospores to the surface and a second phase where hyphae elements are embedded in EPS with water channels that allow the diffusion of nutrients and passage of waste disposal between the bottom layer and the surface [63]. On the other hand, substratum may influence the adhesion process itself, e.g., soft lining materials of dentures lead to higher adhesion when compared to acrylic surfaces [91]. It also influences the size of the developed *Candida* biofilm [90]. *C. albicans* biofilms are larger in latex and silicone elastomer surfaces, and smaller in polyurethane and on silicone, when compared to polyvinyl chloride [31]. Chandra *et al.* have tested the effect of different modifications on the surface of biomaterials on the formation of *C. albicans* biofilms. This work has led to the discovery that polyetherurethane with 6% of polyethylene oxide significantly reduces the total biofilm biomass, as well as the metabolic activity of the cells in the biofilm [92]. In turn, Estivill *et al.* have studied the biofilm formation of *C. albicans, C. glabrata, C. parapsilosis, C. tropicalis,* and *C. krusei* on polyvinyl chloride, polyurethane, and Teflon. All species exhibited increased biofilm formation on Teflon, except for *C. glabrata*, for which the best surface for biofilm formation was found to be polyvinyl chloride. *C. tropicalis* showed the highest number of cells recovered from biofilm development in a polyurethane catheter, while on polyvinyl chloride catheter,

C. parapsilosis was the one with the highest number of cells [93]. These differences in preference for surface material, that again appear to vary in a species- and strain-dependent manner, highlight the importance of selecting the most adequate biomaterials to prevent or, at least limit, the propensity for the development of biofilm-seeded infections by *Candida* species. Besides the substratum, a relevant factor influencing biofilm formation is the available carbon source. When comparing the number of cells per biofilm formed by *C. albicans* and *C. glabrata*, a clear increase is observed when glucose is used as the carbon source, comparatively to sucrose [94] or, in the case of *C. albicans*, also to galactose [87]. The test of different concentrations of glucose, has revealed that even low concentrations of glucose induce *C. glabrata* biofilm [95]. Moreover, the medium used to evaluate biofilm formation *in vitro* has shown to be responsible for differences in morphology. On a polymethylmethacrylate surface, *C. albicans* biofilm cells have been shown to predominantly include yeast shaped cells in YNB medium, and hyphal cells in RPMI 1640 medium [63]. This indicates that biofilm formation does not require a given morphology, reinforcing the fact that biofilm development is intrinsically dependent on the environmental conditions. The presence of saliva has been described as another influencing factor of biofilm formation in *Candida* species. Its addition to the medium leads to a significant decrease of *C. albicans* or *C. glabrata* biofilm formation [94]. Nonetheless, in the presence of saliva *C. albicans* exhibits more biofilm formation than C*. glabrata, C. tropicalis*, and *C. parapsilosis*, while the later exhibits higher adhesion capacity to abiotic surfaces. On buccal epithelial cells, *C. glabrata* exhibits the highest capacity of adhesion [96].

Fluid flow rate also affects biofilm formation, affecting EPS production, among other factors. Hawser *et al.* observed that under static conditions, EPS production was minimal when compared to the use of liquid flow. In fact, increasing the speed of flow, the ECM produced was significantly higher, totally wrapping the cells of *C. albicans* biofilm, whose metabolic activity did not change with such alterations. Nevertheless, a shaking speed of 60 rpm was found to inhibit biofilm formation [97]. Moreover, Al-Fattani and Douglas showed that *C. albicans* and *C. tropicalis* biofilms had more ECM produced when grown under conditions of continuous flow in a modified Robbins device than in static conditions [83]. Furthermore, *C. albicans* biofilms under shear stress were found to become thinner but denser, when compared to static conditions, and once again metabolic activity did not suffer any modification [98].

2.3.3. Regulation of Biofilm Formation in *Candida* species

Biofilm formation is regulated by several transcription factors, including those involved in adhesion, hyphal formation, and EPS production, as assembled in Figure I.2 and Table I.1. The study of the elaborated regulatory network that underlies biofilm formation is a promising field of research, as it is expected to lead to the discovery of the best targets to tackle biofilm formation by *Candida* species in the host.

Nobile *et al.* have identified important transcription factors essential for biofilm formation using a *C. albicans* library of 165 transcription factor deletion mutants that were tested for biofilm growth *in vitro* and *in vivo* on rat denture and catheter models [99]. The biofilm defective deletion mutants identified were *efg1Δ/Δ, bcr1Δ/Δ, tec1Δ/Δ, ndt80Δ/Δ, rob1Δ/Δ*, and *brg1Δ/Δ*. Resorting to Chromatin ImmunoPrecipitation-on-chip, it was possible to unravel the promoter regions bound by each

transcription factor during biofilm formation. The six transcription factors were found to regulate a high degree of overlapping target genes as well as to control the expression of each other [99].

In *C. albicans*, the main regulators of biofilm development are also involved in filamentous growth, given the typical hyphal differentiation that takes place during this process. That is the case of Efg1 and Cph1 that positively control the expression of genes required for hyphal growth, such as *ECE1, HYR1, HWP1,* and *ALS3* [100]–[104]. These transcription factors also control the expression of cell wall-related genes due to the usual morphological alterations involved in the transition from yeast to hyphae [105], [106]. The *Δefg1* and *Δefg1Δcph1* deletion mutants have been shown to be incapable of filamentation or biofilm development, being only able to form a sparse monolayer of adherent elongated cells[107]. *C. albicans* Efh1 was found to be a homolog of Efg1, regulating, together with Efg1, a set of genes involved in filamentation [108]. In *C. parapsilosis,* Efg1 has been shown to be a morphological switch regulator [109], and to have a role in biofilm formation since its absence leads to reduced biofilm [110]. Surprisingly, in *C. glabrata*, which is unable to form hyphae, a homolog of Efg1, encoded by ORF *CAGL0L01771g*, has been found but remains uncharacterized [111]. In turn, Cph1 is the terminal transcription factor of the MAP kinase pathway in *C. albicans*, mediating a feedback regulation of this pathway [104]. This protein belongs to the STE-like transcription factor family being present in *C. albicans, C. tropicalis,* and *C. parapsilosis*. In *C. glabrata*, the Cph1 ortholog is the Ste12 transcription factor involved in the regulation of filamentation induced by nitrogen starvation [111], [112].

Also involved in filamentous growth regulation in *C. albicans* is the Ndt80 transcription factor. This regulator has also been associated to the control of cell separation, azole resistance, virulence and biofilm formation [99], [113], [114]. Likewise, Brg1 has a role in the transcriptional control of hyphal growth-related genes in *C. albicans*, since the absence of both copies of the *BRG1* gene leads to impaired hyphal development. Meanwhile, its overexpression was found to lead to the increased expression of hyphae-specific genes, including *ALS3, HWP1*, and *ECE1*. *C. albicans* Brg1 is, in turn, repressed by the Nrg1 C_2H_2 zinc finger transcription factor, involved in the control of cell morphology and pathogenicity, by repressing filamentous growth [115], [116]. The *C. tropicalis* Nrg1 homolog was similarly found to have a role in repressing filamentation [117], while other predicted homologs in *C. parapsilosis*, *C. tropicalis* and *C. glabrata* remain uncharacterized [111]. Besides Nrg1, *C. albicans* and *C. tropicalis* count with Cup9 and Slf1 regulators to suppress filamentous growth [117]. In turn, Ume6 transcription factor has also been found in *C. parapsilosis*, playing an important role in biofilm development [110], and in *C. albicans* and *C. tropicalis*, as a regulator of filamentous growth [117]. Another negative regulator of filamentous growth and biofilm formation in *C. albicans* is Rfg1 [116], [118], [119]. Together with Nrg1, Rfg1 down-regulates the expression of *ALS3*, *ECE1*, and *HWP1* hyphae-specific genes [120], [121].

Table I.1. Factors influencing *Candida* biofilms.

	Factors influencing *Candida* biofilms							
						Drug resistance		
	EPS	**Adhesins**	**Transcription factors**	**Preferred substratum**	**Preferred carbon source**	**Drug**	**Genes Involved**	**Model/ Evidence**
Candida albicans	Polysaccharides glucose hexosamine lipids, proteins phosphorus uronic acid non-coding DNA	Als1-7 Als9, Hwp1, Hwp2. Rbt1, Eap1, Ywp1	Efg1, Bcr1, Tec1, Ndt80, Rob1, Brg1, Cph1, Nrg1, Tup1, Ume6, Cup9, Slf1, Rfg1, Csr1, Gcn4, Tye7, Rca1, Ace2,	Latex, Silicon elastomer, Teflon	Glucose	Fluconazole Voriconazole Ravuconazole AmphotericinB, Nystatin, Chlorhexidine Terbinafine	-	Bio-prosthetic model
						AmphotericinB, Nystatin, Fluconazole, Chlorhexidine	-	Silicone elastomer model
						Fluconazole	*CDR1, CDR2, MDR1*	Plastic coverlips *in vitro*
						Fluconazole	*MNN9 MNN11, VAN1 MNN4-4, VRG1 PMR, BIG1 KRE5 FKS1*	*In vitro*
Candida glabrata	-	Epa1-7 Hyr1	Cst6, Ace2	Polyvinyl chloride	Glucose	Fluconazole	-	*In vitro* in over denture acrylic strips
						Caspofungin, Amphotericin B, Nystatin, Ketoconazole, 5-flucytosine	-	*In vitro* over poly-styrene surface
Candida tropicalis	Polysaccharides glucose hexosamine proteins phosphorus uronic acid	Als-like proteins	Nrg1 Cup9 Slf1 Ume6 Tec1	Teflon, Polyurethane	-	Fluconazole AmphotericinB	-	*In vitro* over poly-styrene surface
Candida parapsilosis	-	Cpar2_404800 Als-like proteins	Ume6 Efg1 Bcr1 Cph2 Ace2	Teflon	-	Fluconazole Voriconazole Ravuconazole AmphotericinB, Nystatin Chlorhexidine Terbinafine	-	Bio-prosthetic model

Main EPS produced, important adhesins, TFs regulating biofilm, most advantageous substratum and carbon source for biofilm formation and biofilm drug resistance found for Candida albicans, Candida glabrata, Candida tropicalis, and Candida parapsilosis.

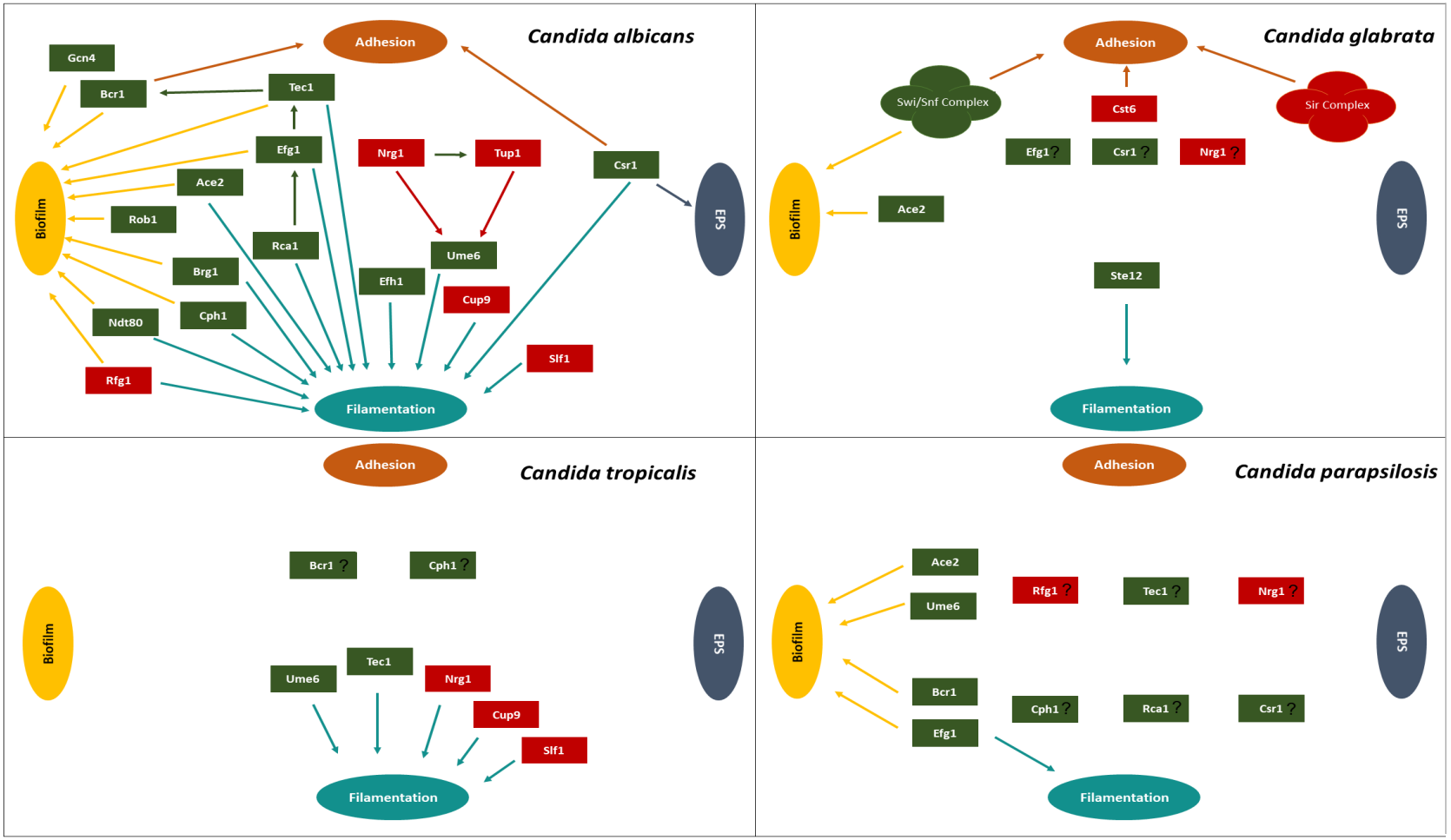

Figure I.2. Transcription regulatory network described for *Candida albicans*, *Candida glabrata*, *Candida tropicalis* and *Candida parapsilosis*, highlighting the transcriptional factors involved in adhesion, extracellular polymeric substances (EPS), filamentation and biofilm. Green boxes indicate activators and red boxes indicate repressors. Participation of each transcription factor in these processes is indicated by the coloured arrows: brown arrows correspond to adhesion, dark blue arrows correspond to EPS, light blue arrows correspond to filamentation, and yellow arrows correspond to biofilm formation.

Bcr1, a C_2H_2 zinc finger transcription factor, is also an important regulator of biofilm formation, but not of hyphal formation. Bcr1 regulates the expression of cell surface proteins encoded by the *HYR1, ECE1, RBT5, ECM331, HWP1, ALS3, ALS1*, and *ALS9* genes [122], controlling the adhesion process in *C. albicans*, during the early phase of biofilm formation. Moreover, the absence of Bcr1 in an *in vivo* rat model of catheter-based infection was found to abrogate biofilm formation after 48 h of infection. Interestingly, the overexpression of *ALS3* in a *bcr1/bcr1* background completely restored the biofilm formation phenotype [77]. In *C. parapsilosis*, a homolog of Bcr1 was identified as one of the most important transcription factors regulating biofilm formation [110], [111], [123], [124]. Bcr1 is itself positively regulated by the transcription factor Tec1, in *C. albicans* [122]. Tec1 positively regulates morphogenesis and is essential for hyphae formation upon serum induction, macrophage evasion and expression of aspartyl proteinase genes [107], [125]. In turn, Efg1 and Cph2 are known to regulate Tec1 [126], [127]. *C. parapsilosis* has been found to have a homolog of Tec1 [111]. Tec1 of *C. tropicalis* is an important transcription regulator promoting filamentation [117].

Regulation of biofilm matrix biogenesis has also been studied, although not so extensively. *C. albicans* Csr1 regulator is involved in the control of adherence [128] and development of the ECM of *C. albicans* biofilms [129]. More specifically, Csr1 negatively controls the concentration of β-1,3-glucan present in the matrix by activating *CSH1* and *IFD6*, and inhibiting the expression of *GCA1*, *GCA2*, and *ADH5*. Csr1 has also been found to participate in the control of filamentous growth [129]. On the other hand, a transcription factor that positively controls glycolytic genes, Tye7, was found to be essential for biofilm cohesiveness in *C. albicans* [130].

The Rca1/Cst6 in *C. albicans,* is a regulator of hyphal formation by positively controlling the expression of hyphal genes like *GWP1*, *ECE1*, *HGC1*, and *ALS3* and the transcription factor Efg1 [131]. In *C. glabrata*, Cst6 is another important transcription regulator of biofilm formation. This protein is a bZIP transcription factor of the ATF/CREB family that negatively controls the expression of the *EPA6* gene, which encodes an important adhesin found in *C. glabrata* biofilms [132].

In *C. albicans,* an Ace2 transcriptional regulator was also found conserving the C_2H_2 zinc finger domain [111]. The absence of Ace2 leads to hyperfilamentation and hypervirulence in *C. albicans* [133], [134], although it has been shown to be required for biofilm formation in normoxia conditions [135] and filamentous growth under hypoxic conditions [136]. The *C. parapsilosis* and *C. glabrata* Ace2 homologs also play important roles in biofilm formation [110], [137].

Although having specific transcription factors regulating biofilm formation, *C. glabrata* has a number of related genes whose expression is controlled by subtelomeric silencing. *HYR1, EPA1, EPA2, EPA3, EPA4, EPA5, EPA6,* and *EPA7* genes of *C. glabrata* have been found to be repressed by this process, given their loci proximity to a telomere. This regulation is mediated by the Sir complex (Sir2–Sir4), Rap1, Rif1, yKu70, and yKu80 [80], [138], as well as the Swi/Snf complex [132]. Both Swi/Snf and Sir complexes appear to underlie the regulation of biofilm formation which is specific for *C. glabrata*, when compared with other *Candida* species.

Given the multifactorial nature of biofilm formation, its regulatory network is highly complex, involving the control of adhesion, hyphal formation, ECM production, and other processes (Figure I.2).

Finding a general regulator to tackle the regulatory control of biofilm in all *Candida* species is thus a very challenging goal.

2.3.4. Antifungal Resistance through Biofilm Formation

Biofilm formation has been tightly linked to the development of resistance to antifungal drugs (Table I.1). For example, resistance acquisition during biofilm formation was observed in a study where 48 h biofilms of *C. albicans* were found to exhibit five- to eightfold higher resistance to all antifungals when compared to planktonic cells [139]. Increased resistance exhibited by *C. parapsilosis* biofilms to fluconazole, voriconazole, ravuconazole, amphotericin B, nystatin, chlorhexidine, and terbinafine have also been registered [140].

This enhancement of resistance when *Candida* species grow as biofilms might be explained by several factors. One of them is the increased metabolic activity occurring in the early development of biofilm. Chandra *et al.* have shown that although MICs of amphotericin B, fluconazole, nystatin, and chlorhexidine were 0.5, 1, 8, and 16 μg/mL, respectively, in the early stage of *C. albicans* biofilm formation on polymethylmethacrylate strips, after 72 h of biofilm formation, MICs of amphotericin B, fluconazole, nystatin, and chlorhexidine had changed to 8, 128, 32, and 256 μg/mL, respectively [63]. Interestingly, however, the defective biofilm formation mutants, *Δefg1* and *Δefg1Δcph1*, which only exhibit an adherent monolayer of elongated cells, show the same resistance toward fluconazole and amphotericin B as the wild-type. These results suggest that resistance to antifungal drugs is related to adherence, regardless of normal biofilm formation [107].

Another issue to consider is the possible role of the ECM in antifungal drug resistance. Some authors advocate that EPS contributes as a barrier to prevent the diffusion of drugs, showing that *Candida* cells resist 20% better to amphotericin B with EPS, when compared to the same cells upon EPS removal [62]. Indeed, the extracellular β-1,3-glucan matrix has been proven to bind to amphotericin B, while its absence from the matrix, increases *C. albicans* susceptibility to fluconazole and amphotericin B [141]. Other evidences were given in a study where radiolabeled drug (^{3}H-fluconazole) is only sequestrated in the presence of matrix mannan and β-1,6-glucan, demonstrating the importance of these molecules in antifungal resistance [86].

Alterations in gene expression during *C. albicans* biofilm formation include the upregulation of *CDR* and *MDR* genes encoding azole resistance transporters [81]. This upregulation seems to be important for the development of antifungal resistance in the early phase of the biofilm formation, while in the maturation process, changes in sterol composition appear to be more relevant [62]. Nevertheless, it has been shown that a set of isogenic *C. albicans* strains carrying single or double deletions of genes encoding efflux pumps (*Δcdr1, Δcdr2, Δmdr1, Δcdr1/cdr2*, and *Δmdr1/cdr1*) could form biofilm like the parental strains, still displaying antifungal resistance. This gives evidence that antifungal resistance in biofilm does not depend on a single mechanism [81]. Interestingly, overexpression of *CDR1*, *CDR2* and *TPO1_2* genes has also been observed in *C. glabrata* biofilms [142], [143]. Tpo1_2 is a major facilitator superfamily transporter known to have a role in antifungal resistance [144] and to be necessary for the normal expression of *ALS1*, *EAP1* and *EPA1* genes involved in adhesion [143]. In fact, *C. glabrata* biofilms have shown to be significantly more resistant than planktonic cells [142], [145].

Showing that some specific mechanism of biofilm formation might be behind the resistance to antifungal drugs, *ALS3* and *HWP1* were found to be induced upon exposure to caspofungin in *C. albicans* biofilms but not in planktonic growing cells [146]. Additionally, the deletion of *MNN9*, *MNN11*, *VAN1*, *MNN4-4*, *VRG4*, *PMR1*, *BIG1*, *KRE5* and *FKS1* genes was found to lead to higher susceptibility to fluconazole in biofilm cells, but not in planktonic cells [86]. Interestingly, exposure to 80 μg/mL of fluconazole was found to lead to almost no changes in gene expression in SC5314 *C. albicans* biofilms, while exposure to caspofungin or amphotericin B results in massive gene expression changes, suggesting that biofilm cells were innately protected against azole drugs [146].

Similar to what has been described for other microorganisms, persister cells are also found within biofilms formed by *C. albicans*. Persister cells are dormant, non-dividing cells that have high tolerance to antimicrobial drugs. This tolerance is believed to be possible thanks to the dormancy of the cell, which enables the binding of antimicrobial drugs to their specific target, while making it impossible to the drug to inhibit the function of the target molecule. This tolerance, however comes at the price of non-proliferation [147]. In *C. albicans*, biofilm persister cells display resistance to fluconazole, while the same cells grown in non-biofilm planktonic culture are sensitive to fluconazole. Interestingly, these persister cells cultivated in biofilm exhibit increased expression of the *CDR* genes [81]. This phenomenon was also observed for *C. albicans* cells in biofilm exposed to amphotericin B and chlorhexidine, but independently of the expression of drug efflux pumps [148].

2.3.5. Multi-species Biofilm Formation and Quorum Sensing

Candida species biofilms have been usually studied as single species biofilm, although *in vivo* a very different reality is observed. Generally, biofilms are composed by multiple species that interact as a community having synergistic and/or antagonistic relationships. The synergistic interactions involve metabolic cooperation while antagonistic interactions include competition for nutrients and the generation of inhibitory compounds [149].

The formation of mixed biofilms of *Candida* species has been described with different combinations between *Candida* species or with *Candida* and bacteria. *C. albicans, C. glabrata, C. krusei*, and *C. tropicalis* have been shown to form biofilm with each other [94], [150]. Although increased biofilm formation was observed for most combinations of *Candida* species, for *C. tropicalis* this increase was only observed when in interaction with *C. albicans* [150].

Candida albicans biofilms have also been shown to be favored by combination with four species of bacteria: *Streptococcus mutans, Streptococcus sanguinis, Actinomyces viscosus*, and *Actinomyces odontolyticus*. Increased hyphae development, accompanied by the overexpression of *HWP1, ALS3,* and *EPA1*, was observed in mixed-species biofilm, both on acrylic surfaces or in reconstituted human oral epithelia (RHOE). Moreover, tissue damage and invasiveness is higher when all these five species are infecting and forming biofilm on RHOE. When compared to single *Candida* or single bacteria biofilms, mixed-species biofilm are significantly more invasive [151].

Multispecies biofilm formed upon denture stomatitis that frequently involves *C. albicans, S. mutans, S. sanguinis,* and *Actinomyces naeslundii* has also been investigated. Evidence of the increased pathogenicity of *C. albicans* in the presence of these bacteria was obtained, suggesting that

in these conditions the use of antibacterial agents could have an effect in decreasing fungal proliferation [152]. Interestingly, *S. mutants* and *C. albicans* have been shown to have a synergetic relationship since their coexistence leads to increased biofilm formation, when compared to single biofilms, despite the negative effect *S. mutants* has on hyphae formation. This dual-species biofilm displays two layers: *S. mutans* cells attached to the surface followed by *C. albicans* cells as a second layer [94]. Interestingly, *S. mutans* was also reported to increase biofilm formation of *C. glabrata* [94]. Multispecies biofilm formation on infected mice has also been investigated, considering *C. albicans* in coexistence with epithelial cells, neutrophils and commensal oral bacteria, such as *Enterococcus/Lactobacillus* sp. and *Staphylococcus* sp. [53].

Staphylococcus aureus interaction with *C. albicans* has been described in more detailed. Both species are able to cooperate in order to form a polymicrobial biofilm, even in the presence of serum which does not allow the formation of *S. aureus* single species biofilm. Visualization of these dual-species biofilm showed a first layer of *C. albicans* biofilm attached to the surface covered by a *S. aureus* monolayer that is included in the ECM formed by *Candida* cells. This ECM has proven to protect *S. aureus* from killing by vancomycin [153]. This positive interaction has shown to be also dependent on hyphae formation by *C. albicans* [154]. *Staphylococcus epidermis* has also been shown to cooperate with *C. albicans*, forming a multispecies biofilm that allows the protection of *S. epidermidis* against vancomycin and of *C. albicans* against fluconazole [83], [155] and amphotericin B [83].

When a synergistic relationship takes place, quorum sensing is an essential process that allows communication between species. Quorum sensing has been described mostly in bacteria, although several studies have already reported the use of quorum sensing between bacteria and *Candida* species [53], [156]. This process comprises the production and release of a signal molecule (autoinducer), which, according to the cell density, will increase in concentration and orchestrate a collective and coordinated expression of given genes, in all the species involved for the development of biofilm [149]. One example of quorum sensing has been described for the interaction between *C. albicans* and *Streptococcus gordonii*. These two species have been shown to coaggregate thanks to two cell wall anchored proteins of *S. gordonii*, SspA and SspB [156], [157], the later interacting directly with exposed *C. albicans* Als3 [158]. The positive interaction between these two species is based on the production and release of a chemical molecule denominated autoinducer 2 by *S. gordonii* [159]. This interaction has several advantages to *C. albicans*, such as the enhancement of hyphae formation and resistance to farnesol [156].

Farnesol is also a quorum-sensing molecule but produced as a secondary product of sterol biosynthesis and secreted by *C. albicans* [160]. When accumulated, it prevents the formation of filamentous growth and biofilm [161]–[164]. Generally, farnesol is mostly secreted in the later stages of biofilm formation by *C. albicans* [164]. Among pathogenic *Candida* species, only *C. albicans* and *C. dubliniensis* are known to secrete farnesol [165]. Farnesol is considered to be an autoinducer molecule that influences the expression of genes involved in antifungal resistance, cell wall maintenance, phagocytic response, surface hydrophobicity, iron metabolism and heat shock [162]. Given its effect and synergistic action with antifungal therapy, it has been considered as a potential therapeutic agent [166]. In *C. parapsilosis*, farnesol has also been described as having an inhibitory

effect on growth and biofilm formation [167], [168]. The presence of exogenous farnesol has been shown to lead to increased expression of oxidoreductases and a change in the expression of genes related to sterol metabolism [167]. Moreover, reference strains of *C. parapsilosis*, *C. tropicalis, C. dubliniensis* and *C. albicans* were found to have reduced biofilm production upon exposure to farnesol. However, *C. glabrata* and *Candida krusei* biofilm development was found to remain unaltered upon exposure of this quorum-sensing molecule.

Along with farnesol, a few other molecules produced by *C. albicans* have been proposed to work as quorum-sensing molecules, including morphogenic autoregulatory substance, phenylethyl alcohol and tryptophol [169], tyrosol, and farnesoic acid. Although through different pathways, farnesoic acid, just like farnesol, is involved in regulating the yeast-to-hyphae transition [161], [169]. Depending on the strain, *C. albicans* might produce farnesol or farnesoic acid, both having an inhibitory effect of filamentous growth [169]. Tyrosol, on the other hand, has an opposite effect on yeast-to-hyphae transition, increasing cell density and promoting the formation of germ tubes and the transition from yeast to hyphae [170]. Tyrosol is produced by planktonic and biofilm cells, having a stimulating effect in hyphae formation in the early stage of biofilm development [164].

Interaction of *C. albicans* with *Aspergillus nidulans* has been shown to be competitive thanks to the production of farnesol. In fact, the presence of exogenous farnesol or the co-culture of *A. nidulans* with *C. albicans* activates apoptosis in *A. nidulans* cells. This activation takes place in a mitochondria dependent way, through the FadA G protein complex signal transduction pathway[171].

Another antagonistic relationship is the one described between *C. albicans* and *Pseudomonas aeruginosa*. In this specific case, *P. aeruginosa* is known to attach to *C. albicans* filaments, forming biofilm over the hyphae instead of the surface. The formation of biofilm ultimately leads to the death of *C. albicans* filamentous cells, although yeast cells remain viable [172]. In fact, the presence of secreted factors by *P. aeruginosa* causes downregulation of genes involved in adhesion and biofilm formation, and increases the expression of genes encoding drug exporters, such as *CDR1* and *SNQ2*, and the *YWP1* gene encoding a protein involved in biofilm dispersal, in *C. albicans* biofilms [173]. This negative effect over *C. albicans* is related to a quorum sensing molecule produced and secreted by *P. aeruginosa*, the 3-oxo-C12 homoserine lactone. Other compounds with a 12-carbon backbone, like dodecanol, have a similar effect on *C. albicans* filamentous growth [174]. On the other hand, farnesol produced by *C. albicans* leads to a decreased quinolone signal from *Pseudomonas* that regulates the production of extracellular proteases, hydrogen cyanide and redox-active phenazines [175]. According to Holcombe *et al.*, the factors secreted by *P. aeruginosa* seem to have a specific effect in the maturation phase of biofilm formation by *Candida* species [173]. *C. glabrata, C. tropicalis, C. parapsilosis* and *C. dubliniensis* biofilm formation is also inhibited upon interaction with *P. aeruginosa* [176], which has a growth inhibitory effect on these *Candida* species [177], [178]. Interestingly, *P. aeruginosa* proliferation is also inhibited in the presence of *C. albicans*, *C. glabrata* and *C. krusei* [176].

2.4. Promising Strategies

Although no definitive solution for *Candida* biofilms has been found yet, there are several promising strategies being implemented nowadays, as well as intense research being developed in the search for novel solutions that alone or together with others might become the answer to this problem.

The current therapies with partial success to fight this challenge are based on two different approaches. The first, called “lock” therapy is directed to eradicate biofilm formation in catheters prior to their contact with the patient. The strategy consists in diffusing a high concentration of an antimicrobial drug into the catheter lumen, letting the agent act during a period of several hours or days. This technique avoids systemic toxicity since the antimicrobial drug only acts in the catheter [179]. Examples of success using the “lock” therapy are the tests performed on silicone catheters infected with different *C. albicans* and *C. glabrata* isolates, where micafungin (5 and 15 mg/L), caspofungin (5 and 25 mg/L), and posaconazole (10 mg/L) were used as antimicrobial agents. All antifungals used with this technique help decrease *Candida* biofilms, being micafungin the most effective [180]. Nevertheless, when using amphotericin B lipid formulation (1,000 mg/L), known to have activity against *Candida* biofilms [140], in a ‘lock’ therapy approach, an effective eradication of *Candida* biofilms was not observed [181]. Moreover, an interesting antimicrobial agent tested in ‘lock’ therapy is ethanol. Combined ‘lock’ therapy using 0.3 mL of 70% ethanol and 5 mg/L of micafungin was effective eliminating a catheter-related candidemia in a male infant [182]. Ethanol is an advantageous antimicrobial agent given its low cost and effectiveness against *Candida* species.

The other approach is catheter coating. Modification of the coating of the catheter with minocycline-rifampin, chlorhexidine, or silver sulfadiazine decreases the number of bloodstream infections caused by central venous catheters [183]. Coating with nanomaterials or nanoparticles has been studied as a possible improvement in the effect of reducing the occurrence of these infections. Although this technology has been developed with the main focus of eliminating bacteria, the use of silane system coatings on titanium and zirconia specimens has been described in a process of implant modification for the elimination of *Candida albicans* biofilms [184].

Given the absence of a real solution, new fields have been explored in order to find a different path to eliminate *Candida* biofilms. Research has been developed to find new natural products or synthetic peptides that might have an antifungal action. The study of different compounds has revealed interesting candidates with antifungal activity. Such is the case of phenylpropanoids and terpenoids of plant origin [185], [186], and phenazines produced by *P. aeruginosa* [187], which inhibit yeast-to-hyphal transition and biofilm formation in *C. albicans*. Besides these compounds, several high-throughput screenings have been performed trying to identify the best candidates to inhibit *Candida* biofilms. Siles *et al.* have screened a library of 1,200 off-patent drugs approved by the Food and Drug Administration, finding 38 active compounds against *C. albicans* biofilms. Another high-throughput screening has identified the SM21 compound as the best inhibitor of yeast-to-hypha transition, from a library of 50,240 small molecules, not having any toxic effect when tested in different human cell lines [188]. Moreover, some synthetic peptides also display significant antifungal activity, as is the case of KSL-W. This peptide significantly affects the growth, yeast-to-hypha transition and biofilm formation of *C. albicans* [189].

Karlsson *et al.* have used an antifungal β-peptide in coating nanotechnology. This approach was based on the design of polymer films that enable the localized release of the β-peptide from the surface. When testing film surfaces coated with this polymer, a significant reduction of cell viability, metabolic activity and hyphal elongation was observed [190].

Besides coating the surfaces with given molecules, another strategy is based on the modification of polymers incorporated in medical devices. Synthesis of water insoluble and organo-soluble polyethylenimine derivates with subsequent quaternization of N-methyl polyethylenimine with alkyl bromides was evaluated regarding the antifungal activity obtained. The resulting cationic polymers are capable of inhibiting *C. albicans, C. tropicalis*, and *C. dubliniensis* growth very effectively. The mode of action of these polymers is believed to be related to the disruption of membrane integrity [191]. Furthermore, chitosan hydrogel is another available polymer from natural origin that may be used to modify the surface of medical devices. Chitosan is very effective in impairing biofilm formation of *C. albicans, C. parapsilosis, C. glabrata, C. tropicalis, C. krusei*, and *C. guilliermondii*, having been tested positively in a *in vivo* catheter mouse model against *C. parapsilosis* biofilm formation [192].

Although most antifungal agents fail to eliminate *Candida* biofilms, there is still hope thanks to some relatively new drug formulations. That is the case of lipid formulations of polyene antifungals, such as liposomal amphotericin B and amphotericin B lipid complex. When used against *C. albicans* biofilms formed in a bioprosthetic model, the results show MICs like those obtained with planktonic cells. Also, the echinocandins, caspofungin and micafungin, have effective action against *C. albicans* and *C. parapsilosis* biofilms in the same model [140]. Interestingly, when biofilm precursor planktonic cells were exposed to subinhibitory levels of voriconazole, nystatin or chlorhexidine, and subsequently left to form biofilm, the same antifungal resistance of biofilms was not observed. In fact, a significant decrease of the capacity of the cells to form biofilm was observed [140]. Another interesting drug that has been discovered to have a role in acting against *in vitro* filamentous growth in *C. albicans* and against biofilms in *C. albicans, C. glabrata*, and *C. parapsilosis* is acetylsalicylic acid, usually known as aspirin. A decrease in biofilm formation was observed for aspirin concentrations between 0.43 and 1.73 mM [193].

An alternative approach to eradicate *Candida* biofilms consists in the photodynamic inactivation. This technique is based on the use of visible light and a nontoxic dye called photosensitizer that when activated leads to the production of reactive oxygen species which subsequently kill the targeted microbial cells due to the damage provoked on DNA, proteins, and/or cell membrane. Different photosensitizers have been tested against *Candida* biofilms demonstrating the great potential of this technique as an antimicrobial therapy. The photosensitizer toluidine blue (0.1 mg/mL) has been used successfully, reducing up to 60% the formation of *C. albicans* biofilms [194]. Another promising photosensitizer is methylene blue, capable of preventing *C. parapsilosis* biofilm formation *ex vivo* on mouse tongues after being activated by red LED light [195]. Interestingly, the combination of photodynamic inactivation strategy, using toluidine blue, together with chitosan, results in an enhancement of the effect of both approaches against *Candida* biofilms [196]. The nontoxicity of the dyes and the low cost of the technique highlight the great potential of this alternative approach [197].

2.5. Conclusion and Future Perspectives

This review highlights the overwhelming complexity of the intracellular mechanisms leading to the formation of *Candida* biofilms, including those controlling adhesion, changes in cell morphology and EPS production, especially considering that these have been shown to be in many cases species, or even strain, specific. Additionally, external factors, including the surface where the biofilm forms, which may be a layer of epithelial cells or very diversified plastic polymers, the cocktail of nutrients and inhibitors that are present in the surrounding environment or the presence of other synergistic or antagonistic microorganisms, have a tremendous effect on the final characteristics of the formed biofilm.

All this variability poses concerning challenges from the clinical point of view, leading to the successful persistence of *Candida* infections associated with high mortality rates. All the tactics against *Candida* biofilms implemented so far are only able to address this problem partially. Therefore, treatment and prevention of *Candida* biofilms must suffer improvements so that an effective solution might be applied. As discussed, more recent strategies have the potential to be improved although continuous research for new therapies or for the best combination between the available ones are also possible approaches. Nonetheless, the specific knowledge on all the mechanisms behind biofilm formation and antifungal resistance in each *Candida* species will be crucial for the delineation of a more effective strategic plan in the fight against *Candida* infections.

Despite all gathered knowledge, there is still a lot to be scrutinized, including many aspects regarding the formation of biofilms by non-*albicans Candida* species, whose study is decades behind that of *C. albicans*. Table I.1 and Figure I.2 highlight a lot of the blanks that are still to be filled regarding the specific mechanisms used by *C. glabrata, C. parapsilosis*, and *C. tropicalis*, which are emerging as important human pathogens. Additionally, it will also be highly relevant to ascertain the differences between biofilms formed by commensal *Candida* populations and those related to increased pathogenesis and persistent infections.

3. In the crossroad between *Candida glabrata* antifungal resistance and virulence

The ability of *Candida glabrata* to prevail in the human host, even upon the administration of antifungal therapy, is linked to the molecular mechanisms of virulence and antifungal resistance set in place by this yeast. This Subchapter focuses on those molecular mechanisms, highlighting examples of cross-talk between antifungal resistance and virulence in *C. glabrata.*

3.1. The Establishment of Antifungal Resistance

Therapeutic failure corresponds to loss of response from a patient to a drug administered at a standard dose. Such failure is usually due to a multitude of factors relative to the drug itself, the host and the microbial pathogen [198]. In the case of *Candida* infections, which are usually linked to immunocompromised patients, the propensity for therapeutic failure is increased. The risk of failure is also linked to the use of antifungal drugs as prophylaxis, which gives the possibility of commensal *Candida* species to develop resistance mechanisms upon exposure to drugs at prolonged periods [198]–[200]. In addition, the capacity of *Candida* species, especially *Candida glabrata*, to exhibit such molecular mechanisms is itself a cause for an increase in the probability of failure to any given therapeutic strategy implemented [201].

According to the factors that are being analysed when studying antifungal resistance, one can describe resistance in different ways. It is possible to discuss resistance in terms of clinical resistance or mycological resistance. The first is the failure to eliminate the patient's fungal infection, though the drug administered has *in vitro* activity against the pathogen in case, while mycological resistance, is the ability of the fungus to survive and grow in the presence of the drug that should eradicate it or at least limit its *in vitro* growth [201]. Within mycological resistance, we may encounter two types of antifungal resistance: primary or secondary. Primary antifungal resistance corresponds to a natural resistance to the antifungal agent exhibit by the pathogen, which does not require pre-exposure of the pathogen to the drug for its development. Secondary resistance is an acquired resistance that results from the exposure of the pathogen to the drug, resulting in the development of new molecular mechanisms of resistance [198], [202].

Different methods may be applied to analyse resistance. Antifungal susceptibility testing is usually applied to the study of a given clinical isolate to evaluate the risk of failure of a given drug. Standardised *in vitro* methods for such testing have been developed by the European Committee on Antimicrobial Susceptibility Testing (EUCAST) and the Clinical and Laboratory Standards Institute (CLSI), being usually applied to identify strains with high probability of leading to clinical resistance. Epidemiological cutoff values have been established but for some drugs/species, like caspofungin and *C. glabrata*, standardised testing cannot be applied due to the unreliable behaviour of the drug or species in case [203]. Nevertheless, antifungal susceptibility testing should always be carefully analysed given that there isn't an absolute association between the results of the test and the clinical response [198].

As pointed out above, by several applications of antifungal susceptibility testing, *C. glabrata* is the *Candida* species found to have a higher number of clinical isolates exhibiting antifungal resistance, to any of the classes of antifungals used [15], [29], which indicates that *C. glabrata* infections are more prone to failure than those of other *Candida* species. This propensity for acquiring antifungal resistance is linked to several antifungal resistance mechanisms developed by *C. glabrata* in response to the action of antifungal drugs. The molecular mechanisms leading to acquired resistance to the different available antifungal drugs will be reviewed herein.

3.1.1. Molecular Mechanisms of Azole Resistance in *Candida glabrata*

Azoles are widely used for the treatment of *Candida* infections [204], by targeting the cytochrome P450 sterol 14α-demethylase, Erg11, that catalyses the conversion of lanosterol into ergosterol [205], [206]. By inhibiting its target, azoles cause the inability to produce and renovate sterols in the plasma membrane, changing its fluidity and hampering important processes, such as signalling, exocytosis and endocytosis [13]. *C. glabrata* displays several different mechanisms to fight these compounds (Figure I.3), and they can present themselves alone or in combination in a single isolate [198]. The most commonly developed mechanisms for reaching antifungal resistance is the upregulation of drug efflux pumps from the ATP binding cassette (ABC) superfamily and Major Facilitator Superfamily (MFS) [207].

Present in all organisms, ABC transporters are ubiquitous proteins that use energy provided by the hydrolysis of ATP to transport through the membrane different types of substrates. ABC proteins are defined by their two nucleotide-binding domain (NBD), which are highly conserved, holding the ATP-binding motif, and two transmembrane domains (TMDs), which are comprised by several transmembrane spanning segments (TMS) that determine substrate specificity [208], [209]. The subfamily found to have a role in azole resistance in *C. glabrata* is the pleiotropic drug resistance (PDR) subfamily, to which CgCdr1, CgCdr2 and CgSnq2 belong. Transporters belonging to this subfamily in yeast are known to extrude several xenobiotics like fungicides, azoles, mycotoxins, herbicides and other antifungal drugs [210]. CgCdr1, CgCdr2 and CgSnq2 were found to be necessary for full resistance of *C. glabrata* to azole drugs [211]–[214]. CgCdr1 expression was shown to cause reduced intracellular accumulation of fluconazole in azole resistant clinical isolates [211]. CgCdr1, CgCdr2, CgSnq2 were found to be upregulated in azole resistant strains, while their deletion compromises significantly the ability to resist azole drugs [211]–[213]. In addition, CgYor1 ABC transporter has been found to be upregulated in *C. glabrata* upon azole exposure, suggesting that at least one more ABC transporter is connected to the acquisition of azole resistance in this yeast [215], [216].

MFS transporters have also been implicated in azole resistance in *C. glabrata*. MFS transporters use the electrochemical proton-motive force for the translocation of different substrates. MFS proteins are characterized by 12 or 14 TMS with a cytoplasmic loop in between, being classified accordingly as belonging to the drug:H+ antiporter-1 (DHA1), (12 TMS), or the drug:H+ antiporter-2 (DHA2), (14 TMS), families [217]. The first MFS transporter implicated in *C. glabrata* drug extrusion was CgAqr1, a homolog of the previously known *S. cerevisiae* ScAqr1, a transporter involved in acetic acid and antifungal resistance. CgAqr1 was found to be necessary for the decrease of intracellular accumulation of ^{3}H-clotrimazole [218]. CgQdr2 is another DHA transporter that has been linked to an important role in

miconazole, tioconazole, clotrimazole, and ketoconazole resistance. It has been shown that this transporter is also necessary for decreased ^{3}H-clotrimazole intracellular accumulation in *C. glabrata* [219]. CgTpo3 and CgFlr2 were also found to decrease ^{3}H-clotrimazole intracellular accumulation, having a role in azole resistance [220], [221]. Moreover, CgTpo1_1 and CgTpo1_2 were also found to confer resistance to clotrimazole, miconazole, ketoconazole, tioconazole, itraconazole and fluconazole, being CgTpo1_2 upregulated upon the response of *C. glabrata* to clotrimazole exposure [144]. In addition, CgAqr1, CgQdr2, CgTpo1_1, and CgTpo3 have been implicated in the clinical acquisition of clotrimazole drug resistance, given that their transcript levels were significantly upregulated in *C. glabrata* azole resistant isolates [222].

ABC and MFS transporters have been shown to be regulated by the transcription factor CgPdr1, which is the main regulator of azole resistance in *C. glabrata*. CgPdr1, a homolog of the ScPdr1 and ScPdr3 regulators of multidrug transporters genes in *S. cerevisiae,* was first analysed by Vermitsky and colleagues (2004). They found that the upregulation of *CgCDR1* and *CgCDR2* genes in an azole resistant isolate was connected with a single amino acid substitution in the CgPdr1 transcription factor, believed to be the cause of azole resistance [214], [215]. Another study has shown that other alterations in the sequence of *CgPDR1* gene also lead to azole resistance in *C. glabrata* [223], these alterations being nowadays identified as gain-of-function (GOF) mutations of CgPdr1 [224], [225]. CgPdr1 autoregulates itself and its overproduction leads to higher upregulation of *CgCDR1* gene and, consequently, to higher azole resistance. In CgPdr1 GOF mutants the production of CgPdr1 polypeptide is synthesized at higher frequency but less stable than the wild-type protein [226]. Interestingly, CgPdr1 is also known to regulate virulence and adhesion in this pathogenic yeast [224], [227], [228], as will be discussed later on. In opposition to CgPdr1, *C. glabrata* expresses a transcription factor that negatively regulates pleiotropic drug resistance, CgStb5 [229].

Given that azole compounds act by disrupting the biosynthesis of ergosterol, leading to ergosterol depletion and the production of toxic sterol intermediates, some of the resistance mechanisms of *C. glabrata* are directly linked with the ergosterol pathway. Although not usually found in *C. glabrata* clinical isolates [225], [230], certain cases show that *C. glabrata* may exhibit the upregulation of *CgERG11* gene or its mutation, a mechanism more common in other *Candida* species [225], [231], [232]. Interestingly, only an azole resistant clinical isolate of *C. glabrata* was found to present a single-amino-acid substitution (G315D) in *CgERG11* gene, which turned CgErg11 non-functional [233]. In addition, a point mutation in *CgERG3* gene was found in an azole resistant clinical isolate, leading to decreased levels of toxic sterols in the plasma membrane and, consequently, to decreased azole toxicity [234]. Upon *C. glabrata* exposure to fluconazole, several other genes involved in the biosynthetic pathway of ergosterol are also found to be upregulated: *CgERG2, CgERG3, CgERG4* and *CgERG10*, as well as genes involved in sterol uptake: *CgAUS1, CgUPC2A, CgUPC2B, CgSUT1, CgSUT2,* and *CgPDR16* [235]. Controlling the gene that encodes the target of azole drugs, *CgERG11*, and the genes encoding enzymes from the sterol biosynthesis pathway, CgUpc2A is an important transcription factor whose role is also linked to azole resistance [236], [237]. The absence of *CgUPC2A* gene in an azole susceptible-dose-dependent and an azole resistant isolate was found to increase the susceptibility of both isolates to fluconazole, and decrease the ergosterol levels of *C. glabrata* [236]. CgUpc2A is also

involved in the control of the expression of *CgAUS1* gene [237]. In the Δ*cgerg1* deletion mutant, the disruption of *CgAUS1*, encoding a sterol uptake transporter, was found to lead to high sensitivity to fluconazole and voriconazole. It seems that upon loss of the biosynthesis of ergosterol, CgAus1 becomes an important player in azole resistance allowing *C. glabrata* to cope with the loss of ergosterol, and, subsequently, fight the action of azole drugs [235].

C. glabrata strains may suffer loss of mitochondrial functions, which has been linked to enhancement of azole resistance. The absence of mitochondrial function translates into the inability to grow in nonfermentable carbon sources and a deficient growth in media supplemented with glucose. This phenotype is called *petite* and its due to the partial or total loss of mitochondrial genome, or mutation in the mitochondrial DNA [238]. In *petite* cells, although *CgERG11* gene is not upregulated, the genes encoding the drug efflux pumps *CgCDR1*, *CgCDR2* and/or *CgSNQ2* usually are, leading to azole resistance [212], [238], [239]. It is believed that the upregulation of multidrug resistance transporters is due to the *petite* mutations, which are known to influence nuclear gene expression in yeast [238]. Moreover, loss of mitochondrial functions leads to the triggering of anaerobic metabolism, which is known to stimulate the action of CgErg11, and subsequently the production of ergosterol, helping *C. glabrata* cope with the action of azole drugs [240]. Indeed, *petite* mutants have been found to have higher levels of ergosterol and in certain cases to be amphotericin B susceptible, due to the increased number of available amphotericin B target molecules [238]. An interesting mitochondrial matrix cochaperone, CgMge1, was found to increase resistance towards fluconazole when overexpressed in *C. glabrata* [241], linking once more mitochondrial functions with resistance. A more recent study shows that the overexpression of *CgMGE1* gene decreases the formation of toxic sterols upon fluconazole exposure, especially under acidic conditions [242].

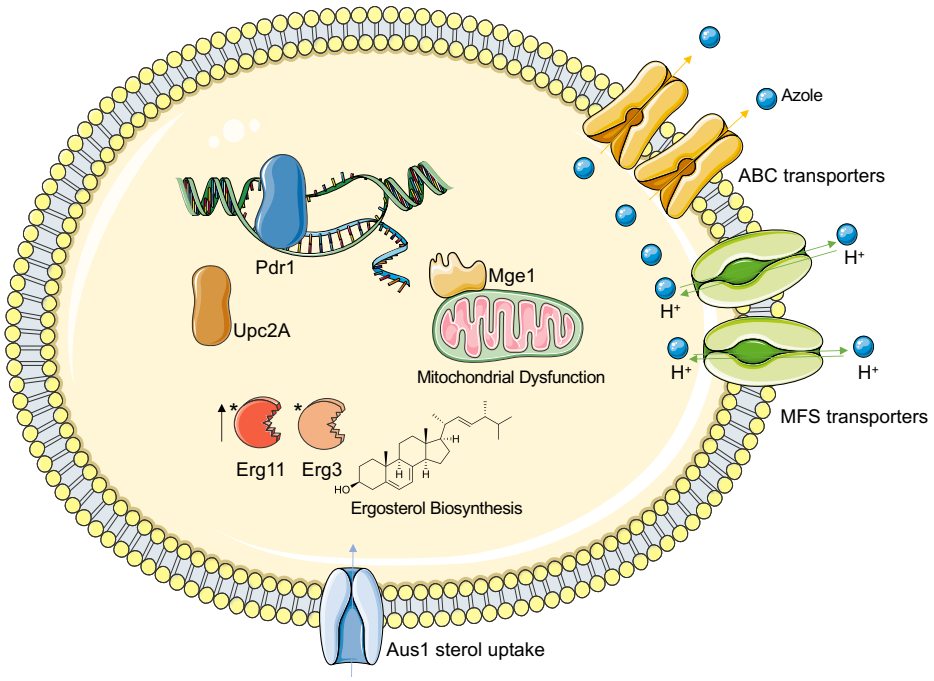

Figure I.3. Main molecular mechanisms of azole resistance in *Candida glabrata*. Upregulation of ABC and MFS transporters by the activation of Pdr1 with GOF mutations and due to mitochondrial dysfunction. Alterations in the ergosterol biosynthetic pathway: upregulation of *ERG11* gene by Upc2A transcription factor, alterations in the structure of Erg11 and Erg3 and sterol uptake by Aus1 and overexpression of *MGE1* contributing to decrease the production of toxic sterols and replace the sterols into the membrane.

3.1.2. Molecular Mechanisms of Echinocandin Resistance in *Candida glabrata*

Echinocandins are the most recent class of antifungal drugs, being in the front-line for the fight against invasive candidiasis [243], [244]. Echinocandins act by inhibiting the β-(1,3)-D-glucan synthase involved in the synthesis of β-(1,3)-glucan, an essential component of the cell wall of *Candida* species. Echinocandins target the FKS subunits of this enzyme, encoded by the *FKS1, FKS2* and *FKS3* genes. By compromising the synthesis of β-(1,3)-glucan, these compounds provoke dramatic changes in the cell wall of fungal cells, which in the case of *C. albicans* become rounded and enlarged before lysis [243].

Although at first efficient even against *C. glabrata* invasive candidiasis, an upraise of resistance has been observed, with 4.9% of *C. glabrata* resistant isolates in 2001 turning into 12.3% in 2010. This increase in *C. glabrata* resistance towards echinocandins was linked with amino acid substitutions in CgFks1 and CgFks2 proteins [244]. Indeed, several mutations in hot spot regions of the encoding genes have been shown to lead to drug resistance [245]–[249]. These mutations, however, were also found to decrease the catalytic efficiency of the enzyme [245] (Figure I.4).

Given that hot spot mutations in *CgFKS1* and *CgFKS2* are the unique molecular mechanism described so far for *C. glabrata* echinocandin resistance, new molecular diagnostic tools, for example a dual assay based on the allele-specific molecular beacon and DNA melt analysis, with subsequently asymmetric PCR, use the detection of such mutations in order to guide antifungal therapy, [250].

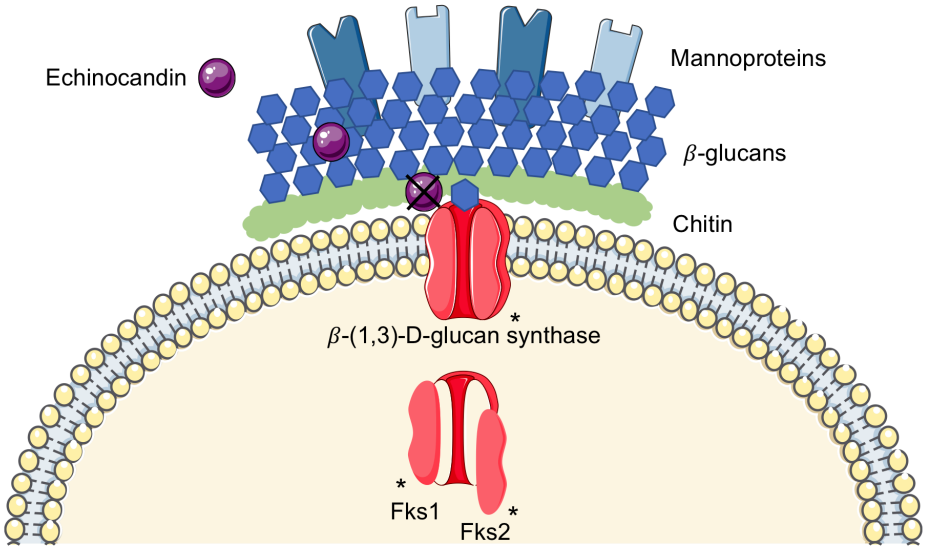

Figure I.4. Echinocandin resistance mechanisms in *Candida glabrata* based on the hot spot mutations in *FKS1* and *FKS2* genes, altering the structure of the β-(1,3)-D-glucan synthase and stopping the inhibition by echinocandins.

3.1.3. Molecular Mechanisms of Polyene Resistance in *Candida glabrata*

Amphotericin B is the main polyene drug used in the treatment of fungal infections, due to the high toxicity found to be associated to the majority of polyenes. Amphotericin B has limited toxicity that allows its intravenous administration. Like all polyene drugs, amphotericin B acts by bind to ergosterol, leading to the formation of pores in the plasma membrane. This ultimately results in disruption of the

osmotic integrity of the plasma membrane, leaking intracellular magnesium and potassium and leading to cell lysis. Polyenes are also known to cause the disruption of oxidative enzymes [251].

Amphotericin B resistance in *C. glabrata* is usually due to changes in the biosynthesis of ergosterol, which modifies the levels or type of ergosterol on the membrane (Figure I.5). For instance, common mechanisms of resistance are mutations in the *CgERG6* gene that lead to lower ergosterol levels on the plasma membrane. Such mechanism was already found in several *C. glabrata* amphotericin B resistant clinical isolates with missense mutations in *CgERG6*, leading to lower levels of ergosterol and to the accumulation of sterol intermediates on the plasma membrane [252], [253].

Moreover, certain MFS transporters have been shown to be necessary in the fight of *C. glabrata* against amphotericin B, such as CgTpo1_1, CgTpo1_2 and CgFlr2 [144], [221], although the clear mechanism as to their action on amphotericin B resistance as not yet been assessed.

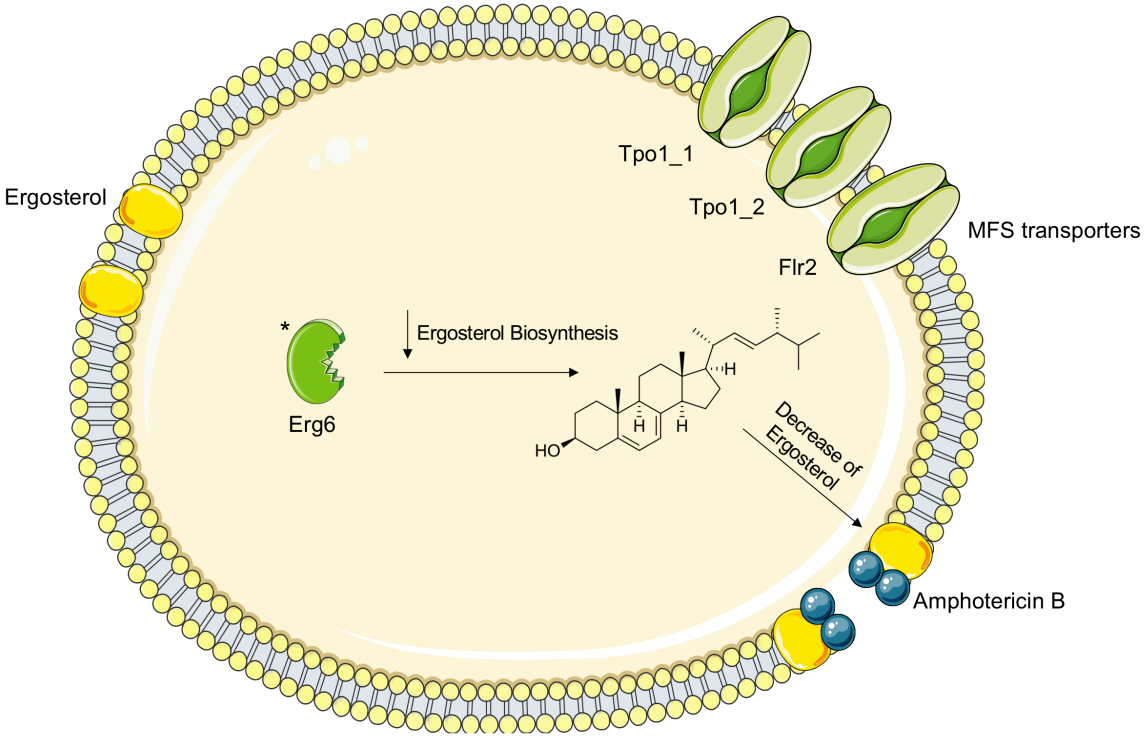

Figure I.5. Amphotericin B mechanisms of resistance in *Candida glabrata* rely on the alterations in the structure of Erg6, which decrease ergosterol levels on the membrane, and on the MFS transporters Tpo1_1, Tpo1_2 and Flr2.

3.1.4. Molecular Mechanisms of Pyrimidine-analogue Resistance in *Candida glabrata*

Pyrimidine-analogues constitute the last class of antifungal drugs used to tackle *Candida* infections. 5-fluorocytosine is the single one of these compounds used for therapy, and is usually used in combination with other antifungal drugs. 5-fluorocytosine is transported into the fungal cell by the cytosine permease. Then, it is converted into 5-fluorouridine monophosphate and 5-fluorouridine diphosphate, which is turned into 5-fluorouridine triphosphate by the action of cytosine deaminase and

uridine phosphoribosyl transferase inside the cells. 5-fluorouridine triphosphate is incorporated into fungal RNA instead of uridylic acid, blocking the synthesis of proteins. In addition, 5-fluorocytosine is also converted into 5-fluorodeoxyuridine monophosphate that inhibits *CDC21* gene of *Candida* species, a thymidylate synthase, essential for DNA synthesis [254]–[256].

Candida resistance to 5-fluorocytosine is generally developed thanks to downregulation or mutations of genes involved in the conversion of this compound into 5-fluorouridine or 5-fluoro-deoxyuridine monophosphate, avoiding their negative actions upon DNA and RNA synthesis [257], [258] (Figure I.6). A study of 3 *C. glabrata* resistant mutants unravelled mutations in *CgFUR1* and *CgFCY1* genes, encoding the uridine phosphoribosyl transferase and cytosine deaminase, respectively, which lead to null phenotypes for CgFur1 and CgFcy1, being the cause of 5-fluorocytosine resistance [259]. Another study links 5-fluorocytosine resistance with the decrease activity of uridine phosphoribosyl transferase, CgFur1 [260]. Moreover, a study of selected resistant mutants of *C. glabrata* revealed missense mutation in *CgFCY1* and *CgFCY2* genes, encoding cytosine deaminase and cytosine permease, respectively. In addition, the *CgCDC21* and *CgFCY2* genes were found to be upregulated in one resistant mutant, while *CgFUR1* gene was downregulated in another resistant mutant. In this study, no differences were found in the uptake of 5-fluorocytosine [256].

An interesting study focused on the global proteomic response of *C. glabrata* to 5-fluorocytosine, assess through an iTRAQ-MS-based approach, shows that 32 proteins are differently expressed, half of which under the control of CgPdr1. This work identified two MFS transporters, CgFlr1 and CgFlr2, found to have a role in controlling the accumulation of 5-fluorocytosine, being an additional resistance mechanism against this drug [221]. It is important to notice that CgFlr2 is also important for azole resistance, being a very likely cause for the failure of combination therapy in *C. glabrata* infections. One other MFS transporter, CgAqr1, and two aquaglyceroporins, CgFps1 and CgFps2, have been implicated in 5-fluorocytosine resistance, being also implicated in decreasing the intracellular concentration of the drug [218], [261].

It is important to notice that besides having different mechanisms to reach 5-fluorocytosine resistance, *C. glabrata* was also shown to display intrinsic resistance towards this antifungal drug. In the study of Pfaller and colleagues (2002), 1% of 1,267 *C. glabrata* isolates were found to have primary resistance towards 5-fluorocytosine [262]. Therefore, the use of this antifungal drug should be carefully evaluated and considered only in combined therapy.

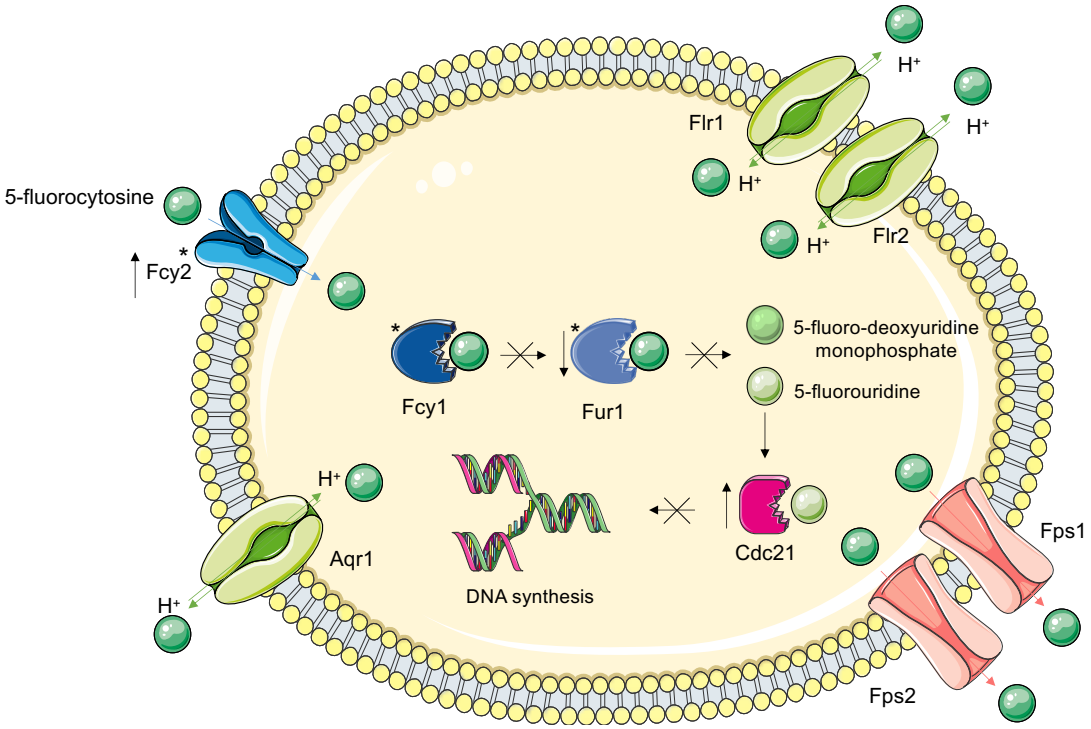

Figure I.6. Pyrimidine-analogue resistance in *Candida glabrata.* Changes of expression or mutations of genes involved in the conversion of 5-fluorocytosine into pyrimidine-analogues. The role of MFS transporters Aqr1, Flr1, Flr2, Fps1 and Fps2 in 5-fluorocytosine resistance.

3.1.5. Mechanisms of Multidrug Resistance in *Candida glabrata*

Although *Candida glabrata* displays specific responses to the exposure of each given drug, this pathogenic yeast also exhibits mechanisms known to be used for the resistance to more than one family of antifungal drugs, resulting in multidrug resistance.

That is the case of CgMsh2 activity, involved in mismatch DNA repair in *C. glabrata*. Disruption of *CgMSH2* and nonsynonymous mutations in its sequence in several clinical isolates were found to lead to a hyper-mutator phenotype with increased resistance to the antifungal drugs caspofungin, fluconazole and amphotericin B. The absence of *CgMSH2* was found to be accompanied by mutations in the hot spot region of *CgFKS1* and *CgFKS2*, mutations in *CgPDR1* and, in one specific case, a mutation in *CgERG6* gene. It is believed that this hyper-mutator phenotype enables *C. glabrata* to more easily develop resistance to different antifungal compounds, resulting in multidrug resistance [263].

3.2. The Virulence Features of the Pathogenic Yeast *Candida glabrata*

To infect the human host, *Candida glabrata* counts with different features that enable this pathogenic yeast to prevail and evade the immune system of the host. The following sections will attend to the main mechanisms used by *C. glabrata* to infect the human host and models of infection, pointing out their importance in the triumph of this pathogen over the host.

3.2.1 *Candida glabrata* Adherence to the Human Mucosa

Fungal pathogens rely on adherence to ensure their survival in the human host. *C. glabrata* has shown to be able to strongly adhere to several mammalian cell types, such as epithelial cell lines [264]–[266] and coronary endothelial cells [267], and to mediate binding to immune cells, like macrophages [268]. This yeast also adheres tightly to fibronectin present in the host ECM [269]. Adherence to host tissues is performed by adhesins (Figure I.7), some of those already presented in the previous Subchapter. *C. glabrata* has a very high number GPI-CWPs, with 67 predicted adhesins identified [270], divided into different adhesins families [271]. GPI-CWPs are composed by a N-terminal hydrophobic signal sequence and a C-terminal consensus sequence, without internal transmembrane domains. The first part targets the protein to the ER, and the C-terminal has another hydrophobic domain that is cleaved and replaced by the GPI anchor in the membrane of the ER, which will become in the end the plasma membrane [271].

The major family of adhesins in *C. glabrata* is the EPA family with 18 or 23 genes sequenced for CBS138 and BG2 strains, respectively [272]. EPA proteins bind to host tissues by recognizing host cell glycans through their adhesin (A) domains. These domains have in their structure eleven strands that form an antiparallel β-sandwich motif called anthrax protective antigen (PA14) domain and count with two inner loops, CBL1 and CBL2, which are also involved in calcium binding, and on L1, L2 and L3 loops, for their binding specificity to glycans with galactose terminal residues, preferentially galactose-β-1-3 glycans [273], [274].

CgEpa1 has been shown to be an essential adhesin for *C. glabrata* adherence to the human laryngeal carcinoma cell line HEp2 [264]. This adhesin is very similar to two other, CgEpa6 and CgEpa7, which share 94% similarity [275]. These three adhesins have been found to play the most important roles when it comes to *C. glabrata* adhesion to host cells. All three are involved in the adhesion to uroepithelial cells *in vitro* and in bladder colonization in a murine urinary tract infection model [276], as well as in the mouse kidney colonization [275]. These proteins are also implicated in the recognition of *C. glabrata* by NCR1, a mouse ortholog of the human natural killer (NK) cells cytotoxic receptor NKp46 [277].

EPA family has other members that seem to also be necessary for the full capacity of adherence of this species. For instance, De Las Peñas and colleagues (2003) have shown that the entire cluster of genes to which *CgEPA1* gene belongs is necessary for the full virulence of *C. glabrata* in a immunocompetent BalbC mice systemic infection model [80]. In addition, *CgEPA2* gene, encoding another EPA adhesin, is expressed in *C. glabrata* cells recovered from the liver of a murine model of

systemic infection and upon hydrogen peroxide exposure [278], suggesting an important role in virulence.

The importance of EPA adhesins in *C. glabrata* virulence is intrinsically related to their function in recognizing and adhering specific ligands on the host cells and ECM. CgEpa1, CgEpa6 and CgEpa7 have been shown to prefer ligands containing a terminal galactose residue, being CgEpa6 the one with a broader ligand specificity range for glycans [279]. One of these ligands is the Galβ-1,3-GalNAc disaccharide, called Thomsen-Friedenreich or T antigen, which is present in mucin-type *O*-glycans [273], [274]. Mucins are well known to be glycans present in several tissues, such as colon tissue and uterine tissue, as well as in saliva, and CgEpa1 recognizes them [280], enabling *C. glabrata* adhesion to host tissues.

Fascinatingly, the expression of given adhesin-encoding genes, seems to depend upon host environmental conditions. For instance, *CgEPA6* expression is induced in hypoxic conditions and in the presence of parabens and sorbate, that if present upon *C. glabrata* adherence to human vaginal epithelial cells, augment the process of adhesion [281]. Moreover, the expression of this adhesin is dependent on the presence of nicotinic acid, a precursor of NAD^+ (nicotinamide adenine dinucleotide), which *C. glabrata* is not able to synthesize. Therefore, upon the presence of nicotinic acid in the environment, the expression of *CgEPA6* is no longer repressed, being activated by the Sir2, a NAD^+-dependent histone deacetylase, promoting adhesion on that specific environment [276]

An interesting aspect of *CgEPA1* gene expression is that it was found to be regulated, not only by subtelomeric silencing described previously, but also by the major regulator of azole resistance in *C. glabrata*, the CgPdr1 transcription factor. In fact, CgPdr1 GOF mutations have been associated with higher virulence of *C. glabrata* strains in murine models of disseminated infection, together with azole resistance [224]. Vale-Silva and colleagues (2013) studied the interaction of *C. glabrata* with murine bone marrow-derived macrophages and human acute monocytic leukemia cell line-derived macrophages, and different epithelial cell lines: Chinese hamster ovary modified cell line Lec2, human cervix adenocarcinoma cells and human colorectal adenocarcinoma cells. Their worked showed that GOF mutations on CgPdr1 result in decreased adherence to and uptake by macrophages, while higher adherence was observed for the epithelial cell lines [266]. This enhanced virulence upon GOF mutations in this transcription factor was correlated with the increased expression of *CgEPA1* gene, highlighting the importance of this adhesin in the colonization of bladder and kidney in a murine model of urinary tract infection [228].

Another interesting family of *C. glabrata* adhesins is the PA14 domain containing cell wall protein (Pwp) family, constituted by 7 members, which have some similarity with EPA adhesins, specially due to the conservation of the PA14 domain [78], [267]. From this family the most well-known adhesin is Pwp7, which participates in *C. glabrata* adhesion to human umbilical vein endothelial cells [267]. The adhesin-like wall protein (Awp) family has 12 members, 6 of those being correlated with the hyperadhesive phenotype of *C. glabrata* clinical isolates [270], [282]. Additionally, the Awp5 adhesin was found to have an important role in the adhesion to human umbilical vein endothelial cells, being better known as Aed1 (adherence to endothelial cells-1) [267]. Both these families of adhesins are still poorly characterize in terms of their importance in adherence and virulence in *C. glabrata*. Although the

majority is not yet characterized, adhesins have a major importance in *C. glabrata* adherence and virulence, being present in high numbers in this yeast's genome. In fact, a recent study found the presence of 101 and 107 adhesin-like genes in two *C. glabrata* clinical isolates [283].

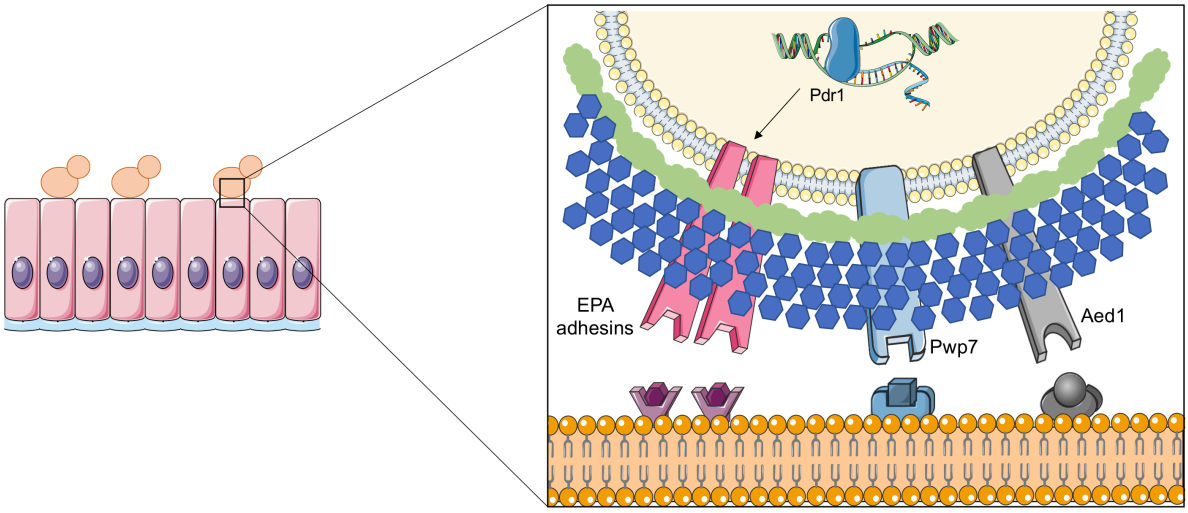

Figure I.7. Adhesins involved in the adhesion to host mucosa upon *Candida glabrata* infections.

C. glabrata possesses yet another family of cell wall proteins, which are not adhesins, but contribute to the interaction of this pathogen with host cells. The YPS family comprises 11 members that are GPI-anchored aspartyl proteases, usually designated yapsins. The YPS family was found to be necessary for the control of CgEpa1 presence on the cell wall, resulting its deletion in an hyperadhesive phenotype towards epithelial cells. In turn, Yps1 and Yps7 participate in the maintenance of the cell wall in stationary phase, while all *YPS* genes are necessary for *C. glabrata* survival within macrophages, thanks to their action avoiding the production of nitric oxide by macrophages. The importance of yapsins in *C. glabrata* virulence was further demonstrated in a murine model of disseminated candidiasis by Kaur and colleagues (2007) [284].

3.2.2. *Candida glabrata* Phenotypic Switching

C. glabrata has the ability to adapt to the human host at different levels, exhibiting altered phenotypes according to the host niche, a feature usually called phenotypic switching. Within the human host, *C. glabrata* may present itself in four different colony morphologies: white, light brown, dark brown and very dark brown [285]. Different clinical isolates have been shown to have the capacity of phenotypic switching, exhibiting different phenotypes upon collection from different parts of the human host. For instance, a clinical isolate recovered from the vaginal tract was found to have dark brown phenotype while being genetically identical to another clinical isolate recovered from the oral cavity, whose phenotype was mostly white [286]. From all possible phenotypes *C. glabrata* may present, the dark brown phenotype is the one that exhibits higher virulence in a mouse model of systemic infection [287]. From the study of the genes differentially expressed between the white and dark brown phenotypes of *C. glabrata*, it was discovered that the two phenotypes differ mainly in terms of copper assimilation, sulfur assimilation, and stress response [288]. Although the specific mechanisms that allow phenotypic

switching in *C. glabrata* are not clear, this feature seems to be of high importance upon this yeast colonization of human body niches.

3.2.3. Evading Macrophage Action: *Candida glabrata* Modulation of the Phagolysosome

Once inside the human host, *C. glabrata* has to face different environmental stresses, and one of the most difficult to fight is phagocytosis, mainly performed by macrophages. The phagolysosome environment is very aggressive towards pathogens, with low pH, ROS, starvation of carbon source and presence of hydrolytic enzymes [289], [290]. Nevertheless, *C. glabrata* is able to survive within such environment and even replicate in such hostile conditions [289], [291], instead of causing high damage to macrophages or macrophage apoptosis, like *C. albicans* [291].

Upon phagocytosis, *C. glabrata* suffers modification to cope with the stresses encountered (Figure I.8). 23 genes (*CCH1, SLM1, SHO1, ARG81, GPR1, GPA2, FRE8, CAGL0M12496g, LRG1, GNT1, ERG5, SLG1, OST6, MNN4, MNS1, PMT2, PMT4, YGR106C, BAR1, CDC12, CKA2, HEK2* and *MPS23*) were found to be necessary for the mechanisms developed by *C. glabrata*, within a screening of 433 deletion mutants. These genes are involved in cell wall biosynthesis, calcium homeostasis, nutritional and stress responses, protein glycosylation and iron homeostasis in *C. glabrata*. However, upon phagocytosis, 18 genes mediate cell surface exposure of β-glucans or chitin, found to mediate also TNF-α induction, and 15 genes are responsible for decreasing ROS production within the phagolysosome, 9 of those participating in *C. glabrata* oxidative stress resistance [292].

Other alterations are also necessary for *C. glabrata* resistance to phagolysosomes, such as the induced expression of *CgCTA1* and peroxisome proliferation [289]. CgCta1 is the single catalase of *C. glabrata* being responsible for resistance to oxidative stress [40], a stress *C. glabrata* suffers within this environment [289]. Although at first increased, the number of peroxisomes declines throughout the process of phagocytosis due to autophagy, which is initiated as a mechanism to cope with phagolysosome-imposed stress. This mechanism allows survival of *C. glabrata* within this environment; indeed, without *CgATG11* or *CgATG17* genes, involved in pexophagy and non-selective autophagy, such survival becomes compromised [289].

C. glabrata was also found to suffer modifications on the chromatin structure and resistance to micrococcal nuclease digestion, and to developed an altered epigenetic signature, with decreased protein acetylation and increased cellular lysine deacetylase activity upon phagocytosis [293]. This adaptation was found to be extremely important given that *ΔCgrsc3-a, ΔCgrsc3-b, Cgrsc3-aΔbΔ,* and *ΔCgrtt109* mutants deficient in chromatin organization and *ΔCgrtt107* and *ΔCgsgs1* mutants defective in DNA damage repair were found to display decreased virulence in a murine model of disseminated candidiasis [293].

The changes occurring within *C. glabrata* cells lead to clear alterations in the behaviour of macrophages and phagolysosomes, which allow their survival and replication within these cells of the human host (Figure I.8). *C. glabrata* was found to be able to inhibit the production of proinflammatory cytokines, such as TNF-α, IL-1β, IL-6, IL-8, and IFN-γ, as well as to decrease ROS production by infected-macrophages [291]. The alterations *C. glabrata* imposes onto macrophages upon being

phagocytized increase until the point of changing the maturation of the phagolysosome, altering the fusion of lysosomes with the phagosome [291]. *C. glabrata* replication within phagolysosomes was found to be accompanied by an increase in the pH within this structure [291], [294], which ranges between 4.5–5.5, being an acidic environment essential for the activity of hydrolytic enzymes [290]. In fact, when analysing replicating *C. glabrata* macrophages, the internal pH of the phagolysosome was found to be 6.1 [291] and with decreased phagosomal hydrolase activity [294]. Such alteration of pH seems to be due to the presence of *C. glabrata* cells [291], whose mannosyltranferases, such as CgMnn10 and CgMnn11, were found to be necessary for extracellular environment alkalinisation *in vitro* and inside phagolysosomes [294].

This altered environment permits the survival of *C. glabrata* cells and they proliferation, ultimately causing the lysis of the macrophage itself, freeing viable *C. glabrata* cells within the host [291].

3.2.4. *Candida glabrata* Production of Hydrolytic Enzymes

In order to progress in the invasion of host tissues, yeast pathogens often resort to hydrolytic enzymes [295], [296]. Although not particularly recognized by it, *C. glabrata* virulence might also rely on specific enzymes that are secreted upon contact with host tissues to ensure this yeast survival and proliferation. Such enzymes destroy the proteins and lipids of the cell host membranes, leading to membrane dysfunction or rupture [297], or host proteins and lipids of the extracellular matrix of host tissues, improving invasion [295]. Hydrolytic enzymes can be divided into proteinases and phospholipases, according to their target, proteins or lipids, hydrolysing peptide bonds or phospholipids, respectively [297].

Although not as much as *C. albicans*, *C. glabrata* was found to display phospholipase activity. Such hydrolytic activity was found to be present in a higher number of persistent isolates than in non-persistent isolates of candidemia cases [297], which highlights its significance in *C. glabrata* virulence. *C. glabrata* clinical isolates recovered from the oral cavity have also shown to have phospholipase activity [298]. *C. glabrata* isolates recovered from the oral cavity and from blood samples were also found to demonstrate proteinase activity [298], [299]. Berila and colleagues (2011) have further showed that apparently both proteinase and phospholipase activities are present in the majority of the *C. glabrata* clinical isolates they analysed, irrespective of their source [300]. However, other studies appear to contradict these results, showing that the majority of *C. glabrata* recovered isolates did not present proteinase or phospholipase activity [301], [302]. Interestingly, clinical isolates of this pathogenic yeast also display hemolysin production [303]. Hemolysin is a very advantageous feature when it comes to degrade hemoglobin to acquire iron, a very difficult to find element within the human host [13].

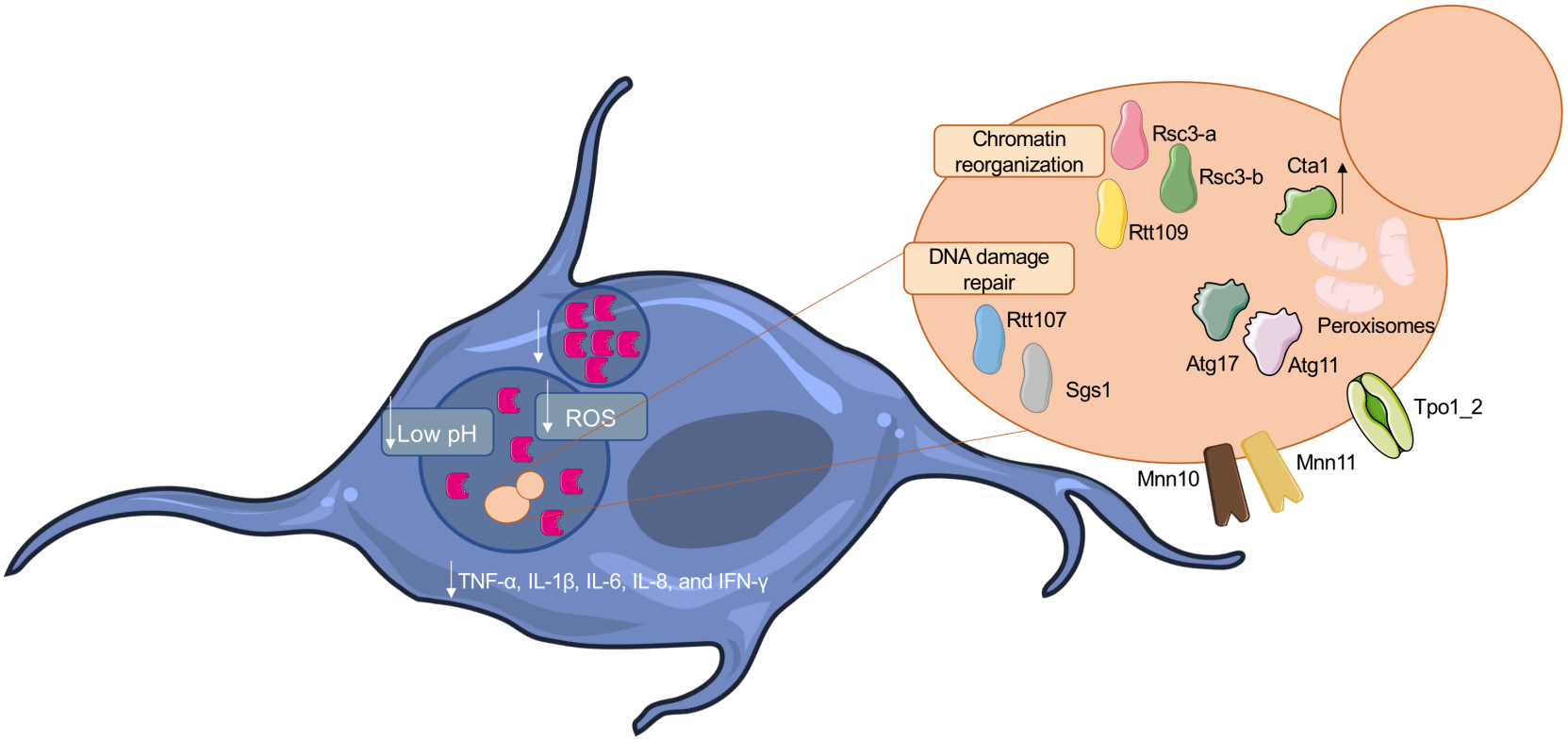

Figure I.8. *Candida glabrata* mechanisms for evading phagocytosis action by macrophages. *C. glabrata* employs mechanisms of chromatin reorganization and DNA damage repair, having essential effectors: Rsc3-a, Rsc3-b and Rtt109, and Rtt107 and Sgs1, respectively; uses the level of peroxisomes together with Atg17 and Atg11 to answer phagolysosomal stress, as well as Cta1 to couple with oxidative stress; and relies on two mannosyltransferases, Mnn10 and Mnn11, for the alkalinisation of the phagolysosome. Such mechanisms allow *C. glabrata* to provoke a decrease in the production of inflammatory cytokines, decrease of acidification, decrease of ROS formation and alters the fusion of lysosomes with the phagosome.

3.2.5. Unexpected Players in *C. glabrata* Virulence

Some virulence features in *C. glabrata* come as a surprise given their absence on the majority of other *Candida* species causing disease. That is the case of the CgAce2 transcription factor responsible for mother and daughter cell separation in *C. glabrata* [304]. CgAce2 is an ortholog of ScAce2, which in *S. cerevisiae* also controls the separation of mother and daughter cells and the expression of early G1-phase genes [305]. This transcription factor was found to be connected to *C. glabrata*'s virulence. Indeed, Δ*cgace2* deletion mutant cells exhibit increased virulence in a murine model of invasive candidiasis [304]. It has been hypothesized that upon the loss of this transcription factor, the abundant display of cytoplasmic proteins on the cell wall leads to an increase of the immunogenicity [137], [306], defined by an elevation of the number of proinflammatory cytokines [304].

Ste12 is another transcription factor found to be necessary for the full virulence of *C. glabrata* in a murine model of systemic candidiasis. Although its role in virulence is not clear, this regulator was found to be necessary for nitrogen starvation induced filamentation [112].

Another interesting feature of *C. glabrata* is pigmentation. Although not much explored, *C. glabrata* has been shown to produce indole pigments: pityriacitrin, malassezia indole, pityriaanhydride and pityriarubin C; in a pigment-induced medium supplemented with tryptophan as the sole source of nitrogen [307]. For the production of indole pigments *C. glabrata* uses the Ehrlich pathway, being indispensable the presence of CgAro8 enzyme, which transforms tryptophan into indole pyruvate. *C. glabrata* pigmented cells were found to exhibit higher virulence than non-pigmented cells. Indole pigments help cells resist the action of neutrophils, as well as the oxidative action of hydrogen peroxide, and increase the capacity of *C. glabrata* to damage human oral epithelial cell line TR146, measured by the activity of released lactate dehydrogenase (LDH) [308]. The pigmentation role in virulence is not that surprising if one considers that other fungal pathogens like *Cryptococcus neoformans*, also use pigments as a virulence factor [309].

3.3. *Candida glabrata* Antifungal Resistance, Virulence and Biofilm Formation Have More in Common Than Meets the Eye

Although usually discussed as separated topics, antifungal resistance, virulence and biofilm formation have been found to share common strategic pathways within fungal pathogens [310]. *C. glabrata* is no exception, having molecular mechanisms found to be behind the development of at least two of these processes (Table I.2).

One of those mechanisms relies on the action of the CgPdr1 transcription factor. As discussed above, CgPdr1 is known as the master regulator of multidrug resistance, controlling the expression of multiple drug efflux pumps. GOF mutations on this transcription factor were found to not only enhance resistance, but also to increase virulence, augmenting tissue colonization in the kidney, spleen and liver of infected mice [224]. The increased virulence found in the colonization of bladder and kidney in a murine model of urinary tract infection, due to CgPdr1 GOF mutations, were found to be connected with the increased expression of *CgEPA1* gene [228]. In turn, CgEpa1 adhesin is an essential player in

C. glabrata biofilm formation, especially in the first step, adhesion, contributing for hydrophilic and hydrophobic interactions [143], [311], [312]. In fact, just like CgEpa1, CgEpa3 is involved in adhesion and biofilm formation [75], [313] and when the *EPA1-3* cluster is deleted, *C. glabrata* virulence in a systemic infection mouse model becomes compromised [80]. Interestingly, CgEpa2 was also implicated in the ability of *C. glabrata* to resist oxidative stress [278].

Meanwhile, different GOF mutations on CgPdr1 were also found to increase the expression of *CgPUP1* gene, encoding a mitochondrial protein, and *CgCDR1* gene, encoding an important multidrug resistance transporter [227]. Deletion of both these genes in an azole resistant isolate was found to lead to a decrease in virulence in mice injected intravenously, with less kidney colonization and tissue burden, comparatively to the initial isolate. In addition, their deletion also resulted in decreased antifungal resistance, indicating the full connection between the two processes in *C. glabrata* [227].

Another mechanism generally associated with increase antifungal resistance is the loss of mitochondrial function. Nevertheless, mitochondrial defects have been found to be associated with changes in the virulence of *C. glabrata*. Brun and colleagues, (2005), have induced the formation of *C. glabrata petite* mutants, whose loss of mitochondrial function was accompanied with decreased virulence against a murine model of systemic infection, comparatively to the parental strains [314]. On the other hand, a *petite* mutant was found to have increased virulence in systemic and vaginal murine infection models, while being azole resistant due to the upregulation of CgCdr1, CgCdr2 and CgSnq2 ABC transporters [239]. Although both studies show different results regarding the virulence of *petite* mutants, mitochondrial defects clearly have influence over *C. glabrata* virulence. Interestingly, downregulation of mitochondrial activity is also observed in cells within *C. glabrata* biofilms, once they become exposed to fluconazole [242]. Nevertheless, such downregulation has already been described to happen during normal maturation of *C. albicans* biofilms [315].

Biofilm formation was recently found to rely on different MFS transporters in *C. glabrata*: CgTpo4, CgDtr1, CgQdr2 and CgTpo1_2 [143], [316], [317]. The absence of these transporters was found to significantly decrease the ability of this pathogenic yeast to form biofilms [316]. CgTpo1_2 has been implicated in the virulence of *C. glabrata*, being necessary for the survival of this pathogenic yeast upon phagocytosis [143], as well as for azole resistance [144]. On the other hand, as described above, CgQdr2 is an important player in azole resistance [219]. Such studies give evidence of the importance of MFS transporters in the three main processes behind the success of *C. glabrata* infections.

Calcineurin is a Ca^{2+}-calmodulin activated protein phosphatase 2B, which consists in two subunits: with a catalytic A subunit and a Ca^{2+}-binding regulatory B subunit. This phosphatase is responsible for the control of intracellular calcium homeostasis. Calcium is a vital secondary messenger for most cellular processes in fungi [318], [319]. Calcineurin has been shown to be essential for crucial processes in *C. glabrata*, like plasma membrane integrity and ER stress response, growth at human host temperature (37ºC) and pH homeostasis [43]. Calcineurin, as well as the CgCzr1 transcription factor, which is activated by its action, are needed for full virulence in murine systemic and ocular infection models, but only calcineurin was found to be necessary for *C. glabrata* infection of a murine urinary tract infection model [43]. In addition, at least one of the calcineurin mutants for either subunit were found to be susceptible to different antifungal drugs: fluconazole, posaconazole, ketoconazole,

itraconazole, miconazole, voriconazole micafungin, caspofungin and anidulafungin [43], [319]. Recovered azole tolerance is observed upon the complementation of the deletion mutant with *CgCNB1* gene [319]. In turn, the absence of *CgCZR1* gene was found to affect more azole resistance than echinocandin resistance [43]. Interestingly, the use of a psychotic drug, fluphenazine, known to be a calmodulin antagonist, which makes impossible its connection with calcineurin for the activation of CgCzr1 regulator, was found to have a significant effect decreasing *C. glabrata* biofilm formation together with caspofungin [320]. The decrease of virulence and antifungal resistance was also observed upon the use of both drugs [320], indicating a very important role of the calcineurin pathway in all of these processes in *C. glabrata*. In fact, in the study of Schwarzmüller and colleagues (2014), the deletion of 14 genes was found to decrease biofilm formation in *C. glabrata*, being *CgCNB1* one of those genes, highlighting its importance, not only in virulence and antifungal resistance, but also in biofilm formation [321]. Given the wide importance of calcineurin in *C. glabrata*, it constitutes a valuable new drug target, with both non-azole ergosterol biosynthesis inhibitors and calcineurin inhibitors being shown to act synergistically, against *C. glabrata*, *C. albicans* and *C. krusei* [322].

There are two endogenous regulators of calcineurin, CgRcn1 and CgRcn2. The first participates in the activation and repression of the calcineurin pathway while CgRcn2 only displays action in the inhibition of the pathway. By stimulating the calcineurin pathway, CgRcn1 leads to the activation of CgCzr1. CgRcn1 was found to also have a role in antifungal resistance in *C. glabrata*. Deletion of *CgRCN1* gene resulted in decrease resistance towards micafungin and fluconazole, while its reintroduction resulted in the recovery of the wild-type phenotype [323].

A putative calcium channel, Cch1-Mid1, has been linked to the ability of *C. glabrata* to resist fluconazole exposure. In yeast, Cch1 is an N-glycosylated integral membrane protein, being the catalytic subunit of the channel, while Mid1 is believed to be a regulatory subunit required for the function of the catalytic subunit. Insertions in *CgCCH1* and *CgMID1* genes lead to increased susceptibility to fluconazole and defective calcium uptake [324]. Interestingly, deletion of *CgCCH1* gene also decreases the ability of *C. glabrata* to form biofilms [321], turning CgCch1 as an important player in azole resistance and biofilm formation.

CgIre1 is a kinase/endoribonuclease that, together with calcineurin and CgSlt2, from the mitogen-activated protein kinase (MAPK) signaling pathway, has the function of activating the unfolded protein response (UPR). CgIre1 interacts with unfolded proteins in the ER, leading to the activation of stress responsive genes. The absence of *CgIRE1* gene was found to decrease the mortality of cyclophosphamide-immunosuppressed mice, and lower fungal burden in the kidney and spleen in a mouse model of disseminated candidiasis [44]. In turn, CgSlt2, which is also involved in cell wall integrity, was found to be necessary for the normal production of chitin and for resistance to caspofungin in *C. glabrata* [325]. Just like calcineurin, CgSlt2 was found to be necessary for the full virulence of *C. glabrata* in a mouse model of disseminated candidiasis [326], highlighting the importance of all these three players, calcineurin, Ire1 and Slt2, in virulence and antifungal resistance in this pathogenic yeast.

The ability of *C. glabrata* to respond to oxidative stress has been found to be necessary for its virulence, but also for biofilm formation. The unique catalase of *C. glabrata*, CgCta1, is regulated by CgYap1, CgSkn7, CgMsn2 and CgMsn4 transcription factors that have important roles in in stress

responses [40]. CgSkn7 has been found to be essential for resistance to oxidative stress, being responsible for activating, upon hydrogen peroxide exposure, *CgTRX2, CgTRR1, CgTSA1* and *CgCTA1* genes encoding important players in the oxidative stress response [327]. Upon the loss of *CgSKN7* gene, *C. glabrata* was found to have decreased virulence in a murine model of disseminated candidiasis [327] and to have decreased capacity to form biofilms [321]. Another transcription factor involved in the response to stress is CgSte20. This transcription factor is involved in the adaptation to hypertonic stress and participates in the maintenance of the cell wall integrity [328]. The absence of *CgSTE20* gene has been found to attenuate the virulence of *C. glabrata* in a model of murine candidiasis [328], and to increase the formation of biofilms [321].

The plasticity of *C. glabrata* genome is by itself a mechanism through which both virulence and antifungal resistance may be enhanced. The formation of new chromosomes in *C. glabrata* happens by the duplication of chromosome segments carrying a centromere, with the subsequent addition of new telomeric ends [329]. The study of Bader and colleagues (2012) shows how specific karyotypic changes may occur in the *C. glabrata* genome, allowing this species to adapt to a different environment. Genomic changes have been found to underlie different cell surface properties, leading to differential resistance to caspofungin [330]. Other studies on *C. glabrata* clinical isolates have highlighted the association of new formed chromosomes with antifungal resistance and virulence. The segments duplicated were found to have the sequence of important genes in antifungal resistance, such as *CgCDR1* and *CgCDR2*, and in virulence, such as several YPS genes and the *CAGL0E02321g* gene, encoding a putative phospholipase B [329], [331].

Overall, antifungal resistance and virulence seem to find themselves in the crossroad for successful infections of *C. glabrata*. All the mechanisms found to enhance both processes in this pathogenic yeast together with the mechanisms of biofilm formation, highlight the potential of this yeast as a pathogen within the human host. The information gathered herein gives evidence of the molecular mechanisms that *C. glabrata* resorts to and that should be thus considered when developing future therapeutic strategies.

Table I.2. *Candida glabrata* common molecular mechanisms and effectors involved in at least two of the main processes used by this yeast to succeed in the human host: antifungal resistance, virulence and biofilm formation.

***Candida glabrata* Common Molecular Mechanisms and Effectors Involved in the Main Processes**				
		Antifungal Resistance	**Virulence**	**Biofilm Formation**
GOF Mutations Pdr1 Transcription Factor		Activation of MDR transporters	Activation of Epa1 adhesin, increase of tissue colonization in the kidney, bladder, spleen and liver of infected mice	Activation of Epa1 adhesin
Epa1 Adhesin		-	Necessary for full virulence in a murine model of urinary tract infection, increase of tissue colonization in the kidney, bladder, spleen and liver of infected mice	Participates in the first step of biofilm formation, adhesion
Cdr1 ABC Transporter		Efflux of antifungal drugs	Necessary for full virulence in mice injected intravenously, increase of kidney colonization and tissue burden	-
Pup1 Mitochondrial Protein		Necessary for azole resistance	Necessary for full virulence in mice injected intravenously, increase of kidney colonization and tissue burden	-
Loss of Mitochondrial Function		Upregulation of CgCdr1, CgCdr2 and CgSnq2 ABC transporters	Contradictory results of virulence in murine model of systemic infection but increase of virulence in a vaginal murine infection model	Observed in biofilms exposed to fluconazole, might be connected to the maturation of the biofilm
Qdr2 MFS Transporter		Efflux of azole drugs	-	Necessary for biofilm formation
Tpo1_2 MFS Transporter		Efflux of azole drugs	Necessary for the survival upon phagocytosis	Necessary for biofilm formation
Calcium-Calcineurin Pathway	Calcineurin	Necessary for azole and echinocandin resistance	Necessary for full virulence in murine systemic, ocular and urinary tract infection models, essential for plasma membrane integrity and ER stress response, growth at human host temperature (37˚C) and pH homeostasis	Necessary for biofilm formation
	Czr1 Transcription Factor	Necessary for azole resistance	Necessary for full virulence in murine systemic and ocular infection models	-
	Rcn1	Necessary for micafungin and fluconazole resistance	Activation of Czr1 transcription factor	-
	Calmodulin	Necessary for caspofungin resistance	Necessary for full virulence in *Galleria mellonella* model of infection	Necessary for biofilm formation
	Cch1 Putative Calcium Channel Subunit	Necessary for fluconazole resistance	-	Necessary for biofilm formation
Slt2 MAPK Signalling Pathway		Necessary for cell wall integrity and chitin production for caspofungin resistance	Necessary for full virulence in a mouse model of disseminated candidiasis	-
Skn7 Transcription Factor		-	Necessary for full virulence in a mouse model of disseminated candidiasis, activates Cta1 for the oxidative stress response	Necessary for biofilm formation
Ste20 Transcription Factor		-	Necessary for full virulence in a model of murine candidiasis, participates in the adaptation to hypertonic stress and maintenance of the cell wall integrity	Negative regulator of biofilm formation
Karyotypic Changes in the Genome		Duplication of *CDR1* and *CDR2* genes increases antifungal resistance, increase of caspofungin resistance	Duplication of several YPS genes and *CAGL0E02321g* gene, encoding a putative phospholipase B, increases virulence	-

4. Thesis Outline

Candida glabrata infections have increased in recent years due to the increase of immunocompromised patients and the extensive use of antifungal drugs for treatment and prophylaxis. This pathogenic yeast is well-known for its fast acquisition of resistance against such antifungal drugs and for its capacity to form biofilms in indwelling devices, which are very hard to eradicate. Antifungal resistance and pathogenesis, characteristics of this species, result at times in the failure of all available therapeutic solutions, which ultimately leads to high mortality rates. In order to surpass this problematic, an in-depth knowledge of the molecular mechanisms *C. glabrata* employs to persist in the human host is thus necessary. Only by achieving such goal, it will be possible to design new therapeutic strategies.

This thesis is focused on this problematic, starting in Chapter I, by describing *C. glabrata* as an opportunistic pathogen, following an introduction of the main molecular mechanisms of biofilm formation in *Candida* species, adapted from a review paper published in 2018. In addition, Chapter I addresses the main molecular mechanisms of antifungal resistance and virulence developed by *C. glabrata,* ending with the description of the main motivation and outline of this thesis.

Chapter II is composed by the study of two new transcription factors, CgEfg1 and CgTec1, found to regulate biofilm formation in *C. glabrata*. The role of these transcription factors in the adhesive properties of *C. glabrata* towards medically relevant surfaces and the transcriptome changes occurring from planktonic growth to mature biofilm development are analysed. Two new MFS transporters, CgDtr1 and CgTpo4, are also characterized in this Chapter, found to have roles in biofilm formation and virulence in *C. glabrata*. This Chapter englobes one published paper and two submitted ones.

Given that the development of new therapeutic strategies should rely not only in fighting biofilm formation and virulence, but also tackle antifungal resistance, evidences of new players in this process are presented in Chapter III. Two cell peripheral proteins, CgEpa3 and CgPil1, with roles in biofilm formation are described in this chapter for conferring resistance to azole drugs, a discovery resulting from an *in vitro* evolution of an azole susceptible clinical isolate towards azole resistance. This Chapter is comprised by one published paper and another in preparation.

Chapter IV discusses all the results presented in this work, highlighting the integration between different molecular mechanisms that cross-talk to favour biofilm formation, antifungal resistance and virulence, and provides a perspective on how this knowledge may be used to improve the success of current therapeutic approaches towards the effective eradication *C. glabrata* infections.

II. *Candida glabrata* biofilm formation: new regulators and effectors of a complex process

Journal papers

Mafalda Cavalheiro, Diana Pereira, Carolina Leitão, Pedro Pais, Easter Ndlovu, Andreia I. Pimenta, Rui Santos, Azusa Takahashi-Nakaguchi, Michiyo Okamoto, Mihaela Ola, Hiroji Chibana, Arsénio M. Fialho, Geraldine Butler, Etienne Dague, Miguel Cacho Teixeira, From the first touch to biofilm establishment by the human pathogen *Candida glabrata*: a genome-wide to nanoscale view (in review in Communications Biology).

Daniela Romão, Mafalda Cavalheiro, Dalila Mil-Homens, Rui Santos, Pedro Pais, Catarina Costa, Azusa Takahashi-Nakaguchi, Arsénio M. Fialho, Hiroji Chibana and Miguel C. Teixeira, A New Determinant of *Candida glabrata* Virulence: The Acetate Exporter CgDtr1. Front. Cell. Infect. Microbiol. 7:473. doi: 10.3389/fcimb.2017.00473, 2017.

Mafalda Cavalheiro, Daniela Romão, Rui Santos, Dalila Mil-Homens, Pedro Pais, Catarina Costa, Mónica Galocha, Diana Pereira, Azusa Takahashi-Nakaguchi, Hiroji Chibana, Arsénio M. Fialho, Miguel C. Teixeira, Role of CgTpo4 in polyamine and antimicrobial peptide resistance: determining virulence in *Candida glabrata* (submitted to Scientific Reports).

1. From the first touch to biofilm establishment by the human pathogen *Candida glabrata*: a genome-wide to nanoscale view

1.1. Abstract

Candida glabrata is an opportunistic pathogen that adheres to human epithelial mucosa and forms biofilm to cause persistent infections. In this work, Single-cell Force Spectroscopy (SCFS) was used to glimpse at the adhesive properties of *C. glabrata* as it interacts with clinically relevant surfaces, the first step towards biofilm formation. Following a genetic screening, RNA-sequencing revealed that half of the entire transcriptome of *C. glabrata* is remodelled upon biofilm formation, around 40% of which under the control of the transcription factors CgEfg1 and CgTec1. Using SCFS, it was possible to observe that CgEfg1, but not CgTec1, is necessary for the initial interaction of *C. glabrata* cells with both abiotic surfaces and epithelial cells, while both transcription factors orchestrate biofilm maturation. Overall, this study characterizes the network of transcription factors controlling massive transcriptional remodelling occurring from the initial cell-surface interaction to mature biofilm formation.

1.2. Introduction

The use of medical devices has increased over the years, driven by the necessity to improve the quality of life and by the fast development of new technology [57]. Although bringing enormous advantages, medical devices also have a dark side related to the emergence of microbial infections [57], [332], [333]. Medical devices, once inserted in the human host, provide a favourable surface in which microorganisms may develop biofilms, giving rise to persistent colonization and, often, a very hard to eradicate source of infection [334]. Once the biofilm is formed on such devices, disseminated cells can move to other host niches, and just as well originate new biofilms [335].

Candida glabrata is an opportunistic pathogen that is able to use such surfaces to form biofilms and prevail in the human host [31], [335], [336]. It is considered the second most common cause of candidiasis [17], [18], being associated to both invasive disseminated infections as well as oral, esophageal or vulvovaginal candidiasis [8]–[11]. *C. glabrata* is able to adhere to abiotic surfaces like polyvinyl chloride, polyurethane, polystyrene, silicone, Teflon and denture acrylic surfaces [31], [66], [75], [93], [337], [338], but it is as well able to adhere to different epithelial cells, like the human cultured epithelial cells HEp2 [264] or the human vaginal epithelial cell line VK2/E6E7 [313].

Adhesion is a complex interplay between physico-chemical interactions (hydrophobicity, electrostatic interactions) and adhesin-mediated interactions. Adhesins are GPI-CWPs divided into seven subfamilies based on the phylogenetic analysis of their putative N-terminal ligand-binding regions [78], [271]. The most studied *C. glabrata* family of adhesins is the EPA family, given the importance of its 17 members in the adherence of this fungal pathogen [78]. The cellular proliferation and production of an ECM gives continuation to *C. glabrata* biofilm formation, in a thick structure of yeast cells that exhibits higher resistance to antifungal drugs than planktonic cells [35], [145], being the perfect niche for the protection of *C. glabrata* cells.

In this work, *C. glabrata*'s ability to adhere to different clinically-relevant surfaces was assessed by SCFS, revealing the forces established between *C. glabrata* and plastic surfaces used in medical devices, but also the ability to establish interactions with human vaginal epithelial cells (VK2/E6E7 cell line). From a screening of potential transcription factors involved in the control of biofilm formation, only two were found to be necessary for adhesion to human vaginal epithelial cells and biofilm formation in *C. glabrata*: CgEfg1 and CgTec1. Given their relevance on biofilm formation, the study of the transcriptomic remodelling occurring in *C. glabrata* cells from planktonic cultivation to 24h of biofilm formation, in the presence or absence of *CgEFG1* or *CgTEC1* genes, was pursuit through RNA-sequencing (RNA-seq). In order to assess the importance of CgEfg1 and CgTec1 at the scale of cell-surface molecular interactions, SCFS was used to measure how the expression of *CgEFG1* and *CgTEC1* modulate the interaction forces between *C. glabrata* and clinically-related surfaces.

1.3. Methods

1.3.1. Strains and Growth Medium

Candida glabrata CBS138, KUE100 [339] and L5U1 (cgura3Δ0 cgleu2Δ0) [340] strains, the later kindly provided by John Bennett, NIAID, NIH, Bethesda, were used in this study. Cells were batch-cultured at 30 ºC with orbital agitation (250 rpm) in the following growth media. Yeast extract Peptone Dextrose (YPD) growth media, containing per liter: 20 g glucose (Merck), 10 g yeast extract (Difco) and 20 g bacterial-peptone (LioChem). BM minimal growth medium contained per liter: 20 g glucose (Merck); 2.7 g $(NH_4)_2SO_4$ (Merck); 1.7 g yeast nitrogen base without amino acids or $(NH_4)_2SO_4$ (Difco). Sabouraud's dextrose broth (SDB) contained 40 g glucose (Merck) and 10 g peptone (LioChem) per liter.

The VK2/E6E7 human epithelium cell line (ATCC® CRL-2616™) was used for adhesion assays. This cell line is derived from the vaginal mucosa of healthy premenopausal female submit to vaginal repair surgery and immortalized with human papillomavirus 16/E6E7. Cells maintenance was achieved with Keratinocyte Serum Free (KSF) medium, containing 0.1 ng/mL human recombinant epidermal growth factor (EGF), 0.05 mg/mL bovine pituitary extract and additional 44.1 mg/L calcium chloride. Cells were maintained at 37 °C, with 95% air and 5% CO_2.

1.3.2. Cloning of the *C. glabrata CgEFG1* and *CgTEC1* genes (ORF *CAGL0M07634g* and *CAGL0M01716g*)

The pGREG576 plasmid from the Drag & Drop collection [341] was used to clone and express the *C. glabrata* ORF *CAGL0M07634g* and *CAGL0M01716g* in *S. cerevisiae*, as described before for other heterologous genes [342]. pGREG576 was acquired from Euroscarf and contains a galactose inducible promoter (*GAL1*) and the yeast selectable marker *URA3*. The *CgEFG1* and *CgTEC1* genes were generated by polymerase chain reaction (PCR), using genomic DNA extracted from the sequenced CBS138 *C. glabrata* strain, with the primers present in Supplementary Table SII.1. To enable expression of the *CgTEC1* gene in *C. glabrata*, the *GAL1* promoter was replaced by the constitutive *PDC1*

C. glabrata promoter, while for *CgEFG1* the replacement was performed using the copper-induced *MT-I C. glabrata* promoter. The *PDC1* and *MT-I* promoters DNA was generated by PCR, using the primers in Supplementary Table SII.1. The recombinant plasmids pGREG576_*CgEFG1,* pGREG576_*CgTEC1,* pGREG576_*MT-I_CgEFG1* and pGREG576_*PDC1_CgTEC1* were obtained through homologous recombination in *S. cerevisiae* and verified by DNA sequencing.

1.3.3. Disruption of the *C. glabrata CgEFG1* and *CgTEC1* genes (ORF *CAGL0M07634g, CAGL0M01716g).*

The deletion of the *CgEFG1* and *CgTEC1* genes was carried out in the parental strain KUE100, using the method described by [339]. The target genes were replaced by a DNA cassette including the *CgHIS3* gene, through homologous recombination. The pHIS906 plasmid including *CgHIS3* was used as a template and transformation was performed as described previously [339]. Recombination locus and gene deletion were verified by PCR using the primers indicated in Supplementary Table SII.1.

1.3.4. Biofilm Quantification

C. glabrata strains were tested regarding their capacity to form biofilm on a polystyrene surface, recurring to the PrestoBlue Cell Viability assay. For that, the *C. glabrata* strains were grown in SDB (pH 5.6) medium and harvested by centrifugation at mid-exponential phase. The cells were inoculated with an initial Optical Density at 600nm (OD_{600nm}) = 0.05±0.005 in 96-well polystyrene microtiter plates (Greiner) in SDB (pH 5.6) medium. Cells were cultivated at 30 ºC during 24±0.5 h with mild orbital shaking (70 rpm). After the incubation time, each well was washed two times with 100 µL of sterile phosphate-buffered saline (PBS) pH 7.4 (PBS contained per liter: 8 g NaCl (Panreac), 0.2 g KCl (Panreac), 1.81 g $NaH_2PO_4{\cdot}H_2O$ (Merck), and 0.24 g KH_2PO_4 (Panreac), to remove the cells unattached to the formed biofilm. Then, Presto Blue reagent was prepared in a 1:10 solution in the medium used for biofilm formation, adding 100 µL of the solution to each well. Plates were incubated at 37 ºC for 30 min. Afterwards, absorbance reading, at the wavelength of 570 nm and 600 nm for reference, was determined in a microplate reader (SPECTROstar Nano, BMG Labtech).

1.3.5. Human vaginal epithelial cell adherence assay

For the adhesion assays, VK2/E6E7 human epithelium cells were grown and inoculated in 24-well polystyrene plates (Greiner) with a density of $2.5x10^5$ cell/mL a day prior to use. Additionally, *C. glabrata* cells were inoculated with an initial OD_{600nm} = 0.05±0.005, cultivated at 30 ºC, during 16±0.5 h, with orbital shaking (250 rpm) in YPD medium. In order to initiate the assay, the culture medium of mammalian cells was removed and substituted by new culture medium, in each well, and, subsequently, *C. glabrata* cells were added to each well, with a density of $12.5x10^5$ Colony Forming Units (CFU)/well, corresponding to a multiplicity of infection (MOI) value of 10. Then, the plate was incubated at 37 °C, 5% CO_2, for 30 min. Afterwards, each well was wash 3 times with 500 µL of PBS pH 7.4, following the addition of 500 µL of Triton X-100 0.5% and incubation at room temperature for 15 min. The cell

suspension in each well was then recovered, diluted and spread onto agar plates to determine CFU count, which represent the proportion of adherent cells to the human epithelium.

1.3.6. RNA sample extraction and preparation

Cells were grown in SDB (pH 5.6) medium. Planktonic cells were cultured at 30 ºC with orbital agitation (250 rpm), while biofilm cells were cultured at 30 ºC, in square Petri dishes, with orbital agitation (30 rpm). Total RNA was extracted from wild-type and single deletion mutant cells during planktonic exponential growth and upon 24 h of biofilm growth. Total RNA was isolated using an Ambion Ribopure-Yeast RNA kit, according to manufacturer's instructions.

1.3.7. RNA-sequencing of *C. glabrata* cells in planktonic and biofilm conditions

Strand specific RNA-seq library preparation and sequencing was carried out as a paid service by the NGS core from Oklahoma Medical Research Foundation, Oklahoma City, Oklahoma, USA. Prior to RNA-seq analysis, quality control measures were implemented. Concentration of RNA was ascertained via fluorometric analysis on a Thermo Fisher Qubit fluorometer. Overall quality of RNA was verified using an Agilent Tapestation instrument. Following initial QC steps sequencing libraries were generated using the Illumina Truseq Stranded Total RNA library prep kit with ribosomal depletion via RiboZero Gold according to the manufacturer's protocol. Briefly, ribosomal RNA was depleted via pull down with bead-bound ribosomal-RNA complementary oligomers. The RNA molecules were then chemically fragmented and the first strand of cDNA was generated using random primers. Following RNase digestion, the second strand of cDNA was generated replacing dTTP in the reaction mix with dUTP. Double stranded cDNA then underwent adenylation of 3' ends following ligation of Illumina-specific adapter sequences. Subsequent PCR enrichment of ligated products further selected for those strands not incorporating dUTP, leading to strand-specific sequencing libraries. Final libraries for each sample were assayed on the Agilent Tapestation for appropriate size and quantity. These libraries were then pooled in equimolar amounts as ascertained via fluorometric analyses. Final pools were absolutely quantified using qPCR on a Roche LightCycler 480 instrument with Kapa Biosystems Illumina Library Quantification reagents. Sequencing was performed on an Illumina HiSeq 3000, producing 2x150 bp paired-end reads, 2 GB clean data, yielding 52 M reads per sample. Paired-end reads were obtained from wild-type (*Candida glabrata* KUE100) and correspondent deletion mutant strains Δ*cgefg1* and Δ*cgtec1* (*CAGL0M07634g* and *CAGL0M01716g,* respectively). Two replicates of each sample were obtained from three independent RNA isolations, subsequently pooled together. Samples reads were trimmed using Skewer [343] and aligned to the *C. glabrata* CBS138 reference genome, obtained from the *Candida* Genome Database (CGD) [344], using TopHat [345]. HTSeq [346] was used to count mapped reads per gene. Differentially expressed genes were identified using DESeq2 [347] with an adjusted p-value threshold of 0.01 and a $\log_2$ fold change threshold of -1.0 and 1.0. Default parameters in DESeq2 were used. Significantly differentially expressed genes were clustered using hierarchical clustering in R [348]. *C. albicans* and *S. cerevisiae* homologs were obtained from the CGD and

Saccharomyces Genome Database (SGD) [349], respectively. **Accession number.** The data sets were deposited at the Gene Expression Omnibus, NCBI database, with the reference number GSE140427.

1.3.8. Transcriptomic analysis

The RNA-sequencing analysis provided three datasets: wild-type in planktonic growth vs wild-type biofilm growth; Δ*cgefg1* vs wild-type upon biofilm growth; and Δ*cgtec1* vs wild-type upon biofilm growth. The genes of each dataset were submitted to several analyses using different databases and bioinformatic tools, so they could be grouped according to their biological functions. This was accomplished mainly by resorting to the description of the *C. glabrata* genes found on the CGD (http://www.candidagenome.org). The uncharacterized genes were clustered based on the description of ortholog genes in *S. cerevisiae* or in *C. albicans*, according to the SGD or in CGD, respectively. Go-Stats from GoToolBox web server [350] allowed the determination of the main Gene Ontology (GO) terms to which the genes were related. From this organization, several genes related to cell adhesion were chosen for the following gene expression analysis.

1.3.9. Single gene expression analysis

The levels of *CgPWP5, CgAED2* and *CgAWP13* transcripts in the KUE100 wild-type, Δ*cgefg1* and Δ*cgtec1* deletion mutant cells upon 6 h, 24 h and 48 h of biofilm formation on polystyrene surface and planktonic conditions, were assessed by quantitative real-time (RT)-PCR. Cells were grown in SDB (pH 5.6) medium. Planktonic cells were cultured at 30 ºC with orbital agitation (250 rpm), while biofilm cells were cultured at 30 ºC, in square Petri dishes, with orbital agitation (30 rpm). Total RNA was extracted from planktonic and biofilm conditions (6 h, 24 h and 48 h of biofilm formation). Synthesis of cDNA for real time RT-PCR experiments, from total RNA samples, was performed using the MultiscribeTM reverse transcriptase kit (Applied Biosystems), following the manufacturer's instructions, and using 10 ng of cDNA per reaction. The RT-PCR step was carried out using NZY qPCR Green Master Mix (2x) (NZYTECH). Primers for the amplification of the *CgPWP5, CgAED2, CgAWP13* and *CgACT1* cDNA were designed using Primer Express Software (Applied Biosystems) (Supplementary Table SII.1). The RT-PCR reactions were conducted in a thermal cycler block (7500 Real-Time PCR System - Applied Biosystems). The *CgACT1* mRNA level was used as an internal control as before [219].

1.3.10. Single-cell force spectroscopy

For the interaction of *C. glabrata* strains with plastic surfaces and human vaginal epithelial cells, SCFS was implemented. Yeast cell probes were prepared by adding stationary-phase *C. glabrata* cells to the petri dish with the plastic materials attached by glue or to the petri dish with prepared epithelial cells. Triangular shaped tipless cantilevers (NP-O10, Microlevers, Bruker Corporation) were coated with concanavalin A (conA). For the coating, the cantilevers were immersed overnight in 100 µg/mL of conA solution and washed in acetate buffer pH 5.2 before use. Single yeast cells placed on the petri dish were attached onto the conA-coated cantilevers using Nanowizard III AFM (Bruker, JPK BIOAFM),

approaching the cantilever onto a single cell for 30 s. Interaction of *C. glabrata* cells with plastic surfaces was followed with force measurements at room temperature (25 ºC), under acetate buffer pH 5.2. For the interaction of *C. glabrata* cells with human vaginal epithelial cells, Nanowizard III AFM equipped with CellHesion module (Bruker, JPK BIOAFM) was used and VK2/E6E7 cells ($7x10^4$) were platted on a petri dish under the KSF culture medium, at 37 °C, with 95% air and 5% CO_2 to grow overnight. Single-cell measurements were conducted under this environment thanks to the petri dish heater (Bruker, JPK BIOAFM). The nominal spring constant (Kc) of the cantilevers used for the interaction with the plastic surfaces was approximately 0.35 N/m, and 0.06 N/m for the cantilevers used to measure interactions between yeast and epithelial cells. The cantilevers were all calibrated. Their sensitivity ranged from ~14 to 30 nm/V and their spring constants, determined by the thermal noise method, were in agreement with the manufacturer: the Kc ranged from 0.03 to 0.12 for the nominal 0.06 N/m and 0.175 to 0.7 for the nominal 0.35 N/m. Several force-distance curves were recorded for an area of 10 µm x 10 µm of the plastic surface and applied force of 1 nN, and with an area of 3 µm x 3 µm of the epithelial cell and applied force of 0.5 nN. Cell probes were approached and retracted to the plastic surfaces with a speed of 5 µm/s and a contact time of 0 s, 0.5 s, 1 s and 5 s and to the human vaginal epithelial cells with a speed of 20 µm/s and 5 s, 10 s, 30 s and 60 s of contact time. At least 5 yeast cells, from at least 3 independent cultures, were immobilized on the cantilever for the interaction of each material, and at least 4 yeast cells, from at least 3 independent cultures, were immobilized on the cantilever for the interaction with epithelial cells. Adhesion force, work of adhesion, rupture distance, number of jumps and tethers histograms were obtained by calculating the maximum adhesion peak, the area under the curve, the last rupture distance and counting the number of jumps and tethers for each force-distance curve. 256, 100 and 25 force-distance curves were recorded for the interaction with the materials, with 0 s, 0.5-1 s and 5 s, respectively, and 64 and 16 force-distance curves were recorded for the interaction with epithelial cells, with 5 and 10 s, and 30 s and 60 s, respectively.

1.3.11. Atomic force microscopy (AFM)

Topographic images of VK2/E6E7 epithelial cells were obtained using the Nanowizard III AFM (JPK Instruments) coupled with an axiovert microscope from Zeiss with QI™ mode. VK2/E6E7 cells ($7x10^4$) were platted on a petri dish under the KSF culture medium, at 37 °C, with 95% air and 5% CO_2 to grow overnight, following imaging under this environment. MLCT cantilevers (Bruker probes) with a spring constant of 0.012 N/m were used. The cantilevers spring constants were determined by the thermal noise method. QI™ settings used are the following: Z-length: 3 µm; applied force: 4 nN; speed: 150 µm/s. JPK data processing (JPK Instrument, Berlin, Germany) software was used for image processing as described before [351].

1.4. Results

1.4.1. *C. glabrata* is strongly adherent to plastic surfaces used in medical devices

Given the importance of adhesion as the first step of biofilm formation, the interaction forces established between a single KUE100 *C. glabrata* cell and glass, polystyrene, silicone elastomer and polyvinyl chloride were quantified. To do so, a noninvasive technique was used, SCFS, with tipless cantilevers coated with conA to immobilize a single *C. glabrata* cell. Each cell probe was slowly approached towards the surface material, for different periods of time: 0 s, 0.5 s, 1 s and 5 s; and withdrawn at constant speed. The cell probes and surfaces were kept submersed in acetate buffer, pH 5.2, for all the experiments. 256 force-distance curves were recorded according to a 10x10 μm^2 force map, between the *C. glabrata* KUE100 single-cell probes and the different materials.

C. glabrata interaction with each surface was studied based on the maximum adhesion force, work of adhesion and rupture distance measured on the force-distance curves and plotted as repartition histograms. The maximum adhesion force measured corresponds to the maximum adhesion force felt during the entire interaction, the work of adhesion consists in the complete set of forces establish during the interaction (area under the retraction force-distance curve) and the rupture distance is the distance from the contact point to the last force establish during interaction. The mean value and their standard deviation were extracted from a gaussian fit.

Interaction forces between a yeast cell and glass show a maximum adhesion force of about 1 nN (Figure II.1a), work of adhesion of $6.58x10^{-16}$ J (Figure II.1b) and rupture distance of approximately 1.2 µm (Figure II.1c). The representative force-distance curve for the interaction with glass is depicted in Figure II.1d (black line), showing a small peak of adhesion and an elongation before the rupture. The adhesion of *C. glabrata* to other hydrophobic surfaces was further tested, using currently used medical materials, namely polystyrene, silicone elastomer and polyvinyl chloride [31], [93], [352]. The values of maximum adhesion force towards polystyrene, silicone elastomer and polyvinyl chloride obtained where ~14 nN, ~10 nN, ~19 nN, respectively. All of these *C. glabrata*-material interactions are significantly more adhesive than towards glass (Figures II.1a and II.1b), although no differences are observed in terms of rupture distance (Figure II.1c). The representative force-distance curves show very high peaks of adhesion with small elongation before the rupture of the interaction, suggesting that mainly non-specific interactions, like hydrophobic or electrostatic [353], [354], are at play when a *C. glabrata* cell adheres to polystyrene, silicone elastomer or polyvinyl chloride (Figure II.1d red, blue and green, respectively). Moreover, an adhesion frequency of 100% was observed for *C. glabrata* interaction with all the abiotic surfaces tested.

Increasing the contact time of the yeast cell and surface from 0 s to 0.5 s, 1 s or 5 s is accompanied by an increase in maximum adhesion force and work of adhesion (Supplementary Figure SII.1). For glass and polystyrene, *C. glabrata* adhesion is promoted by the increase of the contact time between yeast cell and material surface, suggesting sensitivity to contact. However, this behavior was not expected for the interaction with materials given that it is typical for biological interactions, mainly adhesin interactions, depending on the association rate [355]. For silicone elastomer and polyvinyl chloride, any of the contact times tested lead to higher adhesion force than 0 s of contact time, but no

difference exists between 0.5 s, 1 s or 5 s, suggesting that all the possible interactions are established in a short amount of time (less than 0.5 s) and are then unsensitive to contact time. Interestingly, the rupture distance does not change with any of the contact times used: 0 s, 0.5 s, 1 s or 5 s. Nevertheless, it is clear that extending contact time strengthens the adhesion of this pathogenic yeast to the medical materials tested.

1.4.2. *C. glabrata* adheres to human vaginal epithelial cells

To study the interaction of the wild-type *C. glabrata* KUE100 with human epithelial cells, the human vaginal epithelial cell line VK2/E6E7 was selected due to the frequent vulvovaginal infections *C. glabrata* is known to cause [356]. The epithelial cells were first characterized by imaging them using AFM, in the Quantitative Imaging™ (QI™) mode (Figure II.2) [351], [357]. One very obvious characteristic of these cells is the height of the nucleus, more than 10 µm on almost all tested cells, which makes AFM imaging challenging. Comparing Figure II.2 to the QI™ images of other living adherent mammalians cells, like chinese hamster ovary and human colorectal tumor cells, it is possible to observe similarities in height [351].

The interactions established between a single *C. glabrata* cell and a single human vaginal epithelial cell were studied resorting to SCFS. *C. glabrata* cell probes were prepare with tipless cantilevers modified with conA. The epithelial cells were grown in KSF medium, at 37 ºC, 5% CO_2 and maintained in these conditions during the experiments. Each cell probe was approached towards a given epithelial cell with an extended speed of 20 µm/s, for different periods of time: 5 s, 10 s, 30 s and 60 s; and withdrawn at constant speed. Adhesion maps were recorded during constant approach and retraction of the *C. glabrata* KUE100 single-cell probes towards each single epithelial cell.

C. glabrata KUE100 wild-type interaction with each epithelial cell was studied in terms of not only maximum adhesion force, work of adhesion and rupture distance, but also regarding the number of jumps and tethers, that were measured on the force-distance curves and plotted as repartition histograms. Mean value and their standard deviation were extracted from a gaussian fit. A jump translates the attachment of the yeast-cell-probe to an adhesive unit, generally initially coupled to the cytoskeleton, following its unfolding, and finally its rupture [358]. In turn, a tether consists basically on the formation of a membrane nanotube, which is extruded and elongated resulting in a long plateau due to the pulling of the membrane reservoir [358]–[362]. Membrane nanotubes have been found in epithelial cells [363] and other cell types [359] and are considered important for cell-to-cell adhesion and intercellular communication [364], [365]. The formation of tethers is affected by the actin cytoskeleton and glycocalyx connected to the membrane [359]. With just 5 s of contact time between cells, interaction forces can be measured, showing a maximum adhesion force of about 0.55 nN, work of adhesion of 5.98×10^{-15} J, rupture distance of approximately 35 µm and an average of 1.63 jumps per force-distance curve and 2.55 tethers per force-distance curve (Figure II.3a, b, c, d and e, respectively). The force-distance curves of the interaction reveal the presence of jumps and tethers and generally long distances for the rupture of the interaction (Figure II.3f). This analysis results from the measurement of at least 4 yeast cells, from at least 3 independent cultures, recording around 64 force-distance curves per yeast cell.

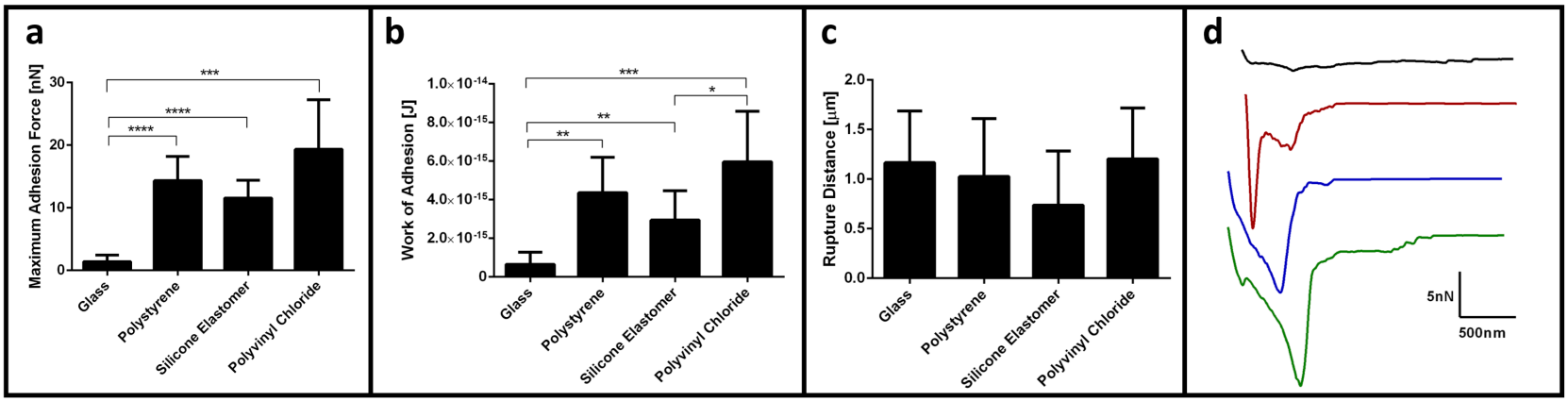

Figure II.1. Interaction of *C. glabrata* wild-type strain KUE100 with glass, polystyrene, silicone elastomer and polyvinylchloride by SCFS. Average of the **a** maximal adhesion force, **b** work of adhesion and **c** rupture distance measured on each retraction curve. **d** Representative force-distance curves of the interaction with glass (black), polystyrene (red), silicone elastomer (blue) and polyvinyl chloride (green). For every condition, at least 5 yeast cells, from at least 3 independent cell cultures, were immobilized on the cantilever for the interaction of each material and 256 force-distance curves were recorded. Error bars indicate standard deviations. *, P<0.05; **, P<0.01; ***, P<0.001; ****, P<0.0001.

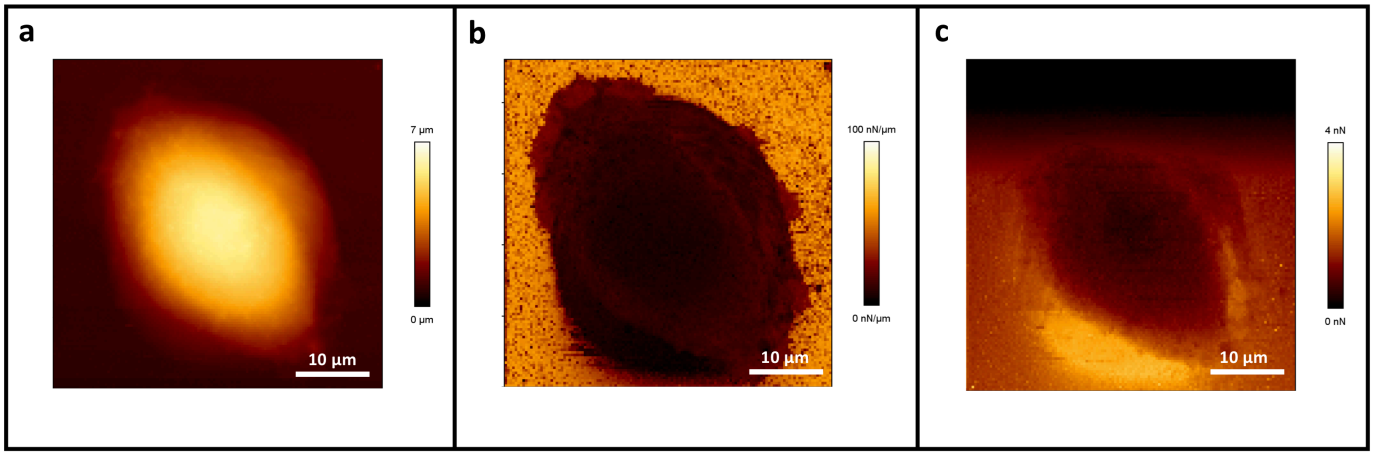

Figure II.2. AFM imaging of human vaginal epithelial VK2/E6E7 cells in the QI™. **a** height image based on the contact point position, **b** spring constant map corresponding to the slope of the approach force-distance curves and **c** adhesion map corresponding to the maximum adhesion force on the retraction force-distance curves.

The overall results show that, in general, different contact times between the yeast and epithelial cells do not alter adhesion force, work of adhesion, rupture distance or number of tethers (Figure II.3a, b, c, e and f). These results are very surprising given that the presence of jumps suggests a role developed by adhesins in the interaction between yeast and epithelial cell, and therefore, a specific biologic interaction, expected to depend on contact time. It is possible that the adhesin/s at play have a remarkably small kinetic association constant (K_{on}) and the differences rely between 0 s and 1 s of contact time. Interestingly, the main aspect that seems to change with contact time for *C. glabrata* is the number of jumps (Figure II.3d). Jumps have previously been described to translate the involvement of integrins in the adhesion process, especially when the number of jumps is higher than the number of tethers [362]. In fact, upon 30 s of contact time *C. glabrata* presents slightly higher numbers of jumps per force-distance curve, which might indicate a role of adhesins in these first moments of the interaction with epithelial cells. Nevertheless, for other contact times the differences are not clear between the number of jumps and tethers (Figure II.3d and e).

Comparing the interaction of *C. glabrata* and human vaginal epithelial cells with the interaction of *C. glabrata* and the plastic materials, the adhesion force measured on the interaction with plastic surfaces was found to be up to 40-fold higher (Supplementary Figure SII.2a). Interestingly, the work of adhesion does not change significantly between the two types of interaction, except regarding the interaction of *C. glabrata* with polyvinyl chloride (Supplementary Figure SII.2b). Logically, the rupture distance analysis shows the exact opposite results, the interaction of wild-type *C. glabrata* shows much higher average values of rupture distance than the interaction of *C. glabrata* with any of the materials tested (Supplementary Figure SII.2c). The differences between *C. glabrata* adhesion to the materials and epithelial cells is also clear by the comparison between the representative force-distance curves of each case (Supplementary Figures SII.2d and e).

1.4.3. CgEfg1 and CgTec1 are involved in *C. glabrata* biofilm formation

Although in *Candida albicans* a lot is already known about the major regulators of biofilm formation, very little has been uncovered for *C. glabrata*. According to the work of Nobile and colleagues (2012) the regulatory network of biofilm formation in *C. albicans* is composed by CaEfg1, CaTec1, CaRob1, CaNdt80, CaBcr1, CaBrg1 [99]. In order to unravel possible transcription factors for biofilm formation in *C. glabrata*, we found the predicted orthologs in *C. glabrata*, of these transcription factors: CgEfg1 (CAGL0M07634g), CgEfg2 (CAGL0L01771g), CgTec1 (CAGL0M01716g), CgTec2 (CAGL0F04081), CgNdt80 (CAGL0L13090g) and Bcr1 (CAGL0L00583g). No orthologs were found in the *C. glabrata* genome for CaRob1 or CaBrg1. Deletion mutants for the selected genes were built and tested for the ability to form 24 h biofilms on a polystyrene surface, with SDB medium, pH 5.6, using the PrestoBlue Cell Viability assay. From this screening, only two genes, *CgEFG1* and *CgTEC1,* were found to be necessary for biofilm formation on these conditions (Figure II.4a). Additionally, the overexpression of *CgEFG1* or *CgTEC1* genes in the *C. glabrata* wild-type strain L5U1 was found to lead to an increase in biofilm formation (Figure II.4b). These differences indicate a clear role of CgTec1 and CgEfg1 in biofilm formation in *C. glabrata*, but also suggests that other regulators must yet be found and are probably different from the ones responsible for *C. albicans* biofilm formation.

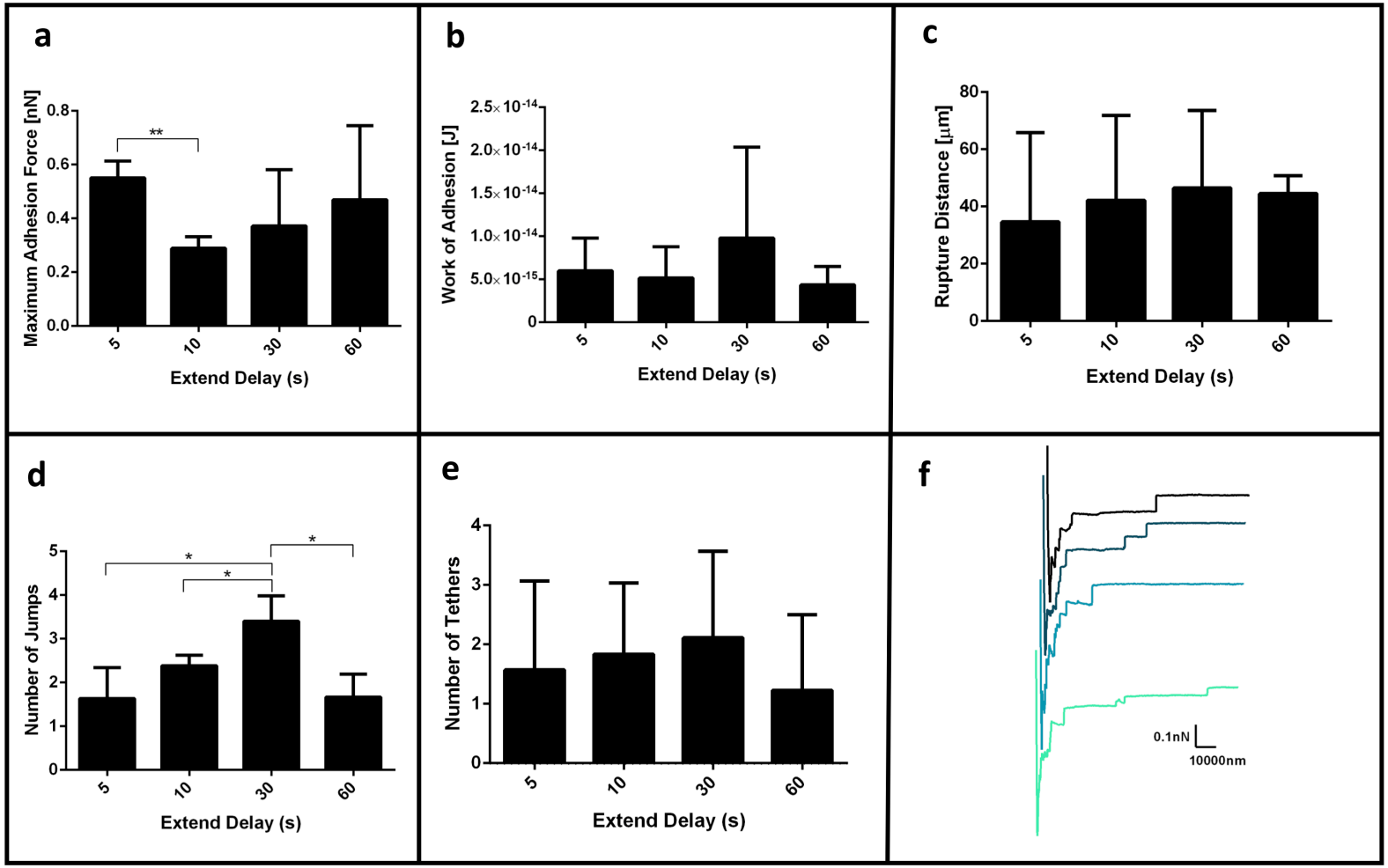

Figure II.3. Interaction of *C. glabrata* wild-type strain KUE100 with human vaginal epithelial VK2/E6E7 cells by SCFS, using different contact times: 5 s, 10 s, 30 s and 60 s. Characterization of these interactions is based on the **a** maximal adhesion force, **b** work of adhesion, **c** rupture distance, **d** number of jumps and **e** number of tethers measured on each retraction curve. **f** Representative force-distance curves are presented for each contact time (the lighter the force curve, the higher the contact time). Horizontal lines indicate the average levels from at least 4 yeast cells, from at least 3 independent cell cultures, immobilized on the cantilever for the interaction with epithelial cells and 64 or 16 force-distance curves were recorded, for 5 s and 10 s, and 30 s and 60 s, respectively. Error bars indicate standard deviations. *, $P<0.05$; **, $P<0.01$.

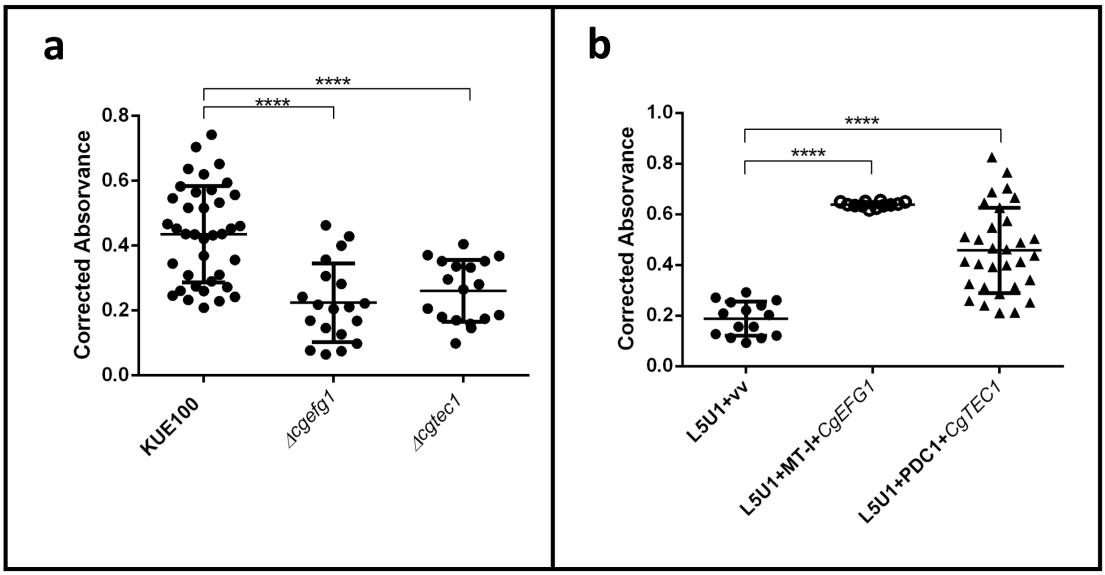

Figure II.4. CgEfg1 and CgTec1 are necessary for *C. glabrata* biofilm formation on polystyrene surface. Assessment of 24 h biofilm formation was performed by Presto Blue Cell Viability assay in microtiter plates of **a** *C. glabrata* KUE100, Δ*cgefg1* and Δ*cgtec1* strains and **b** *C. glabrata* L5U1 strain harboring the pGREG576 cloning vector (vv) and the same strain harboring the pGREG576_*MT-I_CgEFG1* or pGREG576_*PDC1_CgTEC1* plasmids, grown in SDB medium, pH 5.6. The data is displayed in a scatter dot plot, where each dot represents the level of biofilm formed in a sample. Horizontal lines indicate the average levels from at least three independent experiments. Error bars indicate standard deviations. ****, P<0.0001.

1.4.4. CgEfg1 and CgTec1 are involved in *C. glabrata* adherence to the human vaginal epithelium

Given the importance of CgEfg1 and CgTec1 in biofilm formation in *C. glabrata,* their involvement in *C. glabrata*'s adherence capacity to the human vaginal epithelial VK2/E6E7 cell line was also investigated. Adhesion of wild-type *C. glabrata* cells and Δ*cgefg1* and Δ*cgtec1* mutant cells was evaluated after 30 min of contact, at 37 ºC, 5% CO_2, with a MOI of 10. The results are presented as a percentage of adhered cells (ratio between the CFU/ml after incubation with the epithelial cells and the initial CFU/ml estimated for each suspension). The deletion of *CgEFG1* or *CgTEC1* in *C. glabrata* is accompanied by a decrease in its capacity to adhere to the human vaginal epithelium (Figure II.5a). On the other hand, the overexpression of *CgEFG1* or *CgTEC1* genes in the *C. glabrata* wild-type strain L5U1 led to an increase in the adherence capacity of *C. glabrata* (Figure II.5b). These results provide evidence that both CgTec1 and CgEfg1 have important roles in *C. glabrata* adhesion to the human vaginal epithelium, evidencing a new role for CgTec1, which is not found for CaTec1, but a similar one between the Efg1 transcription factors of both species [366].

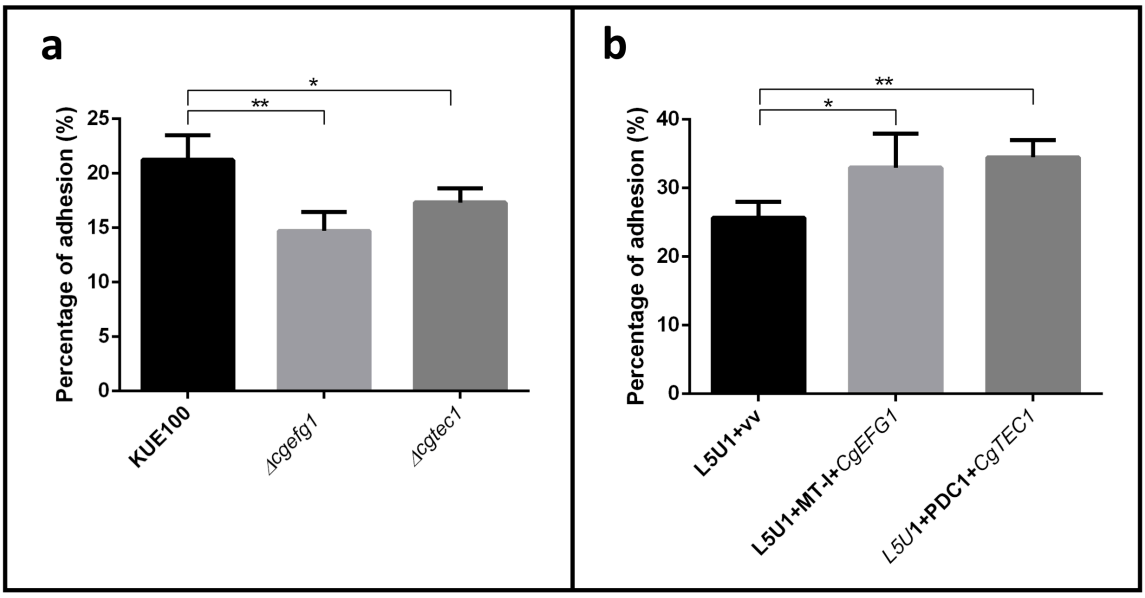

Figure II.5. CgEfg1 and CgTec1 are necessary for *C. glabrata* adhesion to the VK2/E6E7 human vaginal epithelium cell line. Adhesion of **a** the *C. glabrata* parental KUE100 and Δ*cgefg1* and Δ*cgtec1* strains and **b** the *C. glabrata* L5U1 strain harboring the pGREG576 cloning vector (vv) and the same strain harboring the pGREG576_*MT-I_CgEFG1* or pGREG576_*PDC1_CgTEC1* plasmids, to the human vaginal epithelial cells for 30 min at 37 ºC under 5% CO_2. Values are averages of results from at least three independent experiments. Error bars represent standard deviations. *, P<0.05; **, P<0.01.

1.4.5. Transcriptome-wide changes of *C. glabrata* cells upon biofilm formation

Going further on the analysis of the role of CgEfg1 and CgTec1 transcription factors in the control of biofilm formation in *C. glabrata*, an RNA-seq analysis was performed to measure the transcriptome-wide remodeling occurring after 24 h of biofilm formation, in comparison to planktonic cultivation, in the wild-type and the two deletion mutant cells: Δ*cgefg1* and Δ*cgtec1*. This analysis enabled the identification of the transcriptional remodeling that underlies adaptation to biofilm and planktonic growth by *C. glabrata* cells, as well as to identify the genes whose expression is affected by the CgEfg1 and/or CgTec1 transcription factors.

Incredibly, upon 24 h of *C. glabrata* KUE100 biofilm formation, a total of 3072 genes exhibit differential expression, when compared to planktonic growing cells (Supplementary Table SII.2), which represents approximately half of the whole transcriptome. Within this total number, 1567 genes were found to be upregulated and 1505 genes downregulated. In other to see where the main differences lay, we organized the upregulated genes according to the biological processes they are related to (Supplementary Figure SII.3). Biofilm formation requires the upregulation of several functional groups relative to: RNA metabolism and translation, carbon and energy metabolism, cell cycle, response to stress, amino acid metabolism, lipid metabolism, cell wall organization, adhesion and biofilm formation.

Adhesion to surfaces and between cells is the first step of biofilm formation, being required to maintain the mature biofilm [57], [76]. Thus, the observed upregulation of genes related to adhesion was clearly expected. These include *CgEPA1, CgEPA2, CgEPA3, CgEPA9, CgEPA10, CgEPA12, CgEPA20, CgEPA23*, encoding cluster I adhesins, as well as *CgPWP1, CgPWP2*, *CgPWP3, CgPWP5*,

encoding cluster II adhesins, *CgAED1* and *CgAED2*, encoding cluster III adhesins, and *CgAWP1*, *CgAWP3*, *CgAWP4*, *CgAWP6*, *CgAWP13*, encoding cluster IV adhesins. Interestingly, *CgTEC1* and *CgEFG1* were also found to be upregulated in biofilm cells, but not their predicted paralogs *CgEFG2* or *CgTEC2*. This observation is consistent with the role played by the *C. glabrata* CgEfg1 and CgTec1, but not by CgEfg2 and CgTec2, in biofilm formation, as described in this study.

Interestingly, also among the upregulated genes in biofilm cells are a number of genes encoding MDR transporters from the MFS, previously shown to confer antifungal resistance in *C. glabrata*, including *CgQDR2* [219], *CgAQR1*[218], *CgTPO1_2* [144] and *CgTPO3* [220], along with the uncharacterized ORFs *CAGL0B02343g and CAGL0J00363g*, which are predicted MFS-MDR transporters.

1.4.6. CgEfg1 and CgTec1 transcriptional control upon biofilm formation

The absence of *CgEFG1* gene in *C. glabrata*, upon 24 h of biofilm formation on a polystyrene surface leads to 1164 genes differentially expressed. CgEfg1 was found to activate 650 genes and repressed 514 genes, directly or indirectly (Supplementary Table SII.3). In turn, in 24 h *C. glabrata* biofilm cells, CgTec1 transcription factor was found to control a total of 1082 genes, activating 487 genes and repressing 595 genes, directly or indirectly (Supplementary Table SII.4). Out of the 1567 genes found to be upregulated in biofilm cells, 466 are regulated by CgEfg1 and 389 are regulated by CgTec1. The significant number of genes activated and repressed by both transcription factors highlights their impact as regulators of biofilm formation in *C. glabrata*.

When grouping the genes activated by CgEfg1 by function (Supplementary Figure SII.4), it is possible to observe that the main functional groups being activated by this transcription factor upon biofilm formation are unknown function, protein metabolism, response to stress, amino acid metabolism, carbon and energy metabolism, lipid metabolism and adhesion and biofilm formation. When performing the same classification for the genes activated by CgTec1 (Supplementary Figure SII.5), we observe that the main functional groups are unknown function, response to stress, protein metabolism, cell cycle, carbon and energy metabolism and cell wall organization.

Although activating similar functional groups, others seem to be differentially regulated by each transcription factor, suggesting that each one has their own biological targeted processes. For instance, CgEfg1 seems to contribute to the regulation of important genes for adhesion and biofilm formation, activating thirteen of the nineteen adhesin-encoding genes activated upon 24 h of biofilm formation: *CgPWP5*, *CgAED1*, *CgAED2*, *CgAWP13, CgAWP3, CgAWP1, CgPWP1, CgAWP4, CgPWP3, CgEPA9, CgEPA10, CgEPA12* and *CgEPA20* (Supplementary Table SII.5). Interestingly, CgEfg1 also activates the genes encoding CgTec1 and CgBcr1 transcription factors, a behavior similar to what has been described for the biofilm network set in place in *C. albicans* [99]. In turn, CgTec1 seems to be more relevant to other important functional groups upon biofilm formation, such as the cell wall organization, cell cycle and invasive/filamentous growth and virulence.

1.4.7. CgEfg1 and CgTec1-activated adhesins are required for biofilm formation

In order to confirm the previous observations and discern at which stage of biofilm formation CgEfg1 and CgTec1 play a more significant role, the expression of *CgPWP5, CgAED2* and *CgAWP13* adhesin-encoding genes was assessed at planktonic conditions and at 6 h, 24 h and 48 h of biofilm formation, in the KUE100 wild-type strain and deletion mutants Δ*cgefg1* and Δ*cgtec1* cells (Figure II.6a, b and c). These adhesin-encoding genes were selected given their upregulation upon biofilm formation and activation by both transcription factors (Supplementary Table II.5). Also, two of these adhesins, CgPwp5 and CgAed2, were found to be necessary for 24 h biofilm formation on a polystyrene surface (Figure II.6d). CgAwp13 had already been identified as an abundant protein present on the cell wall of a very polystyrene-adherent clinical isolate [282], but herein, the individual deletion of *CgAWP13* was found not to lead to a decrease in *C. glabrata* biofilm formation. However, the role in biofilm formation of CgPwp5 and CgAed2 adhesins is reported here for the first time.

The three tested adhesins are particularly upregulated in later stages of biofilm formation (24 h and 48 h), suggesting that they may be more relevant in yeast cell to yeast cell adhesion than to the initial steps of adhesion to polystyrene. Upon the deletion of CgEfg1 or CgTec1, the expression of *CgPWP5, CgAED2* and *CgAWP13* genes is not downregulated in planktonic conditions nor upon 6 h of biofilm formation. Significantly, upon 24 h and 48 h, the three adhesin-encoding genes are found to be strongly upregulated in the wild-type strain, but not in the Δ*cgefg1* or Δ*cgtec1* deletion mutants, indicating that both CgEfg1 and CgTec1 are relevant in later stages of biofilm formation (Figure II.6).

1.4.8. CgEfg1, but not CgTec1, is involved in *C. glabrata* adhesion to plastic surfaces

Given the results from the transcriptome-wide changes upon the deletion of *CgEFG1* or *CgTEC1* genes, indicating their importance in the control of different adhesin-encoding genes (Figure II.6), we explored their impact in the adhesion of *C. glabrata* to glass, polystyrene, silicone elastomer and polyvinyl chloride. Just like for the wild-type *C. glabrata* KUE100 strain, SCFS was applied with 5 s of contact between the yeast cell and surface, being the force-distance curves analysed regarding maximum adhesion force, work of adhesion and rupture distance (Figures II.7 and II.8). The deletion of *CgEFG1* gene significantly affects the capacity of *C. glabrata* to adhere to any of the plastic surfaces tested, but no difference was found regarding the interaction with glass. *C. glabrata* maximum adhesion force towards polystyrene and polyvinyl chloride, and work of adhesion towards silicone elastomer and polyvinyl chloride, were found to decrease upon *CgEFG1* deletion (Figure II.7a and b). In turn, no clear differences seem to exist between the KUE100 wild-type and the deletion mutant Δ*cgtec1* in terms of maximum adhesion force, work of adhesion or rupture distance (Figure II.8).

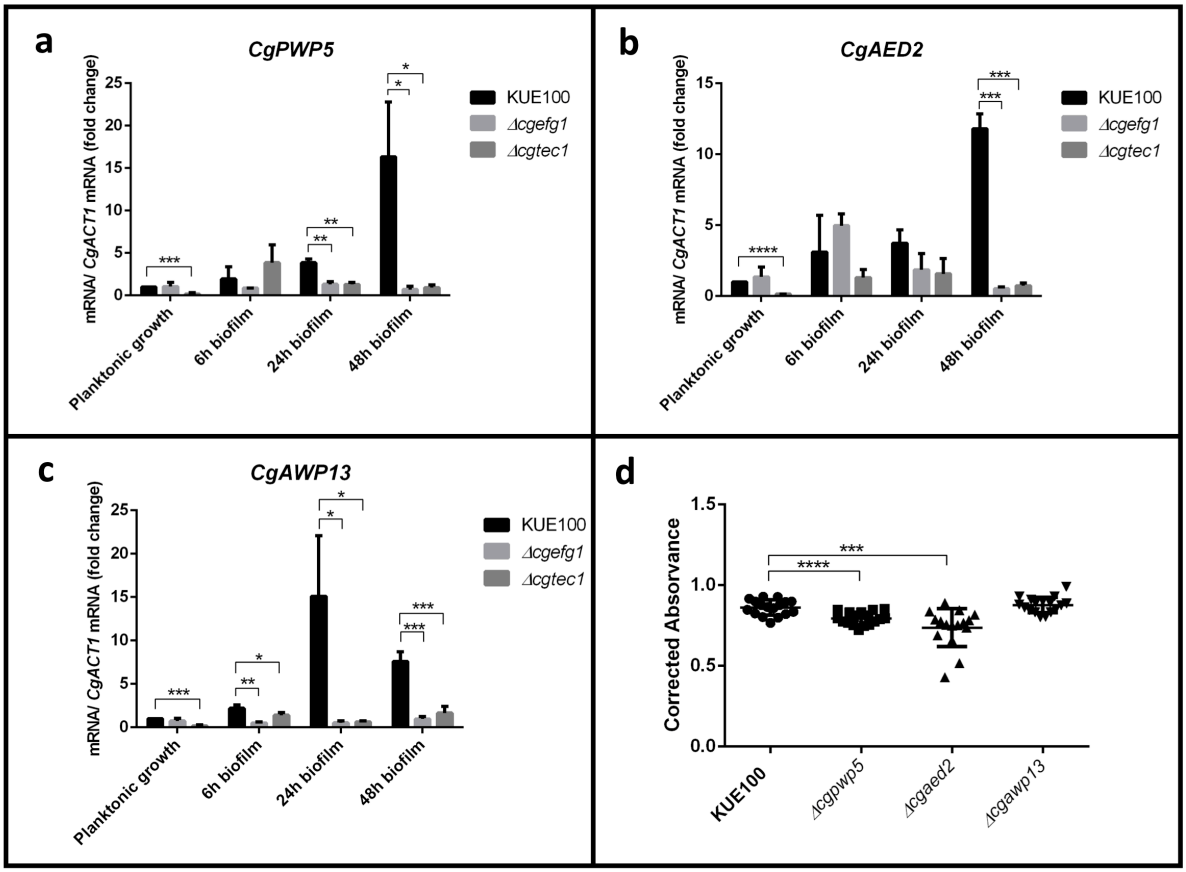

Figure II.6. CgPwp5, CgAed2 and CgAwp13 adhesins are necessary for biofilm formation, being regulated by CgEfg1 and CgTec1 transcription factors. Shown are the transcript levels of **a** *CgPWP5*, **b** *CgAED2*, **c** *CgAWP13* in the *C. glabrata* wild-type strain KUE100 and in the derived deletion mutants Δ*cgefg1* and Δ*cgtec1*, in planktonic conditions and 6 h, 24 h and 48 h of biofilm formation conditions on polystyrene surface in liquid SDB medium, pH 5.6. Transcript levels were assessed by quantitative RT-PCR, as described in Materials and Methods. Values are averages of results from at least three independent experiments. Error bars represent standard deviations. **d** 24 h biofilm formation quantified by Presto Blue Cell Viability assay in microtiter plates of *C. glabrata* KUE100 wild-type and Δ*cgpwp5, Δcgaed2 and* Δ*cgawp13* deletion mutant strains grown in SDB medium, pH 5.6. The data is displayed in a scatter dot plot, where each dot represents the level of biofilm formed in a sample. Horizontal lines indicate the average levels from at least three independent experiments. Error bars indicate standard deviations. *, P<0.05; **P<0.01, ***P<0.001 P; ****, P<0.0001.

1.4.9. CgEfg1, but not CgTec1, is involved in *C. glabrata* adhesion to human vaginal epithelial cells

As shown previously (Figure II.5), both CgEfg1 and CgTec1 are necessary to reach wild-type adherence levels upon 30 min of contact with human vaginal epithelium. To check if they are also required for the initial steps of the adhesion process, that take place in seconds, the interaction forces established by Δ*cgefg1* and Δ*cgtec1* deletion mutant cells with a single epithelial cell were measured through SCFS, for a period of contact of 5 s, and compared to that of the parental wild-type strain. Upon the deletion of *CgEFG1* gene, the maximum adhesion force of the interaction decreases significantly, while the number of jumps and tethers diminishes significantly, which can be depicted in the representative force-distance curves of the interaction of the wild-type and Δ*cgefg1* deletion mutant with

an epithelial cell (Figure II.9). These results point out the importance of CgEfg1 in the capacity of *C. glabrata* to adhere to these epithelial cells, right at the initial point of interaction of the two cells.

On the other hand, the loss of *CgTEC1* gene did not result in such variance from the adherence profile of the wild-type strain (Figure II.10). It seems that CgTec1 transcription factor has a role in the adherence to the human vaginal epithelium but not as important as the role of CgEfg1 and does not contribute to the first moments of interactions between *C. glabrata* and a human vaginal epithelial cell.

1.5. Discussion

C. glabrata is an effective pathogenic yeast, that uses adhesion and biofilm formation to better adapt to the environment and infect the human host. This work increases the understanding of the molecular basis of this process, from the transcriptome remodeling perspective to the nanoscale interaction level.

SCFS has allowed the in-depth study of the adhesion process of *C. glabrata* to several clinically relevant surfaces. The simplest adhesion of a single *C. glabrata* cell to glass was found to be higher than what has been found for other bacterial species like *Staphylococcus epidermidis*, *Staphylococcus aureus* and *Streptococcus mutans*, all ranging values of 4-5 nN of maximum adhesion force to borosilicate glass [367]. *C. glabrata*'s maximum adhesion force towards polystyrene, silicone elastomer and polyvinyl chloride obtained (~14 nN, ~10 nN, ~19 nN, respectively), was even higher than the obtained with glass, and the values found by Valotteau and colleagues (2019), for *C. glabrata* adhesion to hydrophobic methyl-terminated substrates (adhesion force of 0.3-0.5 nN and rupture distance of 0.2-0.4 μm) [311]. Nevertheless, it is lower than the interaction measured with other hydrophobic surfaces (~50 nN) [368]. *C. albicans* presents lower levels of maximum adhesion force (~40 nN) than *C. glabrata*, when comparing the same surfaces, while both present much higher adhesion forces than *Saccharomyces cerevisiae* (about 5 nN) [369], which is consistent with the role of adhesion in pathogenesis.

The interaction of *C. glabrata* with human vaginal epithelial cells (Figure II.3) revealed an adhesion profile similar to what has been found for other pathogens adhering to human epithelia. Similar to what we found, the interaction of *C. albicans* with macrophages exhibited a maximum adhesion force of 0.5 nN and the work of adhesion between 1-10x10^{-15} J. Moreover, the study of force-distance curves also showed the presence of jumps and tethers [370]. In turn, the interaction of a single cell of human bronchial epithelium to a monolayer of *Pseudomonas aeruginosa*, revealed an adhesion force of 0.67 nN and work of adhesion of about 4.14x10^{-15} J [371], a bit higher than what is observed for *C. glabrata* or *C. albicans.* Although considering different microorganisms and epithelial cells, the values obtained are not that far apart from one and other, clearly indicating the capacity of these pathogens to adhere to human cells, an important characteristic in their colonization and infection ability.

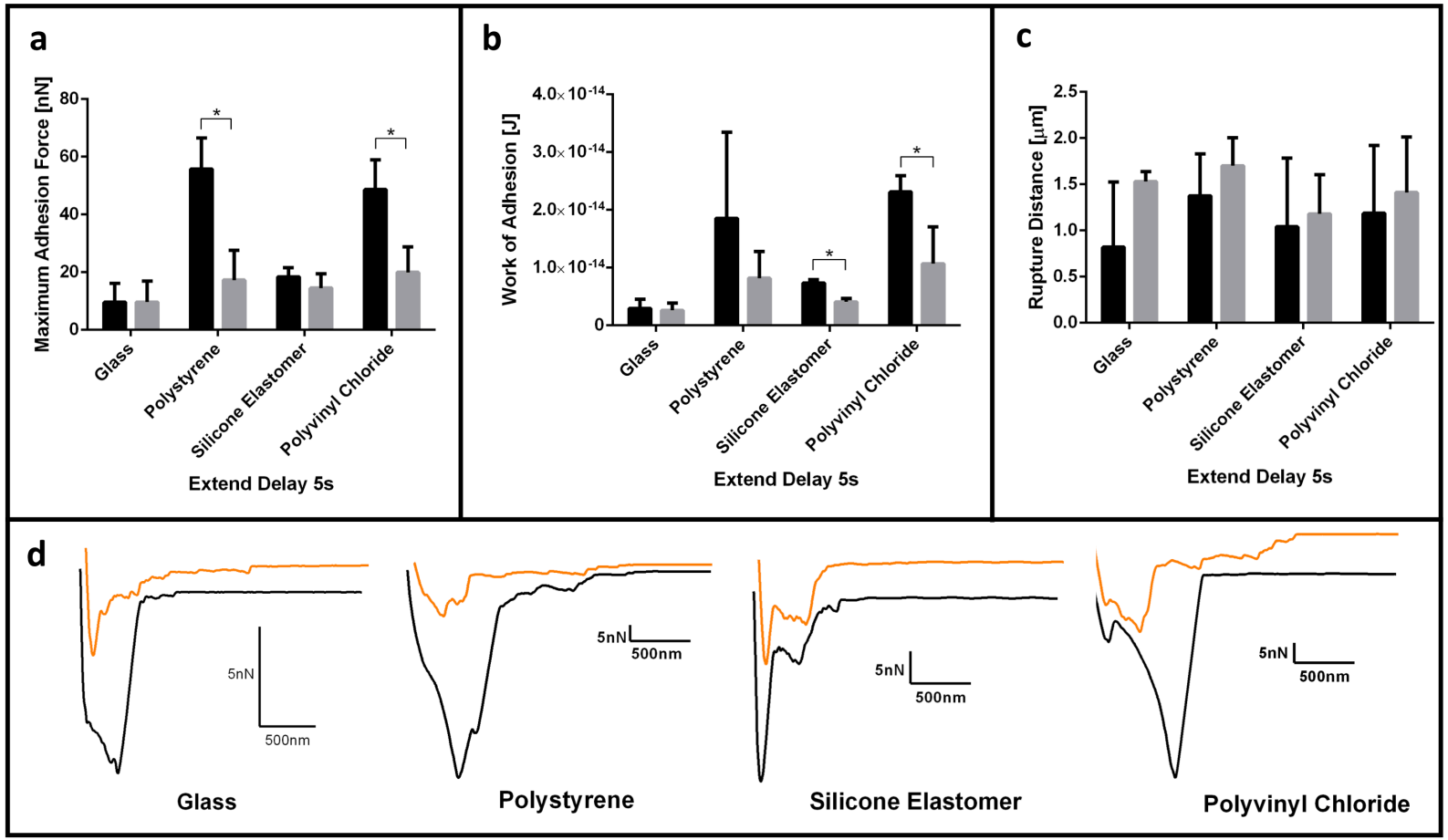

Figure II.7. CgEfg1 is necessary for the adhesion of *C. glabrata* to polystyrene, silicone elastomer and polyvinyl chloride, with 5 s of contact time. Horizontal lines indicate the average levels of *C. glabrata* wild-type KUE100 strain (black) and deletion mutant Δ*cgefg1* (grey) regarding **a** maximum adhesion force, **b** work of adhesion and **c** rupture distance measured on each retraction curve. **d** Representative force-distance curves of the interaction with glass, polystyrene, silicone elastomer and polyvinyl chloride, by *C. glabrata* wild-type KUE100 (black) and Δ*cgefg1* deletion mutant single cells (orange). For every condition, at least 4 yeast cells, from at least 3 independent cell cultures, were immobilized on the cantilever for the interaction with each material. 256 force-distance curves were recorded per yeast cell. Error bars indicate standard deviations. *, P<0.05.

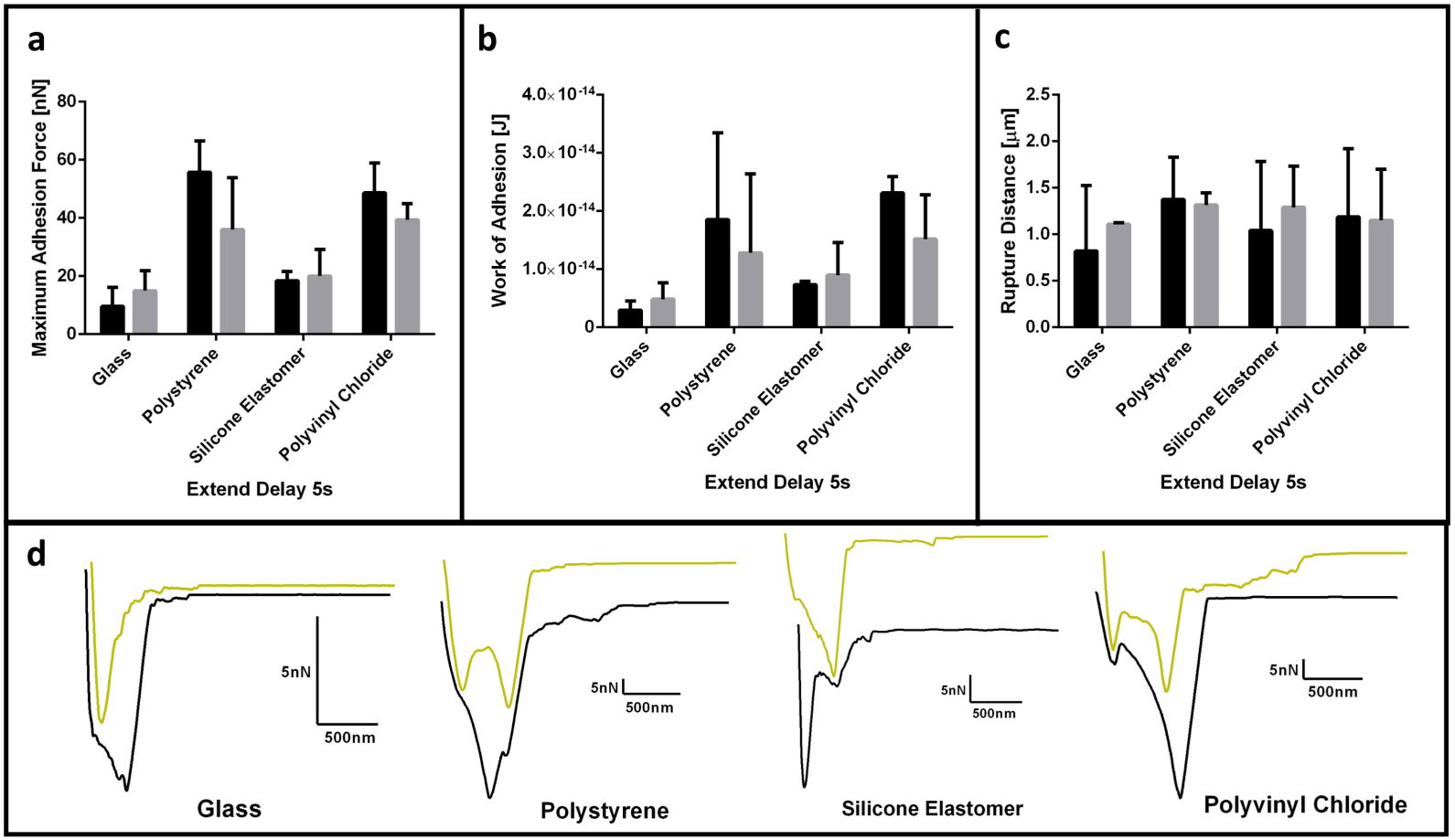

Figure II.8. CgTec1 is not necessary for *C. glabrata* adhesion to polystyrene, silicone elastomer and polyvinyl chloride, with 5 s of contact time. Horizontal lines indicate the average levels of *C. glabrata* wild-type KUE100 strain (black) and deletion mutant Δ*cgtec1* (grey) regarding **a** maximum adhesion force, **b** work of adhesion and **c** rupture distance measured on each retraction curve. **d** Representative force-distance curves of the interaction with glass, polystyrene, silicone elastomer and polyvinyl chloride, by *C. glabrata* wild-type KUE100 (black) and Δ*cgtec1* deletion mutant single cells (green). For every condition, at least 4 yeast cells, from at least 3 independent cell cultures, were immobilized on the cantilever for the interaction with each material. 256 force-distance curves were recorded per yeast cell. Error bars indicate standard deviations.

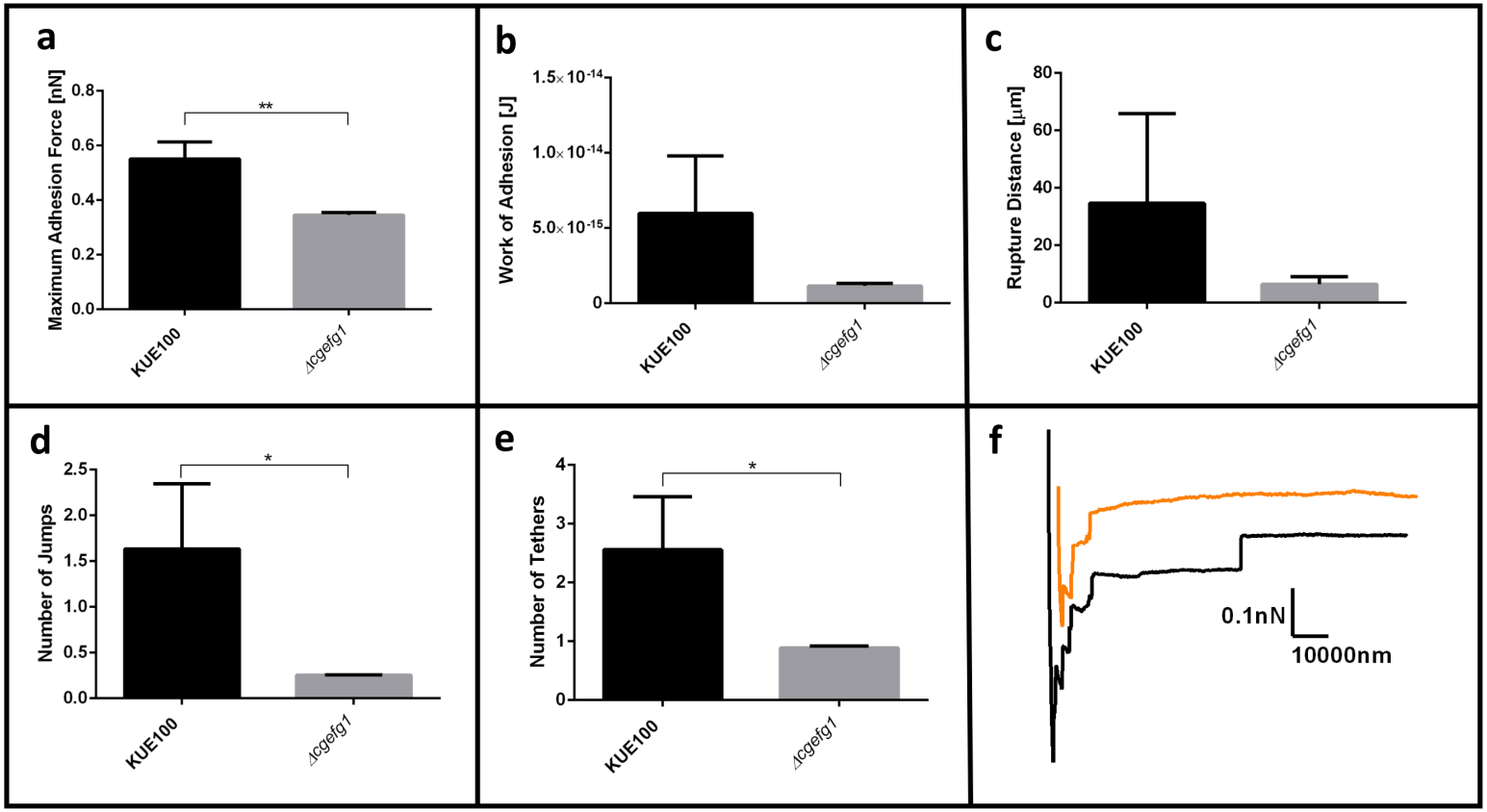

Figure II.9. Interaction of *C. glabrata* wild-type strain KUE100 (black) and deletion mutant Δ*cgefg1* (grey) with human vaginal epithelial VK2/E6E7 cells by SCFS, using 5 s of contact time. Characterization of these interactions is based on the **a** maximal adhesion force, **b** work of adhesion, **c** rupture distance, **d** number of jumps and **e** number of tethers measured on each retraction curve. **f** Representative force-distance curves of the interaction of *C. glabrata* wild-type KUE100 (black) and Δ*cgefg1* deletion mutant single cells (orange) with epithelial cells. Horizontal lines indicate the average levels from at least 4 yeast cells, from at least 3 independent cultures, immobilized on the cantilever for the interaction with epithelial cells 64 force-distance curves were recorded. Error bars indicate standard deviations. *, P<0.05; **, P<0.01.

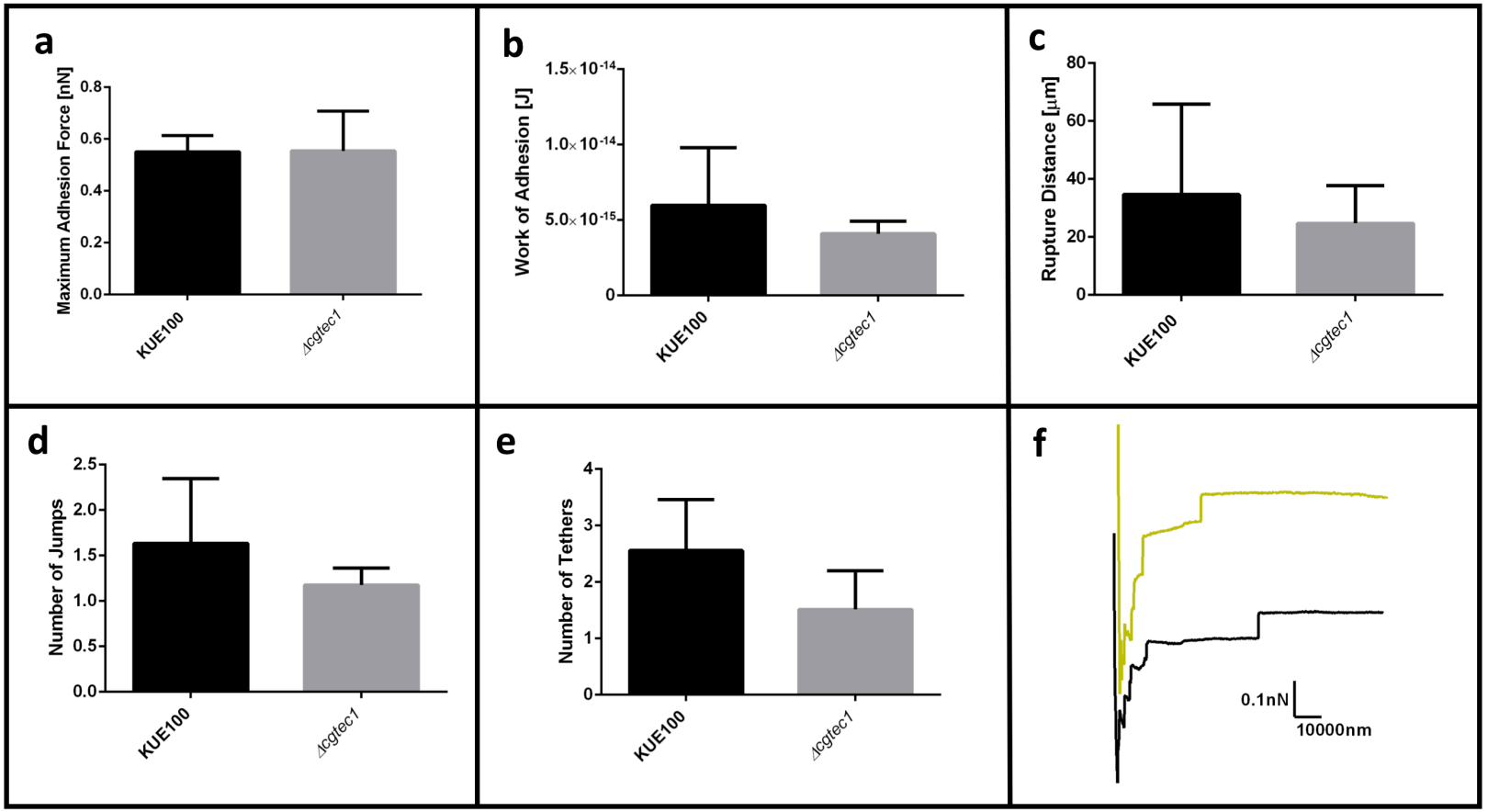

Figure II.10. Interaction of *C. glabrata* wild-type strain KUE100 (black) and deletion mutant Δ*cgtec1* (grey) with human vaginal epithelial VK2/E6E7 cells by SCFS, using 5 s of contact time. Characterization of these interactions is based on the **a** maximal adhesion force, **b** work of adhesion, **c** rupture distance, **d** number of jumps and **e** number of tethers measured on each retraction curve. **f** Representative force-distance curves of the interaction of *C. glabrata* wild-type KUE100 (black) and Δ*cgtec1* deletion mutant single cells (green) with epithelial cells. Horizontal lines indicate the average levels from at least 4 yeast cells, from at least 3 independent cultures, immobilized on the cantilever for the interaction with epithelial cells 64 force-distance curves were recorded. Error bars indicate standard deviations.

The dramatically increased capacity of *C. glabrata* to adhere to medical materials when compared to epithelial cells (Supplementary Figure SII.2), correlates with the difficulty to eradicate *C. glabrata* from the human host, when it is attached to medical devices, when compared to when it is just interacting with host cells. This highlights the need to change the materials used in medical devices, so that they are not a perfect match for adherence to *C. glabrata* and other pathogens.

To further pursuit the study of biofilm formation, we performed a genetic screening that identified CgEfg1 and CgTec1 transcription factors as necessary to biofilm formation and adhesion to the human vaginal epithelium. This screening also revealed that the regulatory network of *C. glabrata* controlling biofilm formation is different from the one described for *C. albicans* [99]. Nevertheless, upon biofilm formation, both species suffer major alterations in the transcriptome, *C. glabrata* with 3072 genes with altered expression, and *C. albicans* with 2235 genes differentially expressed, comparatively to planktonic conditions, according to Nobile et al., (2012) [99]. In both species, genes differently expressed are related to adhesion and metabolism [372]. Adhesion allows the starting point and sustenance of the biofilm, being easy to relate its significance in biofilm formation. Regarding metabolism, our data set shows upregulation of biosynthesis of positively charged amino acids, indicating that the cells are suffering from nitrogen limitation. Moreover, 13 out of the 18 genes required for the biogenesis of peroxisomes, where fatty acid β-oxidation occurs, were found to be upregulated upon *C. glabrata* biofilm formation, suggesting biofilm cells might also be experiencing carbon source limitation. An indication also found by Fox and colleagues study on transcriptomics modulation upon biofilm formation [372].

The importance of CgEfg1 and CgTec1 in the control of biofilm formation is very clear given the number of genes differently expressed upon biofilm formation and controlled by each transcription factor. It seems from our data sets, that both CgEfg1 and CgTec1 have an important role contributing to the production of ECM and biofilm proteins, given the activation of genes belonging to the functional groups of protein metabolism and carbon and energy metabolism. Although CgEfg1 controls a lot of genes regarding adhesion, CgTec1 seems to be more relevant to cell wall organization, cell cycle and invasive/filamentous growth and virulence. Such results suggest that CgTec1 might be involved in the control of pseudohyphae formation, similar to one of the roles of its *C. albicans* ortholog [125].

When evaluating the capacity of wild-type and Δ*cgefg1* and Δ*cgtec1* deletion mutants to adhere to clinically relevant surfaces by SCFS, agreeing results were found. Although CgTec1 is not necessary for the first moments of adhesion to plastic surfaces or epithelial cells, CgEfg1 was found to have a significant role. The clear importance of CgEfg1 in *C. glabrata* adhesion is most likely related to its role in the activation of 13 adhesin-encoding genes, upon 24 h of biofilm formation. Such influence on adhesion is likely extended to the beginning of biofilm formation, given that upon *CgEFG1* deletion, but not *CgTEC1* deletion, a decreased in the expression of *CgAWP1*, *CgAWP4, CgEPA6, CgEPA7* and *CgEPA8* adhesin-encoding genes was observed in planktonic cells (Supplementary Table SII.5), a feature that may underlie the differential ability of these cells to adhere to biotic and abiotic surfaces in their first contact. To corroborate this idea, the work of El-Kirat-Chatel and colleagues (2015) shows that Δ*cgepa6* deletion mutant has decreased adhesion force to hydrophobic surfaces when compared to the

wild-type [368], suggesting that CgEpa6 is one of the adhesins controlled by CgEfg1, responsible for its importance in *C. glabrata's* first moments of adhesion to the plastic surfaces studied herein.

Overall, this work describes two new major regulators of adhesion and biofilm formation, CgEfg1 and CgTec1, constituting promising targets for the development of new therapeutic strategies to fight *C. glabrata* promoted candidiasis.

1.6. Acknowledgements

This work was supported by "Fundação para a Ciência e a Tecnologia" (FCT) (Contracts PTDC/BBB-BIO/4004/2014 and PTDC/BII-BIO/28216/2017 and BIOTECnico PhD grants to MC, PP and AIP). Funding received by iBB-Institute for Bioengineering and Biosciences from FCT-Portuguese Foundation for Science and Technology (UID/BIO/04565/2013) and from Programa Operacional Regional de Lisboa 2020 (Project N. 007317), as well as from project LISBOA-01-0145-FEDER-022231-the BioData.pt Research Infrastructure, is acknowledged. We acknowledge John Bennett, of the National Institute of Allergy and Infectious Diseases, NIH, Bethesda, USA, for kindly providing the L5U1 strain.

2. A new determinant of *Candida glabrata* virulence: the acetate exporter CgDtr1

2.1. Abstract

Persistence and virulence of *Candida glabrata* infections are multifactorial phenomena, whose understanding is crucial to design more suitable therapeutic strategies. In this study, the putative multidrug transporter CgDtr1, encoded by ORF *CAGL0M06281g*, is identified as a determinant of *C. glabrata* virulence in the infection model *Galleria mellonella*. *CgDTR1* deletion is shown to decrease the ability to kill *G. mellonella* larvae by decreasing *C. glabrata* ability to proliferate in *G. mellonella* hemolymph, and to tolerate the action of hemocytes. The possible role of CgDtr1 in the resistance to several stress factors that underlie death induced by phagocytosis was assessed. *CgDTR1* was found to confer resistance to oxidative and acetic acid stress. Consistently, CgDtr1 was found to be a plasma membrane acetic acid exporter, relieving the stress induced upon *C. glabrata* cells within hemocytes, and thus enabling increased proliferation and virulence against *G. mellonella* larvae.

2.2. Introduction

Infections caused by *Candida* species are recognized as the 4th most common cause of nosocomial infections [373]. Candidiasis is considered to be responsible for more than 400,000 life-threatening infections worldwide every year [374]. *Candida glabrata* is the second most common cause of invasive candidiasis, with an estimated death rate of 40–50% [58]. Infections caused by this pathogenic yeast have increased worldwide [13], [61], which is likely due to the relatively high prevalence of antifungal drug resistance among *C. glabrata* clinical isolates [58], [375]. It may also be the result of its ability to survive under stress conditions, such as those imposed by the host immune system [375]. Additionally, *C. glabrata* is able to survive on inanimate surfaces for more than 5 months, while *C. albicans* can only sustain about 4 months and *C. parapsilosis* only 2 weeks [376]. It is, thus, crucial to fully understand these pathogenesis-related phenomena in order to design better ways to prevent and control superficial and invasive candidiasis caused by *C. glabrata*.

In this work, the predicted *C. glabrata* Drug:H+ antiporter (DHA) CgDtr1, encoded by the ORF *CAGL0M06281g*, is shown to play a role in virulence and biofilm formation. ORF *CAGL0M06281g* is predicted to encode an ortholog of the *S. cerevisiae* Dtr1 protein, which was characterized as a dityrosine transporter required for spore wall synthesis [377]. Dtr1 was further shown to confer resistance to the antimalarial drug quinine, the antiarrhythmic drug quinidine and weak acids [377]. Within the DHA family in *C. glabrata*, seven other homologous transporters have been characterized so far [378], and found to confer resistance to drugs and other stress factors, such as azoles, flucytosine, benomyl, acetic acid, and polyamines, mostly by contributing to decrease the intracellular accumulation of those molecules [144], [218]–[221], [340]. Interestingly, the *C. albicans* DHA transporters CaMdr1, CaNag3, CaNag4 and, more recently, CaQdr1, CaQdr2, and CaQdr3 were found to further play a role

in its virulence, although the molecular mechanisms behind this observation are still to be fully elucidated [379]–[381]. More recently, the DHA transporters CgTpo1_1 and CgTpo1_2 were also found to contribute to increase *C. glabrata* virulence, through increasing antimicrobial peptide resistance and tolerance against phagocytosis, respectively [143].

In this study, the impact of CgDtr1 expression in the context of virulence was studied, using *Galleria mellonella* as an infection model. The influence of CgDtr1 in *C. glabrata* proliferation in this host and in the presence of *G. mellonella* hemocytes was further evaluated. Additionally, the activity of CgDtr1 against phagocytosis-related stresses, including oxidative and acidic stress, was inspected.

2.3. Methods

2.3.1. Strains, plasmids and growth medium

Candida glabrata CBS138 (prototrophic), KUE100 (prototrophic) [339] and L5U1 (cgura3Δ0; cgleu2Δ0) [340] strains were used in this study. *C. glabrata* cells were cultivated in rich YEPD medium, RPMI 1640 medium or BM minimal medium. YEPD medium contained per liter: 20g D-(+)- glucose (Merk), 20 g bacterial-peptone (LioChem) and 10 g of yeast-extract (Difco); whereas RPMI 1640 medium (pH 4) contained 10.4 g RPMI 1640 (Sigma), 34.5 g morpholinepropanesulfonic acid (MOPS, Sigma) and 18 g glucose (Merck) per liter. BM media contained 20 g/L of D-(+)-glucose (Merck), 1.7 g/L of Yeast-Nitrogen-Base, without amino acids or ammonium sulfate (Difco) and 2.65 g/L ammonium sulfate (Merck). L5U1 strain was grown in BM medium supplemented with 60 mg/L leucine (Sigma). *Saccharomyces cerevisiae* strain BY4741 (MATa, ura3Δ0, leu2Δ0, his3Δ1, met15Δ0) and the derived single deletion mutant BY4741_Δ*dtr1* were obtained from the Euroscarf collection and grown in BM medium supplemented with 20 mg/L methionine, 20 mg/L histidine, 60 mg/L leucine, and 20 mg/L uracil (all from Sigma). Solid media contained additionally 20 g/L of Bactoagar (Difco).

2.3.2. Cloning of the *C. glabrata CgDTR1* gene (ORF *CAGL0M06281g)*

The pGREG576 plasmid from the Drag & Drop collection [341] was used to clone and express the *C. glabrata* ORF *CAGL0M06281g* in *S. cerevisiae*, as described before [219]. *CAGL0M06281g* DNA was generated by PCR, using genomic DNA extracted from the sequenced CBS138 *C. glabrata* strain, and the following specific primers: 5′-GAATTCGATATCAAGCTTATCGATACCGTCGACAATGAGCACCTCCAGCAACAC-3′ and 5′ -GCGTGACATAACTAATTACATGACTCGAGGTCGACTCAGAAACTGTCTTTAACCC- 3′. The designed primers contain, besides a region with homology to the first and last 20 nucleotides of the *CAGL0M06281g* coding region (italic), nucleotide sequences with homology to the cloning site flanking regions of the pGREG576 vector (underlined). The amplified fragment was co-transformed into the parental *S. cerevisiae* strain BY4741 with the pGREG576 vector, previously cut with the restriction enzyme SalI, to obtain the pGREG576_*CgDTR1* plasmid. To enable gene expression in *C. glabrata*, the *GAL1* promoter present in the pGREG576_*CgDTR1* plasmid was replaced by the copper-inducible *C. glabrata MTI* promoter, giving rise to the pGREG576_*MTI*_*CgDTR1* plasmid. The *MTI* promoter DNA

was generated by PCR with the specific primers: 5′-TTAACCCTCACTAAAGGGAACAAAAGCTGGAGCTCTGTACGACACGCATCATGTGGCAATC-3′ and 5′-GAAAAGTTCTTCTCCTTTACTCATACTAGTGCGGCTGTGTTTGTTTTTGTATGTGTTTGTTG-3′. The designed primers contain, besides a region with homology to the first and last 27 nucleotides of the first 1,000 bp of the *MTI* promoter region (italic), nucleotide sequences with homology to the cloning site flanking regions of the pGREG576 vector (underlined). The amplified fragment was co-transformed into the parental strain BY4741 with the pGREG576_*CgDTR1* plasmid, previously cut with SacI and NotI restriction enzymes to remove the *GAL1* promoter, to generate the pGREG576_*MTI*_*CgDTR1* plasmid. The recombinant plasmids pGREG576_*CgDTR1* and pGREG576_*MTI*_*CgDTR1* were verified by DNA sequencing.

2.3.3. Disruption of the *C. glabrata CgDTR1* gene (ORF *CAGL0M06281g*)

The deletion of the *CgDTR1* gene was carried out in the parental strain KUE100, as described before [339]. The target genes were replaced by a DNA cassette including the *CgHIS3* gene, through homologous recombination. The replacement cassette was prepared by PCR using the following primers: 5′-TTTTGATTTTTTTACCATAATTTGTTTAAGATTATTTACCATAATAGCAGTAACGGGGCCGCTGATCACG-3′ and 5′ -ACACTAAATTTTAAACTTAGAATTCATTGAAGGCCCCTTAGAAATTATAAGTTTCACATCGTGAGGCTGG-3′. The pHIS906 plasmid including *CgHIS3* was used as a template and transformation was performed as described previously. The 3′ sequences of the primers, GGCCGCTGATCACG and CATCGTGAGGCTGG were attached to flanking region of *CgHIS3*. The underlined 56 bp sequences were flanking sequence of each gene. The replacement of *CgDTR1* by the *CgHIS3* cassette was verified by PCR, using as primers: 5′-CAGCTTTATCTCAGAAAACCAG-3′, which is complementary to a region in the cassette; and 5′ -GCTAAGAGATTGGCTGAGAG-3′, which is complementary to a region downstream of the *CgDTR1* 3′ end. Additionally, gene deletion was further verified by PCR using the following pairs of primers: 5′-CAACACTAGCGGTGAGTG-3′ and 5′-CTGCCTCCTTTATCTGCGA-3′. No PCR product was identified from template DNA of the mutant, while clear PCR products were identified from template DNA of parental strain KUE100.

2.3.4. *Galleria mellonella* survival and proliferation assays

Galleria mellonella larvae were reared in our lab insectariums, on a pollen grain and bee wax diet at 25 °C in the darkness. Last instance larvae weighting 250±25 mg were used in the killing assays and the larvae infection was based on the protocol previously described [143], [382], [383]. *C. glabrata* strains were cultivated in YEPD until stationary phase, harvested by centrifugation and resuspended in PBS (pH 7.4). 3.5 μL of yeast cell suspension, containing ~$5x10^7$ cells, were injected into each caterpillar via the last left proleg. For each condition, 10 larvae were used to follow the larval survival over a period of 72 h. Control larvae were injected with PBS (pH 7.4). For proliferation assays, three

living larvae at 1, 24, and 48 h post-injection were punctured in the abdomen with a sterile needle and hemolymph was collected.

2.3.5. *C. glabrata* phagocytosis assays in *G. mellonella* hemocytes

G. mellonella hemocytes were isolated as described before [384]. Hemocytes suspended in Grace insect medium (GIM) (Sigma) supplemented with 10% fetal bovine serum, 1% glutamine, and 1% antibiotic (10,000 U penicillin G, 10 mg streptomycin).

Cultures of *C. glabrata* cells were grown until mid-exponential phase (OD_{600nm}=0.4–0.6) and the appropriate volume was collected to have $7x10^2$ cells/mL in PBS. *Galleria* hemocyte monolayer medium was replaced with GIM without antimycotics, and then cells were infected with the yeast suspensions with a multiplicity of infection (MOI) of 1:5. After 1 h of infection at 37 °C, the hemocytes were carefully washed twice with cell culture medium. Viable intracellular yeast cells were measured after 1, 4, 24, and 48 h of infection, upon hemocyte lysis with 0.5% Triton X-100.

2.3.6. Susceptibility assays in *C. glabrata* and *S. cerevisiae*

The susceptibility of the *C. glabrata* or *S. cerevisiae* cells toward toxic concentrations of the selected drugs and acetic acid was evaluated as before, through spot assays or cultivation in liquid growth medium [218], [219]. The tested drugs included the following compounds, used in the specified concentration ranges: the azole antifungal drugs fluconazole (10-200 mg/L), ketoconazole (10-50 mg/L), clotrimazole (1-20 mg/L), thioconazole (0.2-1 mg/L) and miconazole (0.2-1 mg/L), the polyene antifungal drug amphotericin B (0.1-0.5 mg/L), and the fluoropyrimidine 5-flucytosine (0.02-5 mg/L).

2.3.7. CgDtr1 sub-cellular localization assessment

The sub-cellular localization of the CgDtr1 protein was determined based on the observation of BY4741 *S. cerevisiae* or L5U1 *C. glabrata* cells transformed with the pGREG576_*CgDTR1* or pGREG576_*MTI_CgDTR1* plasmids, respectively. *S. cerevisiae* cell suspensions were prepared by cultivation in BM-U medium, containing 0.5% glucose and 0.1% galactose, at 30 °C, with orbital shaking (250 rev/min), until a standard culture OD_{600nm} (Optical Density) = 0.4 ± 0.04 was reached. At this point cells were transferred to the same medium containing 0.1% glucose and 1% galactose, to induce protein expression. *C. glabrata* cell suspensions were prepared in BM-U medium, until a standard culture OD_{600nm}=0.5 ± 0.05 was reached, and transferred to the same medium supplemented with 50 μM $CuSO_4$ (Sigma), to induce protein overexpression. After 5 h of incubation, the distribution of CgDtr1_GFP fusion protein in *S. cerevisiae* or in *C. glabrata* living cells were detected by fluorescence microscopy in a Zeiss Axioplan microscope (Carl Zeiss MicroImaging), using excitation and emission wavelength of 395 and 509 nm, respectively, and images captured using a cooled CCD camera (Cool SNAPFX, Roper Scientific Photometrics).

2.3.8. ^{14}C-acetate accumulation assay

Accumulation assays using radiolabelled, [^{14}C]-acetate were carried out as described before [218]. To estimate the accumulation of radiolabelled compound (Intracellular/Extracellular) in yeast cells, cells were grown in BM medium, resuspended in BM medium, to obtain dense cell suspensions (OD_{600nm}=5.0 ± 0.1, equivalent to ~2.2 mg/(dry weight) mL). The radiolabeled compound was added to the cell suspensions (3.5µM of [^{14}C]-acetic acid (American Radiolabeled Chemicals; 0.1 mCi/mL) and 65 mM of unlabeled acetic acid) and accumulation of radiolabeled compound was followed for 30 min until equilibrium was reached. Radioactivity was measured in a Beckman LS 5000TD scintillation counter.

2.3.9. Gene expression measurement

The transcript levels of *CgDTR1* were determined by quantitative real-time PCR (RT-PCR). Total RNA was extracted from cells grown in the presence of acetic acid or hydrogen peroxide, and also when internalized within larvae hemocytes. At the end of each incubation period, total RNA obtained from the *C. glabrata* cell population was extracted using the hot phenol method [385]. Total RNA was converted to cDNA for the real-time Reverse-Transcription PCR (RT-PCR) using the MultiScribe Reverse Transcriptase kit (Applied Biosystems) and the 7500 RT-PCR thermal cycler block (Applied Biosystems). The real time PCR step was carried out using adequate primers (*CgDTR1* Forward: 5′-GGAGCCAAAATGAGAATGATATGTC−3′ ; *CgDTR1* Reverse: 5′-ACCACCTTGAAATCGGTGATG−3′ ; *CgACT1* Forward: 5′-AGAGCCGTCTTCCCTTCCAT-3′ ; *CgACT1* Reverse: 5′ - TTGACCCATACCGACC ATGA-3′), SYBR Green® reagents (Applied Biosystems) and the 7500 RT-PCR thermocycler block (Applied Biosystems). Default parameters set by the manufacturer were followed, and fluorescence was detected by the instrument and plotted in an amplification graph (7500 Systems SDS Software, Applied Biosystems). *CgACT1* gene transcript level was used as an internal reference. To avoid false positive signals, the absence of non-specific amplification with the chosen primers was confirmed by the generation of a dissociation curve for each pair of primers.

2.4. Results

2.4.1. CgDtr1 is a determinant of *C. glabrata* virulence against the *G. mellonella* infection model

Using *G. mellonella* larvae as an infection model, the possible effect of *CgDTR1* deletion in *C. glabrata* ability to exert its virulence was assessed. The survival of the larvae was followed for 72 h upon injection of 5x10^7 cells. The wild-type KUE100 *C. glabrata* strain was found to be able to kill 30% more larvae than the derived Δ*cgdtr1* deletion mutant (Figure II.11A). Additionally, the overexpression of *CgDTR1* in the L5U1 *C. glabrata* wild-type was found to lead to a 50% decrease in *G. mellonella* survival rate, when compared with L5U1 cells harboring the cloning vector pGREG576 (Figure II.11B). Interestingly, it was also possible to observe that the L5U1 wild-type strain appears to be much less

virulent than the KUE100 wild-type strain. This data strongly suggest that the CgDtr1 transporter is involved in the pathogenesis of *C. glabrata*.

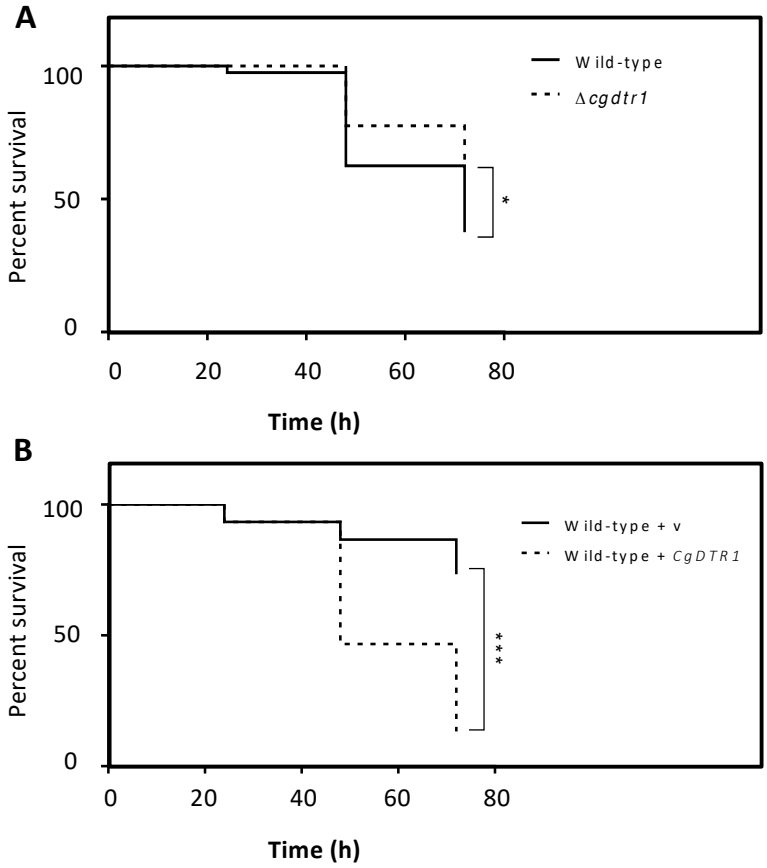

Figure II.11. *CgDTR1* expression increases *C. glabrata* virulence against the *G. mellonella* infection model. (A) The survival of larvae injected with ~5x10^7 CFU/larvae of KUE100 *C. glabrata* wild-type (full line), or derived Δ*cgdtr1* deletion mutant (dashed line), is displayed as Kaplan-Meier survival curves. (B) The survival of larvae injected with ~5x10^7 CFU/larvae of L5U1 *C. glabrata* wild-type strain, harboring the pGREG576 cloning vector (full line) or the pGREG576_*MTI_CgDTR1* expression plasmid (dashed line), is displayed as Kaplan-Meier survival curves. The displayed results are the average of at least three independent experiments. *P < 0.05; ***P < 0.001.

2.4.2. *CgDTR1* expression increases *C. glabrata* cell proliferation in *G. mellonella* hemolymph

Given the observation that CgDtr1 expression increases the ability of *C. glabrata* cells to kill *G. mellonella* larvae, a deeper analysis of the underlying mechanisms was undertaken. The proliferation of *C. glabrata* cells within this infection model was then assessed. The hemolymph of injected larvae was recovered 1, 24, and 48 h after injection and the number of viable *C. glabrata* cells evaluated. After 1 and 24 h of injection the number of wild-type and Δ*cgdtr1* cells was found to be undistinguishable (Figure II.12). However, upon 48 h of injection, a time in which a greater difference was detected in terms of larvae survival rate, the concentration of wild-type cells was found to be 4.5-fold higher than that of the mutant population (Figure II.12). This difference in terms of cell proliferation may very well explain the different ability to kill the host, especially considering that the mutant displays no growth defect *in vitro*.

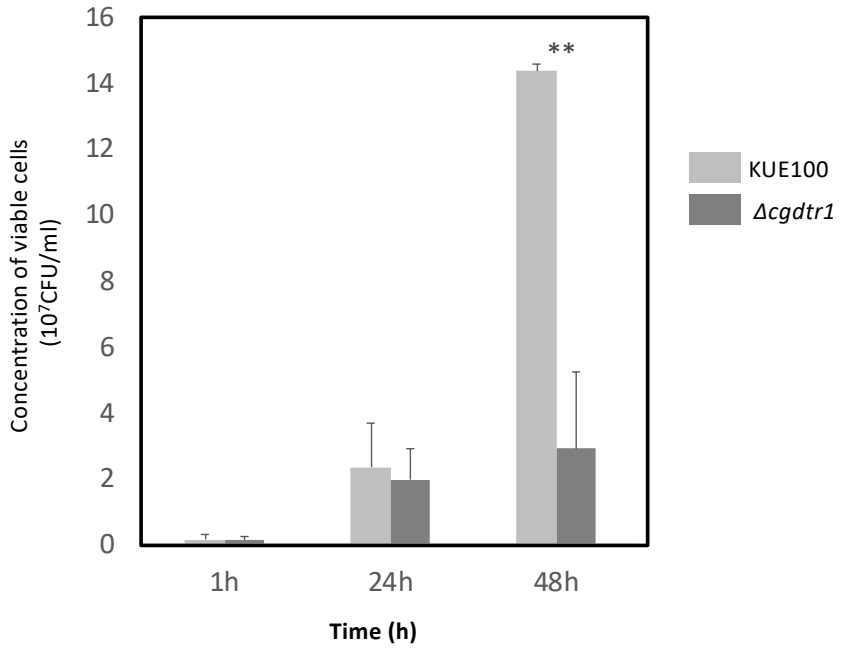

Figure II.12. *CgDTR1* deletion decreases *C. glabrata* proliferation in *G. mellonella* hemolymph. The concentration of viable *C. glabrata* KUE100 wild-type (light gray) and Δ*cgdtr1* (dark gray) cells assessed within total hemolymph recovered from *G. mellonella* larvae upon 1, 24, and 48 h of injection with ~5x10^7 CFU/larvae is shown. The displayed results are the average of at least three independent experiments, standard deviation being represented by the error bars. **P < 0.01.

The exact reason why the Δ*cgdtr1* mutant is unable to proliferate as much as the wild-type within the *G. mellonella* hemolymph was then pursued. First, the hypothesis that the two strain exhibit differences at the level of antimicrobial peptide (AMP) resistance was explored. The resistance of both strains to the AMP histatine-5 was evaluated, however, no differences were observed (results not shown). Second, the resistance of each strain to phagocytosis by hemocytes, the insect equivalent to mammalian macrophages, was inspected. *C. glabrata* cells were exposed to a cell culture of *G. mellonella* hemocytes. The concentration of viable *C. glabrata* cells found within the hemocytes was measured after 1, 4, 24, and 48 h after co-culture. After 1, 4, and 24 h of phagocytosis the number of viable wild-type cells internalized within hemocytes was found to be undistinguishable of the number of Δ*cgdtr1* cells internalized within hemocytes (Figure II.13A). After 48 h of injection, the population of wild-type cells found within hemocytic cells was found to be 3-fold higher than Δ*cgdtr1* mutant cells (Figure II.13A). A similar experiment was carried out using the L5U1 *C. glabrata* wild-type cells harboring the pGREG576_*MTI_CgDTR1*, leading to *CgDTR1* overexpression upon $CuSO_4$ induction, or the cloning vector pGREG576. Consistent with the previous results, the overexpression of *CgDTR1* was found to lead to a 25% increase in cell proliferation within hemocytes (Figure II.13B).

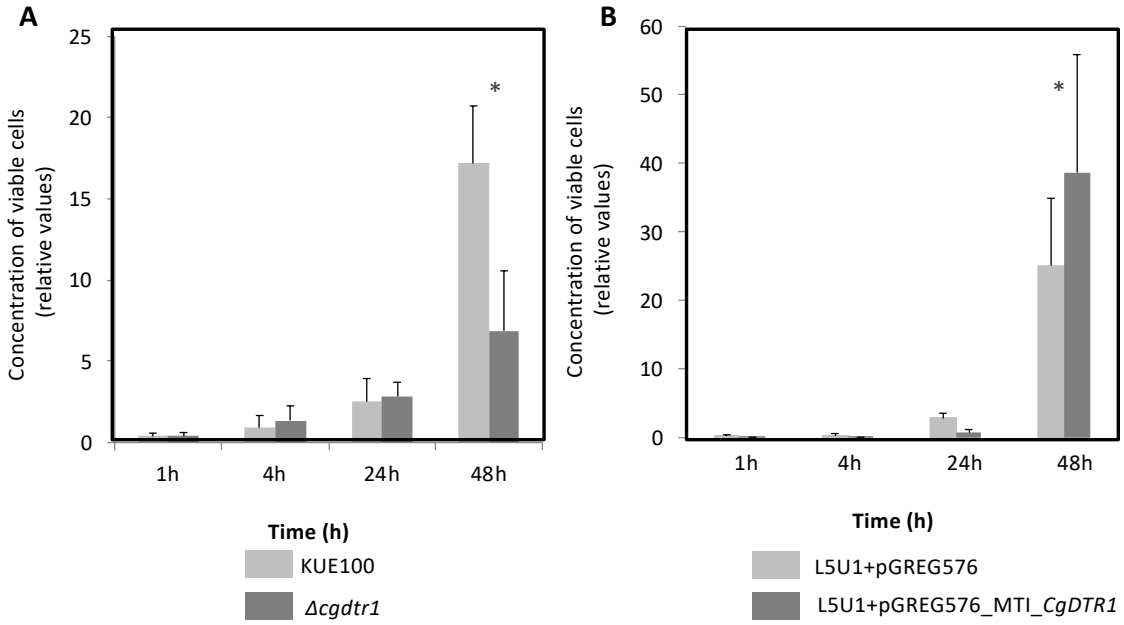

Figure II.13. *CgDTR1* expression increases *C. glabrata* proliferation in *G. mellonella* hemocytes. The concentration of viable KUE100 *C. glabrata* wild-type (light gray) and Δ*cgdtr1* (dark gray) cells (A), or of viable L5U1 *C. glabrata* wild-type harboring the pGREG576 cloning vector (light gray) or the pGREG576_*MTI_CgDTR1* expression plasmid (dark gray) cells (B) assessed upon 1, 4, 24, and 48 h of co-culture with *G. mellonella* hemocytes, using a MOI of 1:5. The displayed results are relative to the concentration of viable cells inoculated at time zero and are the average of at least three independent experiments, standard deviation being represented by the error bars. *P < 0.05.

2.4.3. CgDtr1 confers resistance to weak acid and oxidative stress, but not to antifungal drugs

Given its predicted function as a multidrug resistance transporter, together with the results described above, it appeared reasonable to hypothesize that the role of CgDtr1 in *C. glabrata* proliferation within *G. mellonella* hemocytes is related to defending the yeast cell against the stress factors encountered within hemocytic cells. Considering the identification of the *S. cerevisiae DTR1* gene as a determinant of weak acid resistance, the eventual role of *CgDTR1* in this context was evaluated, especially considering that the phagolysosomes of mammalian macrophages are highly acidic and rich in acetic acid [386]. Based on spot assays, the deletion of *CgDTR1* was found to moderately decrease acetic and benzoic acid tolerance in the KUE100 *C. glabrata* strain (Figure II.14A). Given the importance of Reactive Oxygen Species (ROS) in the killing of phagocytosed yeast cells, the effect of the expression of *CgDTR1* in the resistance to hydrogen peroxide was further assessed. Significantly, the deletion of *CgDTR1* was also found to severely impair growth in the presence of 20 mM H_2O_2 (Figure II.14A). Based on the analysis of the growth curves of the same populations in liquid medium, it is possible to see that the deletion of the *C. glabrata CgDTR1* gene dramatically increases yeast susceptibility to acetic acid, increasing in about 20 h the period of lag-phase induced upon stress exposure (Figure II.15). Upon exposure to 2 mM benzoic acid, wild-type cells were found to undergo a period of 40 h of lag-phase, before exponential growth could be resumed, but in these conditions the Δ*cgdtr1* deletion mutant population was found to be unable to resume growth even after 80 h of

lag-phase (Figure II.15). Consistent with the previous results, the overexpression of the *CgDTR1* gene in the L5U1 *C. glabrata* wild-type strain was found to increase its resistance to the acetic and benzoic acid stress, as well as to H_2O_2 (Figure II.14B). Interestingly, it was also possible to observe that the L5U1 wild-type strain appears to be much more susceptible to weak acid and oxidative stress than the KUE100 wild-type strain. Furthermore, the heterologous expression of the *CgDTR1* gene was found to slightly increase the resistance of the *S. cerevisiae* wild-type and Δ*dtr1* deletion mutant strains against both weak acids and H_2O_2 (results not shown).

Given the predicted role of CgDtr1, as a member of the drug:H+ antiporter family, in drug/chemical stress resistance, the susceptibility to antifungal drugs was additionally assessed. The tested drugs include the azoles miconazole, thioconazole, clotrimazole, ketoconazole, itraconazole, and fluconazole, the polyene amphotericin B, and the fluoropyrimidine 5-flucytosine. However, no difference in terms of drug susceptibility was observed when comparing the proliferation of wild-type and Δ*cgdtr1* deletion mutant strains (results not shown).

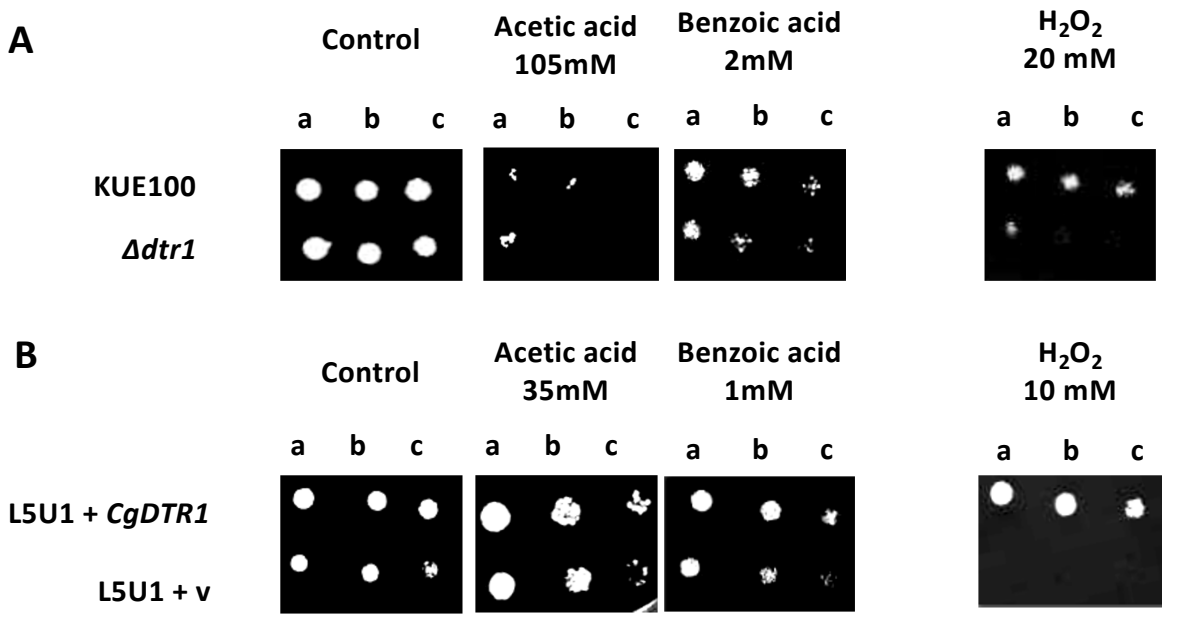

Figure II.14. *CgDTR1* confers resistance to weak acids and hydrogen peroxide in *C. glabrata*. (A) Comparison of the susceptibility to acetic acid, benzoic acid or to H_2O_2, at the indicated concentrations, of the KUE100 *C. glabrata* (wild-type—wt) and Δ*cgdtr1* strains, in BM agar plates, pH 4.5, by spot assays. (B) Comparison of the susceptibility to acetic acid, benzoic acid or to H_2O_2, at the indicated concentrations, of the L5U1 *C. glabrata* strain (wild-type—wt), harboring the pGREG576 cloning vector (v) or the pGREG576_*MTI_CgDTR1* in BM agar plates, pH 4.5, without uracil, by spot assays. The inocula were prepared as described in the materials and methods section. Cell suspensions used to prepare the spots were 1:5 (b) and 1:25 (c) dilutions of the cell suspension used in (a). The displayed images are representative of at least three independent experiments.

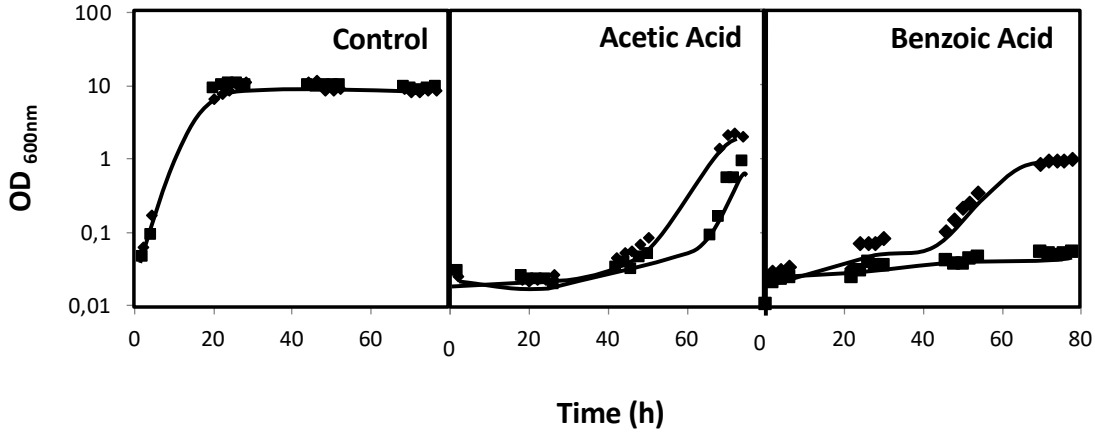

Figure II.15. *CgDTR1* confers resistance to weak acids in *C. glabrata*. Comparison of the susceptibility of KUE100 *C. glabrata* wild-type (◆) and Δ*cgdtr1* (■) deletion mutant strain to cultivation in the presence of 100 mM acetic acid or of 2 mM benzoic acid in BM liquid medium, pH 4.5, in comparison to control conditions, measured in terms of variation of Optical Density at 600nm (OD_{600nm}). The inocula were prepared as described in the materials and methods section. Growth curves are representative of at least three independent experiments.

2.4.4. *CgDTR1* is a plasma membrane acetate exporter

C. glabrata cells harboring the pGREG576_*MTI_CgDTR1* plasmid were grown to mid-exponential phase in minimal medium, and then transferred to the same medium containing 50 μM $CuSO_4$, to induce the expression of the fusion protein. At a standard OD_{600nm} of 0.5±0.05, obtained after around 5 h of incubation, cells were inspected through fluorescence microscopy. In *C. glabrata* cells, the CgDtr1_GFP fusion protein was found to be predominantly localized to the cell periphery (Figure II.16A). *S. cerevisiae* cells harboring the pGREG576_*CgDTR1* plasmid were also tested for the subcellular localization of CgDtr1, to verify that in these cells, the *C. glabrata* transporter was localized similarly. At a standard OD_{600nm} of 0.5±0.05, obtained after around 5 h of incubation with 1% galactose to induce protein expression, fluorescence was found mostly in the cell periphery (Figure II.16A). Intracellular Dtr1-GFP staining is also observed, possibly corresponding to mislocalized protein aggregates resulting from exaggerated overexpression. Altogether, these results strongly suggest plasma membrane localization, differently from what was observed for its *S. cerevisiae* homolog, Dtr1, shown to be localized only at the prospore membrane [377].

Given the registered plasma membrane localization, the possible role of CgDtr1 as an acetate exporter was analysed. The accumulation of [^{14}C]-labeled acetic acid in non-adapted *C. glabrata* cells suddenly exposed to the presence of 65 mM cold acetic acid, which induces a mild growth inhibition in both the parental strain and Δ*cgdtr1* cells, was thus tested. The intracellular accumulation of radiolabelled acetate was found to be 2-fold higher in cells devoid of *CgDTR1* than in parental KUE100 cells (Figure II.16B). Altogether, the presented evidences point out to CgDtr1 as a plasma membrane acetate exporter.

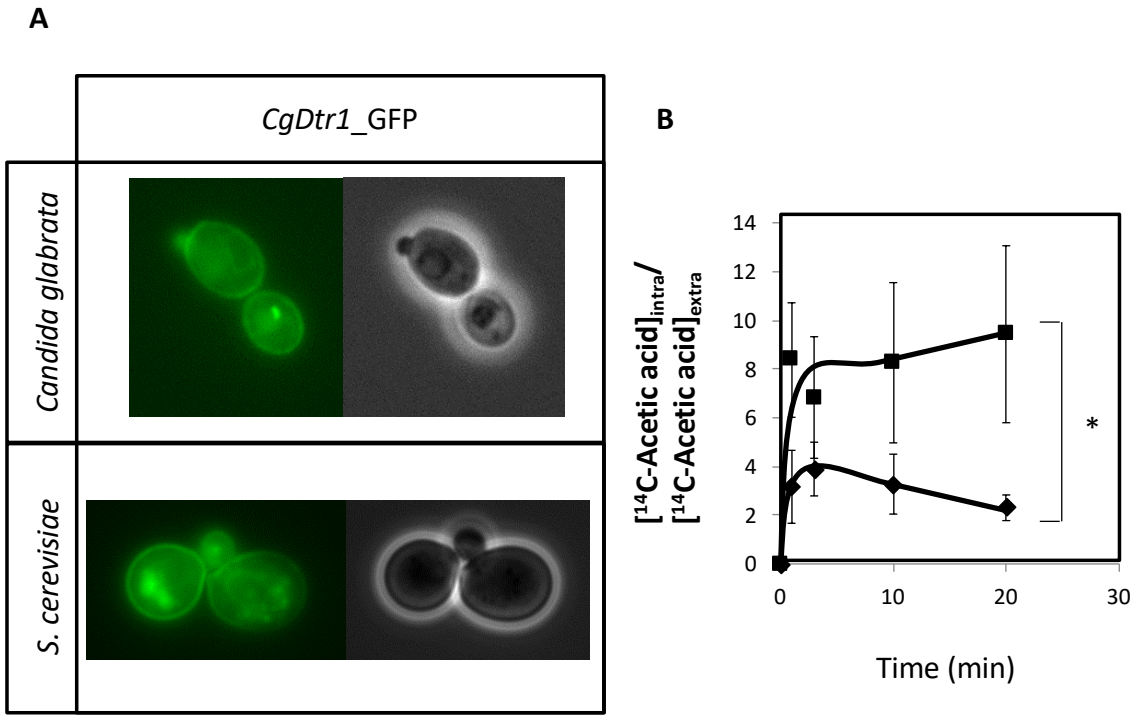

Figure II.16. CgDtr1 is a plasma membrane acetate exporter in *C. glabrata* cells. (A) Fluorescence of exponential-phase L5U1 *C. glabrata* cells or BY4741 *S. cerevisiae* cells, harboring the pGREG576_*MTI_CgDTR1* or pGREG576_*CgDTR1* plasmids, after 5 h of copper- or galactose-induced recombinant protein production, respectively. Results indicate that the CgDtr1-GFP fusion protein localizes to the plasma membrane of both *S. cerevisiae* and *C. glabrata* cells. (B) Time course accumulation ratio of [^{14}C]-Acetic acid in non-adapted cells of KUE100 *C. glabrata* wild-type (◆) or Δ*cgdtr1* (■) strains, during cultivation in BM liquid medium in the presence of 65 mM unlabeled acetic acid. The accumulation ratio values are averages of at least three independent experiments. Error bars represent the corresponding standard deviations. *$p < 0.05$.

2.4.5. *CgDTR1* transcript levels are upregulated during internalization in hemocytes and in the presence of hydrogen peroxide stress

Considering the importance of CgDtr1 for proliferation within hemocytes, its transcript levels were followed during internalization in hemocytes. A dramatic upregulation of *CgDTR1* expression was registered during the internalization of *C. glabrata* cells by *G. mellonella* hemocytes (Figure II.17A). Interestingly, upon 1 h of co-culture with hemocytes, *C. glabrata* cells that were not internalized by hemocytes already exhibit a 4-fold upregulation of *CgDTR1* transcript levels. Upon 24 or 48 h of internalization of *C. glabrata* cells in hemocytes the transcript levels of *CgDTR1* were found to be 100-fold upregulated, which highlights the importance of this gene in the context of the adaptation of this pathogen to growth inside macrophages. In order to evaluate which could be the stimuli that leads to this upregulation, changes in *CgDTR1* transcript levels occurring in *C. glabrata* cells upon 1 h of exposure to either acetic acid or hydrogen peroxide were assessed. Of the two stresses only hydrogen peroxide was found to induced a significant upregulation of *CgDTR1* expression, while surprisingly exposure to acetic acid led to the downregulation of *CgDTR1* expression (Figures II.17B, C).

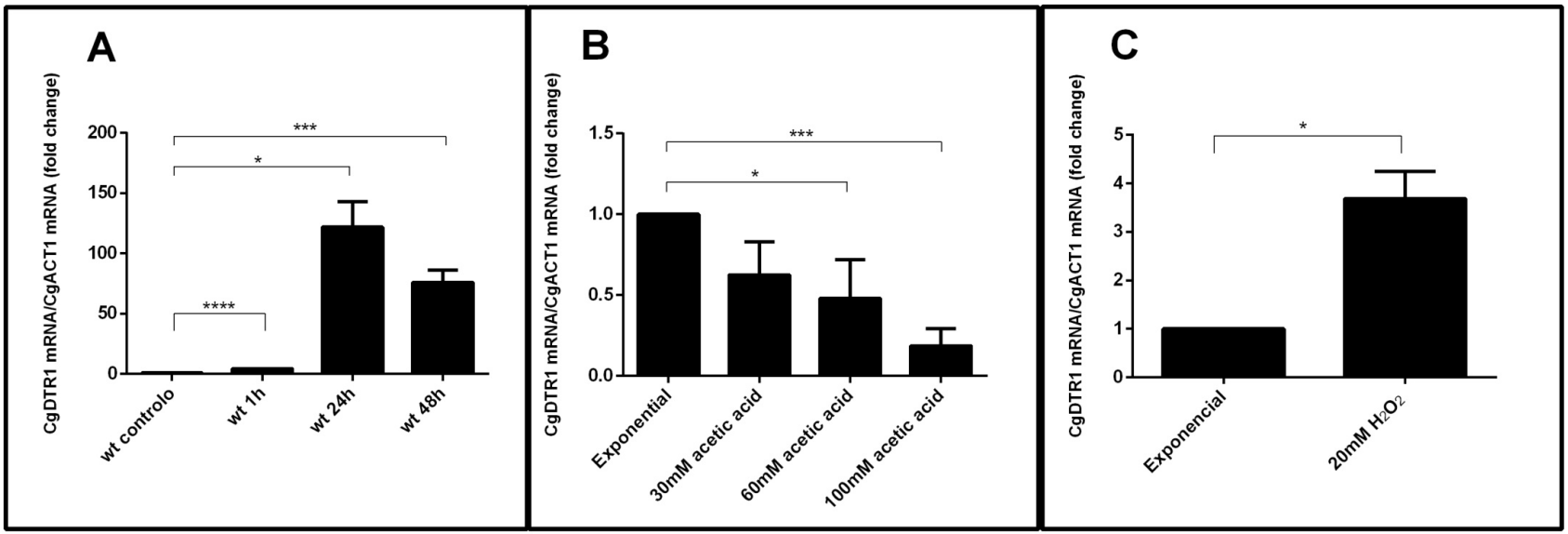

Figure II.17. The *CgDTR1* gene transcript level is upregulated during internalization in hemocytes and upon exposure to oxidative stress. Comparison of the variation of the *CgDTR1* transcript levels in KUE100 *C. glabrata* wild-type cells upon exposure to: (A) *G. mellonella* hemocytes, comparing non-internalized cells collected in the supernatant of hemocyte-*C. glabrata* 1 h co-cultures, and after 24 and 48 h of internationalization by hemocytes; (B) 30, 60, or 100 mM of acetic acid for 1 h; or (C) 20 mM of hydrogen peroxide for 1 h, in comparison with exponentially growing *C. glabrata* cells. The presented transcript levels were obtained by quantitative RT-PCR and are *CgDTR1*mRNA/*CgACT1*mRNA levels, relative to the values registered in wild-type exponential cells cultivated in planktonic conditions. The indicated values are averages of at least three independent experiments. Error bars represent the corresponding standard deviations. *P < 0.05; ***P < 0.001; ****P < 0.0001.

2.5. Discussion

In this study, the multidrug transporter CgDtr1 was shown to play a role in *C. glabrata* pathogenesis, protecting these cells from stress agents present in macrophagic cells.

The deletion of *CgDTR1* was found to lead to an increased larvae survival upon infection, decreasing in 30% the killing ability of *C. glabrata* cells. The use of *G. mellonella* as a model, had been previously exploited for the study of *Candida albicans* [387] and *C. glabrata* [143] virulence, and appears to be particularly useful in this context since it is difficult to cause *C. glabrata*-induced mortality in mice, even when facing neutropenia [388]. Furthermore, the larval innate immune system has a strong similarity to the mammalian innate immune system, especially when considering the hemocyte-dependent cellular response, very similar to that displayed by mammalian macrophages [389], in which *C. glabrata* is able to survive and replicate for a very prolonged time [291]. These features make the use of *G. mellonella* larvae an interesting and simplified model to further understand what happens inside the human host.

Although previous reports had shown that some *Candida* DHA genes [143], [380], [381], homologs of *CgDTR1*, play a role in virulence, the exact mechanisms underlying these observations remained unclear. In this work, the deletion of the *CgDTR1* gene was found to decrease the ability of *C. glabrata* to kill *G. mellonella* larvae. This decreased killing ability was found to correlate with diminished proliferation in *G. mellonella* hemolymph. Our results of *in vitro* interaction between yeast cells and hemocytes seem to support the hypothesis that CgDtr1 contributes for cell proliferation within macrophages. It is clear that Δ*cgdtr1* cells are more susceptible to stress factors found inside phagocytic cells, including acidic and oxidative stress. Additionally, the dramatic upregulation of *CgDTR1* transcript levels in *C. glabrata* cells upon internalization in *G. mellonella* hemocytes, which correlates with increased *CgDTR1* expression induced upon exposure to oxidative stress, further suggests that CgDtr1 is an important factor for adaptation to proliferate inside host macrophages.

Consistent with a role in weak acid stress resistance, CgDtr1 was found in this study to be a plasma membrane acetate exporter. Weak acids have an impact on membrane organization and function, while their intracellular accumulation may lead to higher oxidative stress, protein aggregation, membrane trafficking inhibition and changes in plasma and vacuolar membrane spatial organization [390], [391]. The expression of a number of genes encoding DHAs have been found to contribute to weak acid tolerance in *S. cerevisiae,* including *AQR1* and *AZR1* [392], [393], *TPO2* and *TPO3* [394] and *TPO1* [395]. Interestingly, CgDtr1 shares with its *S. cerevisiae* homolog Dtr1 a role in weak acid stress tolerance. However, given its plasma membrane localization and the inability of *C. glabrata* to undergo sporulation, it is unlikely that CgDtr1 shares Dtr1's role as dityrosine transporter in *S. cerevisiae* prospore membrane [377]. Tolerance against weak acids is important for at least *C. albicans*, as well as probably other pathogenic *Candida* species, to thrive within the host, since significant concentrations of both acetic and lactic acids have been found in the vaginal tract [396], and within the phagolysosome of human macrophages [386]. Furthermore, a synergistic action between some drugs and acetic acid was found, reinforcing the importance of weak acid resistance mechanisms in the context of antifungal therapy [218].

Altogether, the results from the present study strongly suggest that CgDtr1 plays an important role in the virulence of *C. glabrata* infections, possibly as a fitness factor [397], facilitating its proliferation within the host by protecting against weak acid stress.

2.6. Author Contributions

DR and MC made most of the experimental work and drafted the manuscript. RS, PP and CC contributed to the experimental work. DM-H and AF designed and conducted the infection experiments. AT-N and HC designed and conducted the molecular biology of *C. glabrata* strains. HC is a co-corresponding author of this manuscript. MT designed the experimental workflow, supervised the experimental work, and wrote the manuscript.

2.7. Acknowledgements and Funding

We acknowledge John Bennett, of the National Institute of Allergy and Infectious Diseases, NIH, Bethesda, USA, for kindly providing the L5U1 strain.

This work was supported by “Fundação para a Ciência e a Tecnologia” (FCT) (Contract PTDC/BBB- BIO/4004/2014; PhD grants to MC (PD/BD/116946/2016) and PP (PD/BD/113631/2015) and post-doctoral grants to CC (SFRH/BPD/100863/2014) and DM-H (SFRH/BPD/91831/2012). Funding received by iBB-Institute for Bioengineering and Biosciences from FCT-Portuguese Foundation for Science and Technology (UID/BIO/04565/2013) and from Programa Operacional Regional de Lisboa 2020 (Project N. 007317) is acknowledged. This study was partly supported by a Joint Usage/Research Program of the Medical Mycology Research Center, Chiba University. We acknowledge John Bennett, of the National Institute of Allergy and Infectious Diseases, NIH, Bethesda, USA, for kindly providing the L5U1 strain.

3. Role of CgTpo4 in polyamine and antimicrobial peptide resistance: determining virulence in *Candida glabrata*

3.1. Abstract

Candida glabrata is an emerging fungal pathogen, whose success depends on its impressive ability to resist antifungal drugs but also to thrive against host defenses.

In this study, the predicted multidrug transporter CgTpo4 (encoded by ORF *CAGL0L10912g*) is described as a new determinant of virulence in *C. glabrata*. CgTpo4 expression was found to increase *C. glabrata* ability to kill the infection model *Galleria mellonella*. This effect was found to correlate with the role found for Tpo4 in AMP resistance, specifically against histatin-5. Interestingly, *G. mellonella* was found to strongly activate AMP expression in response to *C. glabrata* infection, suggesting AMPs are a key antifungal defense in this infection model. CgTpo4 was also found to be a plasma membrane exporter of polyamines, especially spermidine, suggesting that CgTpo4 is able to export polyamines and AMPs, thus conferring resistance to both stress agents. *CgTPO4* deletion was also found to alter the membrane potential of *C. glabrata* cells, a physiological parameter affected by polyamine homeostasis.

Altogether, this study presents the polyamine exporter CgTpo4 as a determinant of *C. glabrata* virulence, which acts by protecting the yeast cells from the overexpression of AMPs, deployed as a host defense mechanism.

3.2. Introduction

Candida species are among the top 10 most frequently isolated nosocomial bloodstream pathogens, with an annual incidence rate of up to 4.8 cases, in Europe, and 13.3 cases, in the US, *per* 100 000 inhabitants [16]. Despite the fact that *Candida albicans* is still the predominant cause of invasive candidiasis, a higher proportion of patients has been infected by non-*albicans Candida* species [398]. *Candida glabrata* is one of the main examples, since it has risen as the most frequently isolated non-*albicans* pathogenic *Candida* species, accounting for 20% of the diagnosed cases of candidiasis in both Europe and North America [58], [399]. The frequency and relative high mortality levels (up to 45% for *C. glabrata*) of these infections [374] are generally attributed to the capacity of these pathogenic yeasts to efficiently develop MDR, to tolerate host defenses mechanisms, to maintain high proliferative and repopulation capacity through biofilm formation, and to display ability to withstand prolonged harmful conditions such as nutrient starvation and oxidative stress [400], [401].

C. glabrata can resist the confrontation with host immune cells, as a significant fraction of phagocytised cells are able to survive and replicate inside the macrophages. Since the host defense mechanisms are multifaceted, a number of different evasion strategies have evolved [397]. These include avoidance of contact with macrophages, rapid escape from host immune cells, ability to withstand macrophage antimicrobial activities and, most importantly, use macrophages as an

intracellular niche for protection and replication processes [397]. Besides this, in the event of *Candida* infection, other virulence factors, such as biofilm development and resistance to antimicrobial peptides, also play crucial roles for colonization and infection establishment [402]. Antimicrobial peptides, small positively charged amphipathic molecules, work directly against microbes, mainly through a mechanism that involves membrane disruption and pore formation, meaning that being able to resist them can be highly positive for the yeast to complete its infection cycle [403].

During the past three decades, antifungal drug resistance became a serious concern for the medical community. The fact that *C. glabrata* isolates are able to quickly develop resistance to new drugs enables them to keep causing prevalent infectious that are difficult to eliminate [404]. Transporters of the DHA family, belonging to the MFS, well characterized in the model yeast *Saccharomyces cerevisiae*, are known to take part in multi-drug resistance as well as in other important physiological stress response mechanisms, including weak acid and polyamine resistance and transport [144], [378], [405].

In this work, the predicted *C. glabrata* DHA, CgTpo4, encoded by the ORF *CAGL0L10912g*, is shown to play a role in virulence against the infection model *Galleria mellonella*. ORF *CAGL0L10912g* was predicted to encode an ortholog of the *S. cerevisiae TPO4* gene, which was characterized as a determinant of resistance to polyamines [406]. Within the DHA family in *C. glabrata*, eight other homologous transporters have been characterized so far [378]. These include CgAqr1, CgDtr1, CgFlr1, CgFlr2, CgQdr2, CgTpo1_1, CgTpo1_2 and CgTpo3, that were found to confer resistance to drugs and other stress factors, such as azoles, flucytosine, benomyl, mancozeb, acetic acid and polyamines, mostly by contributing to decrease the intracellular accumulation of those molecules [144], [218], [220], [221], [340], [407]. Additionally, the *C. albicans* DHA transporters CaMdr1, CaNag3, CaNag4, CaQdr1, CaQdr2 and CaQdr3, as well as the *C. glabrata* DHA transporters CgTpo1_1, CgTpo1_2 and CgDtr1, were found to further play a role in its virulence, although the exact molecular mechanisms behind this observation are still to be fully elucidated [143], [379]–[381], [407], [408].

Here, the impact of *CgTPO4* expression in the context of virulence against the infection model *Galleria mellonella* was addressed. The larval immune system has high similarity to the mammalian innate immune system in what concerns both the phagocytic cells and the humoral response, involving antimicrobial peptides, to eliminate infecting microbes [409]. The influence of CgTpo4 in *C. glabrata* success of the infections in this host and the consequent impacts on the larval survival rate was evaluated. Given the obtained indications, the role of CgTpo4 in this process was investigated, with emphasis in its activity in antimicrobial peptide and polyamine resistance. These elements allow a deeper understanding of the mechanisms involved in *C. glabrata* virulence, a poorly characterized subject.

3.3. Methods

3.3.1. Strains, plasmids and growth medium

Candida glabrata KUE100 [339] and L5U1 (cgura3Δ0 cgleu2Δ0) [340] strains, the later kindly provided by John Bennett, NIAID, NIH, Bethesda, were used in this study. *C. glabrata* cells were cultivated in YPD medium, containing: 20 g/L D-(+)- glucose (Merck), 20 g/L bacterial-peptone (LioChem) and 10 g/L of yeast-extract (Difco). BM basal minimal medium used for the susceptibility assays contained 20 g/L glucose (Merck), 1.7 g/L yeast nitrogen base without amino acids or NH_4+ (Difco) and 2.65 g/L $(NH_4)_2SO_4$ (Merck). *S. cerevisiae* BY4741 wild-type strain, used in gene cloning through homologous recombination was grown in either YPD medium or BM-U medium, that resulted from BM supplementation with 20 mg/L methionine, 20 mg/L histidine and 60 mg/L leucine (all from Sigma). *C. glabrata* L5U1 strains were cultured in BM medium supplemented with 20 mg/L uracil and 60mg/L leucine.

3.3.2. Cloning of the *C. glabrata CgTPO4* gene (ORF *CAGL0L10912g*)

The pGREG576 plasmid from the Drag & Drop collection [341] was used to clone and express the *C. glabrata* ORF *CAGL0L10912g* in *S. cerevisiae*, as described before for other heterologous genes [219]. *CAGL0L10912g* DNA was generated by PCR, using genomic DNA extracted from the sequenced CBS138 *C. glabrata* strain, and the primers indicated in Table II.1. The amplified fragment was co-transformed into *S. cerevisiae* BY4741 strain with the pGREG576 vector, digested with SalI, to obtain through homologous recombination the pGREG576_*CgTPO4* plasmid. To enable *CgTPO4* expression in *C. glabrata*, the *GAL1* promoter was replaced by the copper-inducible *MT-I C. glabrata* promoter, giving rise to the pGREG576_*MT-I_CgTPO4* plasmid. The *MT-I* promoter DNA was generated by PCR, using genomic DNA extracted from the CBS138 *C. glabrata* strain, and the primers indicated in Table II.1. The amplified fragment was co-transformed into *S. cerevisiae* BY4741 strain with the pGREG576_*CgTPO4* plasmid, digested with SacI and NotI to remove the *GAL1* promoter, to generate through homologous recombination the pGREG576_*MT-I_CgTPO4* plasmid. Constructs were verified by DNA sequencing.

3.3.3. Deletion of the *C. glabrata CgTPO4* gene (ORF *CAGL0L10912g*)

The deletion of the *C. glabrata CgTPO4* gene (ORF *CAGL0L10912g*) was carried out in the parental strain KUE100, using the method described by Ueno *et al.* [339]. The target gene *CgTPO4* was replaced by a DNA cassette including the *CgHIS3* gene, through homologous recombination. The replacement cassette was prepared by PCR using the primers indicated in Table II.1. The pHIS906 plasmid including *CgHIS3* was used as a template and transformation was performed as described previously [339]. Recombination locus and gene deletion were verified by PCR using the primers indicated in Table II.1.

3.3.4. *Galleria mellonella* survival assays

Galleria mellonella larvae were reared in our lab insectarium, on a pollen grain and bee wax diet at 25 °C in the darkness. Last instance larvae weighting 250±25 mg were used in the survival assays and the larvae infection was based on the protocol previously described [383]. *C. glabrata* strains were cultivated in YPD until stationary phase, harvested by centrifugation and resuspended in PBS (pH 7.4). A micrometer device was used to control a microsyringe and inject 3.5 µL of yeast cell suspension (approximately $5x10^7$ cells per injection) into each caterpillar via the last left proleg, which had been previously surface sanitized with 70% (v/v) ethanol. Following injection, larvae were placed in Petri dishes and stored in the dark at 37 °C. For each condition, 10 larvae were used to follow the larval survival over a period of 72 h. Caterpillars were considered dead when they displayed no movement in response to touch. Control larvae were injected with PBS (pH 7.4).

3.3.5. *Galleria mellonella* hemocyte-yeast interaction assays

To isolate *G. mellonella* hemocytes, larvae previously anesthetized on ice and surface sterilized with 70% (v/v) ethanol were punctured in the abdomen with a sterile needle and the outflowing hemolymph was immediately collected into a sterile microtube containing anticoagulant buffer (98 mM NaOH, 145 mM NaCl, 17 mM EDTA, 41 mM citric acid [pH 4.5]) in a 1:1 proportion. The hemolymph was centrifuged at 250 × g for 10 min at 4 °C to pellet hemocytes and washed twice with PBS (centrifuged at 250 × g for 5 min at 4 °C). The hemocyte pellet was then gently suspended in 1 mL of GIM (Sigma) supplemented with 10% fetal bovine serum, 1% glutamine, and 1% antibiotic (10,000 U penicillin G, 10 mg streptomycin). Suspended hemocytes were counted with a hemocytometer and incubated at 25 °C in 24-well plates at a concentration of $2x10^5$ cells/mL. Monolayers of primary *Galleria* hemocytes were used for experiments the next day. All preparations and assays were carried out under sterile conditions.

Cultures of *C. glabrata* cells were grown in YPD medium until mid-exponential phase (OD_{600nm} = 0.4-0.6). The optical density of the cultures was measured, and the appropriate volume was collected to have $7×10^2$ cells/mL in PBS. *Galleria* hemocyte monolayer medium was replaced with GIM without antimycotics, and then cells were infected with the yeast suspensions with a MOI of 1:5. After 1 h of infection at 37 °C, the hemocytes were carefully washed twice with PBS, followed by the addition of GIM. The viable intracellular yeast cells were quantified 1 h, 4 h, 24 h and 48 h after infection. Cell monolayers were lysed with 0.5% Triton X-100, and CFU were determined by plating dilutions of cell lysates on YPD-agar plates followed by incubation at 30°C for 24 h.

3.3.6. Gene expression measurement

The transcript levels of genes encoding the *G. mellonela* antimicrobial peptides gallerimycin, galliomycin, IMPI (insect metalloproteinase inhibitor), lysozyme and cecropin were determined by RT-PCR. Three larvae per treatment for each time point (10 and 21 h post infection) were cryopreserved, sliced and homogenized in 1 mL of Trizol reagent (Sigma Aldrich). Whole animal RNA was extracted according to the manufacturer's protocol. RNA was treated with Turbo DNase (Ambio, Applied

Biosystems) according to manufacturer's recommendations and quantified spectrophotometrically (NanoDrop ND-1000). Total RNA was converted to cDNA for the real-time Reverse Transcription PCR using the MultiScribe Reverse Transcriptase kit (Applied Biosystems) and the 7500 RT-PCR thermal cycler block (Applied Biosystems). The real time PCR step was carried out using adequate primers (Table II.1), SYBR Green® reagents (Applied Biosystems) and the 7500 RT-PCR thermocycler block (Applied Biosystems). Default parameters set by the manufacturer were followed, and fluorescence was detected by the instrument and plotted in an amplification graph (7500 Systems SDS Software, Applied Biosystems). *G. mellonella* Actin encoding gene transcript level was used as an internal reference.

3.3.7. Candidacidal assays of histatin-5 and spermidine

To evaluate the effect of *CgTPO4* expression in histatin-5 resistance and spermidine resistance, wild-type and Δ*cgtpo4 C. glabrata* mutants were batch cultured in minimal medium until mid-exponential phase (OD_{600nm}=0.4-0.6), while *C. glabrata* L5U1 cells harboring the pGREG576_*MT-I_CgTPO4* plasmid were grown to mid-exponential phase (OD_{600nm}=0.5±0.05) in minimal medium containing 50 μM $CuSO_4$. Cells were then washed twice and resuspended in sterile PBS to an OD_{600nm}=0.01±0.001 and supplemented with 35 μM and 65 μM of histatin-5 (Sigma) for the wild-type KUE100 and Δ*cgtpo4*, and for *C. glabrata* L5U1 cells, respectively, or supplemented with 5 mM of spermidine. Cell suspensions were incubated at 30 °C under agitation (250 rpm) and cell viability was measured at 30 min intervals, based on the counting of CFU, determined by plating dilutions of the cell suspensions on YPD-agar plates followed by incubation at 30 °C for 24 h. Each result was compared with the initial cell content of the suspension in order to obtain a survival curve.

3.3.8. Subcellular localization of the CgTpo4 transporter

C. glabrata L5U1 cells harboring the pGREG576_*MT-I_CgTPO4* plasmid were grown to mid-exponential phase in minimal medium containing 50 μM $CuSO_4$. At a standard OD_{600nm}=0.5±0.05, obtained after around 5 h of incubation, cells were inspected through fluorescence microscopy. *S. cerevisiae* BY4741 cells harboring the pGREG576_*CgTPO4* plasmid were grown in BM-U medium with 1% galactose to induce protein expression. The distribution of CgTpo4_GFP protein in *S. cerevisiae* or in *C. glabrata* living cells was detected by fluorescence microscopy in a Zeiss Axioplan microscope (Carl Zeiss MicroImaging), using excitation and emission wavelength of 395 and 509 nm, respectively. Fluorescence images were captured using a cooled CCD camera (Cool SNAPFX, Roper Scientific Photometrics).

3.3.9. Susceptibility assays in *C. glabrata*

The susceptibility of *C. glabrata* cells towards toxic concentrations of the selected drugs and polyamines was evaluated as before, through spot assays [218], [219]. *C. glabrata* cell suspensions used to inoculate the agar plates were mid-exponential cells grown in adequate minimal medium, until culture OD_{600nm}=0.4±0.02 was reached and then diluted in sterile water to obtain suspensions with OD_{600nm}=0.05±0.005. These cell suspensions and subsequent dilutions (1:5; 1:25) were applied as 4 μL

spots onto the surface of solid medium, without uracil for strains transformed with the pGREG576 derived plasmids, and supplemented with adequate chemical stress concentrations. The tested drugs and chemicals included the following compounds, used in the specified concentration ranges: the polyamines spermine (10-15 mM), spermidine (4-10 mM) and putrescine (10-20 mM), the azole antifungal drugs fluconazole (10-200 mg/L), ketoconazole (10-50 mg/L), clotrimazole (1-20 mg/L), tioconazole (0.2-1 mg/L) and miconazole (0.2-1 mg/L), the polyene antifungal drug amphotericin B (0.1-0.5 mg/L), and the fluoropyrimidine 5-flucytosine (0.02-5 mg/L).

3.3.10. Spermidine accumulation assays

To analyse the accumulation ratio (intracellular/extracellular concentration) of radiolabeled [^{3}H]-spermidine (Amersham Biosciences) in *C. glabrata* wild-type and Δ*cgtpo4* strains, the two were grown in YPD medium (at pH 4.0) until mid-exponential phase (OD_{600nm}=0.5 ± 0.05), harvested by filtration, washed with fresh medium and finally resuspended in 5 mL of this same medium to obtain dense cell suspensions (OD_{600nm}=0.7 ± 0.05). These cell suspensions were incubated for 5 min at 30 °C with agitation (150 rpm). After that time, 0.1 µM of [^{3}H]-spermidine (Amersham Biosciences) was added to the cell suspension together with 8.5 mM unlabelled spermidine (Sigma). The intracellular accumulation of radiolabelled spermidine was followed during 60 min by filtering, at adequate intervals, 200 µL of the cell suspension through pre-wetted glass microfibre filters (Whatman GF/C). The filters were washed with ice-cold Tris-Magnesium Sulfate buffer (0.1 M Mes, 41 mM Tris, both from Sigma, adjusted to pH 4.0) and the radioactivity was measured in a Beckman LS 5000TD scintillation counter. Extracellular concentration of [^{3}H]-spermidine was estimated by measuring the radioactivity of 50 µL of the culture supernatant. Intracellular concentration of [^{3}H]-spermidine was calculated considering the internal cell volume (Vi) of the two strains constant and equal to 2.5 mL (mg dry weight)$^{-1}$ [410].

3.3.11. Estimation of plasma membrane potential

The estimation of the plasma membrane potential was carried out by measuring the fluorescence intensity of cells exposed to the fluorescent carbocyanine 3,3'-Dihexyloxacarbocyanine Iodide (DiOC6(3)) [411]. Cells were cultivated in YPD medium until mid-exponential phase, washed twice in Mes/glucose buffer [10 mM Mes, 0.1 mM MgCl2 and 20 g/L glucose (pH 5.6)] and resuspended in Mes/glucose buffer, supplemented with 250 nM DiOC6(3) (Molecular Probes), followed by incubation in the dark for 30 min at 30 °C with orbital agitation (250 rpm). After centrifugation cells were observed with a Zeiss Axioplan microscope equipped with adequate epifluorescence filters (BP450- 490 and LP520). Fluorescence emission was collected with a CCD camera (CoolSNAPFX, Roper Scientific Photometrics). For the excitation of the fluorescent molecule, radiation with a wavelength of 480 nm was used. The images were analysed using MetaMorph 3.5. The fluorescence intensity values, obtained pixel-by-pixel in the region of interest, were calculated for a minimum of 100 cells per experiment, considering a minimum of 3 independent experiments, *per* strain.

Table II. 1. List of primers used in this study. Unless otherwise indicated, the primers were generated in this study.

Name	Sequence (5'-3')
CgTPO4 gene cloning	
pGREG_CgTPO4 _FW	GAATTCGATATCAAGCTTATCGATACCGTCGACAATGGCCGGTACAAATCAAG
pGREG_CgTPO4_Rev	GCGTGACATAACTAATTACATGACTCGAGGTCGACCTATACCATTCTAGAGGAG
pGREG576 GAL-to-MTI promotor replacement	
pGREG_MTI_ FW	TTAACCCTCACTAAAGGGAACAAAAGCTGGAGCTCTGTACGACACGCATCATGTGGCAATC
pGREG_MTI_Rev	GAAAAGTTCTTCTCCTTTACTCATACTAGTGCGGCTGTGTTTGTTTTTGTATGTGTTTGTTG
CgTPO4 gene disruption	
ΔCgTPO4_FW	GAACTGGTGAAATATAGTATAAGCGTTACAAAGCGAATAACGAATACATACACCACGGCCGC TGATCACG
ΔCgTPO4_Rev	AAGAGCAAAAGTATTCAATTTTTTAAAAATTTAAAGCAAATCGAAAAAAAGGACTACATCGTGAGG CTGG
ΔCg TPO4_conf_FW	CAAGTTGGTGATACTAATAGCA
ΔCg TPO4_conf _Rev	CACTTCACTCAAGGGAGC
RT-PCR experiments	
P1RT Galle	CGCAATATCATTGGCCTTCT [412]
P2RT Galle	CCTGCAGTTAGCAATGCAC [412]
P1RT Galli	TCGTATCGTCACCGCAAAATG [413]
P2RT Galli	GCCGCAATGACCACCTTTATA [413]
P1RT IMPI	AGATGGCTATGCAAGGGATG [412]
P2RT IMPI	AGGACCTGTGCAGCATTTCT [412]
P1RT Lys	TCCCAACTCTTGACCGACGA [412]
P2RT Lys	AGTGGTTGCGCCATCCATAC [412]
P1RT Cecr	ATTTGCCTGCATCGTAGCG [414]
P2RT Cecr	CTTGTACTGCTGGACCAGCTTTT [414]
P1RT Act	ATCCTCACCCTGAAGTACCC [412]
P2RT Act	CCACACGCAGCTCATTGTA [412]

3.4. Results

3.4.1. *CgTPO4* is a determinant of *C. glabrata* virulence against the *G. mellonella* infection model

Using *G. mellonella* larvae as infection model, the possible effect of *CgTPO4* deletion in *C. glabrata* ability to exert its virulence was assessed. The survival of the larvae was evaluated after 24 h, 48 h and 72 h upon injection of $5x10^7$ fungal cells. The wild-type KUE100 *C. glabrata* strain was, thus, found to be able to kill 30% more larvae than the derived *Δcgtpo4* deletion mutant (Figure II.18A). Additionally, the overexpression of *CgTPO4* in the L5U1 *C. glabrata* wild-type, using the expression vector pGREG576_*MT-I_CgTPO4*, was found to lead to a 70% decrease in *G. mellonella* survival rate, when compared with L5U1 cells harboring the cloning vector pGREG576 (Figure II.18B). This data shows that CgTpo4 is a determinant of *C. glabrata* virulence against the infection model *G. mellonella.*

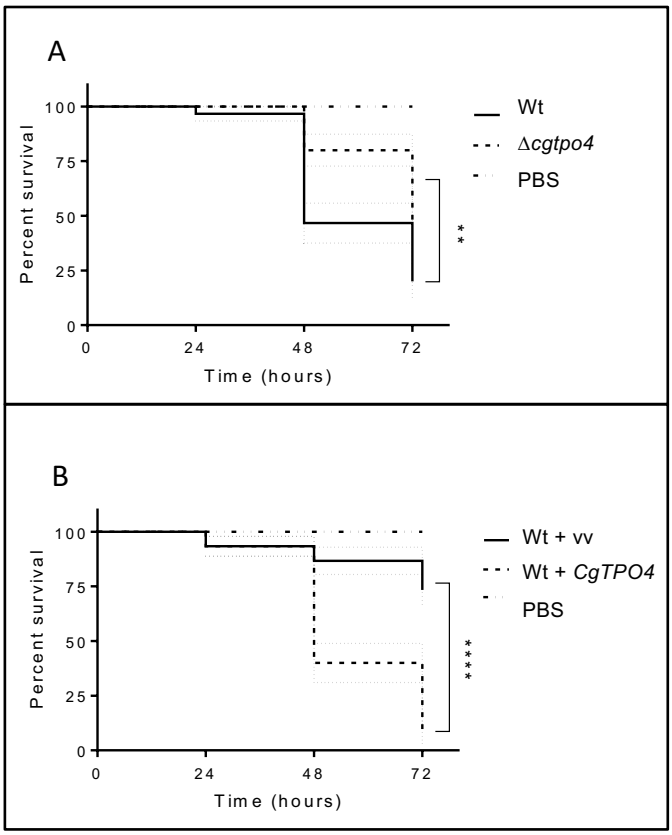

Figure II.18. *CgTPO4* expression increases *C. glabrata* virulence against the *G. mellonella* infection model. A) The survival of larvae injected with approximately $5x10^7$ CFU/larvae of KUE100 *C. glabrata* wild-type, derived Δ*cgtpo4* deletion mutant or PBS as control, is displayed as Kaplan-Meier survival curves. B) The survival of larvae injected with approximately $5x10^7$ CFU/larvae of L5U1 *C. glabrata* wild-type strain, harboring the pGREG576 cloning vector or the pGREG576_*MT-I_CgTPO4* expression plasmid, or injected with PBS as control, is displayed as Kaplan-Meier survival curves. The displayed results are the average of at least three independent experiments, standard deviation being represented by the grey lines. **P<0.01; ****P<0.0001.

3.4.2. *CgTPO4* confers resistance to the human antimicrobial peptide histatin-5, but not to phagocytosis

Based on the observation that *CgTPO4* increases *C. glabrata* ability to kill *G. mellonella* larvae, an effort was put into the identification of the role of CgTpo4 in this context.

The first hypothesis tested was that CgTpo4 could protect the yeast cells from stress induced during phagocytosis. To assess that, *C. glabrata* cells were exposed to a cell culture of *G. mellonella* hemocytes. The concentration of viable *C. glabrata* cells found within the hemocytes was measured after 1 h, 4 h, 24 h and 48 h after co-culture. At all time-points, the number of viable wild-type cells internalized within hemocytes was found to be undistinguishable of the number of *Δcgtpo4* cells internalized within hemocytes (results not shown).

Another possible mechanism by which the CgTpo4 transporter may increase *C. glabrata* ability to kill *G. mellonella* larvae is by mediating resistance to AMPs present in the insect's hemolymph. To test if this transporter is involved in AMP resistance, cell cultures of both wild-type and derived Δ*cgtpo4* deletion mutant were grown until mid-exponential phase and incubated in the presence of histatin-5, which is known to possess candidacidal properties [415]. Upon 1 h of incubation in the presence of 35 μM histatin-5, about the same concentration found in the human saliva, 60% of the *C. glabrata* wild-type population was seen to survive, whereas only 30% of the Δ*cgtpo4* mutant population remains viable in the same period (Figure II.19A). Furthermore, overexpression of *CgTPO4* in a wild-type background increases *C. glabrata* resistance to this antimicrobial peptide (Figure II.19B). This might explain why the deletion of this transporter causes yeast cells to become less virulent, since the increased effectiveness of antimicrobial peptides action on the mutant cells might be compromising the progress of infection.

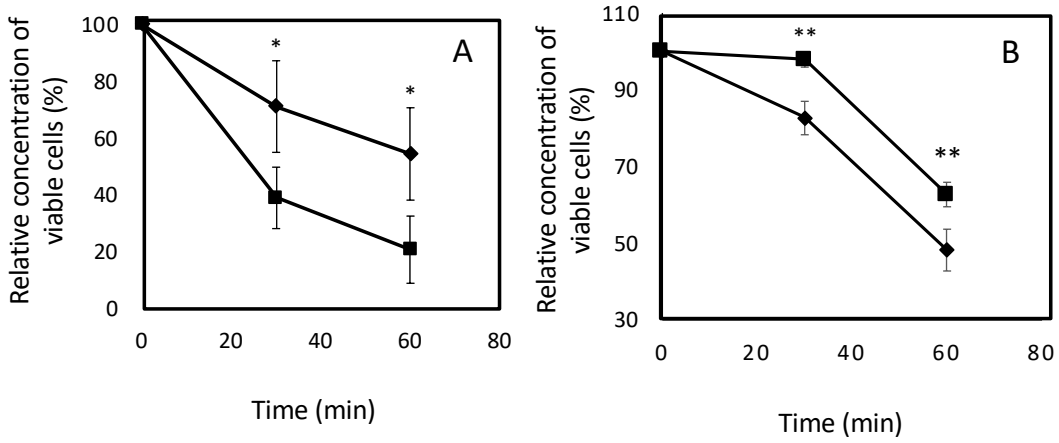

Figure II.19. CgTpo4 is a determinant of histatin-5 resistance. Survival curves of *C. glabrata* KUE100 wild-type (♦) and derived Δ*cgtpo4* deletion mutant (■) cells in the presence of 35 μM of histatin-5 (A) or of *C. glabrata* L5U1 wild-type cells, harboring the cloning vector pGREG576 (♦) or the expression plasmid pGREG576_*MT-I_CgTPO4* (■) in the presence of 65 μM of histatin-5 (B), were determined over a 60 min period. The average percentage of survival, obtained from at least three independent experiments, is indicated by the black lines, standard deviation being represented by error bars. *P<0.05; **P<0.01.

3.4.3. Antimicrobial peptide gene expression is highly activated in *G. mellonella* larvae in response to infection by *C. glabrata*

In order to evaluate the importance of AMPs in the response to *C. glabrata* infection, the transcript levels of five immune-responsive genes, encoding peptides with antimicrobial properties were assessed through quantitative RT-PCR. The assessed AMPs were gallerimycin, galliomycin, IMPI, lysozyme and cecropin. Interestingly, a stepwise increase in the expression of gallerimycin and galliomycin in larvae injected with *C. glabrata* cells was observed, this increase reaching dramatic 60-fold and 25-fold higher transcript levels at 24 h after infection, when compared to control larvae, respectively (Figure II.20A-B). The results obtained for the three other tested AMPs were less impressive, but still significant with lysozyme and cecropin encoding genes showing a 4-fold upregulation after 24 h of *C. glabrata* infection (Figure II.20D-E), suggesting that these AMPs constitute a later response to fight the fungal infection. No significant change in IMPI expression during infection by *C. glabrata* was registered (Figure II.20C).

To evaluate whether the decreased virulence exhibited by Δ*cgtpo4* deletion mutant, when compared to the wild-type strain, could be related to decreased ability of *G. mellonella* to detect the mutated pathogen and activate its immune response, the expression of the same AMP encoding genes was measured in *G. mellonella* larvae exposed to Δ*cgtpo4* mutant cells. Interestingly, the deletion of *CgTPO4* did not change significantly the larval response to infection in terms of AMP expression, except for the levels registered after 1 h and 12 h of exposure, where the larvae appear to respond even more intensely to the mutant strain, when compared to the wild-type strain (Figure II.20A-E).

Altogether, these results show that *C. glabrata* cells are recognized as external agents stimulating the host immune responses in the infection model *G. mellonella*. Additionally, CgTpo4 does not seem to affect the host's ability to activate its defenses.

3.4.4. *CgTPO4* is a determinant of polyamine resistance in *C. glabrata*

Given that the TPO transport proteins have been characterized as polyamine transporters in *S. cerevisiae* [406], [416], it seemed relevant to evaluate if CgTpo4 had similar transport abilities. This effect appeared particularly relevant since AMP transport has been linked to polyamine transporters, as exemplified in the case of histatin-5 in *C. albicans* cells [417].

To this end, the susceptibility against inhibitory concentrations of polyamines exhibited by *Δcgtpo4* deletion mutant cells was compared to that of the parental wild-type strain. Using spot assays, the *Δcgtpo4* mutant showed higher spermidine and putrescine susceptibility than the wild-type strain, a stronger effect being apparent for spermidine (Figure II.21A). Consistently, overexpression of *CgTPO4* from an expression plasmid in a wild-type *C. glabrata* strain, in comparison with the same strain harboring the corresponding cloning vector, was found to lead to increased resistance to spermidine and putrescine (Figure II.21B). Additionally, cell cultures of both wild-type and derived Δ*cgtpo4* deletion mutant were grown until mid-exponential phase and incubated in the presence of spermidine. Upon 1 h of incubation in the presence of 5 mM spermidine, 70% of the *C. glabrata* wild-type population was seen to survive, whereas only 50% of the Δ*cgtpo4* mutant population remains viable in the same period (Figure II.22), confirming the results obtained through spot assays.

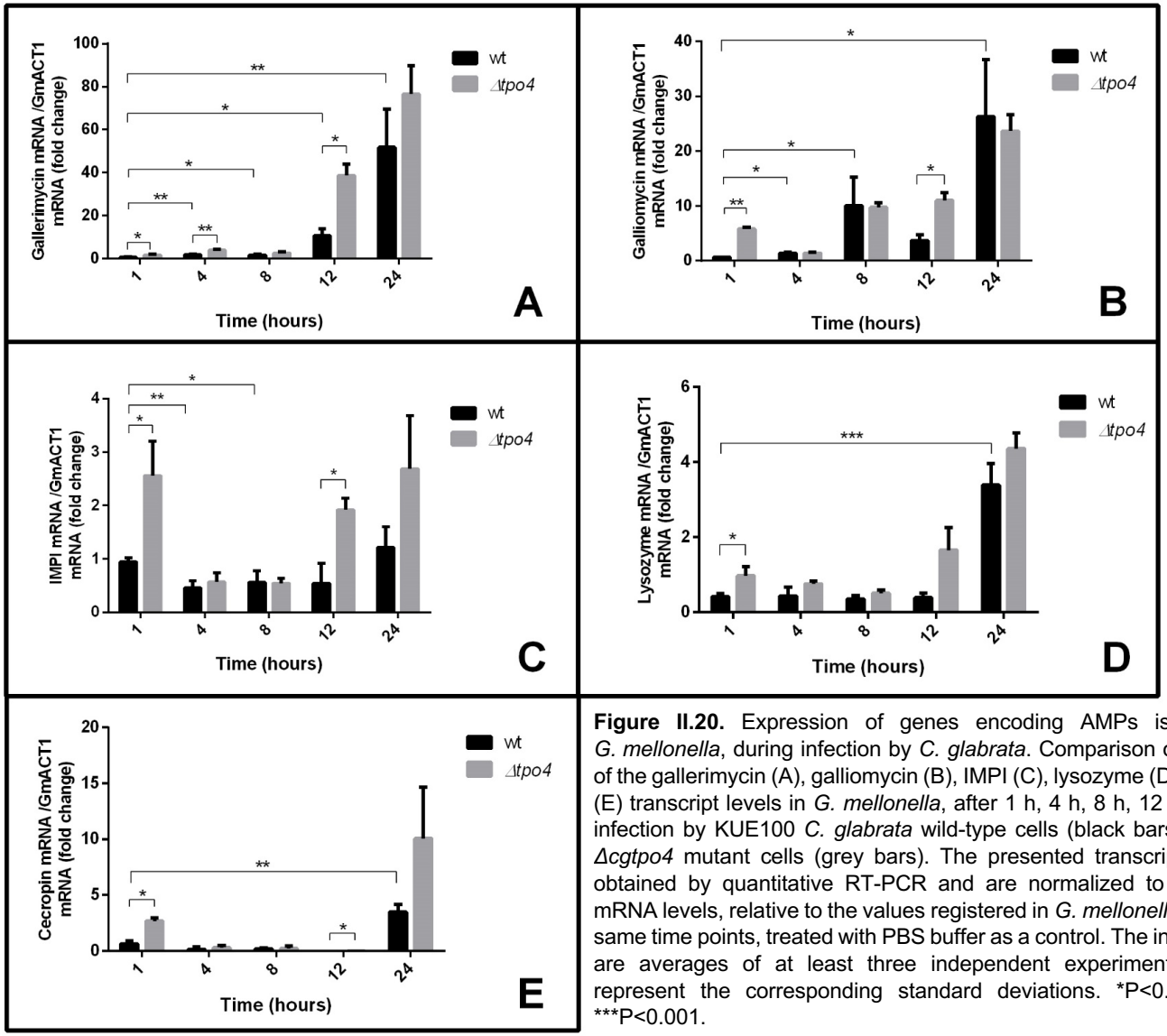

Figure II.20. Expression of genes encoding AMPs is activated in *G. mellonella*, during infection by *C. glabrata*. Comparison of the variation of the gallerimycin (A), galliomycin (B), IMPI (C), lysozyme (D) and cecropin (E) transcript levels in *G. mellonella*, after 1 h, 4 h, 8 h, 12 h, and 24 h of infection by KUE100 *C. glabrata* wild-type cells (black bars) and derived *Δcgtpo4* mutant cells (grey bars). The presented transcript levels were obtained by quantitative RT-PCR and are normalized to the *GmACT1* mRNA levels, relative to the values registered in *G. mellonella* larvae, in the same time points, treated with PBS buffer as a control. The indicated values are averages of at least three independent experiments. Error bars represent the corresponding standard deviations. *P<0.05; **P<0.01; ***P<0.001.

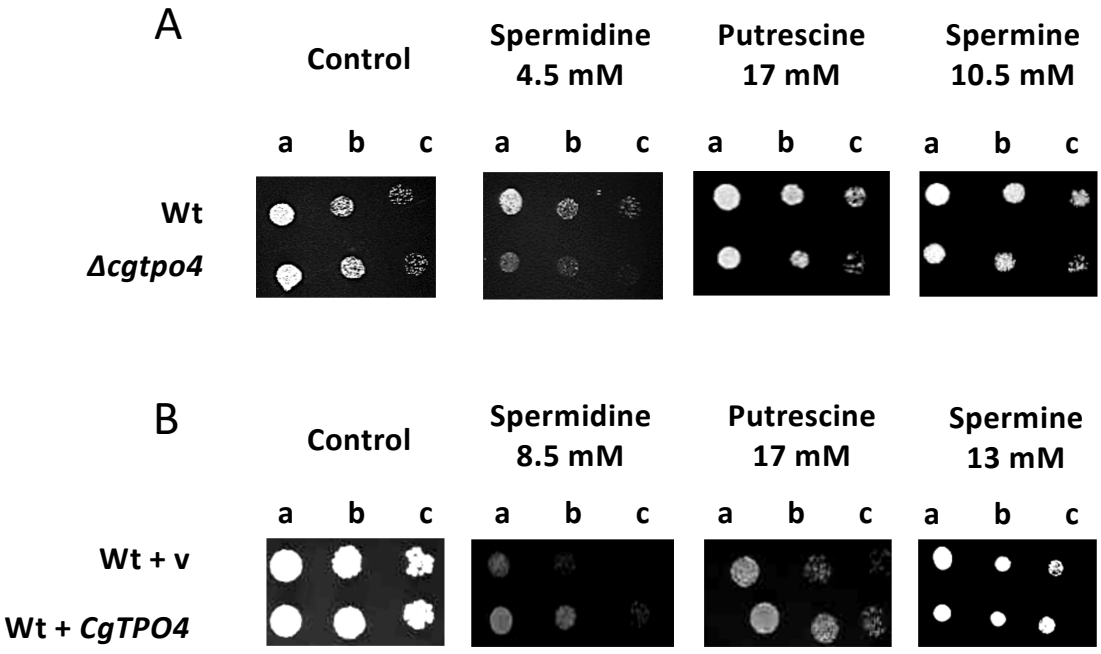

Figure II.22. *CgTPO4* confers resistance to polyamines in *C. glabrata*. A) Comparison of the susceptibility to the polyamines, spermidine, putrescine or spermine, at the indicated concentrations, of the *C. glabrata* KUE100 (Wt) and derived KUE100_*Δcgtpo4* mutant cells, in YPD agar plates, by spot assays. B) Comparison of the susceptibility to spermidine, putrescine or spermine at the indicated concentrations, of the *C. glabrata* L5U1 strain (wild-type - wt), harboring the pGREG576 cloning vector (v) or the pGREG576_*MT-I_CgTPO4* in YPD agar plates, by spot assays. The inocula were prepared as described in the materials and methods section. Cell suspensions used to prepare the spots were 1:5 (b) and 1:25 (c) dilutions of the cell suspension used in (a). The displayed images are representative of at least three independent experiments.

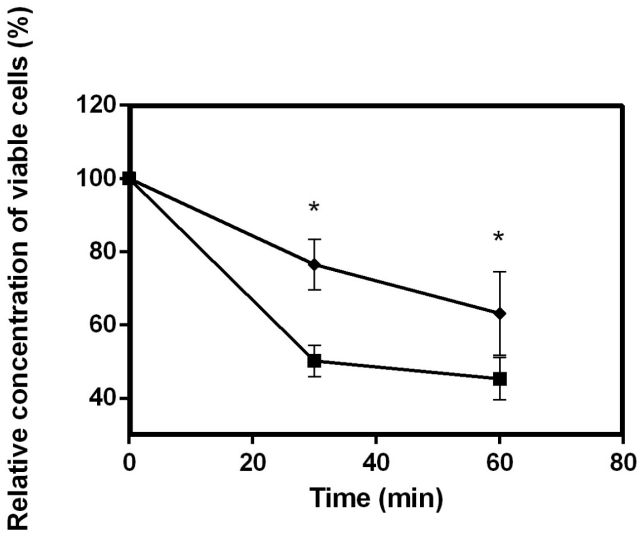

Figure II.21. CgTpo4 is a determinant of spermidine resistance. Survival curves of *C. glabrata* KUE100 wild-type (♦) and derived Δ*cgtpo4* deletion mutant (■) cells were determined over a 60 min period, in the presence of 5 mM of spermidine. The average percentage of survival, obtained from at least three independent experiments, is indicated by the black lines, standard deviation being represented by error bars. *P<0.05.

3.4.5. CgTpo4 is a plasma membrane polyamine exporter

In order to assess the role of CgTpo4 in polyamine resistance, it is crucial to confirm its subcellular localization. In *C. glabrata* cells harboring the pGREG576_*MT-I_CgTPO4* plasmid, the CgTpo4_GFP fusion protein was found to be predominantly localized to the cell periphery (Figure II.23). *S. cerevisiae* cells harboring the pGREG576_*CgTPO4* plasmid were also tested for the subcellular localization of CgTpo4, to verify if, this transporter was localized similarly (Figure II.23).

To assess the exact role of this transporter in polyamine resistance, the intracellular accumulation of radiolabeled [^{3}H]-spermidine was performed for both wild-type and *Δcgtpo4* cells. The *Δcgtpo4* deletion mutant exhibited three-fold higher intracellular accumulation of radiolabeled spermidine when compared with the wild-type strain, meaning that *CgTPO4* expression is strongly related to a decreased polyamine accumulation in *C. glabrata* cells (Figure II.24). Therefore, and in resemblance to its orthologue in *S. cerevisiae*, there are strong indications to suggest that the CgTpo4 transporter plays a role in polyamine resistance, by mediating the extrusion of polyamines from within the yeast cell to the extracellular medium.

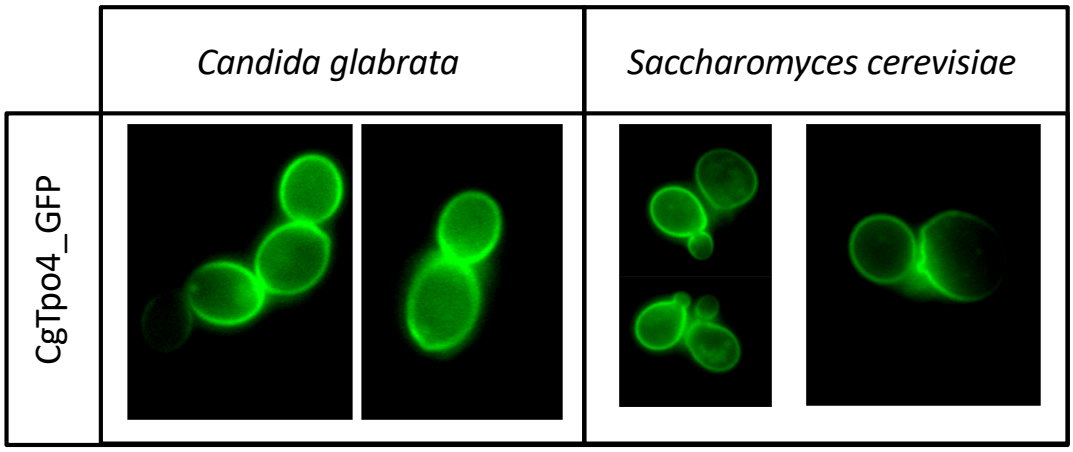

Figure II.23. CgTpo4 is localized in the plasma membrane of yeast cells. Fluorescence of exponential-phase L5U1 *C. glabrata* cells or BY4741 *S. cerevisiae* cells, harboring the pGREG_*MT-I_CgTPO4* or pGREG576_*CgTPO4* plasmids, after 5 h of copper- or galactose-induced recombinant protein production, respectively. Results indicate that the CgTpo4-GFP fusion protein localizes to the plasma membrane in both *S. cerevisiae* and *C. glabrata* cells.

3.4.6. *CgTPO4* deletion leads to increased membrane potential in *C. glabrata* cells

Given the cationic nature of polyamines, their homeostasis impacts the plasma membrane potential. As such, the role of CgTpo4 in this physiological parameter was evaluated indirectly, by monitoring the accumulation of the fluorescent dye DIOC6(3) [411]. The obtained results show that the *Δcgtpo4* deletion mutant cells exhibit higher membrane potential than wild-type cells. The deletion of *CgTPO4* leads to a 2-fold increase in the average cellular fluorescent intensity (Figure II.25). Altogether these results suggest that this gene may play a role in maintaining the plasma membrane potential, directly or indirectly through the transport of polyamines.

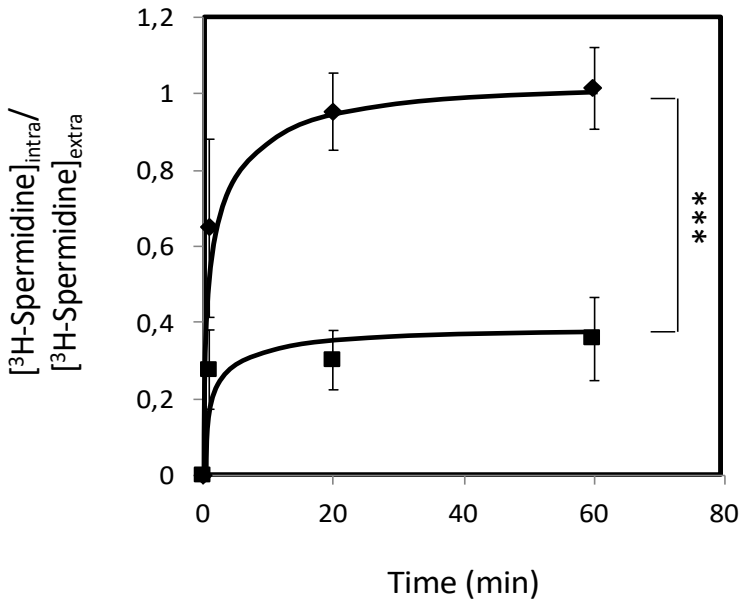

Figure II.25. *CgTPO4* expression leads to decreased spermidine accumulation in *C. glabrata.* Time course accumulation ratio of [^{3}H]-Spermidine in non-adapted cells of KUE100 *C. glabrata* wild-type (■) or KUE100_*Δcgtpo4* (♦) strains, during cultivation in YPD liquid medium in the presence of 8.5 mM unlabeled spermidine. The accumulation ratio values are averages of at least three independent experiments. Error bars represent the corresponding standard deviations. ****p*<0.001.

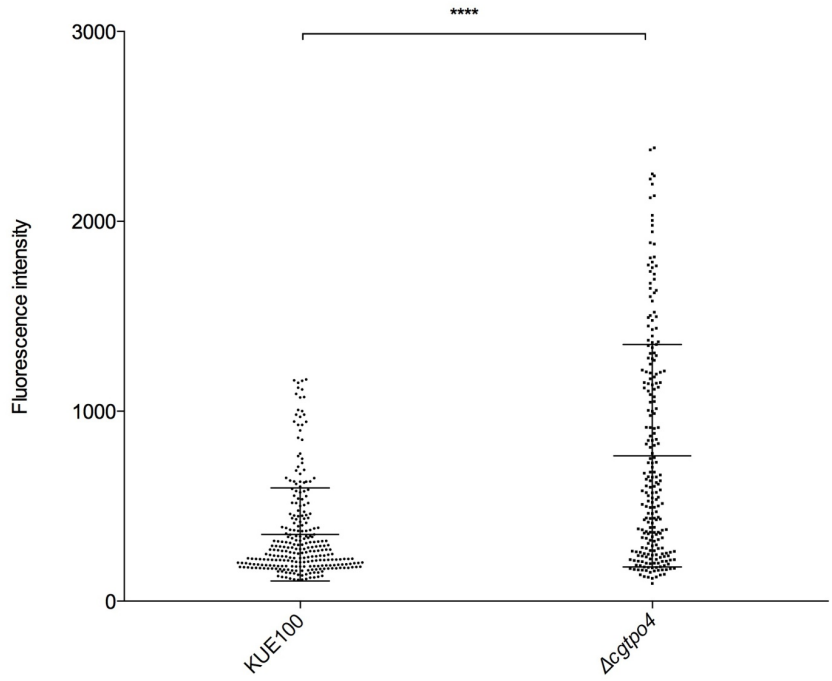

Figure II.24. The deletion of *CgTPO4* increases plasma membrane potential. Comparison of the fluorescence intensity of *C. glabrata* KUE100 wild-type and derived *Δcgtpo4* mutant cells incubated with the fluorescent dye DiOC6(3), whose uptake and accumulation depends on the plasma membrane potential. A scatter dot plot representation of the data is shown, where each dot represents the fluorescence intensity of individual cells. The average level of intensity, considering at least three independent experiments, and at least 100 cells per experiment, is indicated by the black line (-), standard deviation being represented by error bars. ****p<0.0001.

3.5. Discussion

In this study, the CgTpo4 transporter, predicted to be a multidrug transporter of the MFS, is demonstrated to play a role in *C. glabrata* virulence, this effect being proposed to be based on its ability to confer AMP resistance, and to act as a plasma membrane polyamine exporter (Figure II.26).

CgTpo4 was shown to increase the ability of *C. glabrata* cells to kill the infection model *G. mellonella*. Since this model system presents an immune system which is highly similar to the mammalian innate immune system, dependent of phagocytic cells (hemocytes and macrophages, respectively) that allow *C. glabrata* to survive and replicate for a prolonged time, and the release of antimicrobial stress inducers such as AMPs, the use of *Galleria mellonella* is considered a suitable model to understand virulence mechanisms in the human host [143], [227], [418].

During the triggering of an inflammatory response, neutrophils and macrophages are recruited and basophils and mast cells in the nearby connective tissues are stimulated to produce peptides that help eliminating the foreign pathogen [419]. Increased levels of AMP expression in *G. mellonella* had been observed upon exposure to *Salmonella enterica* serovar *typhimurium*, reaching after 16 h of injection an 80-fold, 10-fold and 15-fold increase in gallerimycin, galliomycin and lysozyme expression, respectively [420]. In the case of infection by *Legionella pneumophila*, *G. mellonella* larvae displayed 3-fold higher expression of gallerimycin and galliomycin after 24 h of injection [421]. In this study, the activation of immune-response genes encoding AMPs in response to *C. glabrata* were observed for the first time, demonstrating that these mechanisms are indeed activated in *G. mellonella* against *C. glabrata* infections. Interestingly, antifungal activity had been registered in *G. mellonella* hemolymph [422]. Additionally, some of the *G. mellonella* AMPs have been shown to display antifungal activity, specifically lysozyme has been shown to inhibit *C. albicans* growth [423], while gallerimycin was found to exhibit activity against the environmental fungi *Matarhizium anisophiae* [424], *Sclerotinia minor* and *Erysiphe cichoracearum* [425]. The profile of AMP activation induced by *C. glabrata* is slightly different from that registered during infections with other species, suggesting that *G. mellonella* perception and reaction to the presence of pathogens varies from species to species. In the case of *C. glabrata*, registered herein, gallerimycin and galliomycin seem to be the most activated AMPs, eventually corresponding to the most effective AMPs against this fungal pathogen in *G. mellonella*.

In the attempt to find the molecular basis of CgTpo4 activity as a virulence determinant, CgTpo4 was found not to affect *C. glabrata* proliferation upon phagocytosis, but rather to contribute to the resistance to AMPs. Indeed, CgTpo4 was found to confer resistance to the human AMP histatin-5. Histatins are histidine-rich antimicrobial proteins found in saliva secreted by Ebner's glands, and they offer early defense against incoming microorganisms, especially fungi [426]. Histatin-5 is the smallest of the major salivary histatins and the most active in terms of its antifungal properties that resorts to proteolysis to eliminate threats [426]. The observation made in this study that CgTpo4 confers histatin-5 resistance is coherent with the previous observation that two other members of the DHA family, CaFlu1, in *C. albicans* [427], and CgTpo1_1, in *C. glabrata* [143], also confer resistance to this AMP. These facts point out to the possibility that several members of the DHA family, including CgTpo4, are required for

full protection against AMPs, in both larval and human hosts, contributing in that fashion to increase yeast survival and proliferation during the infection cycle.

Given that the TPO transport proteins have been characterized as polyamine exporters in *S. cerevisiae* [406], [416] and in *C. glabrata* [144], [220], and the fact that AMP transport has been linked to polyamine transporters [417], it seemed relevant to evaluate if CgTpo4 had similar polyamine transport functions. Although no role in antifungal drug resistance could be attributed to CgTpo4, this transporter was found to act as a plasma membrane polyamine exporter. Since *Δcgtpo4* deletion mutant cells were shown to display on average a 2-fold higher plasma membrane potential than wild-type cells, it is possible to suggest that this transporter is involved, directly or indirectly, in the maintenance of plasma membrane potential, by controlling the homeostasis of polycationic polyamines and entrance of H^+ inside the cell. This appears to be consistent with the participation of several DHA transporters in the transport of cations and polycations in *S. cerevisiae* [406], [428], [429] and in *C. glabrata* [144], [220], a process that is bound to affect plasma membrane potential. This role is even more necessary upon the presence of both spermidine and histatin-5 simultaneously. Polyamines are present in the saliva of healthy individuals and increases in concentration in pancreatic cancer patients [430]. Given the presence of both molecules in the saliva, it is important to consider the effects of histatin-5 together with other components of the saliva.

Previous reports have already shown that DHA encoding genes *CaQDR1*, *CaQDR2* and *CaQDR3*, in *C. albicans* [381], and *CgDTR1*, *CgTPO1_1* and *CgTPO1_2*, in *C. glabrata* [143], [407], are involved in the infection outcome of pathogenic yeasts. This study adds CgTpo4 to this battery of virulence factors coming from a family of transporters of drugs, xenobiotics and inhibitory chemical compounds, reinforcing the notion that effectors of resistance to host-induced stress are key factors in pathogenesis, and constitute interesting new drug targets for antifungal therapy.

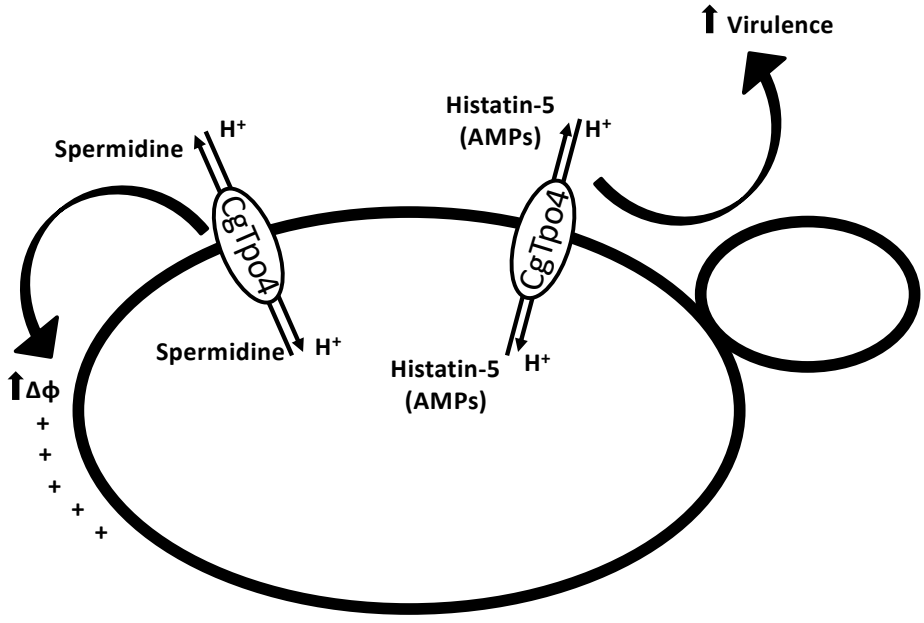

Figure II.26. CgTpo4 is a new determinant of *C. glabrata* virulence. Schematic of the proposed roles of CgTpo4 in the resistance to histatin-5, as a plasma membrane spermidine exporter, and in the regulation of plasma membrane potential.

3.6. Acknowledgements

This work was supported by “Fundação para a Ciência e a Tecnologia” (FCT) (Contract PTDC/BBB-BIO/4004/2014; PhD grants to MC (PD/BD/116946/2016) and PP (PD/BD/113631/2015) and post-doctoral grants to CC (SFRH/BPD/100863/2014) and DMH (SFRH/BPD/91831/2012). Funding received by iBB-Institute for Bioengineering and Biosciences from FCT-Portuguese Foundation for Science and Technology (UID/BIO/04565/2013) and from Programa Operacional Regional de Lisboa 2020 (Project N. 007317) is acknowledged. We acknowledge John Bennett, of the National Institute of Allergy and Infectious Diseases, NIH, Bethesda, USA, for kindly providing the L5U1 strain.

3.7. Author Contributions

MCT, DMH, AMF and HC designed the research plan, with contributions from MC, DR and RS. MC and DR conducted most of the experiments, with contributions from RS, PP, CC and MG. ATN and HC participated in the molecular biology of *C. glabrata* strains, while DMH and AMF participated the virulence and phagocytosis experiments. MCT, MC and DR wrote the manuscript. All authors discussed the results and contributed to the final manuscript.

III. Cell Peripheral Proteins Involved in Biofilm Formation are Key Players in *Candida glabrata* Azole Resistance

Journal papers

Mafalda Cavalheiro, Catarina Costa, Ana Silva-Dias, Isabel M. Miranda, Can Wang, Pedro Pais, Sandra N. Pinto, Dalila Mil-Homens, Michiyo Sato-Okamoto, Azusa Takahashi-Nakaguchi, Raquel M. Silva, Nuno P. Mira, Arsénio M. Fialho, Hiroji Chibana, Acácio G. Rodrigues, Geraldine Butler, Miguel C. Teixeira, A Transcriptomics Approach To Unveiling the Mechanisms of *In Vitro* Evolution towards Fluconazole Resistance of a *Candida glabrata* Clinical Isolate. Antimicrob Agents Chemother. 63(1). pii: e00995-18. doi: 10.1128/AAC.00995-18, 2018.

Mafalda Cavalheiro, Pedro Pais, Catarina Costa, Rui Santos, Michiyo Okamoto, Azusa Takahashi-Nakaguchi, Hiroji Chibana, Miguel Cacho Teixeira, 2. Eisosome component Pil2 participates in azole drug resistance and biofilm formation in *Candida glabrata* (in preparation).

1. A transcriptomics approach to unveiling the mechanisms of *in vitro* evolution towards fluconazole resistance of a *Candida glabrata* clinical isolate

1.1. Abstract

Candida glabrata is an emerging fungal pathogen. Its increased prevalence is associated with its ability to rapidly develop antifungal drug resistance, particularly to azoles. In order to unravel new molecular mechanisms behind azole resistance, a transcriptomics analysis of the evolution of a *C. glabrata* clinical isolate (isolate 044) from azole susceptibility to posaconazole resistance (21st day), clotrimazole resistance (31st day), and fluconazole and voriconazole resistance (45th day), induced by longstanding incubation with fluconazole, was carried out. All the evolved strains were found to accumulate lower concentrations of azole drugs than the parental strain, while the ergosterol concentration remained mostly constant. However, only the population displaying resistance to all azoles was found to have a gain-of-function mutation in the *C. glabrata PDR1* gene, leading to the upregulation of genes encoding multidrug resistance transporters. Intermediate strains, exhibiting posaconazole/clotrimazole resistance and increased fluconazole/voriconazole MIC levels, were found to display alternative ways to resist azole drugs. Particularly, posaconazole/clotrimazole resistance after 31 days was correlated with increased expression of adhesin genes. This finding led us to identify the Epa3 adhesin as a new determinant of azole resistance. Besides being required for biofilm formation, Epa3 expression was found to decrease the intracellular accumulation of azole antifungal drugs. Altogether, this work provides a glimpse of the transcriptomics evolution of a *C. glabrata* population toward multiazole resistance, highlighting the multifactorial nature of the acquisition of azole resistance and pointing out a new player in azole resistance.

1.2. Introduction

Candida glabrata is today the second or third most common cause of candidiasis, most likely because of its resistance to antifungal drugs, particularly azole drugs, which are used as prophylaxis and first- or second-line therapy [202], [431]. Early azole formulations, such as the imidazoles miconazole, clotrimazole and ketoconazole are frequently used for the treatment of fungal mucocutaneous infections even though they exhibit some toxicity in the treatment of systemic infections [432]. The triazole drug fluconazole has been extensively used in prophylaxis and in the treatment of candidiasis, favoring the increase of drug-resistant *C. glabrata* infections [431], [433]. Triazole drugs are significantly safer and more tolerable in systemic therapy then imidazoles [434], while newer triazoles such as posaconazole and voriconazole, exhibit broader-spectrum and more-potent activity than fluconazole [435].

The most common cause of clinically acquired azole resistance is the upregulation of genes encoding drug efflux pumps from the ATP-binding cassette (ABC) superfamily and the major facilitator

superfamily (MFS). One particular ABC transporter, *Candida glabrata* Cdr1 (CgCdr1), is often involved in the acquisition of fluconazole resistance in *C. glabrata* isolates [211], [214]. Additionally, CgCdr2/Phd1 and CgSnq2, two other ABC drug efflux pumps, have also been associated with fluconazole resistance in *C. glabrata*, their overexpression often resulting from the acquisition of gain-of-function (GOF) mutations in *CgPDR1* gene [213], [214]. Several MFS multidrug transporters have also been linked to fluconazole resistance in *C. glabrata* [378]. For example, azole resistance has been associated with the overexpression of the drug:H^+ antiporters (DHA) CgQdr2, CgTpo1_1, CgTpo1_2 and CgTpo3 [144], [219]–[221]. In the case of posaconazole, a study of seven posaconazole-resistant *Candida albicans* isolates revealed no changes in the expression of the drug transporters Cdr1, Cdr2, and Mdr1 [436], suggesting that posaconazole resistance may be dissociated from antifungal transport.

In many *C. albicans* clinical isolates, azole resistance arises from point mutations that lead to conformational changes in Erg11, the primary target of azoles [437]. In *C. glabrata,* a G944A mutation in *ERG11* gene was associated with fluconazole, voriconazole and polyene resistance in one specific isolate [233]. A second fluconazole-resistant isolate of *C. glabrata* was revealed to have increased expression of *ERG11* due to duplication of the entire chromosome containing this gene [438]. However, in all other studies on azole-resistant clinical isolates of *C. glabrata*, no mutation or upregulation of *ERG11* gene was observed, suggesting that this is not an important mechanism for clinical acquisition of resistance to azoles [230], [238], [439]. On the other hand, an E139A mutation in the *ERG3* gene, also involved in the ergosterol biosynthesis, was found to lead to increased resistance to fluconazole in *C. glabrata* strains [234], while in *Candida parapsilosis,* a similar mutation appeared in a posaconazole-resistant strain [440]. Mutation of the *ERG3* gene leads to the formation of ergosta-7,22-dien-3β-ol as the major sterol produced, instead of ergosta-5,7,24(28)-trienol [441]. This alteration prevents azole action, since the toxic sterols that accumulate upon the inhibition of Erg11 can no longer be synthesized by this pathway.

Resistance to azole drugs has mostly been examined as a whole, with little distinction between the mechanisms that may be specific to each azole drug. However, several epidemiological surveys on fluconazole, voriconazole and posaconazole resistance in *C. glabrata* have revealed that several clinical isolates display different levels of resistance to each of these drugs [28], [442], [443]. In this work, the azole-susceptible *C. glabrata* isolate 044, recovered from a positive blood culture, was exposed for prolonged periods to serum-level concentrations of fluconazole resulting in multiazole resistance: after 21 days, posaconazole resistance was reached, followed by clotrimazole resistance after 31 days and, finally, fluconazole and voriconazole resistance upon 45 days of induction. A transcriptomics characterization of the evolution of the 044 clinical isolate from azole susceptibility to stepwise acquisition of resistance to multiple azoles was carried out. On the basis of transcriptomics data, the role of adhesin-encoding genes, especially *CgEPA3*, was investigated in the context of azole drug resistance, establishing a fascinating link between cell to cell adhesion, biofilm formation and drug resistance.

1.3. Materials and Methods

1.3.1. Strains and growth medium

The 044 clinical isolate of *Candida glabrata* studied herein was collected from a patient attending Centro Hospitalar de São João, in Porto, Portugal. *C. glabrata* strains 044Fluco21 (posaconazole resistant), 044Fluco31 (resistant to posaconazole and clotrimazole), and 044Fluco45 (resistant to posaconazole, clotrimazole, fluconazole and voriconazole) were obtained in this study through the directed evolution of the 044 clinical isolated, as described below. Additionally, the wild-type KUE100 and CBS138 *C. glabrata* strains were used. Cells were batch-cultured at 30 ºC with orbital agitation (250 rpm) in the following growth media: yeast extract-peptone-dextrose (YPD) growth media, containing per liter: 20 g glucose (Merck), 20 g yeast extract (Difco) and 10 g bacterial-peptone (LioChem); BM minimal growth medium contained per liter: 20 g glucose (Merck), 2.7 g $(NH_4)_2SO_4$ (Merck), 1.7 g yeast nitrogen base without amino acids or $(NH_4)_2SO_4$ (Difco); The Roswell Park Memorial Institute (RPMI) 1640 medium contained 18 g glucose (Merck), 10.4 g RPMI-1640 (Sigma), 34.53 g morpholinepropanesulfonic acid (MOPS; Sigma) per liter; Sabouraud's dextrose broth (SDB) contained 40 g glucose (Merck) and 10 g peptone (LioChem) per liter.

The VK2/E6E7 human epithelium cell line (ATCC® CRL-2616™) was used for adhesion assays. This cell line is derived from the vaginal mucosa of healthy premenopausal female subjected to vaginal repair surgery and was immortalized with human papillomavirus 16/E6E7. Cells maintenance was achieved with keratinocyte-serum free medium, containing 0.1 ng/mL human recombinant epidermal growth factor (EGF), 0.05 mg/mL bovine pituitary extract and an additional 44.1 mg/L calcium chloride. Cells were maintained at 37 °C, with 95% air and 5% CO_2.

1.3.2. *In vitro* induction of multiple azole resistance

Three, randomly selected colonies of the 044 clinical isolate, exhibiting susceptibility to all azoles tested, was incubated in 10 mL of YPD medium overnight in a rotating drum at 150 rpm, 35 °C. A 1-mL aliquot of this culture, containing 10^6 blastoconidia, was transferred to different vials, each containing 9 mL of culture medium with or without 16mg/mL fluconazole, a concentration of drug that corresponds to therapeutic levels in serum obtained during antifungal treatment [444], and was incubated overnight as described above. The following day, aliquots from each culture containing 10^6 blastoconidia were again transferred to fresh medium containing the same antifungal and were reincubated as described above. Each day, for the 80 days of the assay, a 1-mL aliquot from each subculture was mixed with 0.5 mL of 40% glycerol and was frozen at -70 °C for later testing. To assess resistance stability, the resistant isolates obtained were subcultured daily in the absence of the drug for 30 days. Three colonies from each isolate were incubated in 10 mL drug-free YPD medium at 35 °C, 150 rpm. The following day, aliquots were transferred into fresh medium. At each subculture, a 1-mL aliquot of the suspension was mixed with 0.5 mL of 40% glycerol, and the mixture was frozen at -70°C, for further testing.

1.3.3. Drug susceptibility assays

The MIC values of each antifungal drug were determined according to the M27-A3 protocol and the M27-S4 supplement of the Clinical and Laboratory Standards Institute (CLSI) [445]. Interpretative criteria for fluconazole and voriconazole were those of the CLSI: for fluconazole, a susceptible–dose-dependent (S-DD) MIC of ≤32mg/ml and a resistance (R) MIC of ≥64mg/ml; for voriconazole, a wild-type MIC of ≤0.5 mg/ml and a non-wild-type MIC of ≥1 mg/ml. Although susceptibility breakpoints have not yet been established for posaconazole or clotrimazole, strains inhibited by ≤4 mg/ml were considered to be susceptible to posaconazole or clotrimazole, respectively, considering that their breakpoints should be 4-fold higher in *C. glabrata* than in *C. albicans*, as is the case for fluconazole [446], [447]. Every 5 days of incubation, with or without the antifungal, MIC values were redetermined for fluconazole, voriconazole, posaconazole, and clotrimazole. *Candida glabrata* type strain CBS138 was used in each testing assay, as recommended.

The antifungal drug susceptibilities of the 044 clinical isolate and the derived azole-resistant strains (1), of the KUE100 parental strain and the derived Δ*cgepa1*, Δ*cgepa3*, and Δ*cgepa10* deletion mutants (2), and of the *C. glabrata* wild-type strain L5U1 harboring the pGREG576 vector or the pGREG576_*PDC1_CgEPA3* plasmids (3) were evaluated by spot assays, as described previously [219].

1.3.4. Transcriptomic analysis

The *C. glabrata* 044 clinical isolate and the derived 044Fluco21 (posaconazole-resistant), 044Fluco31 (posaconazole- and clotrimazole-resistant), and 044Fluco45 (posaconazole-, clotrimazole-, fluconazole-, and voriconazole-resistant) strains were harvested in the mid-exponential phase of growth in YPD medium. Three independent cultures from each strain were used for transcriptional profiling. RNA extraction was performed as described elsewhere [448]. The quality and integrity of the purified RNA were confirmed using a bioanalyzer. The DNA chips used for this microarray analysis were manufactured by Agilent using a design for *C. glabrata* [167]. The microarray was designed using eArray by Agilent Technologies, based on the annotation of *C. glabrata* CBS138 available at the Yeast Gene Order Browser in 2014 [449]. cDNA synthesis, hybridization, and scanning were performed using protocols similar to those described in reference [167], except that hybridization was carried out using an Agilent hybridization oven at 65 °C for 17 h at 100 rpm, according to a previously described protocol [448]. Data were analyzed using the LIMMA package in Bioconductor (www.bioconductor.org), as described before [448]. Each gene was represented by two probes spotted in duplicate, which were used separately to calculate the log fold change (FC) (Tables S1 to S3 at http://ibb.tecnico.ulisboa.pt/Cavalheiro_etal_SuplData.pdf). Only genes exhibiting a $\log_2$ FC of >1 and a *P* value of ≤0.05 for at least one probe were selected for further analysis. GO enrichment analysis was performed with the GOToolBox Web server [350] for each group of upregulated and downregulated genes, considering *C. glabrata* genes or their *Saccharomyces cerevisiae* homologs. Predictive analysis of the transcription factors controlling the observed transcriptional alterations was conducted using the PathoYeastract database [450].

1.3.5. Cloning of the *C. glabrata CgEPA3* gene (ORF *CAGL0E06688g*)

The pGREG576 plasmid from the Drag&Drop collection [341] was used to clone and express the *C. glabrata* open reading frame (ORF) *CAGL0E06688g* in *S. cerevisiae*, as described before for other heterologous genes [342]. pGREG576 was acquired from Euroscarf and contains a galactose-inducible promoter (*GAL1)* and the yeast selectable marker *URA3*. The *CgEPA3* gene was cloned in two sections, both generated by PCR, using CBS138 genomic DNA and the primers listed in Table III.1. To enable expression of the *EPA3* gene in *C. glabrata*, the *GAL1* promoter was replaced by the constitutive *C. glabrata PDC1* promoter. The *PDC1* promoter DNA was generated by PCR using the primers listed in Table III.1. The recombinant plasmids pGREG576_*CgEPA3* and pGREG576_*PDC1_CgEPA3* were obtained through homologous recombination in *S. cerevisiae* and were verified by DNA sequencing.

1.3.6. Disruption of the *C. glabrata CgEPA1, CgEPA3, CgEPA9, CgEPA10, CgAWP12* and *CgAWP13* (ORF *CAGL0E06644g*, *CAGL0E06688g*, *CAGL0A01366g*, *CAGL0A01284g*, *CAGL0G10219g*, and *CAGL0H10626g*) genes

The deletion of the *CgEPA1*, *CgEPA3*, *CgEPA9*, *CgEPA10*, *CgAWP12*, and *CgAWP13* genes was carried out in the parental strain KUE100, using the method described in reference [339]. The target genes were replaced, through homologous recombination, by a DNA cassette including the *CgHIS3* gene. The pHIS906 plasmid including *CgHIS3* was used as a template, and transformation was performed as described previously [339]. The deletion of *CgEPA3* in the 044Fluco31 background was carried out using the method described in reference [451]. The gene was replaced through homologous recombination by a *SAT1* flipper cassette. PCR was used to prepare the replacement cassettes and to verify recombination loci and gene deletions, using the primers listed in Table III.1.

1.3.7. Gene expression analysis

The levels of *CgEPA1* and *CgEPA3* transcripts in the azole-susceptible isolate 044 and the azole-resistant derived strains, as well as the levels of *CgCDR1* transcripts in the wild-type strain KUE100 and its derived Δ*cgepa3* deletion mutant strain, and in strain L5U1 harboring the cloning vector pGREG576 or the *CgEPA3* expression plasmid pGREG576_*PDC1_CgEPA3*, were assessed by quantitative real-time PCR. Total-RNA samples were obtained from cell suspensions harvested under control conditions, in the absence of drugs. Synthesis of cDNA for real-time RT-PCR experiments, from total-RNA samples, was performed using the Multiscribe reverse transcriptase kit (Applied Biosystems), following the manufacturer's instructions, and using 10 ng of cDNA per reaction. The RT-PCR step was carried out using SYBR green reagents. Primers for the amplification of the *CgEPA1*, *CgEPA3*, *CgCDR1*, and *CgACT1* cDNA were designed using Primer Express software (Applied Biosystems) (Table III.1). The RT-PCRs were conducted in a thermal cycler block (7500 Real-Time PCR system; Applied Biosystems). The *CgACT1* mRNA level was used as an internal control. The relative values obtained for the wild-type strain under control conditions were set at 1, and the remaining values are presented relative to that control.

Table III. 1. List of primers used in this study.

Name	Sequence (3'-5')
CgEPA3 gene cloning	
pGREG_CgEPA3_I_FW	TGCTATTAGGTCAACCTTGTAACAGCTGCCATAGCTATTCGAACTATAGCTTAAG
pGREG_CgEPA3_I_Rev	CAGTTGCCACGATGACTAGTCAGCTGGAGCTCAGTACATTAATCAATACAGTGCG
pGREG_CgEPA3_II_FW	GTCATCGTGGCAACTGTGATTTTCTTTCTAGATTCCTACT
pGREG_CgEPA3_II_Rev	CGTGAAAAAAAGACTAAATTCAGCTGGAGCTCAGTACATTAATCAATACAGTGCG
pGREG576 GAL-to-PDCI promotor replacement	
pGREG_PDCI_FW	TTAACCCTCACTAAAGGGAACAAAAGCTGGAGCTCAGCATTTTTATACACGTTTTAC
pGREG_PDCI_Rev	GAAAAGTTCTTCTCCTTTACTCATACTAGTGCGGCTGTTAATGTTTTTTGGCAATTG
CgEPA1, CgEPA3, CgEPA9, CgEPA10, AWP12 and AWP13 gene disruption	
ΔCgEPA1_FW	GCACTAGTCGCCGGACAAAATCAAACCAATTAACGTTTCTGATTTAGAGTTCTTACTTCT TTTTCGAAAC
ΔCgEPA1_Rev	GGTCGGAGTGCTACATTTTGGTCCTTTATATTATTGAAGGTATCAAATCGTAACATTTTC GACACCACCG
ΔCgEPA3_FW	GCACTAGTCGCCGGTAACTAAAAAAAAGAAAACATTGAAAAAGACTAGTTAAATTAAGC TAATACTACCA
ΔCgEPA3_Rev	GGTCGGAGTGCTACATTAAGACAAGGGAATTAAAGATAATACTATAACAAAGAGAAATA AGTAACTAATT
ΔCgEPA3_SAT1_FW	ATCATTCCTGGTTTGACAATGGAACTTTACTCTTACCCTATTGTCAGTGGTACTCCTCCC ATGGACGGTGGTATGTTTTA
ΔCgEPA3_SAT1_Rev	GCTTCGAAGCTTTACCCTTGTACTCTGAAAAATTAGGGATATTAAAGACAGAACTAGAG GTTAGGCGTCATCCTGTGCTC
ΔCgEPA9_FW	TCACTAAGTGGATGAAATGCAGAAAGAATACAATTTAACCCTCTTCAATGCGATCCGGC GGCCGCTGATCACG
ΔCgEPA9_Rev	CAACTGCCAAAGGGTTCACAAGTTGAATACCAGGCCAACCATCATCAGTGGCAGGGCG ACATCGTGAGGCTGG
ΔCgEPA10_FW	GCACTAGTCGCCGGGCTAATACCTGATCGTAGACTATATTACTTCATAAAACTTTTGTTA CCTACCCGTA
ΔCgEPA10_Rev	GGGAAAGAAAAATCAACCACATTGGCAAAACGTAGACATCTTGTCAACTGCCAAAGCAT CGTGAGGCTGG
ΔCgAWP12_FW	TACTTAAAATTTCCTTTCTCAATCAACAAAAATATCCATTAACTGAAAAAGAATACGGCG GCCGCTGATCACG
ΔCgAWP12_Rev	TATCAATGTTCATATTGAAAGAAACAGCCTATCTAAAAATCATGGCTGGACGAACGCGA CATCGTGAGGCTGG
ΔCgAWP13_FW	ATTACGTGACAAAAGACAGATAAAGGAATTCTAAATATCCATCTACAAGACCATTCGGC GGCCGCTGATCACG
ΔCgAWP13_Rev	CCTATCTAAAAATCATGGCTGGACGAACGTTTGTATTACTGTACATGTTGGGCATTCGA CATCGTGAGGCTGG
ΔCgEPA1_conf_FW	TAAATAAGTTTTTATCTCGACC
ΔCgEPA1_conf_Rev	GGTTTTCATTGACCGAAG
ΔCgEPA3_conf_FW	CGGAACTTCATTGGTATG
ΔCgEPA3_conf_Rev	CATACCAATGAAGTTCCG
ΔCgEPA3_SAT1_conf_FW	CCCAGAACCCATTTGGTTATCC
ΔCgEPA3_SAT1_conf_Rev	GCCCAGATAACAACACAAGTCC
ΔCgEPA9_conf_FW	CTTTTGGTATCTGACTCTGTTAT
ΔCgEPA9_conf_Rev	GGTCCCAAGAGATTTTACC
ΔCgEPA10_conf_FW	TGTCTCAGTCTATGGCTTTC
ΔCgEPA10_conf_Rev	CTCAAGTGTCTCCCAACA
ΔCgAWP12_conf_FW	GCCTGTGGATATTGCTACT
ΔCgAWP12_conf_Rev	GTCACTGATTGAAAGTTCTCG
ΔCgAWP13_conf_FW	GTATATTTTCAAGTGCTGCAT
ΔCgAWP13_conf_Rev	CTACCGTGGTTTCACTTG
RT-PCRexperiments	
CgEPA1_FW	TTGATTGCTGCAGAAGGGATT
CgEPA1_Rev	ATGGCGTAGGCTTGATAATTTCC
CgEPA3_FW	GTTCCTGTCACCAGCACCATATACTA
CgEPA3_Rev	CCTTGGCAACTAGGTGTTTGG
CgCDR1_FW	GCTTGCCCGCACATTGA
CgCDR1_Rev	CCTCAGGCAGAGTGTGTTCTTTC
CgACT1_FW	AGAGCCGTCTTCCCTTCCAT
CgACT1_Rev	TTGACCCATACCGACCATGA

1.3.8. [^{3}H]clotrimazole accumulation assays

[^{3}H]clotrimazole transport assays were carried out as described before [219]. To estimate the accumulation of clotrimazole (intracellular/extracellular [^{3}H]clotrimazole), yeast cells were grown in BM medium until the mid-exponential phase and were harvested by filtration. Cells were washed and resuspended in BM medium to obtain dense cell suspensions (optical density at 600nm [OD_{600nm}]=5.0$\pm$0.2, equivalent to approximately 2.2 mg [dry weight] mL^{-1}). After a 5-min incubation at 30 °C, with agitation (150 rpm), 0.1µM [^{3}H]clotrimazole (American Radiolabelled Chemicals; 1 mCi/mL) and 30 mg/L of unlabeled clotrimazole were added to the cell suspensions. The intracellular accumulation of labeled clotrimazole was followed for 30 min, as described elsewhere [219]. To calculate the intracellular concentration of labeled clotrimazole, the internal cell volume (Vi) of the exponential cells was considered constant and equal to 2.5μL (mg [dry weight]$^{-1}$) [452].

1.3.9. Quantification of total cellular ergosterol

Ergosterol was extracted from cells using the following method adapted from reference [453], as described before [143]. Cells were cultivated in YPD medium with orbital agitation (250 rpm) until stationary phase, harvested by centrifugation, and resuspended in methanol. Cholesterol (Sigma) was added as an internal standard to estimate the ergosterol extraction yield. The extracts were analysed by high-pressure liquid chromatography (HPLC) with a 250-mm by 4-mm C18 column (LiChroCART Purospher STAR RP-18, end-capped, 5 mm) at 30 °C. Samples were eluted in 100% methanol at a flow rate of 1 mL/min. Ergosterol was detected at 282 nm with a retention time of 12.46$\pm$0.24 min, while cholesterol was detected at 210 nm with a retention time of 15.36$\pm$0.35 min. Results are expressed in micrograms of ergosterol per milligram (wet weight) of cells.

1.3.10. Biofilm quantification

C. glabrata strains were tested for their capacity for biofilm formation by use of the crystal violet method. For that, the *C. glabrata* strains were grown in SDB medium and harvested by centrifugation at mid-exponential phase. The cells were inoculated with an initial OD_{600nm}=0.05$\pm$0.005 in 96-well polystyrene microtiter plates (Greiner) in either SDB (pH 5.6) or RPMI (pH 4) medium. Cells were cultivated at 30 °C for 15$\pm$0.5 h or 24$\pm$0.5 h with mild orbital shaking (70 rpm). After the incubation time, each well was washed three times with 200 μL of deionized water to remove cells not attached to the biofilm matrix. Then 200 μL of a 1% crystal violet (Merck) alcoholic solution was used to stain the biofilm present in each well. Following 15 min of incubation with the dye, each well was washed with 250 μL of deionized water. The stained biofilm was eluted in 200 μL of 96% (vol/vol) ethanol, and the absorbance of each well was read in a microplate reader at a wavelength of 590 nm (SPECTRO-star Nano; BMG Labtech).

1.3.11. Human vaginal epithelial cell adherence assay

For the adhesion assays, VK2/E6E7 human epithelial cells were grown and inoculated in 24-well polystyrene plates (Greiner) with a density of $2.5x10^5$ cells/ml a day prior to use. Additionally, *C. glabrata* cells were inoculated with an initial OD_{600nm}=0.05±0.005 and were cultivated at 30 °C for 16±0.5 h with orbital shaking (250 rpm) in YPD medium. In order to initiate the assay, the culture medium of mammalian cells was removed and replaced by new culture medium in each well, and, subsequently, *Candida glabrata* cells were added to each well, with a density of $12.5x10^5$ CFU/well, corresponding to a multiplicity of infection (MOI) of 10. Then the plate was incubated at 37 °C under 5% CO_2 for 30 min. Afterwards, each well was washed 3 times with 500 μL of 1x phosphate-buffered saline (PBS) (pH 7.2), followed by the addition of 500 μL of 0.5% Triton X-100 and incubation at room temperature for 15 min. The cell suspension in each well was then recovered, diluted, and spread onto agar plates to determine the CFU count, which represents the proportion of cells adherent to the human epithelium.

1.3.12. Acession number

The data sets were deposited at the Array Express Database with reference number E-MTAB-6787.

1.4. Results

1.4.1. Acquisition of resistance in a susceptible *C. glabrata* clinical isolate

The 044 clinical isolate was found to exhibit susceptibility to all the azole drugs tested. Specifically, the MIC values obtained for fluconazole, voriconazole, posaconazole, and clotrimazole are 4 μg/mL, 0.25 μg/mL, 0.5 μg/mL, and 0.125 μg/mL, respectively. After exposure to therapeutic serum fluconazole concentrations, the 044 yeast population evolved in a stepwise manner toward multiazole resistance. Specifically, after 21 days, posaconazole resistance was reached (MIC, ≥4 μg/mL), followed by clotrimazole resistance (MIC, ≥4 μg/mL) after 31days and, finally, fluconazole and voriconazole resistance upon 45 days of induction (MICs, ≥64 and ≥4 μg/mL, respectively) (Figure 1; Table S.1 at http://ibb.tecnico.ulisboa.pt/Cavalheiro_etal_SuplData.pdf). The populations obtained at these time points were designated 044Fluco21 (posaconazole resistant), 044Fluco31 (posaconazole and clotrimazole resistant), and 044Fluco45 (posaconazole, clotrimazole, fluconazole, and voriconazole resistant).

By use of spot assays, the 044 clinical isolate and derived populations were further characterized in terms of antifungal drug resistance. This additional assay confirmed the progressive acquisition of resistance to fluconazole and clotrimazole (Figure III.2A and B) and showed that these strains had indeed become multiazole resistant, since increased resistance to ketoconazole, miconazole, and tioconazole was also observed (Figure III.2A). Interestingly, no change in resistance to flucytosine or amphotericin B, two other antifungal drugs of different classes, was observed (Figure III.2C).

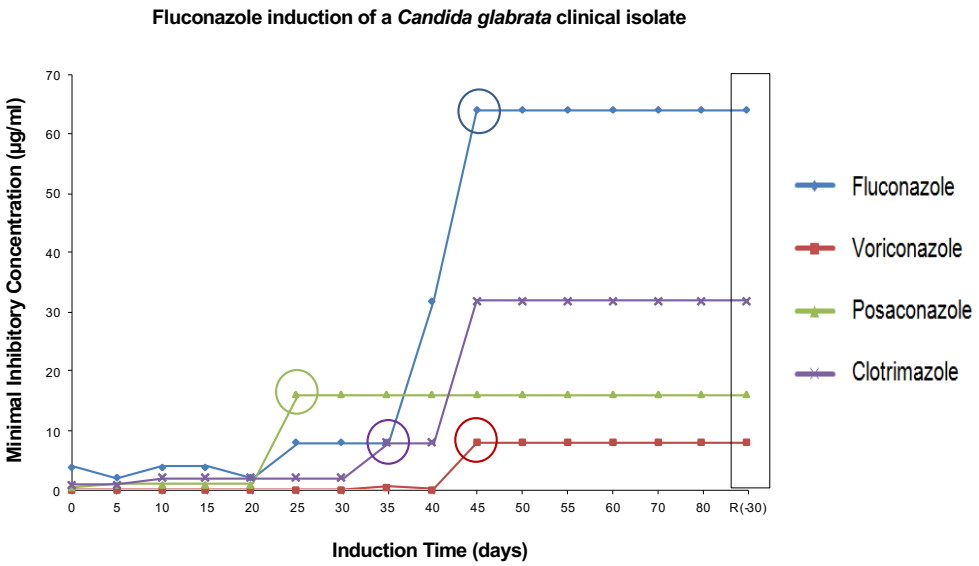

Figure III.1. Azole MIC distribution pattern for a *C. glabrata* cell population during evolution toward multiazole resistance. Shown is a comparison of the MICs of fluconazole, voriconazole, posaconazole, and clotrimazole for the 044 *C. glabrata* clinical isolate during prolonged exposure to therapeutic serum fluconazole concentrations (16 µg/ml), as described in Materials and Methods. The time point at which the clinical resistance breakpoint for each azole drug was reached is indicated by a circle.

1.4.2. Transcriptional remodeling underlying the stepwise acquisition of resistance to posaconazole, clotrimazole and fluconazole/voriconazole

In order to gain insights into the molecular mechanisms underlying the phenotypic changes leading to differential acquisition of resistance to four azoles, the transcriptome-wide changes occurring on the 21st, 31st, and 45th days of fluconazole induction were analyzed by microarray hybridization. It should be noted that the design of the microarrays used was based on the available CBS138 genome; thus, it is possible that specific characteristics of the transcriptome of the clinical isolate analyzed may have been missed in this study. To make sure that the transcriptome observations reflected the evolving population, and not just a specific isolate, a large number of colonies were mixed and analyzed as a whole. Total RNA was extracted from cell populations growing exponentially in YPD medium in the absence of fluconazole in order to ensure that the transcriptome changes observed corresponded to stable transcriptional modifications. Each sample was compared to the azole-susceptible *C. glabrata* 044 clinical isolate (control), considering a 1.5-fold threshold, with an associated *P* value of <0.05. Overall, the expression of 355 genes was downregulated, whereas the expression of 299 genes was upregulated, in the posaconazole-resistant population obtained after 21 days of fluconazole induction (Tables S2 and S3 at http://ibb.tecnico.ulisboa.pt/Cavalheiro_etal_SuplData.pdf). At day 31, when the population had further acquired clotrimazole resistance, the expression of 73 genes was downregulated, whereas that of 199 genes was found to be upregulated, relative to expression in the parental clinical isolate (Table S4 and S5). Finally, at day 45, upon the acquisition of fluconazole/voriconazole resistance, the expression of 6 genes was downregulated, whereas that of 27 genes was found to be upregulated, relative to expression in the parental clinical isolate (Tables S6 and S7). There is very little overlap between the differentially expressed genes in the different populations, with only 44 genes whose altered expression was maintained from day 21 to day 31, and 9 upregulated genes on day 31

whose activated expression was maintained until day 45 (Figure S1 at http://ibb.tecnico.ulisboa.pt/Cavalheiro_etal_SuplData.pdf). GOToolBox was used to identify the Gene Ontology (GO) biological-process terms overrepresented in each data set (Figure S2).

1.4.3. Acquisition of azole drug resistance is accompanied by decreased azole drug accumulation

Two of the most typical changes that occur in azole-resistant strains are alterations in the concentration of ergosterol [454]–[456] and the activation of drug efflux pumps, leading to reduced accumulation of the drug. Indeed, in the strains that evolved from clinical isolate 044, changes at the level of the expression of ergosterol biosynthetic genes were observed, especially in the case of *ERG11*, whose expression was almost 3-fold higher in the 044Fluco31 strain than in the parental strain but returned to basal levels in the 044Fluco45 strain (Figure III.3A). The total ergosterol concentrations in the susceptible clinical isolate 044 and the derived 044Fluco21, 044Fluco31, and 044Fluco45 cells were therefore determined; they were found to remain constant in the 044Fluco21 and 044Fluco31 cells and to decrease slightly in the 044Fluco45 strain (Figure III.3B). No change in the sequence of the *ERG11* gene was identified in the four strains studied.

The expression levels of the multidrug transporter genes *CDR1* and *CDR2* were increased $>$ 2-fold only in 044Fluco45 cells (Figure III.4A). This is consistent with the identification of a nonsynonymous point mutation in the sequence of the transcription factor gene *PDR1*. This point mutation, leading to a Y372C substitution, is in the same position as the Pdr1 Y372N gain-of-function (GOF) mutation identified in other azole-resistant isolates of *C. glabrata* [224] and is similar to that mutation. It is indeed likely that this Y372C substitution constitutes a new Pdr1 GOF mutation, since Pdr1 was found to control nearly 50% of the upregulated genes in this population in cells growing exponentially in the absence of fluconazole or any other stress. Indeed, in an attempt to identify the transcription factors (TFs) that underlie the observed transcriptome-wide remodeling, the PathoYeastract database [450] was used (Table III.2). In this search, the PathoYeastract data used were based solely on data published specifically for *C. glabrata*, demonstrating experimentally the regulatory association between the transcription factors and their target genes in this yeast. The regulators of the expression of the majority of the genes upregulated during the acquisition of multiazole resistance are unknown. The TF that controls the highest number of upregulated genes is Hal9, a TF of unknown function, for the posaconazole-resistant strain and Pdr1 for the remaining two evolved strains.

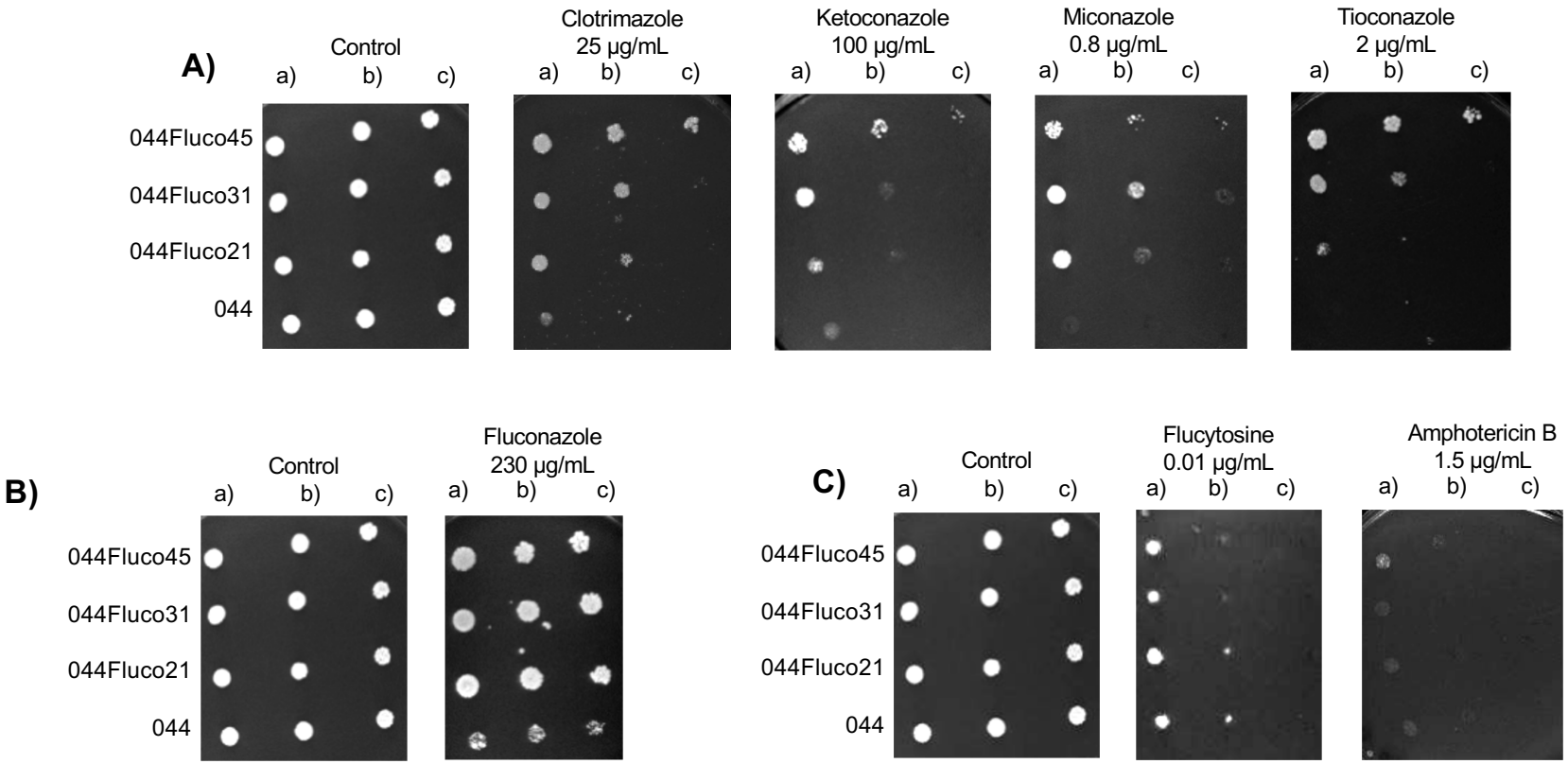

Figure III.2. The evolved strains 044Fluco21, 044Fluco31, and 044Fluco45 display increased azole drug tolerance over that of the parental *Candida glabrata* 044 clinical isolate. Shown are comparisons of the susceptibilities of these strains to the imidazole drugs clotrimazole, ketoconazole, miconazole, and tioconazole (A), the triazole drug fluconazole (B), and amphotericin B and flucytosine (C), at the indicated concentrations, using spot assays on BM agar plates. The inocula were prepared in liquid BM growth medium until the exponential phase of growth was reached, followed by dilution to an OD_{600} of 0.05. Cell suspensions used to prepare the spots were 1:5 (b) and 1:25 (c) dilutions of the cell suspensions used in the plates shown on the left (a). The images displayed are representative of those obtained in at least 3 independent experiments.

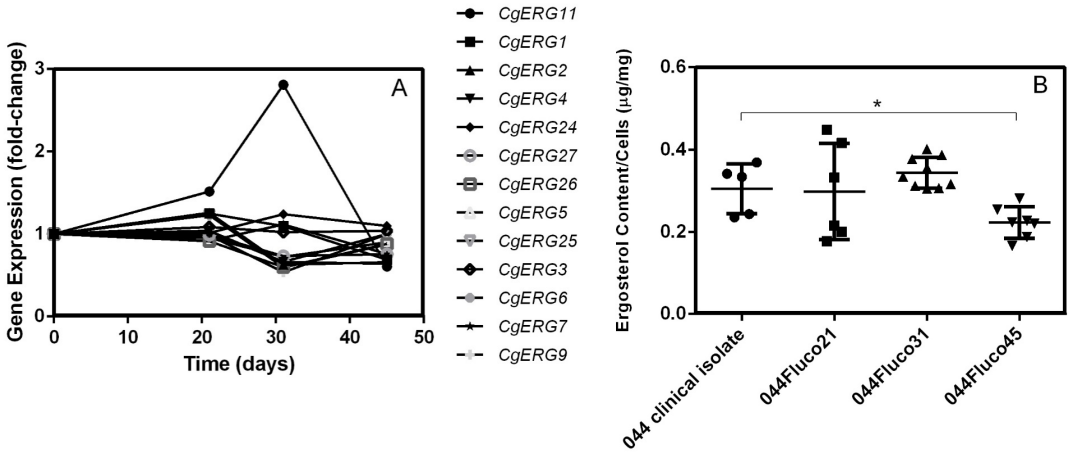

Figure III.3. Role of ergosterol metabolism in the acquisition of azole resistance in the 044 clinical isolate. (A) Gene expression changes registered for ergosterol biosynthetic genes along the evolution of the 044 clinical isolate toward multiazole resistance. Transcript levels were obtained by microarray hybridization, and for each, the fold change relative to the level registered for the 044 parental clinical isolate is shown. Values are averages of results from at least three independent experiments. $P<0.05$. (B) Total ergosterol contents of 044 and azole-derived *C. glabrata* cells. Cells were harvested after 15 h of growth in YPD medium, and total ergosterol was extracted and quantified by HPLC. Cholesterol was used as an internal standard in order to evaluate the yield of the ergosterol extraction. The ergosterol contents displayed are averages of the results of at least three independent experiments. Error bars represent standard deviations. *, $P<0.05$.

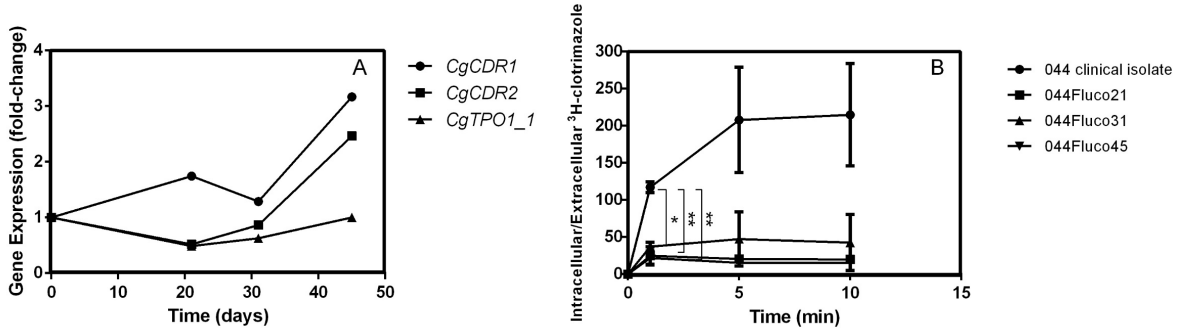

Figure III.4. Role of drug export in the acquisition of azole resistance in the 044 clinical isolate. (A) Gene expression changes registered for the multidrug transporter-encoding genes, whose expression reached >2-fold differences, along the evolution of the 044 clinical isolate toward multiazole resistance. Transcript levels were obtained by microarray hybridization, and for each, the fold change relative to the level registered for the 044 parental clinical isolate is shown. Values are averages of results from at least three independent experiments. $P<0.05$. (B) Time course accumulation of rabiolabeled [^{3}H]clotrimazole in strain 044 and the derived strains 044Fluco21, 044Fluco31, and 044Fluco45 during cultivation in liquid BM medium in the presence of 30 mg/liter unlabeled clotrimazole. Accumulation values are the averages of results from at least three independent experiments. Error bars represent standard deviations. *, $P<0.05$; **, $P<0.01$.

Table III. 2. Distribution of the transcription factors predicted to regulate the genes upregulated in the evolved strains relative to expression in the 044 clinical isolate[a].

Strain	TF	% of regulated genes
044Fluco21 (posaconazole resistant)	Hal9	10.51
	Pdr1	**4.07**
	CAGL0G08844g	2.71
	Ace2	2.37
	Yap1	2.37
	Skn7	0.68
	Yap5	0.68
	Yap6	0.68
044Fluco31 (clotrimazole/posaconazole resistant)	**Pdr1**	**6.77**
	Yap1	4.69
	Hal9	4.17
	CAGL0G08844g	1.56
	Yap5	1.04
	Yap6	1.04
	Upc2a	0.52
	Skn7	0.52
044Fluco45 (multiazole resistant)	**Pdr1**	**43.75**
	Yap1	18.75
	CAGL0G08844g	6.25
	Skn7	6.25

[a]The transcription factors (TFs) are listed in the order of the percentage of upregulated genes for each strain, based on the information gathered in the PathoYeastract database, filtered to consider only transcriptional associations known to occur under stress (32). The different rankings of Pdr1 are shown in boldface.

The ability of the evolved cells to reduce the intracellular accumulation of azole drugs was then evaluated using [^{3}H]clotrimazole as a model azole drug. Remarkably, the intracellular accumulation of [^{3}H]clotrimazole decreased in all three resistant cell populations (Figure III.4B). Specifically, the 044Fluco21 cell population was found to accumulate 4 times less clotrimazole than the 044 parental clinical isolate. The 044Fluco31 and 044Fluco45 cells exhibited even lower levels of accumulated clotrimazole, reaching levels nearly 10-fold-lower than those registered in the 044 clinical isolate (Figure III.4B). Although reduced drug accumulation is consistent with the expression profile of the multiazole-resistant strain 044Fluco45, no clear changes in the expression of drug-resistant transporters were observed in the 044Fluco21 and 044Fluco31 intermediate strains (Figure III.4A), and no change in the sequence of the *PDR1* gene was observed.

1.4.4. Acquisition of clotrimazole drug resistance is accompanied by increased adhesion

The expression of adhesin-encoding genes, including the epithelial adhesins Epa1, Epa3, Epa9, and Epa10 and the putative adhesins Awp12, Awp13, Pwp1, Pwp3, Pwp4, and CAGL0E00231g (Figure III.5A), was increased. The transcript levels of the *CgEPA1* and *CgEPA3* genes were verified using quantitative reverse transcription (RT-qPCR), confirming their transient upregulation, which reached maximal levels in the 044Fluco31 population (Figure III.5B).

This observation prompted us to test the ability of the strains in which azole resistance had evolved to adhere and form biofilms. Indeed, 044Fluco31 cells were found by bright-field microscopy to exhibit a significantly higher level of cell aggregates than 044 and 044Fluco21 cells. The percentage of 044Fluco31 cells found to constitute cell aggregates, considering at least 10 cells/aggregate, reached an average of >50%, in contrast to only 10% for the remaining cell populations (Figure III.6A). Additionally, the number of cells per aggregate, determined by microscopy, was found to be consistently higher for the 044Fluco31 strain (Figure III.6A). Moreover, 044Fluco31 exhibited higher adherence to human vaginal epithelial cells than the other strains (Figure III.6B). Interestingly, the evolved strain 044Fluco21 also exhibited moderately increased adhesion to the epithelial cells tested, despite the observation that there was no clear upregulation of adhesin-encoding genes in this population (Figure III.6B). This suggests that alternative mechanisms whose nature is unclear mediate increased adhesiveness in these *C. glabrata* cells. Since no differences in biofilm formation on polystyrene dishes was observed (Figure III.6C), the increased expression of adhesin-encoding genes in 044Fluco31 cells appears to correlate with their ability to display cell-to-cell adherence and to adhere to epithelial cells.

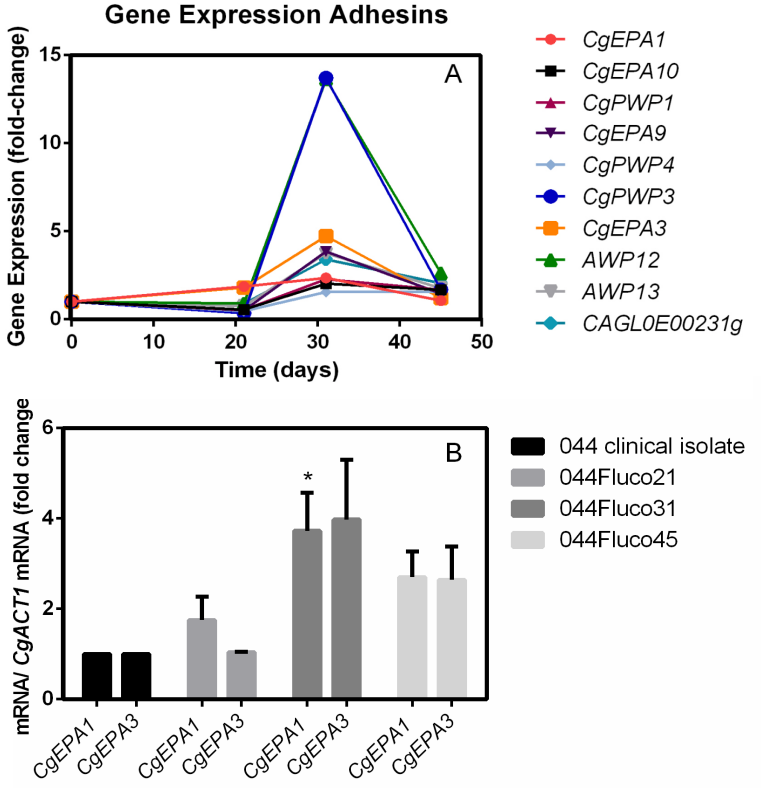

Figure III.5. Correlation between adhesin gene expression and the acquisition of clotrimazole/posaconazole resistance in the 044Fluco31 strain. (A) Gene expression changes registered for adhesin-encoding genes along the evolution of the 044 clinical isolate toward multiazole resistance. Transcript levels were obtained by microarray hybridization, and for each, the fold change relative to the level registered for the 044 parental clinical isolate is shown. Values are averages of results from at least three independent experiments. $P<0.05$. (B) Comparison of the differences in the *CgEPA1* and *CgEPA3* transcript levels along the evolution of the 044 clinical isolate toward multiazole resistance. Transcript levels were obtained by quantitative RT-PCR and were normalized to *CgACT1* mRNA levels. The fold change in the level of each transcript for each evolved strain relative to the level registered for 044 parental cells is shown. Values are averages of results from at least three independent experiments. Error bars represent standard deviations. *, $P<0.05$.

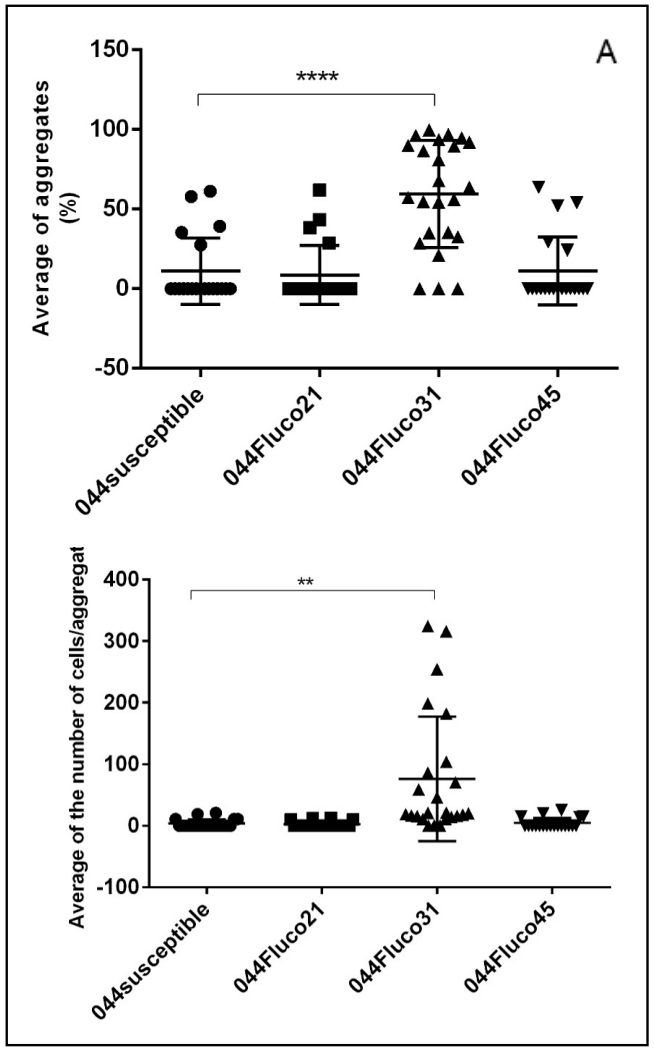

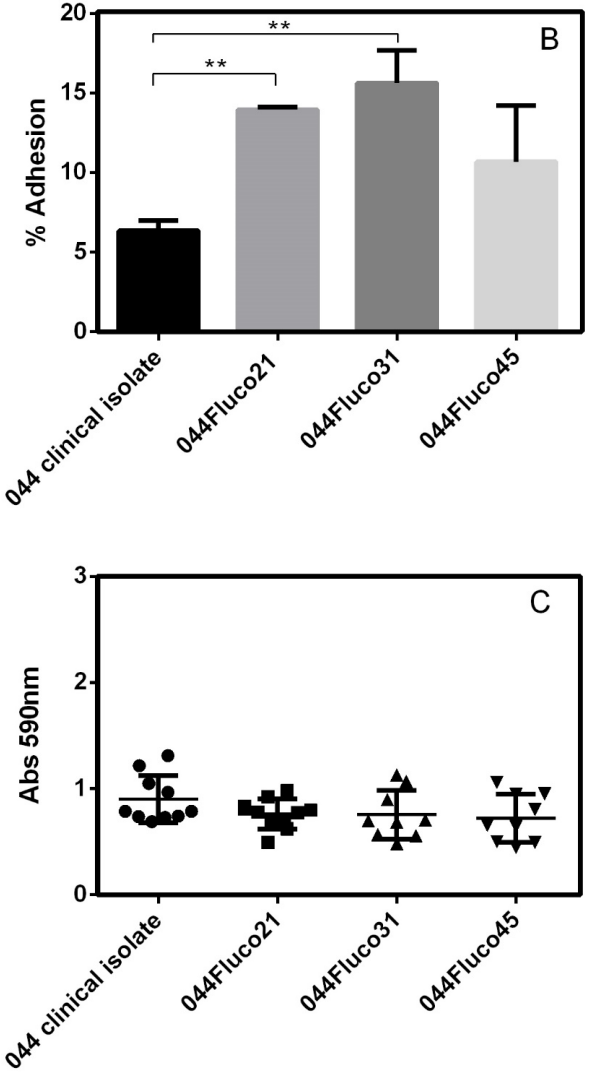

Figure III. 6. The evolved strain 044Fluco31 exhibits increased cell-to-cell adhesion over that of the 044 clinical isolate. Cell-to-cell aggregation was evaluated based on microscopic observation. (A) Displayed, as scatter dot plots, are the percentage of cell aggregates per total cell population and the number of cells per aggregate, considering aggregates of at least 10 cells. **, $P<0.01$; ****, $P<0.0001$. (B) Adhesion of the *C. glabrata* 044 clinical isolate and derived strains evolving toward azole resistance to VK2/E6E7 human vaginal epithelial cells for 30 min at 37 °C under 5% CO_2. Values are averages of results from at least three independent experiments. Error bars represent standard deviations. **, $P<0.01$. (C) Biofilm formation on polystyrene surfaces was assessed based on crystal violet staining of the *C. glabrata* 044 clinical isolate and derived strains evolving toward azole resistance, which had been grown for 15 h in RPMI medium, pH 4.0, in microtiter plates. The data are displayed in a scatter dot plot, where each dot represents the level of biofilm formed in a sample. Horizontal lines indicate the average levels from at least 8 independent experiments. Error bars indicate standard deviations.

1.4.5. The CgEpa3 adhesin is a new determinant of azole drug resistance

Given the observation that a high level of expression of adhesin-encoding genes correlates with increased azole resistance in the evolved strain 044Fluco31, the possible role in azole drug resistance of *CgEPA1*, *CgEPA3*, *CgEPA9*, *CgEPA10*, *CgAWP12*, and *CgAWP13*, accounting for most of the more highly upregulated adhesin-encoding genes, was assessed. Deletion of the *CgEPA3* gene, but not the remaining adhesin-encoding genes, increased the susceptibility of *C. glabrata* to miconazole, ketoconazole, tioconazole, clotrimazole, and fluconazole (Figure III.7A). These results were confirmed by standard assessment of the fluconazole and clotrimazole MICs for the wild-type strain (16 and 2 mg/L, respectively) and the Δ *cgepa3* deletion mutant strain (8 and 1 mg/L, respectively). Overexpression of *CgEPA3* in the wild-type strain L5U1 was consistently found to increase *C. glabrata* resistance to miconazole, ketoconazole, tioconazole, clotrimazole, and fluconazole, confirming the role of this gene as a determinant of azole drug resistance (Figure III.7B). To ensure that the deletion of *CgEPA3* also influences drug resistance in the 044Fluco31 background, the effect of its deletion on azole resistance was tested. Deletion of *CgEPA3* was found to increase the susceptibility of the 044Fluco31 strain to clotrimazole and fluconazole (Figure III.8), suggesting that the effect of this adhesin is not strain dependent.

Since *C. glabrata* CgEpa3 was identified as conferring resistance to azole drugs, its possible involvement in reducing clotrimazole accumulation in yeast cells was examined. The accumulation of radiolabeled clotrimazole in nonadapted *C. glabrata* cells suddenly exposed to 30 mg/L clotrimazole was approximately 2 times higher in cells devoid of CgEpa3 than in wild-type KUE100 cells (Figure III.9A). Overexpression of *CgEPA3* in the wild-type strain L5U1 was consistently found to decrease the accumulation of radiolabeled clotrimazole (Figure III.9B). These findings strongly suggest that CgEpa3 contributes to *C. glabrata* resistance to azole drugs by reducing their accumulation within yeast cells.

To exclude the possibility that the results observed were due to an indirect effect of *CgEPA3* expression on the expression of the drug efflux pump CgCdr1, the effect of deletion or overexpression of *CgEPA3* on the levels of *CgCDR1* transcripts was evaluated. Interestingly, the expression of *CgEPA3* was found to have no effect on *CgCDR1* transcript levels (Figure III.10), suggesting that CgEpa3 affects azole drug accumulation independently of drug efflux pump activity.

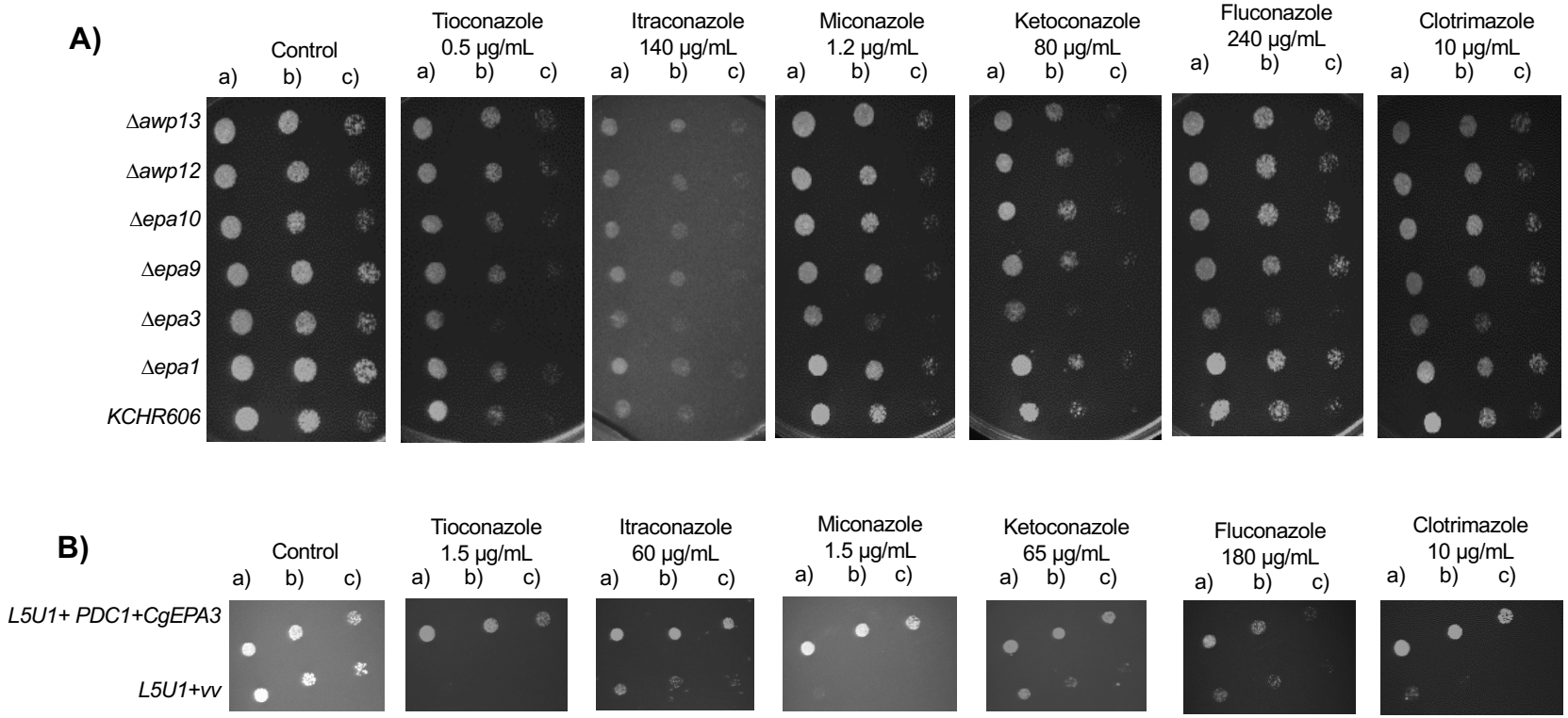

Figure III.7. CgEpa3 confers resistance to azole antifungal drugs in *C. glabrata* cells. (A) Comparison of the susceptibilities of the *C. glabrata* parental strain KUE100 and the Δ*cgepa1*, Δ*cgepa3*, Δ*cgepa9*, Δ*cgepa10*, Δ*cgawp12*, Δ*cgawp13* derived strains to the imidazole drugs clotrimazole, ketoconazole, miconazole, and tioconazole and the triazole drugs fluconazole and itraconazole at the indicated concentrations by use of spot assays on BM agar plates. (B) Comparison of the susceptibilities to several antifungal drugs, at the indicated concentrations, of the *C. glabrata* L5U1 strain harboring the pGREG576 cloning vector (vv) and the same strain harboring the pGREG576_*PDC1_CgEPA3* plasmids in BM agar plates without uracil by use of spot assays. The inocula were prepared as described in Materials and Methods. The cell suspensions used to prepare the spots were 1:5 (b) and 1:25 (c) dilutions of the cell suspension used in the plates shown on the left (a). The images displayed are representative of at least three independent experiments.

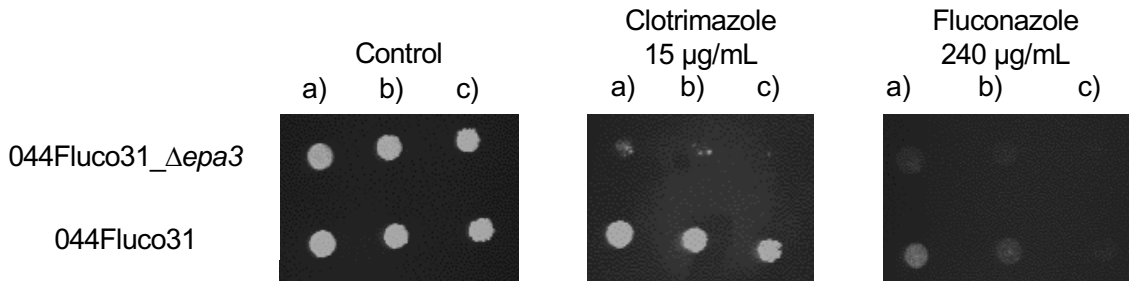

Figure III. 9. CgEpa3 confers resistance to azole antifungal drugs in the *C. glabrata* evolved clinical isolate 044Fluco31. Shown is a comparison of the susceptibilities of the 044Fluco31 *C. glabrata* strain, and the derived 044Fluco31_Δ*cgepa3* deletion mutant strain to the azole drugs clotrimazole and fluconazole, at the indicated concentrations, determined by use of spot assays on BM agar plates. The inocula were prepared as described in Materials and Methods. The cell suspensions used to prepare the spots were 1:5 (b) and 1:25 (c) dilutions of the cell suspension used in the plates shown on the left (a). The images displayed are representative of at least three independent experiments.

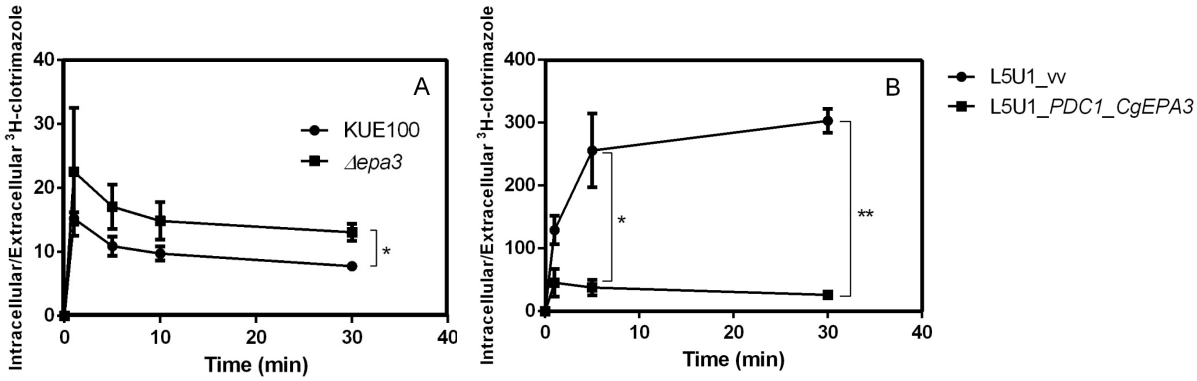

Figure III.8. CgEpa3 leads to decreased intracellular accumulation of [^{3}H]clotrimazole in *C. glabrata* cells. Shown are time courses of accumulation of rabiolabeled [^{3}H]clotrimazole in the wild-type strain KUE100 and KUE100_ Δ *cgepa3* (A) and in strain L5U1 harboring the pGREG576 cloning vector (vv) or the pGREG576_*PDC1_CgEPA3* vector (B) during cultivation in liquid BM medium in the presence of 30 mg/L unlabeled clotrimazole. Accumulation values are the averages of results from at least three independent experiments. Error bars represent standard deviations. *, $P<0.05$; **, $P<0.01$.

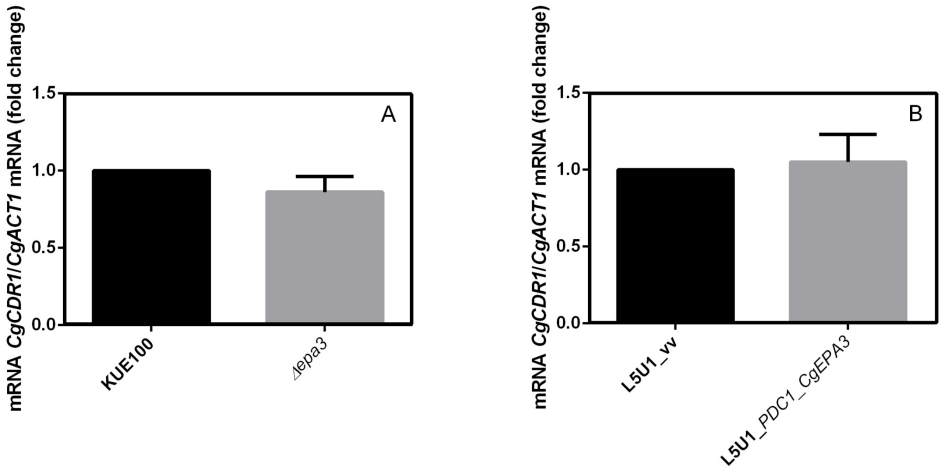

Figure III.10. *CgEPA3* expression does not affect *CgCDR1* transcript levels. Shown are transcript levels of *CgCDR1* in the *C. glabrata* wild-type strain KUE100 and KUE100_Δ*cgepa3* (A) and in strain L5U1 harboring the pGREG576 cloning vector (vv) or the pGREG576_*PDC1_CgEPA3* vector (B) during cultivation in liquid BM medium. Transcript levels were assessed by quantitative RT-PCR, as described in Materials and Methods. Values are averages of results from at least three independent experiments. Error bars represent standard deviations.

1.4.6. The CgEpa3 adhesin promotes biofilm formation.

The effect of deleting *CgEPA3*, *CgEPA1*, or *CgEPA10* on *in vitro* biofilm formation on 96-well polystyrene microplates was further assessed. Deletion of *CgEPA3*, but not deletion of *CgEPA1* or *CgEPA10*, resulted in an almost 2-fold decrease in the level of total biofilms formed relative to that for the parental strain (Figure III.11A). The overexpression of *CgEPA3* in the wild-type L5U1 strain was consistently found to increase the ability of *C. glabrata* to form biofilms on polystyrene (Figure III.11B).

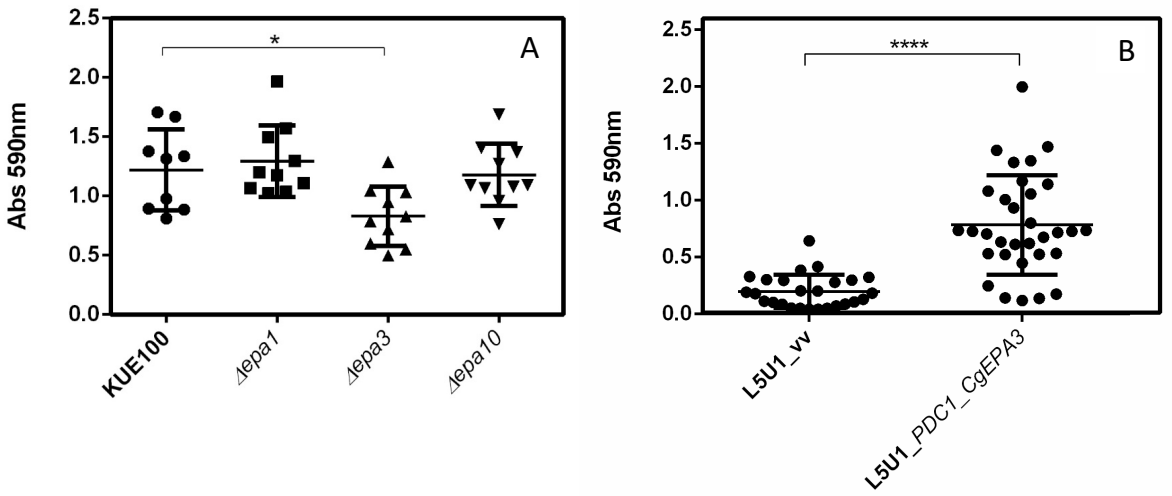

Figure III.11. CgEpa3 is required for biofilm formation. (A) Biofilm formation was assessed based on crystal violet staining of cells of wild-type *C. glabrata* KUE100 and the indicated single deletion mutants, which had been grown for 15 h in SDB medium, pH 5.6, in microtiter plates. The data are displayed on a scatter dot plot, where each dot represents the level of biofilm formed in a sample. Horizontal lines indicate the average levels of biofilm formed in at least 8 independent experiments. Error bars represent standard deviations. *, $P<0.05$. (B) Biofilm formation on polystyrene surfaces was assessed based on crystal violet staining of wild-type *C. glabrata* L5U1 cells harboring either the cloning vector pGREG576 (control) (vv) or the pGREG576_*PDC1_CgEPA3* plasmid, which had been grown for 24 h in SDB medium, pH 5.6, in microtiter plates. The data are displayed on a scatter dot plot, where each dot represents the level of biofilm formed in a sample. Horizontal lines indicate the average levels of biofilm formed in at least 8 independent experiments. Error bars represent standard deviations. ****, $P<0.0001$.

1.5. Discussion

In this study, a transcriptomics analysis of the evolution of an azole-susceptible clinical isolate toward azole resistance, induced by long-standing incubation with a therapeutic concentration of fluconazole in serum, was carried out. The selected approach enabled the identification of the changes in gene expression occurring with time during 45 days of evolution toward a simple and stable solution. One of the surprising observations is that the number of differentially expressed genes, relative to expression in the initial azole-susceptible strain, decreases with time of evolution. At day 21, when the cells were resistant to posaconazole only, 654 genes were found to be expressed differently, while that number decreased to 272 after 31 days and to just 33 at day 45, when the cells reached multiazole resistance. The evolved azole-resistant populations at each time point were found to display significant differences in the molecular mechanisms that are set in place to develop resistance, as summarized in Figure III.12. The multiazole-resistant strain 044Fluco45 exhibits the upregulation of genes encoding

multidrug resistance (MDR) transporters *CgCDR1*, *CgCDR2*, and *CgTPO1_2*, decreased accumulation of azole drugs, and a likely gain-of-function (GOF) mutation in the multidrug transcription factor Pdr1. Although the point mutation observed in the *PDR1* sequence, leading to a Y372C substitution, has not been described before, it is indeed very likely to constitute a GOF mutation, given that it is in the same position as the Pdr1 Y372N GOF mutation identified previously [224]. Altogether, the results for strain 044Fluco45 are consistent with the recurrent observation that the development of GOF mutations in Pdr1, leading to the upregulation of drug efflux pumps, is the main mechanism of azole resistance acquisition in clinical isolates [213], [214]. Based on the evolutionary path observed in the transcriptomics analysis, our current model is that the fluconazole-exposed population appears to be iteratively selected toward resistance at minimum cost, which appears to be, in the long term, the acquisition of Pdr1 GOF mutations, associated with drug efflux pump overexpression. Before reaching that optimal solution, the population goes through transcriptome-wide remodeling, likely reflecting the transient selection of more-fit subpopulations. When the Pdr1 GOF solution is reached by part of the population, these optimized cells are selected, leading to the dilution of other subpopulations until their disappearance.

Interestingly, the 044Fluco21 and 044Fluco31 populations do not exhibit the typical molecular mechanisms related to azole resistance in *C. glabrata* but still exhibit increased MICs for all azole drugs, resistance to posaconazole and to both posaconazole and clotrimazole, respectively, and increased ability to limit the intracellular accumulation of [^{3}H]clotrimazole, compared to the 044 clinical isolate. In the 044Fluco21 posaconazole-resistant strain, the expression of cellular processes such as protein synthesis, cell cycle, and DNA damage response, which are apparently unrelated to azole resistance, is upregulated. Thus, although the slight upregulation of *CgCDR1* in the 044Fluco21 strain may, at least partially, account for the posaconazole resistance phenotype, further characterization of the mechanisms of posaconazole resistance acquisition in *C. glabrata* are required.

The 044Fluco31 strain was found to display upregulation of the *ERG11* gene; however, the concentration of ergosterol was found to remain constant in this strain. Assuming that the increased *ERG11* gene expression results in increased Erg11 protein expression, this may at least prevent the decrease in the ergosterol content that fluconazole exposure is bound to induce and may thus decrease azole susceptibility by maintaining the Erg11/drug molecule ratio. Although upregulation of the *ERG11* gene [231], [457] and the augmentation of ergosterol levels [456] are associated with azole resistance in *Candida albicans*, in the case of *C. glabrata*, the expression level or amino acid substitutions of the *ERG11* gene do not seem to correlate with azole resistance acquisition in the clinical setting [230], [238], [458]. Given that there is no corresponding increase in ergosterol levels (as observed), the increased expression of *ERG11* may only partially, not completely, explain the observed gain in azole resistance in strain 044Fluco31. This observation prompted us to analyze in more detail the molecular basis underlying the posaconazole and clotrimazole resistance exhibited by strains 044Fluco31. Strain 044Fluco31 was found to exhibit upregulation of several adhesin-encoding genes, accompanied by an increased ability to adhere to other *C. glabrata* cells and to epithelial cells. Among the adhesin-encoding genes upregulated in the 044Fluco31 strain, we focused our research on three adhesins of the EPA family, encoded by the *CgEPA1*, *CgEPA3*, and *CgEPA10* genes. Significantly, the expression of Epa3

was found to decrease *C. glabrata* susceptibility to azole drugs, directly or indirectly leading to decreased accumulation of azole drugs. These results indicate Epa3 as an important, though unexpected, player in azole resistance. Our current model is that the role of CgEpa3, and possibly that of other adhesins, in azole resistance, might be to protect the cells from the extracellular concentration of the drug by promoting cell aggregation. Interestingly, comparing the genome of an azole-susceptible *C. glabrata* isolate with that of an azole-resistant *C. glabrata* isolate showed a higher number of adhesin-like genes in the resistant isolate [283]. As expected, CgEpa3 was also found to play a role in *C. glabrata* adhesion and biofilm formation, a finding consistent with the predicted role of CgEpa3 and its upregulation in *C. glabrata* biofilms *in vitro* [312].

Altogether, the analysis of the evolution toward multiazole resistance of the 044 clinical isolate suggests that prolonged exposure to fluconazole progressively selects the subpopulation that evolves to higher resistance with lower costs, leading to what appears to be a unique response to fluconazole induction. Indeed, the final transcriptional profile reached by the 044Fluco45 strain gives evidence of the important role of Pdr1 GOF mutations and the activation of MDR transporters in this context. Nevertheless, in the path to full resistance, several other, eventually more subtle, mechanisms of azole resistance may be employed by the evolving population, including the overexpression of adhesin-encoding genes. This study highlights the role of one of these genes, CgEpa3, in azole drug resistance, further supporting the notion that azole resistance is a multifactorial process, composed of different molecular mechanisms that should be considered in the design of better-suited therapeutic strategies.

1.6. Acknowledgements

This work was supported by FEDER and the “Fundação para a Ciência e a Tecnologia” (FCT) (contracts PTDC/BBB-BIO/4004/2014 and PTDC/BII-BIO/28216/2017 and by Ph.D. and postdoctoral grants to M.C. (PD/BD/116946/2016), P.P. (PD/BD/113631/2015), C.C. (SFRH/BPD/100863/2014), D.M.-H. (SFRH/BPD/91831/2012), S.N.P. (SFRH/BPD/ 92409/2013), and I.M.M. (SFRH/BPD/113285/2015). Funding received from FCT (grant UID/BIO/04565/2013), Programa Operacional Regional de Lisboa 2020 (project no. 007317), and Science Foundation Ireland (grant 12/IA/1343) is also acknowledged. This study was partially supported by a Joint Usage/Research Program of the Medical Mycology Research Center, Chiba University, Chiba, Japan.

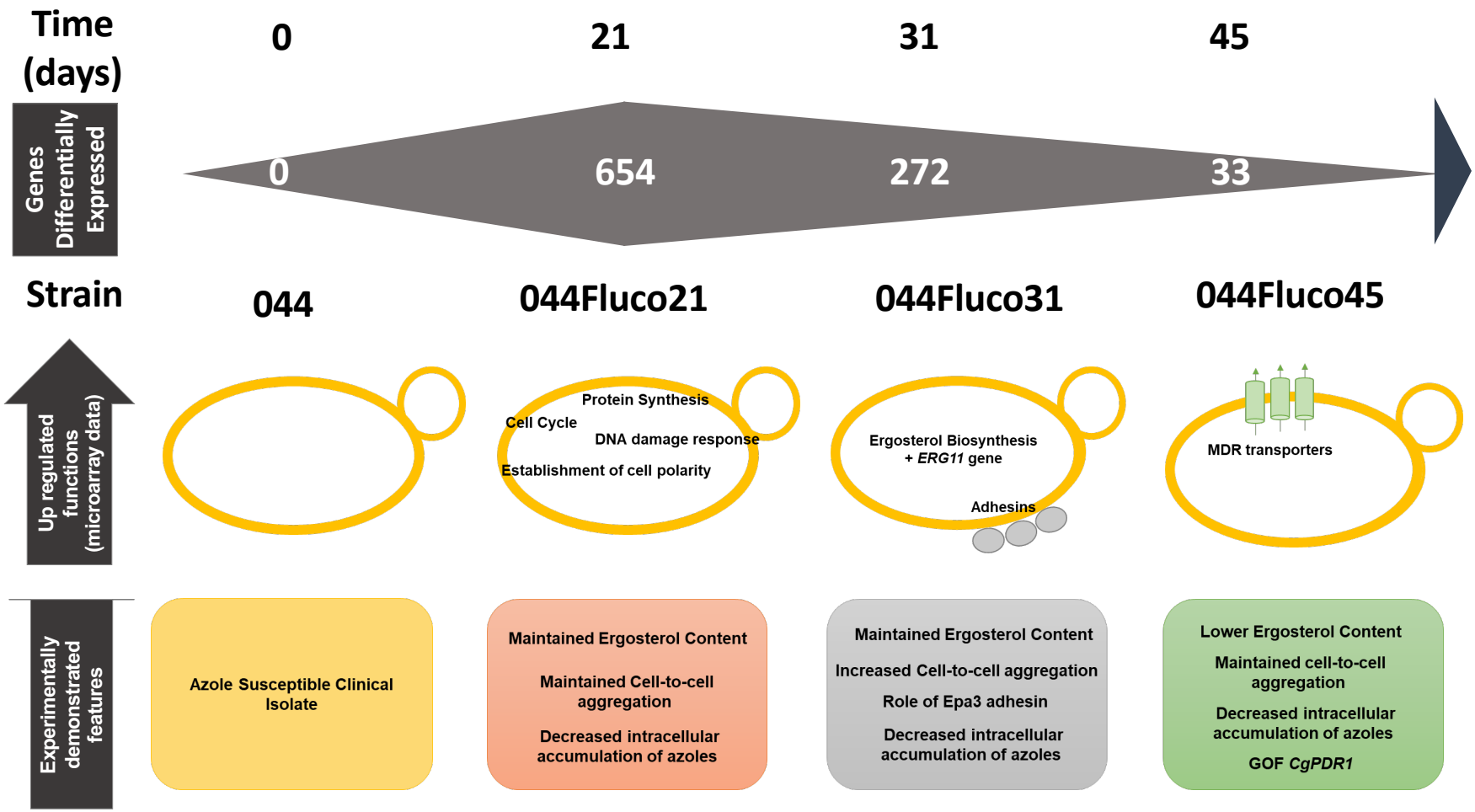

Figure III.12. Current model for the mechanisms underlying the evolution of the 044 clinical isolate toward multiazole resistance. Under the timeline of prolonged fluconazole exposure, indicating the days at which resistance to each azole drug was achieved, the main biological processes found to be upregulated in each of the azole-resistant strains are highlighted. Below, the conclusions of the experimental results obtained are given, suggesting that while for 044Fluco21, drug resistance appears to rely mostly on decreased drug accumulation due to increased CgCdr1 expression, the 044Fluco31 strain displays increased drug tolerance due to increased cell-to-cell adhesion, and 044Fluco45 exhibits multiazole resistance due to the acquisition of a CgPdr1 GOF mutation leading to increased expression of CgCdr1 and CgCdr2.

2. Eisosome component Pil2 participates in azole drug resistance and biofilm formation in *Candida glabrata*

2.1. Abstract

The second most common cause of candidiasis is *Candida glabrata*, a resourceful pathogenic yeast able to acquire resistance to all antifungal drugs used as therapy and to form biofilms on medical devices. Understanding the multiple molecular events that underlie the success of *C. glabrata* infections is crucial to overcome therapeutic failure.

In this work, the role of eisosome components was assessed, leading to the identification of CgPil2 (encoded by ORF *CAGL0G01738g*) as an azole resistance determinant, participating in biofilm formation in *C. glabrata*. Aiming to understand the role of CgPil2, a CgPil2-GFP fusion was used to find that this protein is localized in a punctate pattern at the plasma membrane, typical of eisosome localization. CgPil2 was also found to be required to decrease the accumulation of ^{3}H-radiolabeled-azoles, as well as to the normal biofilm formation in *C. glabrata*. Also, *CgPIL2* deletion was found to affect sphingolipids and ergosterol composition, suggesting that this component of eisosomes is necessary to maintain lipid homeostasis at the plasma membrane. Interestingly, the CgPil2 control of lipid composition at the plasma membrane affects the expression and localization of MDR transporters, like CgQdr2, that are responsible for azole resistance and biofilm formation in this pathogenic yeast.

Our current model is that CgPil2 confers azole resistance and influences biofilm formation by affecting plasma membrane lipid composition and, consequently, the correct localization and expression levels of multidrug transporters in *C. glabrata*.

2.2. Introduction

Candida glabrata is a pathogenic yeast responsible for mucosal and invasive candidiasis within immunocompromised patients, being considered the second most common cause of such diseases, right after *Candida albicans* [17], [18]. Invasive candidiasis caused by *C. glabrata* is known to lead to high mortality rates, ranging from 30-60% [17], [459]. Although different classes of antifungal drugs are available for treatment, their recurrent use as prophylaxis and treatment, has led to enhanced antifungal resistance, especially in the case of *C. glabrata* [460]. It's fast ability to develop resistance to a wide range of antifungal drugs, particularly azoles, raises concern on long-term therapeutic failure and highlights the need to understand the mechanisms underlying drug resistance in this pathogen.

The main known mechanism described as responsible for the rapid development of azole resistance in *C. glabrata* is the activation of multidrug efflux pumps of the ABC transporter superfamily, namely Cdr1, Cdr2 and Snq2 [461], and of the MFS, such as Qdr2, Aqr1, Tpo3, Tpo1_1, Tpo1_2 [144], [218]–[220]. This activation is usually due to GOF mutations in the Pdr1 transcription factor encoding gene, controlling the expression of some of these transporters [214], [219]. Another *C. glabrata* mechanism of azole resistance found mainly *in vitro* corresponds to the loss of mitochondrial function,

the so called *petite* phenotype, that signals for the activation of Pdr1, and indirectly leads to the upregulation of MDR transporters [462]. Nevertheless, such mechanism is very rarely found on resistant clinical isolates [463].

Besides antifungal resistance, *C. glabrata* is able to form biofilms on medical devices and human mucosa, as a means to infect and persist in the human host [35]. *C. glabrata* develops a biofilm composed mainly by a thick layer of yeast cells well aggregated to each other, wrapped by an ECM [464]. Besides enabling *Candida* species survival, biofilm formation is in itself a mechanism for antifungal resistance. The EPS of the ECM, as well as the different metabolism exhibited by persister cells, contribute to increased tolerance to antifungal compounds [335], making biofilm formation a precious pathogenic feature for this yeast.

In a previous study from our group, the evolution towards azole resistance, occurring upon prolonged exposure to serum-like concentrations of fluconazole, was followed at the transcriptome level [313]. Progressive acquisition of resistance to different azoles was found to rely on the selection of subpopulations that evolve towards a higher and more efficient resistance process, that culminated in the acquisition of a GOF mutation in *PDR1* [313]. The final multi-azole resistant strain displayed changes in the expression of only a few genes, including an uncharacterized ORF *CAGL0G01738g* very similar to the *Saccharomyces cerevisiae PIL1* gene, that encodes a component of a lipid-raft like structure called eisosome. The observed upregulation of *CgPIL2* in a multi-azole resistance strain prompted us to analyse whether eisosomes and eisosome components could be correlated with *C. glabrata* azole resistance and biofilm formation.

Eisosomes are very stable plasma membrane half-pipe linear invaginations, composed by the lipid domain described as Membrane Compartment of Can1 (MCC) and membrane-associated proteins, which together form a complex [465]. In *S. cerevisiae*, the eisosome components/proteins are quite well identified and described, having specific functions within this complex [466]. In this non-pathogenic yeast, eisosome proteins include Pil1, the core eisosome protein that confers its half-pipe shape, Lsp1, which also contains BAR (Bin/Amphiphysin/Rvs) domains [467] that bind to the plasma membrane promoting its curvature [468], and Seg1, responsible for recruiting Pil1 to the plasma membrane, for eisosome formation [469]. Eisosomes affect cell wall synthesis, serve as scaffolds to recruit proteins and are involved in stress resistance [470]. Regulation of the synthesis of sphingolipids and ergosterol also influences the formation of eisosomes in *S. cerevisiae* [470]. Both *S. cerevisiae* Δ*pil1* and *C. albicans* Δ*pil1*Δ*lsp1* deletion mutants lead to broad invaginations of the material of the cell wall [465], [471], suggesting they play an important role in the stability of the cell wall and plasma membrane.

To our knowledge, nothing is known about the formation and function of eisosomes in *C. glabrata*, although different homologs of *S. cerevisiae* and *C. albicans* have been identified. In this study, *C. glabrata* CgPil2, CgLsp1 and CgSeg1 were screened for a possible role in antifungal resistance. Given its identification as an azole resistance determinant, the impact of *CgPIL2* deletion in azole accumulation, biofilm formation, sphingolipid and ergosterol metabolism and the expression and sub-cellular localization of drug efflux pumps was evaluated providing interesting clues on the role played by Pil2 and eisosomes in azole resistance in *C. glabrata.*

2.3. Methods

2.3.1. Strains and growth medium

Candida glabrata KUE100 [339] and L5U1 (cgura3Δ0 cgleu2Δ0) [340] strains, the later kindly provided by John Bennett, NIAID, NIH, Bethesda, were used in this study. *Saccharomyces cerevisiae* strain BY4741 (MATa *ura3Δ0 leu2Δ0 his3Δ1 met15Δ0*) and its single deletion mutant BY4741_Δ*pil1* were obtained from the Euroscarf collection. Cells were batch-cultured at 30 ºC with orbital agitation (250 rpm) in the following growth media. YPD growth media, containing per liter: 20 g glucose (Merck), 10 g yeast extract (Difco) and 20 g bacterial-peptone (LioChem). Minimal growth (MG) medium contained per liter: 20 g glucose (Merck); 2.7 g $(NH_4)_2SO_4$ (Merck); 1.7 g yeast nitrogen base without amino acids or $(NH_4)_2SO_4$ (Difco). Wild-type *S. cerevisiae* BY4741 and strains derived from it were grown in MGI medium, obtained by supplementation of MG with 20 mg/L methionine, 20 mg/L histidine and 60 mg/L leucine, (all from Sigma). *C. glabrata* strains derived from L5U1, were grown in MGII medium, obtained by supplementation of MG with 60 mg/L leucine (all from Sigma). SDB contained 40 g glucose (Merck) and 10 g peptone (LioChem) per liter.

2.3.2. Cloning of the *C. glabrata CgPIL2* (ORF *CAGL0G01738g)*

The pGREG576 plasmid from the Drag & Drop collection [341] was used to clone and express the *C. glabrata* ORF *CAGL0G01738g* in *S. cerevisiae*, as described before for other heterologous genes [342]. pGREG576 was acquired from Euroscarf and contains a promoter *GAL1* and the yeast selectable marker *URA3*. The *CgPIL2* gene was generated by PCR, using genomic DNA extracted from the sequenced CBS138 *C. glabrata* strain, with the primers present in Table III.3. To enable expression of the *CgPIL2* gene in *C. glabrata*, the *GAL1* promoter was replaced by the constitutive *PDC1 C. glabrata* promoter. The *PDC1* promoter DNA was generated by PCR, using the primers in Table III.3. The recombinant plasmids pGREG576_*GAL1_CgPIL2* and pGREG576_*PDC1_CgPIL2* were obtained through homologous recombination in *S. cerevisiae* and verified by DNA sequencing.

2.3.3. Disruption of *C. glabrata* genes

The deletion of *CgPIL2, CgLSP1 and CgSEG1* genes (ORFs *CAGL0G01738g*, *CAGL0L08932g* and *CAGL0J01419g,* respectively) was carried out in the parental strain KUE100, using the method described by [339]. The target genes were replaced by a DNA cassette including the *CgHIS3* gene, through homologous recombination. The pHIS906 plasmid including *CgHIS3* was used as a template and transformation was performed as described previously [339]. Recombination locus and gene deletion were verified by PCR using the primers indicated in Table III.3.

2.3.4. Drug susceptibility assays

The MIC values of each antifungal drug were determined according to the M27-A3 protocol and the M27-S4 supplement of the CLSI [445], for the wild-type KUE100 and deletion mutant Δ*cgpil2.*

The antifungal drug susceptibilities of the *C. glabrata* KUE100 parental strain and the derived Δ*cgpil2* deletion mutant, and of the *C. glabrata* strain L5U1 harboring the pGREG576 vector or the pGREG576_*PDC1*_*CgPIL2* plasmids were evaluated by spot assays, as described previously [219].

2.3.5. [^{3}H]clotrimazole accumulation assays

[^{3}H]clotrimazole transport assays were carried out as described before [219] for the wild-type KUE100 and Δ*cgpil2* deletion mutant cells. To estimate the accumulation of clotrimazole (intracellular/extracellular [^{3}H]clotrimazole), yeast cells were grown in MG medium until the mid-exponential phase and were harvested by filtration. Cells were washed and resuspended in MG medium to obtain dense cell suspensions (optical density at 600nm [OD_{600}] = 5.0±0.2, equivalent to approximately 2.2 mg [dry weight]/mL). After a 5 min incubation at 30 °C, with agitation (150 rpm), 0.1 µM [^{3}H]clotrimazole (American Radiolabelled Chemicals; 1 mCi/mL) and 30 mg/L of unlabelled clotrimazole were added to the cell suspensions. The intracellular accumulation of labelled clotrimazole was followed for 30 min, as described elsewhere [219]. To calculate the intracellular concentration of labelled clotrimazole, the internal cell volume (Vi) of the exponential cells was considered constant and equal to 2.5 µl (mg [dry weight]$^{-1}$) [452].

2.3.6. Biofilm quantification

C. glabrata strains were tested regarding their capacity to form biofilm on a polystyrene surface, recurring to the PrestoBlue Cell Viability assay. For that, the *C. glabrata* strains were grown in SDB (pH 5.6) medium or MGII medium in the case of L5U1 wild-type strain harboring pGREG576 vector or the pGREG576_*PDC1*_*CgPIL2* plasmids, and harvested by centrifugation at mid-exponential phase. The cells were inoculated with an initial OD_{600nm} = 0.05±0.005 in 96-well polystyrene microtiter plates (Greiner) in SDB (pH 5.6) medium. Cells were cultivated at 30 ºC during 24±0.5 h with mild orbital shaking (70 rpm). After the incubation time, each well was washed two times with 100 µL of sterile PBS pH 7.4 (PBS contained per liter: 8 g NaCl (Panreac), 0.2 g KCl (Panreac), 1.81 g $NaH_2PO_4{\cdot}H_2O$ (Merck), and 0.24 g KH_2PO_4 (Panreac), to remove the cells unattached to the formed biofilm. Then, Presto Blue reagent was prepared in a 1:10 solution in the medium used for biofilm formation, adding 100 µL of the solution to each well. Plates were incubated at 37 ºC for 30 min. Afterwards, absorbance reading, at the wavelength of 570 nm and 600 nm for reference, was determined in a microplate reader (SPECTROstar Nano, BMG Labtech).

2.3.7. Assessment of the subcellular localization of CgPil2, CgCdr1 and CgQdr2

pGREG576-*GAL1*-*CgQDR2* plasmid was constructed previously [219], while pDS716_*CgCDR1* plasmid was kindly provided by Dominique Sanglard, Institute of Microbiology, University Hospital of Lausanne, (IMUL), Switzerland, Lausanne. The subcellular localization of the CgPil2, CgCdr1 and CgQdr2 proteins was determined based on the observation of *S. cerevisiae* BY4741 and Δ*scpil1* cells transformed with the pGREG576_*GAL1*_*CgPIL2* or pGREG576-*GAL1*-*CgQDR2* or pDS716_*CgCDR1* plasmids, and *C. glabrata* L5U1 cells transformed with pGREG576_*PDC1*_*CgPIL2*. These cells express

either CgPil2_GFP, CgCdr1_GFP and CgQdr2_GFP fusion proteins, whose localization may be determined using fluorescence microscopy. *S. cerevisiae* cell suspensions were prepared by cultivation in MGl medium, containing 0.5% glucose and 0.1% galactose, at 30 °C, with orbital shaking (250 rpm), until a standard culture optical density at OD_{600}=0.4±0.04 was reached. At this point, cells were transferred to the same medium containing 0.1% glucose and 1% galactose to induce protein expression. *C. glabrata* cell suspensions were prepared in MGlI medium until a standard culture OD_{600} of 0.4±0.04 was reached; they were then transferred to the same medium, protein overexpression was induced for 5 h. The distribution of the CgPil2_GFP, CgCdr1_GFP and CgQdr2_GFP fusion proteins in *S. cerevisiae* or in *C. glabrata* living cells was detected by fluorescence microscopy with a Zeiss Axioplan microscope (Carl Zeiss Microimaging) using excitation and emission wavelengths of 395 and 509 nm, respectively. Fluorescence images were captured using a cooled Zeiss Axiocam 503 color (Carl Zeiss Microscopy).

2.3.8. Assessment of the subcellular localization of sphingolipids by NBD-DHS staining

The subcellular localization of the sphingolipids in *C. glabrata* KUE100 and Δ*cgpil2* deletion mutant cells was determined based on C6 NBD-dihydrosphingosine (NBD-DHS; 1 mg/mL in methanol; Santa Cruz Biotechnology) staining, using fluorescence microscopy. Cells were grown in MG medium, at 30 °C, with orbital shaking (250 rpm), overnight. Cells were transferred to the same medium and grown until a standard culture OD_{600} of 0.2±0.04 was reached. NBD-DHS was added to 2mL of $4x10^7$ cells/mL, to a final concentration of 5 µM, and cell suspensions were incubated for 30 min, at 30 °C, with orbital shaking (250 rpm). Cells exposed to NBD-DHS were centrifuged (13,500 rpm for 2 min), washed twice and resuspended in sterile H_2O to final 10^7 cells/mL aliquots. NBD fluorescence was detected by fluorescence microscopy with a Zeiss Axioplan microscope (Carl Zeiss Microimaging) using excitation and emission wavelengths of 395 and 509 nm, respectively. Fluorescence images were captured using a cooled Zeiss Axiocam 503 color (Carl Zeiss Microscopy).

2.3.9. Assessment of the subcellular localization of ergosterol by filipin III staining

The subcellular localization of the ergosterol in *C. glabrata* KUE100 and Δ*cgpil2* deletion mutant cells was determined based on filipin III (1 mg/mL in PBS, pH 7.4, Sigma) staining, using fluorescence microscopy. Cells were grown in YPD medium, at 30 °C, with orbital shaking (250 rpm), overnight. Cells were transferred to the same medium and grown until a standard culture OD_{600} of 0.4±0.04 was reached. Cells were washed twice with PBS, pH 7.4, and filipin III was added to a final concentration of 5 µg/mL and cell suspensions were incubated for 30 min, in the dark, at room temperature. Cells exposed to filipin III were centrifuged (13,500 rpm for 2 min), washed twice and resuspended in PBS, pH 7.4. Filipin III fluorescence was detected by fluorescence microscopy with a Zeiss Axioplan microscope (Carl Zeiss Microimaging) using excitation and emission wavelengths of 340 and 385 nm, respectively. Fluorescence images were captured using a cooled Zeiss Axiocam 503 color (Carl Zeiss Microscopy).

2.3.10. Quantification of total cellular ergosterol

Ergosterol was extracted from cells using the following method adapted from reference [453], as described before [143]. *C. glabrata* KUE100 and Δ*cgpil2* cells were cultivated in YPD medium with orbital agitation (250 rpm) until stationary phase, harvested by centrifugation, and resuspended in methanol. Cholesterol (Sigma) was added as an internal standard to estimate the ergosterol extraction yield. The extracts were analysed by HPLC with a 250 mm by 4 mm C18 column (LiChroCART Purospher STAR RP-18, end-capped, 5 mm) at 30 °C. Samples were eluted in 100% methanol at a flow rate of 1 mL/min. Ergosterol was detected at 282 nm with a retention time of 12.46±0.24 min, while cholesterol was detected at 210 nm with a retention time of 15.36±0.35 min. Results are expressed in micrograms of ergosterol per milligram (wet weight) of cells.

2.3.11. Gene expression analysis

The levels of *CgCDR1, CgCDR2* and *CgQDR2* transcripts in the wild-type strain KUE100 and its derived Δ*cgpil2* deletion mutant strain, at exponential phase or exposed 1 h to 30 mg/L of clotrimazole, were assessed by quantitative real-time PCR. Total-RNA samples were obtained from cell suspensions harvested under control conditions, in the absence of drugs. Synthesis of cDNA for real-time RT-PCR experiments, from total-RNA samples, was performed using the Multiscribe reverse transcriptase kit (Applied Biosystems), following the manufacturer's instructions, and using 10 ng of cDNA per reaction. The RT-PCR step was carried out using SYBR green reagents. Primers for the amplification of the *CgCDR1*, *CgQDR2*, and *CgACT1* cDNA were designed using Primer Express software (Applied Biosystems) (Table III.3). The RT-PCRs were conducted in a thermal cycler block (7500 Real-Time PCR system; Applied Biosystems). The *CgACT1* mRNA level was used as an internal control. The relative values obtained for the wild-type strain under control conditions were set at 1, and the remaining values are presented relative to that control.

Table III. 3. List of primers used in this study.

Name	Sequence (5'-3')
***CgPIL1* gene cloning**	
pGREG_CgPIL1_Fw	GAATTCGATATCAAGCTTATCGATACCGTCGACAATGCACAGAACTTACTCTTTGA
pGREG_CgPIL1_Rv	GCGTGACATAACTAATTACATGACTCGAGGTCGACTCAAGCAGCTTGAGATTCTTCA
pGREG576 GAL1-to-PDCI promoter replacement	
pGREG_PDC1_Fw	TTAACCCTCACTAAAGGGAACAAAAGCTGGAGCTAGCATTTTTATACACGTTTTAC
pGREG_PDC1_Rv	GAAAAGTTCTTCTCCTTTACTCATACTAGTGCGGCTGTTAATGTTTTTTGGCAATTG
Deletion of *CgPIL1*, *CgLSP1*, *CgSEG1* and *CgURA3*	
∆*CgPIL2_Fw*	CTTATTTCTAGTAGAATGTGTAGTTTTTCATTTGTGGATAAGCACTGTAACAACAAGGCC GCTGATCACG
∆*CgPIL2_Rv*	GGGTATTCTCAGAAGTTAAGATAATGGAAAAACGTCGTCCAGTAGTAAAGACACATCAT CGTGAGGCTGG
∆*CgPIL2_Fw_conf*	GCACAAGACATATTCATTGA
∆*CgPIL2_Rv_conf*	CATGTAAGCGATCTTGTC
∆*CgLSP1_Fw*	GTGCGAAGCTGAAGCTTGCAATAGCTTGTCTTTAATTAGAGAAGGGGAGTTCGAACGGC CGCTGATCACG
∆*CgLSP1_Rv*	ATAAAGGTACAATCCAATTTTTATAGATTGGATCCTTAGTTTTCACCTTCATGGTGCATCG TGAGGCTGG
∆*CgLSP1_Fw_conf*	GCTGTCAAGCCAACTCTATCCT
∆*CgLSP1_Rv_conf*	CTTCCTGTTGTTCTTCTTCCCATTGT
∆*CgSEG1_Fw*	AAACGCTTATTTTAGTGGCAAGATATCCTTGATAAAGGCCAACAGGTGGATATAAAGGC CGCTGATCACG
∆*CgSEG1_Rv*	TAAAAATTTAATACAAATATCTTGAATTAATAGTATATCTTGCCCCTTAGTGATTCCATCG TGAGGCTGG
∆*CgSEG1_Fw_conf*	GAAATTACAATGACCAGATGC
∆*CgSEG1_Rv_conf*	ACGAACATTAGCAACACC
RT-PCR experiments	
CgACT1_Fw	AGAGCCGTCTTCCCTTCCAT
CgACT1_Rv	TTGACCCATACCGACCATGA
CgCDR1_Fw	GCTTGCCCGCACATTGA
CgCDR1_Rv	CCTCAGGCAGAGTGTGTTCTTTC
CgQDR2_Fw	TCACTGCATAGTTTCATATCGGACTA
CgQDR2_Rv	CAACTTCAGATAGATCAGGACCATCA

2.4. Results

2.4.1. CgPil2 confers azole resistance in *C. glabrata*

Given the previous observation that *CgPIL2* is upregulated in a *C. glabrata* multi-azole resistant strain [313], the possible role of the *C. glabrata* predicted eisosome protein components in antifungal resistance was assessed. Susceptibility assays were performed for the wild-type strain KUE100 and the derived deletion mutants ∆*cgpil2,* ∆*cglsp1,* ∆*cgseg1,* for different azole antifungal drugs. The ∆*cgpil2* deletion mutant, but not the remaining strains, was found to be more susceptible to the imidazoles ketoconazole, tioconazole and, particularly, clotrimazole, when compared to the parental strain, but not to the triazoles fluconazole and itraconazole (Figure III.13).

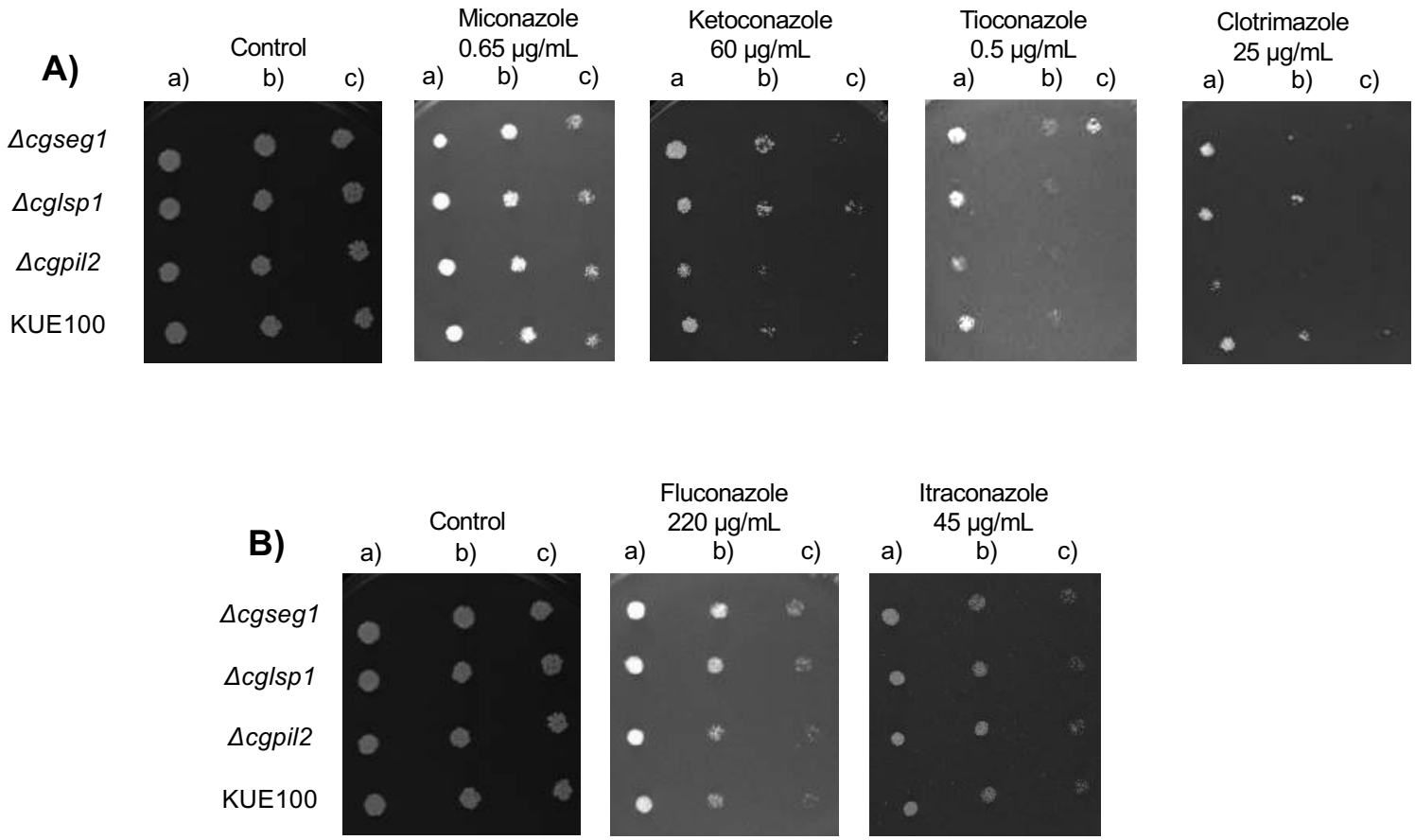

Figure III.13. Spot assays of the susceptibilities of *C. glabrata* strains KUE100 and Δ*cgpil2,* Δ*cglsp1,* Δ*cgseg1* deletion mutants to (A) miconazole, clotrimazole, ketoconazole, tioconazole and (B) fluconazole, itraconazole, at the concentrations indicated, in MG agar plates. The inocula were prepared as described in Methods. The cell suspensions used to prepare the spots were 1:5 (b) and 1:25 (c) dilutions of the cell suspension used for column (a). The images displayed are representative of at least three independent experiments.

The MIC_{50} determined for the Δ*cgpil2* deletion mutant by the standard National Committee for Clinical Laboratory Standards (NCCLS) method, confirmed the increased susceptibility exhibited by this strains to clotrimazole (MIC of 1mg/L), when compared to the wild-type strain (MIC of 2mg/L), while no difference in MIC levels could be detected for fluconazole.

Consistent with the previous results, the overexpression of CgPil2, from the pGREG576_*PDC1 _CgPIL2* recombinant plasmid, in *C. glabrata* was found to increase the resistance to imidazoles (Figure III.14A) and, to a lower extent, to triazoles as well (Figure III.14B).

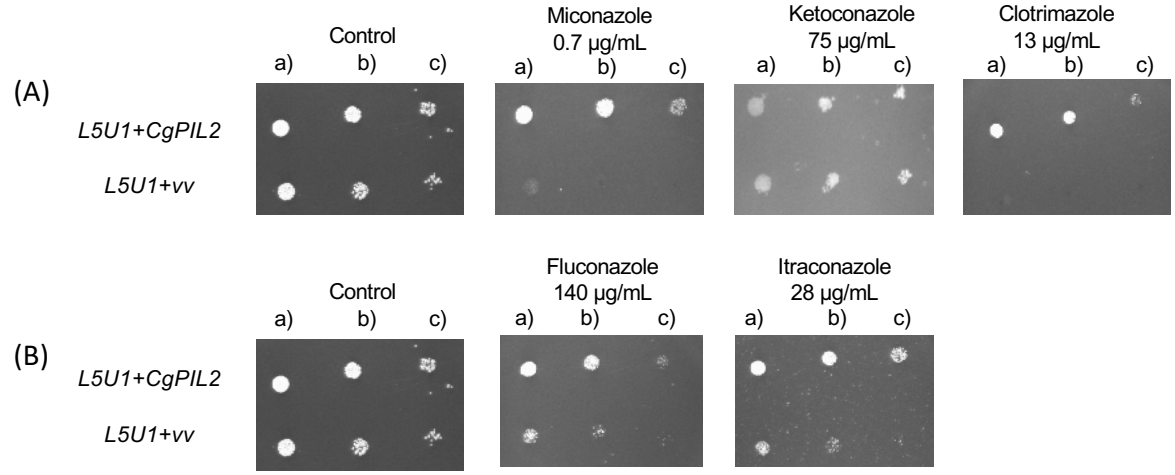

Figure III.14. Spots assays of the susceptibility of *C. glabrata* L5U1 strains harboring the pGREG576 (vv) plasmid or the pGREG576_*PDC1_CgPIL2* plasmid (*CgPIL2*) to (A) miconazole, ketoconazole and clotrimazole, and to (B) fluconazole and itraconazole, at the concentrations indicated, in MG agar plates. The inocula were prepared as described in Methods. The cell suspensions used to prepare the spots were 1:5 (b) and 1:25 (c) dilutions of the cell suspension used for column (a). The images displayed are representative of at least three independent experiments.

2.4.2. CgPil2 localization exhibits a punctate pattern at the plasma membrane

Given the clear importance of CgPil2 in azole resistance, the localization of CgPil2 coupled to GFP was evaluate in *S. cerevisiae* and *C. glabrata* by fluorescence microscopy. *S. cerevisiae* cells harboring the pGREG576_*GAL1_CgPIL2* plasmid, and *C. glabrata* cells harboring the pGREG576_*PDC1 _CgPIL2* plasmid showed the CgPil2-GFP fusion localized in specific patches of the plasma membrane (Figure III.15), most likely corresponding to the eisosomes of the plasma membrane. In fact, such specific punctate pattern of localization has been observed previously by the expression of components of eisosomes fused with GFP, like CaPil1, CaLsp1 and CaSur7, in *C. albicans* [465], [472], and ScCan1 in *S. cerevisiae* [473].

2.4.3. CgPil2 is required to reduce the intracellular accumulation of azoles in *C. glabrata*

To assess if the role of CgPil2 in clotrimazole resistance could be related with altering the partition of the drug across the plasma membrane, the accumulation of ^{3}H-labeled clotrimazole in non-adapted *C. glabrata* cells was followed after sudden exposure to the presence of 30 mg/L cold clotrimazole. Upon the deletion of *CgPIL2* gene, *C. glabrata* cells were found to accumulate 2-fold higher levels of radiolabeled clotrimazole than its parental strain (Figure III.16), suggesting that the role of CgPil2 in clotrimazole resistance indeed involves an effect in drug partitioning.

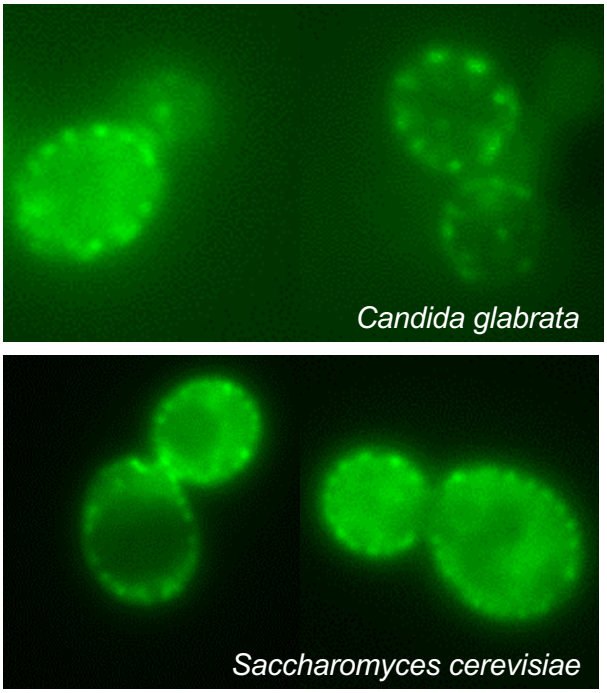

Figure III. 16. Fluorescence of exponential-phase *C. glabrata* L5U1 and *S. cerevisiae* BY4741 cells harboring the pGREG576_*PDC1*_*CgPIL2* and pGREG576_GAL1_*CgPIL2* plasmid (CgPil2_GFP), respectively. The results indicate that the CgPil2-GFP fusion protein localizes to the eisosomes of the plasma membranes of both *S. cerevisiae* and *C. glabrata* cells.

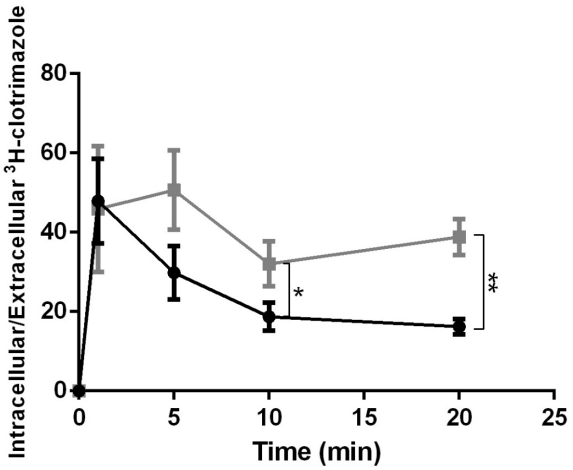

Figure III.15. Time course accumulation ratio of [^{3}H]clotrimazole in the *C. glabrata* KUE100 (black) and Δ*cgpil2* (grey) strains during cultivation in liquid MG in the presence of 30 mg/L unlabeled clotrimazole. The accumulation ratio values are averages for at least three independent experiments. Error bars represent standard deviations. *,P<0.05; **, P<0.01.

2.4.4. CgPil2 component of eisosomes is necessary for biofilm formation

Given the importance of biofilm formation for the success of *C. glabrata* infections, the possible role of CgPil2 in this process was assessed. For that, *in vitro* biofilm formation of the *C. glabrata* KUE100 wild-type strain, Δ*cgpil2* deletion mutant, L5U1 wild-type strain harboring the pGREG576 (vv) plasmid or the pGREG576_*PDC1_CgPIL2* plasmid, on 96-well polystyrene microplates with SDB (pH 5.6) medium was evaluated. The deletion of *CgPIL2* gene was found to decrease significantly the level of biofilm formed when compared to the parental strain, while the overexpression of *CgPIL2* in the L5U1 wild-type strain increases its ability to form biofilm (Figure III. 17).

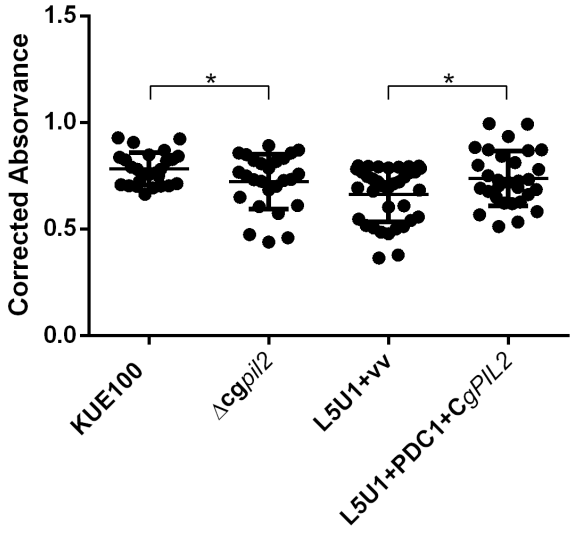

Figure III.17. CgPil2 is required for biofilm formation. Biofilm formation was assessed by Presto Blue Cell Viability assay in microtiter plates of wild-type *C. glabrata* KUE100 and the Δ*cgpil2* deletion mutant, and *C. glabrata* L5U1 strains harboring the pGREG576 (vv) plasmid or the pGREG576_*PDC1_CgPIL2* plasmid, which had been grown for 24 h in SDB medium, pH 5.6. The data are displayed on a scatter dot plot, where each dot represents the level of biofilm formed in a sample. Horizontal lines indicate the average levels of biofilm formed in at least three independent experiments. Error bars represent standard deviations. *, $P<0.05$.

2.4.5. CgPil2 expression affects membrane sphingolipids and ergosterol concentration

The specific localization of CgPil2 in a punctate pattern in the plasma membrane indicates its relation with eisosomes, similar to what is found in *S. cerevisiae* and *C. albicans* [465], [472], [473]. Eisosomes in both these species have been shown to regulate the homeostasis of different lipids, specially phosphatidylinositol 4,5-bisphosphate ($PI_{4,5}P_2$) and sphingolipids [470], [474]. The first is known to affect cell wall synthesis and morphogenesis in *S. cerevisiae, Schizosaccharomyces pombe* and *C. albicans* [470]. In *S. pombe*, SpPil1 regulates the levels of $PI_{4,5}P_2$ by a genetic pathway with SpSyj1 (synaptojanin-like lipid phosphatase), which dephosphorylates $PI_{4,5}P_2$ [475].

Given the importance of eisosomes in lipid composition regulation, we analysed the possible influence of CgPil2 on sphingolipid incorporation in the plasma membrane, using the NBD-DHS stain. By fluorescence microscopy, we assessed the presence of sphingolipids in the wild-type KUE100 and Δ*cgpil2* deletion mutant stained with NBD-DHS. The results point out the different levels of sphingolipids

between the two strains, having the deletion mutant higher levels of sphingolipids than its parental strain (Figure III.18).

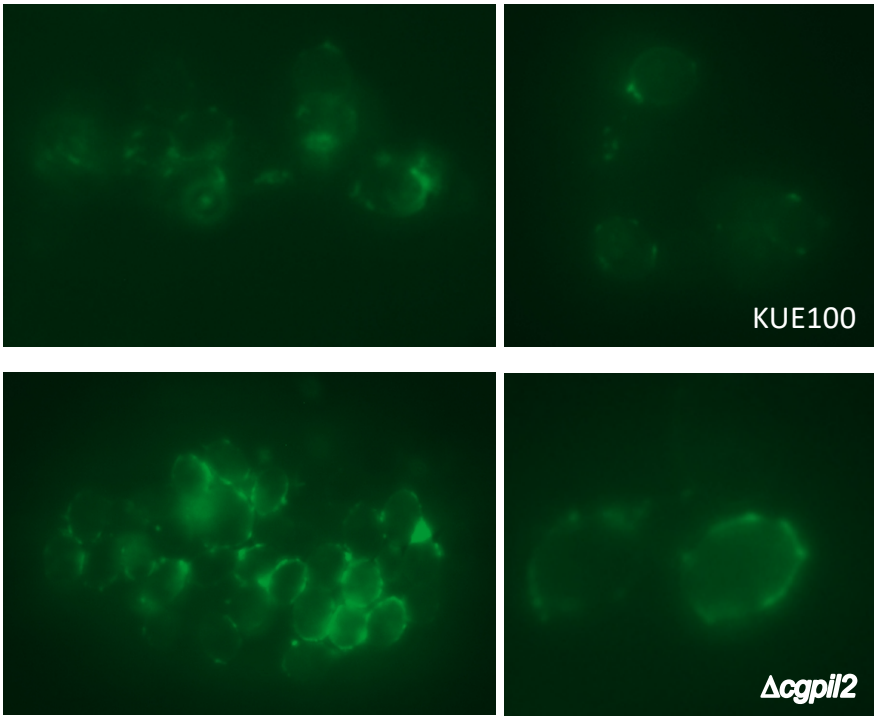

Figure III. 18. Fluorescence of exponential-phase *C. glabrata* KUE100 wild-type cells (above) and Δ*cgpil2* deletion mutant (below) cells stained with NBD-DHS. Results indicate that the CgPil2 controls the concentration and distribution of sphingolipids at the plasma membrane of *C. glabrata* cells.

Given that ergosterol is part of eisosomes in *S. cerevisiae* [476], we hypothesized that the role of CgPil2 in azole resistance might also be connected to its possible regulation of ergosterol levels on the membrane, as observed for sphingolipids. Therefore, filipin III staining of *C. glabrata* wild-type and Δ*cgpil2* deletion cells was performed to assess the distribution of ergosterol on the membrane. A different pattern is observed between wild-type and deletion mutant, where the wild-type exhibits some punctuated patterns that are not observed so frequently in the deletion mutant, which exhibits a more uniform distribution of filipin III on the membrane, and at certain cases, some intracellular accumulation (Figure III.19). Interestingly, ergosterol levels measured by HPLC are higher in the absence of *CgPIL2* gene, comparatively to the wild-type strain KUE100 (Figure III.20).

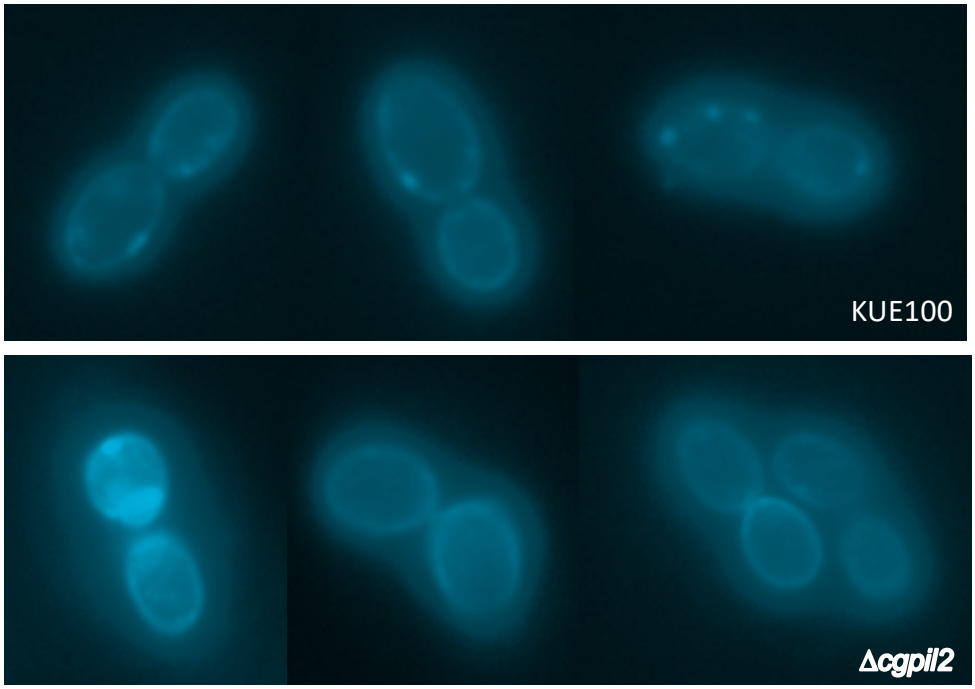

Figure III. 19. Fluorescence of exponential-phase *C. glabrata* KUE100 wild-type cells (above) and Δ*cgpil2* deletion mutant (below) cells stained with Filipin III. Results indicate that the CgPil2 controls the concentration and distribution of ergosterol at the plasma membrane of *C. glabrata* cells.

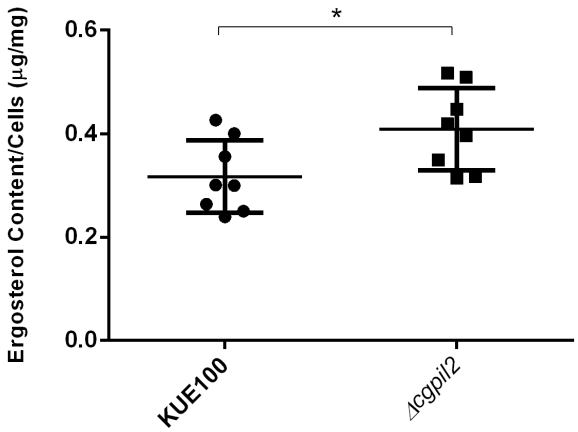

Figure III. 20. Total ergosterol contents of *C. glabrata* KUE100 and Δ*cgpil2* cells. Cells were harvested after 15 h of growth in YPD medium, and total ergosterol was extracted and quantified by HPLC. Cholesterol was used as an internal standard in order to evaluate the yield of the ergosterol extraction. The ergosterol contents displayed are averages of the results of at least three independent experiments. Error bars represent standard deviations. *, P<0.05.

2.4.6. CgPil2 affects the concentration of drug transporters at the plasma membrane, but not at the transcriptional level

Given the observation that CgPil2 controls azole accumulation levels, we assessed its possible influence on the expression or incorporation of MDR azole transporters at the plasma membrane.

The localization of CgCdr1 and CgQdr2 was assessed through the use of previously constructed GFP fusion proteins, by fluorescence microscopy. A decrease of the presence of these transporters at the plasma membrane upon the loss of Pil1 in *S. cerevisiae* was observed (Figure III.21A and B, respectively), suggesting that CgPil2 presence may also be necessary for the accumulation of the tested MDR transporters at the plasma membrane of *C. glabrata*.

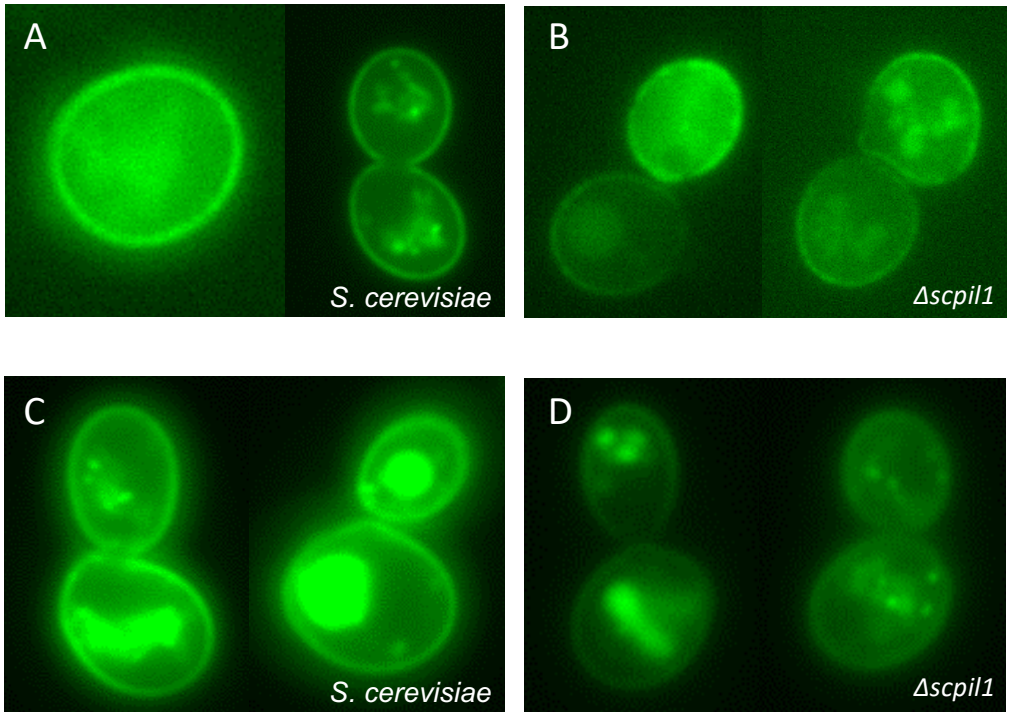

Figure III. 21. Fluorescence of exponential-phase *S. cerevisiae* BY4741 wild-type (A and C) and deletion mutant Δ*scpil1* cells (B and D) harboring the pDS716 recombinant plasmid (A and B) and harboring the pGREG576_*GAL1_CgQDR2* recombinant plasmid (C and D), after 5 h of galactose induction of recombinant protein production. The images displayed are representative of at least three independent experiments.

In addition, the effect of CgPil2 in the transcript levels of *CgCDR1* and *CgQDR2* genes in *C. glabrata* was assessed by RT-PCR. The transcript levels of these genes were measured in the wild-type strain and the deletion mutant Δ*cgpil2* at exponential phase, as well as after 1h of clotrimazole exposure. The results show the expression of both genes is upregulated under azole stress, but that *CgPIL2* expression has no effect on them, in any of the conditions tested (Figure III.22).

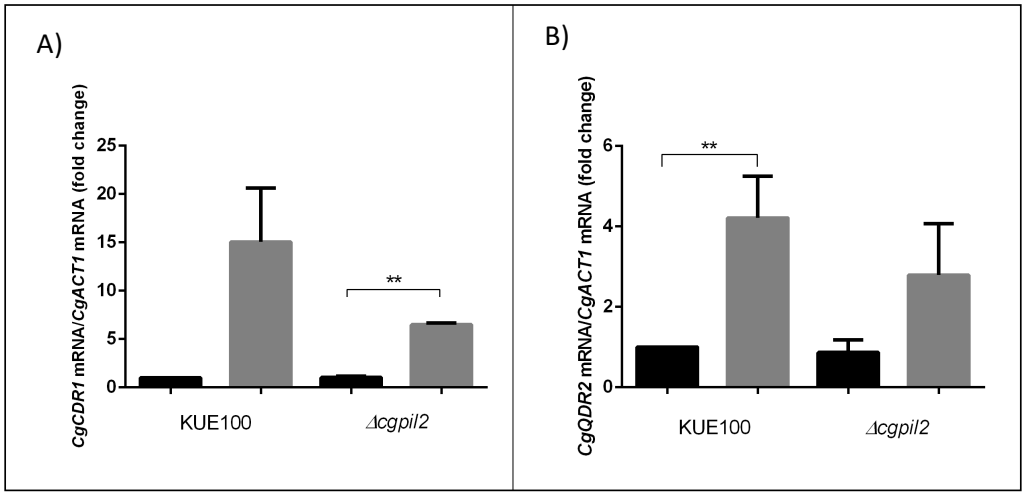

Figure III. 22. Comparison of the transcript levels of (A) *CgCDR1,* (B) *CgQDR2* in *C. glabrata* KUE100 wild-type strain and deletion mutant Δ*cgpil2* cells, in exponential phase (black) and after 1h of 30 mg/L clotrimazole exposure (grey). Transcript levels were determined by quantitative RT-PCR, as described in Methods, and are expressed as *CgGene/CgACT1* mRNA ratios. The value reported for wild-type cells under control conditions was considered equal to 1. The values shown are averages for at least three independent experiments. Error bars represent standard deviations. **, P<0.01.

2.5. Discussion

In this work, the CgPil2 eisosome component is shown to play a role in azole resistance, as well as in biofilm formation in the fungal pathogen *C. glabrata*.

A previous study of the evolution of a clinical isolate towards azole resistance [313] raised the hypothesis that CgPil2 could play a role in this process given its upregulation in the multi-azole resistance strain. Through drug susceptibility assays it was possible to conclude that indeed the absence of CgPil2 leads to a decreased resistance to imidazoles. The same effect could not be seen for other eisosome components, an observation that is likely due to the pivotal role played by Pil1 in the integrity of this lipidic structure [470].

The molecular basis of the observed phenotype was also scrutinized. After observing that CgPil2 displays a subcellular distribution compatible with eisosomal localization [465], [472], [473], and contributes to reduce the intracellular accumulation of clotrimazole and for biofilm formation, two hypotheses were raised for the importance of this eisosome component. Firstly, given that eisosomes are important for different processes, like nutrient uptake, secretion, morphogenesis and response to stress, in *S. cerevisiae* [470], it is possible that in *C. glabrata,* eisosomes also contribute to such processes influencing directly the resistance to azole drugs and the formation of biofilms. Secondly, CgPil2 might also contribute for the control of lipids and proteins on the plasma membrane, and therefore, for the homeostasis of the plasma membrane and cell wall [465], [471], which indirectly influences greatly the ability of *C. glabrata* to fight antifungal drugs and adhere and secret EPS for the ECM upon biofilm formation.

The obtained results indicate clearly that CgPil2 influences lipid homeostasis at the plasma membrane. Differences in sphingolipids and ergosterol levels were observed upon the deletion of *CgPIL2* comparatively to the parental strain. Although the underlying mechanism is still not clear, this

seems to be a conserved trait since changes of sphingolipids and ergosterol on the plasma membrane have been linked to components of eisosomes in *S. cerevisiae* [476] [477]. For instance, Slm1 and Slm2 proteins of eisosomes were found to feel membrane stress and activate the target of rapamycin kinase complex 2 (TORC2), which regulates sphingolipid metabolism [477]. Moreover, Nce102, another component of eisosomes, was proposed to act as a sphingolipid sensor, blocking or activating the downstream functions of Phk kinases, which regulate actin patch organization, endocytosis or eisosome assembly, according to sphingolipid distribution at the membrane [478]. The effect of CgPil2 in sphingolipid and ergosterol concentrations, may on its own, justify the change in azole accumulation, by changing drug partitioning across the plasma membrane.

Indirectly, nonetheless, it is reasonable to hypothesize that eisosomes may also affect the localization and stability of membrane proteins. Significantly, our results show that the localization in *S. cerevisiae* of CgCdr1 and CgQdr2 MDR transporters appears to be affected by ScPil1. Upon the absence of this eisosome component, the localization of CgCdr1 and CgQdr2 at the plasma membrane decreases significantly, although CgPil2 does not affect the expression of this transporters in *C. glabrata*. These results suggest that, although MDR transporters are not localized in eisosomes [144], [218]–[220], CgPil2 is probably necessary for their adequate localization at the plasma membrane, like in *S. cerevisiae*, and therefore, for azole resistance in *C. glabrata*.

Given that CgQdr2 is one of the MFS transporters found recently to be necessary for biofilm formation in *C. glabrata* [316], is possible that the importance of CgPil2 for its localization is one of the motives for its necessity during biofilm formation, as the correct distribution of CgQdr2, and probably other transporters with a role in biofilm formation [316], depends on the presence of eisosomes.

Overall, this work highlights a new player in clotrimazole resistance and biofilm formation, CgPil2, that acts indirectly through its role in lipid membrane homeostasis, affecting the localization of MDR transporters, such as CgCdr1 and CgQdr2, at the plasma membrane. Such effect on MDR transporters localization turns CgPil2 into an interesting target for the development of new therapeutic strategies.

2.6. Acknowledgements

This work was supported by “Fundação para a Ciência e a Tecnologia” (FCT) (Contract PTDC/BII-BIO/28216/2017 and BIOTECnico PhD grant to MC). Funding received by iBB-Institute for Bioengineering and Biosciences from FCT (UIDB/04565/2020) is acknowledged. We acknowledge John Bennett, of the National Institute of Allergy and Infectious Diseases, NIH, Bethesda, USA, for kindly providing the L5U1 strain.

IV. Final Discussion

Candida glabrata is a pathogenic yeast that adapts rapidly to the environment. Its ability to form biofilms guarantees its survival in harder conditions, where nutrient availability is low, or where a stressful niche is encountered. The virulence of this species, based on adherence and the ability to surpass exposure to different stresses, further increases the odds for its success as a pathogen. By being able to infect the human host, *Candida glabrata* constitutes the second most common cause of candidiasis [15], [17]–[19], being responsible for 15% of all invasive candidiasis [23], which have 40-60% mortality rates [12]. Even upon treatment, *C. glabrata* is known to resist better than other *Candida* species to the action of antifungal drugs [15], prevailing in the host, proliferating and causing a disease for which there is no perfectly effective therapeutic solution. The set of mechanisms behind biofilm formation, virulence and azole resistance are the secret behind the success of this pathogenic yeast. One needs to fully understand those in order to find the weak spot of *C. glabrata*, which may then be used as target for the development of new and efficacious therapeutic approaches for *C. glabrata* infections.

This thesis attempts to gather more insights about *C. glabrata* mechanisms of biofilm formation, virulence and antifungal resistance, which allow this yeast to persist and prevail as a human pathogen. The first chapter gathers the current knowledge about *C. glabrata* and the main mechanisms responsible for biofilm formation in all *Candida* species. Chapter I also englobes a revision of the main molecular mechanisms behind antifungal resistance and virulence in this pathogenic yeast, and how particular mechanisms seem to be behind biofilm formation, antifungal resistance and virulence, simultaneously. The notion that some molecular mechanisms are more central for the survival of *C. glabrata* should guide us to find the most significant mechanisms to target as therapy.

C. glabrata's capacity to form biofilms is one of the major problems in the clinical treatment of *C. glabrata* infections. This yeast is able to develop biofilms on different types of medical devices, such as vascular and urinary catheters or dentures [69], decreasing the changes of improvement of patients that exhibit an already compromised immune system. Biofilms are also a strategy employed by *C. glabrata* to survive within the human host, providing a protective environment for the yeast cells colonizing host niches [242]. Chapter II is a first attempt to go further and identify new regulators and effectors of biofilm formation, highlighting how this process might be connected to virulence through specific effectors involved in both processes.

With this purpose in mind, Chapter II is focused on the specific nature of biofilm formation in *C. glabrata,* from the first step of adhesion, either to an abiotic or biotic surface, until the development of a mature biofilm, analysing the transcriptomic changes that occur during this complex process. This work has shown how *C. glabrata* adheres very strongly to medical-related surfaces, similarly to other pathogens, and much more strongly than what has been previously observed for *Saccharomyces cerevisiae* [369]. This observation highlights the risk of using materials, like polystyrene, silicone elastomer and polyvinyl chloride, in the fabrication of medical devices. Nevertheless, *C. glabrata* is also able to adhere to human vaginal epithelial cells, exhibiting an adhesion profile similar to other pathogens, such as *Candida albicans* and *Pseudomonas aeruginosa* [370], [371], which shows how molecules from both human and yeast cells interact during the first moments of adhesion. This result

strongly points out the incredible adherence capacity of this yeast applied during both biofilm formation and development of virulence, correlated to the difficulty in the eradication of *C. glabrata* infections.

To further understand the continuous process of biofilm formation, a genetic screening was employed to ascertain which *C. glabrata* predicted orthologs of *C. albicans* transcription factors controlling biofilm formation, do have the same role in *C. glabrata*. This screening led to the identification of CgEfg1 and CgTec1, which, together, are responsible for 40% of the total changes of transcriptome that occur upon biofilm formation. It is quite incredible how *C. glabrata* changes half of its entire transcriptome to form a biofilm, although the same process in *C. albicans* also results in major transcriptomic changes [99]. Upregulation of adhesion and metabolic changes are the most significantly altered processes occurring within biofilm formation, highlighting the importance of aggregation between cells and adherence to the substrate and suggests that the cells are experiencing carbon and nitrogen limitation, a typical feature of inner biofilm cells which are exposed to lower nutrient concentrations. Moreover, the changes in metabolism may also be related to the production of EPS for the development of an ECM.

From a detailed analysis of the function of CgEfg1 and CgTec1 in this work, it is possible to conclude that both transcription factors regulate the metabolic changes during the continuous process of biofilm formation, but only CgEfg1 controls the adherence process from the first seconds of surface contact. CgEfg1 is most likely necessary for the adhesion of *C. glabrata* to biotic and abiotic surfaces, due to the regulation it exerts over adhesin-encoding genes, having been found to activate 5 adhesin-encoding genes in planktonic conditions and 13 other, upon 24 h of biofilm formation. In fact, one of the activated adhesins in planktonic conditions, by CgEfg1, is CgEpa6, which has been found to be necessary for *C. glabrata* adhesion to hydrophobic surfaces [368], just as CgEfg1. It is thus very likely that the necessary role of CgEfg1 in adhesion is the control of the expression of *CgEPA6* and other adhesin-encoding genes mediating adherence to the hydrophobic surfaces. The main processes regulated by CgEfg1 and CgTec1 in *C. glabrata* biofilm formation are depicted in Figure IV.1.

Interestingly, upon 24h *C. glabrata* biofilm formation, activation of response to stress and drugs is also observed. In fact, several MDR transporters were found to be upregulated upon biofilm formation: CgSnq2, CgAqr1, CgTpo3, CgTpo1_2, CgQdr2 and the not previously characterized DHA transporter, ORF *CAGL0L10912g*, now designated CgTpo4 in this thesis. Both CgEfg1 and CgTec1 were found to be responsible for the activation of some of those MDR transporters and others. CgCdr2 and CgTpo1_2 are activated by both transcription factors while CgEfg1 also induces CgCdr1, CgSnq2, CgTpo1_1, and CgFlr1, and CgTec1 activates CgTpo3 and CgQdr2. These results suggest MDR transporters are involved in biofilm formation, besides antifungal and stress resistance.

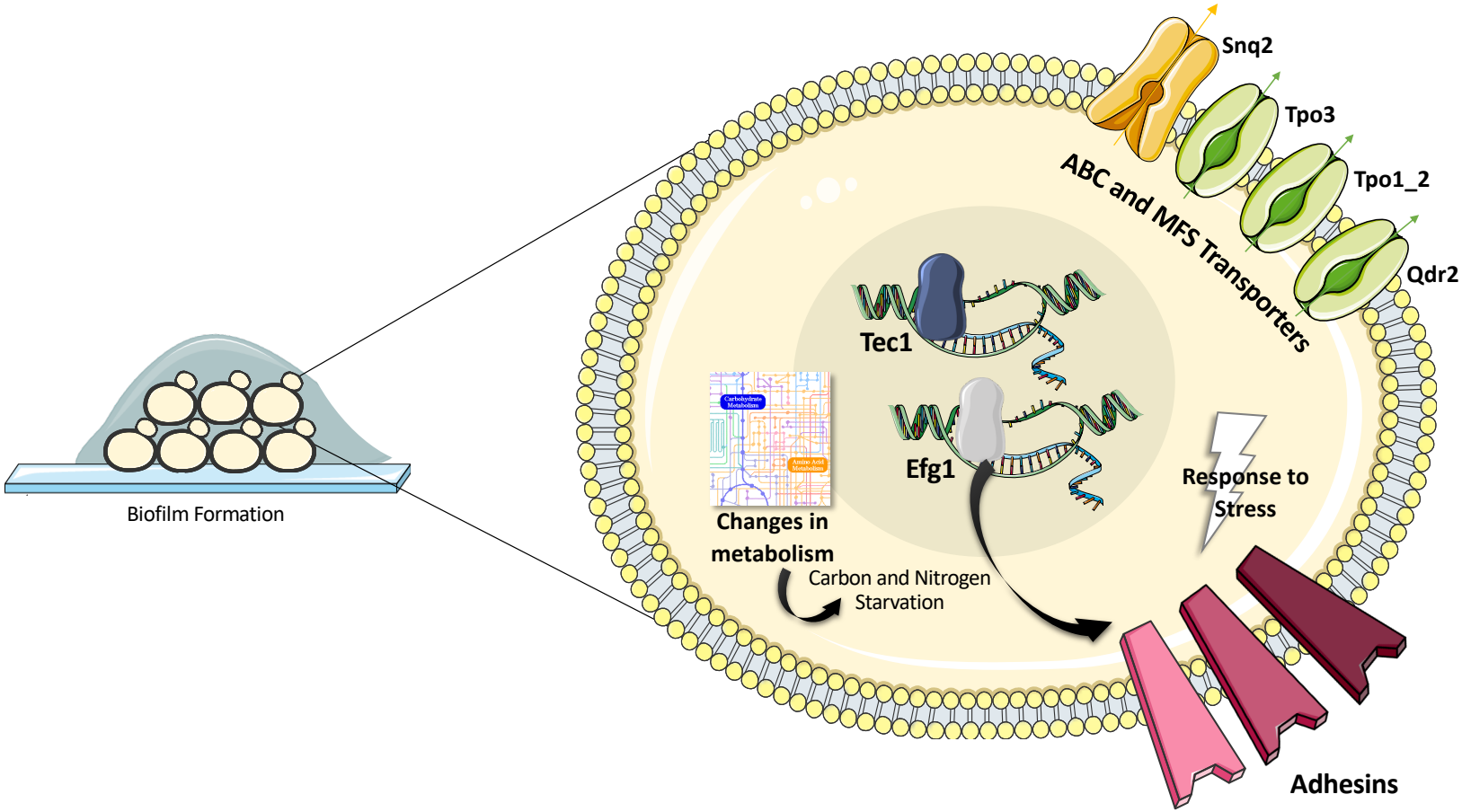

Figure IV.1. Regulation CgEfg1 and CgTec1 exert upon 24h of *C. glabrata* biofilm formation on polystyrene. Upregulation of ABC and MFS transporters and adhesins, increased response to stress, changes in the metabolism that indicate yeast cells are suffering from carbon and nitrogen limitations.

A recent work within our group has characterized several DHA transporters in light of their possible role in biofilm formation, unraveling the unmistakable need for *CgTPO1_2, CgQDR2, CgDTR1* and *CgTPO4* genes for this process [316]. The absence of theses transporters was found to significantly increased the membrane potential, indicating a role in the control of this potential by the transport of small charged molecules, like cations and polycations [316]. It is thus very likely that MFS transporters, as well as other MDR transporters, have a similar role to the bacterial MFS transporters, which by controlling the uptake of certain nutrients, stimulate or not, the formation of bacterial biofilms [479]. In fact, the absence of *CgTPO1_2, CgQDR2, CgDTR1* and *CgTPO4* genes have shown to decrease the expression of certain adhesins in biofilm conditions, and, in turn, CgTec1 was also found to activate *CgQDR2, CgTPO4* and *CgDTR1* genes at an early stage of biofilm formation [316]. This work has confirmed the results of previous studies that have identified the importance of CgQdr2 [317] and CgTpo1_2 [143] and identifies two new transporters, CgDtr1 and CgTpo4 necessary for biofilm formation, whose roles are depicted in Figure IV.2.

Interestingly, although having no role in antifungal resistance like other MFS transporters, CgDtr1 and CgTpo4 were also found to participate significantly in the virulence demonstrated by *C. glabrata* in the *G. mellonella* model of infection, as Subchapters II.2 and II.3 give evidence of. Upon larvae infection, *C. glabrata* was found to activate the expression of *CgDTR1* gene to cope with the stress felt within the larvae hemolymph and hemocytes, being also activated *in vitro* upon exposure to oxidative stress. In Subchapter II.2 , CgDtr1 is shown to be necessary for the full virulence of *C. glabrata* in the *G. mellonella* model of infection, more specifically, being required for the normal proliferation of this yeast in the hemolymph of the larvae, as well as inside the hemocytes, that have very similar functions to human macrophages [389]. The importance of CgDtr1 in this proliferation was found to be related to its central role in resisting oxidative and acidic stresses, which might also happen within the human host, specially within macrophages and the vaginal tract known for their acidic environment [386], [396]. CgDtr1 role in this resistance is related to its function as an acetate exporter, eliminating the acidic stress, and oxidative stress caused by the first, within the yeast cell. CgDtr1 role is thus essential for *C. glabrata* fight against the host immune system (Figure IV.3).

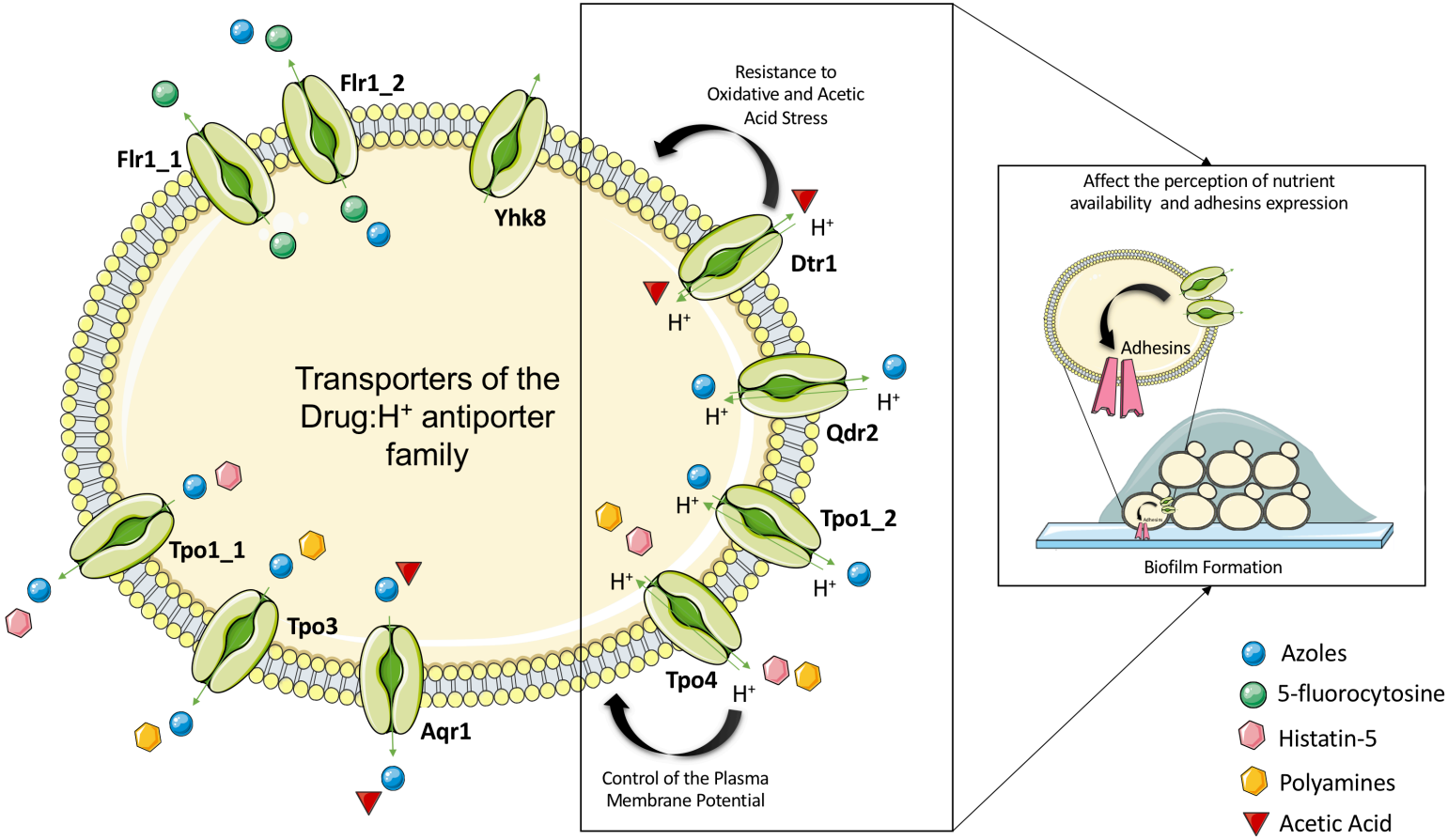

Figure IV.2. Transporters of the DHA family with a role in biofilm formation: CgDtr1, CgQdr2, CgTpo1_2 and CgTpo4 control the plasma membrane potential and affect the perception of nutrient availability and control de expression of adhesin-encoding genes. CgDtr1 is also able to resist oxidative and acetic acid stress, while CgTpo4 is necessary for the resistance against the AMP histatin-5.

On the other hand, the contribution of CgTpo4 for virulence is further elucidated in Subchapter II.3, being related to the capacity of *C. glabrata* to resist AMP and polyamines. The upregulation of the genes encoding AMP of *G. mellonella*, upon *C. glabrata* infection, show that this larva does indeed use this defense mechanism to cope with *C. glabrata* infection. CgTpo4 is thus necessary for the virulence of *C. glabrata* in the *Galleria* model of infection, fighting the AMPs used as a first line of defense. The absence of this DHA transporter did not change the AMPs immune response upon *C. glabrata* infection, indicating that CgTpo4 does not contribute for the identification of this yeast by the *Galleria* immune system. Moreover, CgTpo4 was shown to be necessary for the resistance against the human AMP, histatin-5, a defense against incoming microorganisms, especially fungi [431]. This role is also share by CgTpo1_1, in *C. glabrata* [143] and by CaFlu1, in *C. albicans* [427], indicating that probably other members of the DHA family are also involved in the full protection of *C. glabrata* against AMP of the human host, as well as other models of infection. In addition, CgTpo4 is another TPO transporter found to have a role in the transport of polyamines, which is not so surprising since AMP transport has been already linked to polyamine transport [417] (Figure IV.3). By controlling the homeostasis of polycationic polyamines and entrance of H^+ inside the cell, CgTpo4 has also a role in the regulation of the plasma membrane potential that we have described to be connected with its role in biofilm formation [316].

These studies characterizing two new DHA transporters, increase the number of DHA encoding genes in *C. albicans*, *CaQDR1*, *CaQDR2* and *CaQDR3* genes, and in *C. glabrata*, *CgTPO1_1* and *CgTPO1_2* genes, contributing to the success of these pathogenic yeasts. The roles of all the members of the DHA family in the transport of drugs, xenobiotics and inhibitory chemical compounds, is thus intrinsically related to *Candida* species virulence, biofilm formation and antifungal resistance, making them very interesting new drug targets for antifungal therapy.

In turn, Chapter III collects two new studies focused on previously uncharacterized cell peripheral proteins, which have very different functions within the yeast cell but that have been found to participate in both azole resistance and biofilm formation. The study of such proteins resulted from a global analysis whose main purpose was to induce azole resistance in a susceptible clinical isolate to unravel new molecular mechanisms behind such development of resistance, connected to the clinical setting. This ambition resulted from the observation that, although several azole resistant clinical isolates exhibit as main resistance mechanisms the presence of GOF mutation in CgPdr1, there are others whose ability to resist azole drugs remains unlinked to any known molecular mechanisms. Therefore, there's a current need to identify such molecular mechanisms, which may not be as frequent as CgPdr1 GOF mutations, but that also represent part of the reason for the arise of azole resistant clinical isolates.

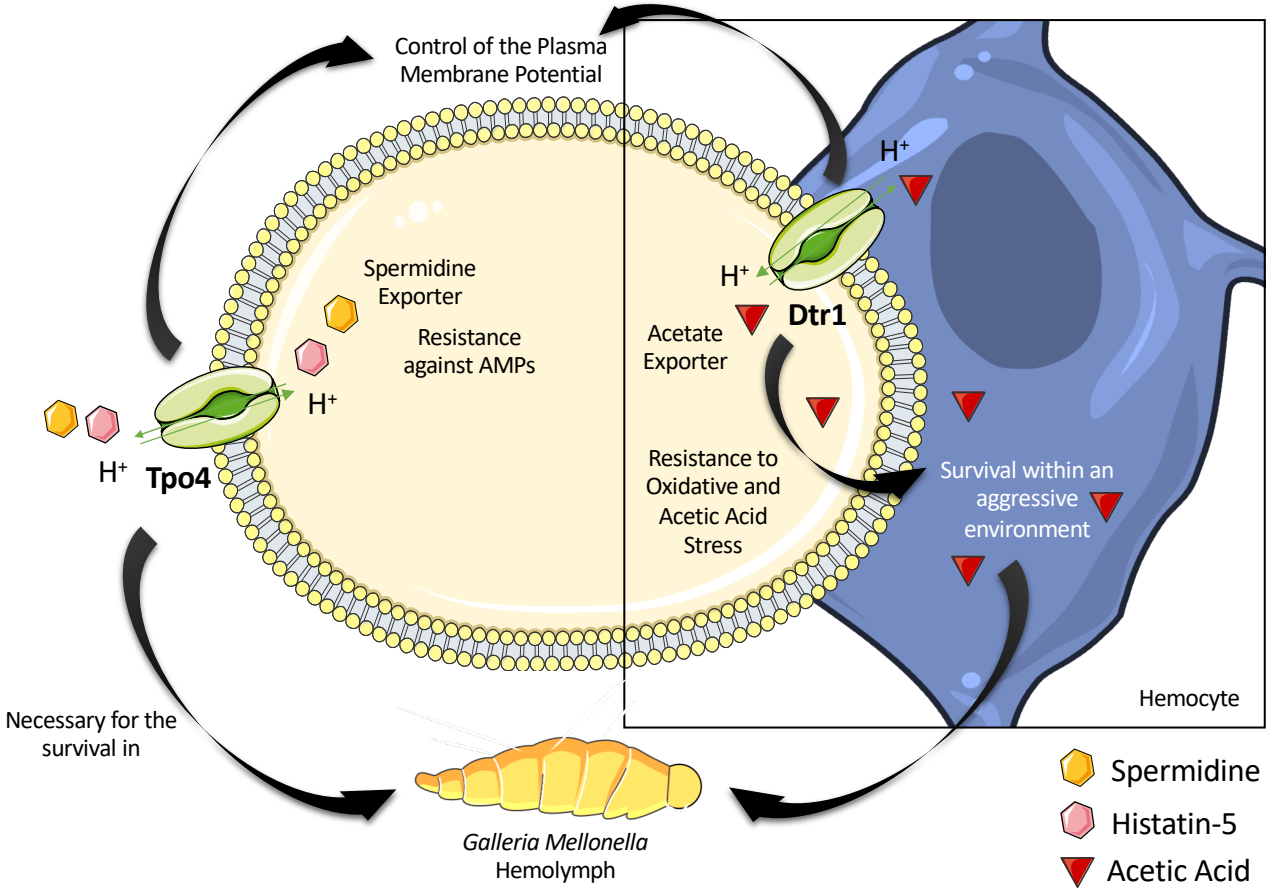

Figure IV.3. Proposed role of CgDtr1 and CgTpo4 in *C. glabrata's* virulence within *G. mellonella* model of infection. CgDtr1 is necessary for the survival within the hemolymph and hemocytes due to a possible role as an acetate exporter, allowing the development of resistance towards oxidative and acetic acid stress. CgTpo4 is necessary for the resistance against AMPs and polyamines (probable spermidine exporter), which allows the survival of *C. glabrata* within this model of infection. Both transporters influence the potential of the plasma membrane.

In the search for new molecular mechanisms of azole resistance, the 044 susceptible clinical isolate was exposed to a therapeutic serum concentration of fluconazole and its evolution towards azole resistance was followed. The isolate acquired resistance to four azole drugs: posaconazole, clotrimazole, voriconazole and fluconazole. Upon the acquisition of posaconazole or clotrimazole resistance, at days 21 and 31, respectively, no known molecular mechanisms were found to explain the acquisition of resistance, except a small upregulation of CgCdr1 ABC transporter and of CgErg11 target of azole drugs, respectively. Although the levels of ergosterol are maintained between the initial isolate until the acquisition of clotrimazole resistance, it is possible that *CgERG11* upregulation helps keeping the necessary levels of ergosterol for the survival of *C. glabrata.* Nevertheless, it is not totally responsible for the observed resistance in 044Fluco31 evolved strain. The upregulation of the expression of several adhesin-encoding genes upon the gain of clotrimazole resistance led to a screening for the possible role of different adhesins in azole resistance, identifying *CgEPA3* gene as required for the resistance to different azole drugs, being necessary for less intracellular accumulation of [^{3}H]clotrimazole. It is possible that CgEpa3, and other adhesins, have an impact on azole resistance through their adhesive function. By increasing the presence of adhesins on the cell wall, an increase of cell-to-cell aggregation will occur, decreasing the contact area of each single yeast cell, turning the aggregate more protected against the exposure to azole drugs (Figure IV.4).

In fact, when *CgEPA3* gene is deleted in the 044Fluco31 evolved strain, it loses the ability to resist fluconazole and clotrimazole. In addition to this important role, CgEpa3 was found also to be necessary for biofilm formation, a not so surprising role for an adhesin. Once again, a new molecular mechanism with high relevance in two major processes in *C. glabrata* was found, revealing how some mechanisms participate in different resources employed by *C. glabrata* for its survival in the human host.

If we continue along the evolution of our initially susceptible clinical isolate, we reach the point upon which the isolate acquires resistance to, not only posaconazole and clotrimazole, but also to voriconazole and fluconazole. At this time point, a mutation in CgPdr1 is observed, accompanied by the upregulation of MDR transporters, indicating a possible new GOF mutation in this transcription factor. Moreover, the number of genes differently expressed decreases throughout this evolution, indicating that the *C. glabrata* clinical isolate progresses to a more simple and effective solution for displaying azole resistance.

Interestingly, it is upon that final evolved strain, that it is possible to observe a slight upregulation of the ORF *CAGL0G01738g*, similar to the *PIL1* gene in *S. cerevisiae*, that prompted us to investigate CgPil2 within the scope of azole resistance. This study shows that CgPil2_GFP protein is localized in a punctuated pattern just like eisosome components in *C. albicans* and *S. cerevisiae* [465], [472], [473]. This eisosome component was found to be necessary for imidazole resistance, being necessary to decrease the intracellular accumulation of [^{3}H]clotrimazole. Further analysis of the function of CgPil2 unravelled its importance in lipid homeostasis at the plasma membrane. Upon deletion of *CgPIL2* gene, differences on the concentration and distribution of sphingolipids and ergosterol on the plasma membrane were observed, as well as an increase in the total level of ergosterol. Although it is not yet fully understood how, alterations in sphingolipid and ergosterol composition have been linked to the components of eisosomes in *S. cerevisiae* [476], [477] [477], [478]. The control CgPil2 exerts on the

homeostasis of lipids at the plasma membrane may itself explain the importance of this component of eisosomes in azole resistance, since changes in azole accumulation depend on the drug partitioning across the plasma membrane. Nevertheless, by changing the lipid content at the plasma membrane, CgPil2 may be indirectly influencing the distribution and presence of given MDR transporters at the plasma membrane. In fact, the absence of ScPil1 leads to a decrease of the presence of CgCdr1 and CgQdr2 when expressed in *S. cerevisiae*, which suggests that the same effect may happen in *C. glabrata*. However, the possible effect CgPil2 may have on CgQdr2 and CgCdr1 presence on the plasma membrane, does not happen at the transcription level (Figure IV. 4).

Interestingly, CgPil2, just like CgEpa3, was found to be necessary for biofilm formation. The role of CgPil2 in the lipid homeostasis, possibly affecting MDR transporters, may also be the reason behind its importance for biofilm formation. In fact, CgQdr2 is one of the MFS-DHA transporters found to be necessary for the control of the plasma membrane potential, influencing the formation of biofilms in *C. glabrata* (Figure IV.2). It seems likely that CgPil2 importance in azole resistance and biofilm formation is indirect, acting through the regulation of lipids on the plasma membrane, which, in turn, influence the membrane localization of MDR transporters.

Chapter III reunites evidences that unknown players are yet to be found regarding azole resistance in *C. glabrata,* especially in the clinical setting where several azole resistant isolates with unknown mechanisms of resistance are still found. Only when a full understanding of all the mechanisms of resistance is available, it will be possible to design more efficient therapeutic strategies to account for all possible scenarios.

The data gathered through this thesis also raises a number of important questions and perspectives for future work. For instance, regarding Subchapter II.1, it would be interesting to perform chromatin immunoprecipitation (ChIP)-sequencing to ascertain the direct target genes of the two new regulators of biofilm formation in *C. glabrata*, CgEfg1 and CgTec1. This would as well confirm the role of CgEfg1 and CgTec1 as main regulators of biofilm formation, giving additional information about new essential players in this complex process. Studies about the influence of CgEfg1 and CgTec1 on the formation and composition of the ECM would also be helpful to delineate which parts of biofilm formation these regulators are responsible for. Furthermore, it would be important to ascertain the significance of these regulators for biofilm formation *in vivo*, which could be performed using bioluminescence imaging in mouse models *in vivo,* avoiding host sacrifice [480]. And it would also be interesting to assess the possible role of CgEfg1 and CgTec1 in antifungal resistance of *C. glabrata* biofilms, given the upregulation of so many MDR transporters upon 24h of biofilm development.

Moreover, in Subchapters II.2 and II.3, it would be also interesting to test the results obtained in another model of infection to further ascertain the role of this MFS transporters in virulence and biofilm formation. Mouse models with *in vivo* catheter conditions would be ideal to assess the importance of these transporters in both processes. Given the importance of CgDtr1 for *C. glabrata* resistance in hemocytes of *G. mellonella*, it would be important to test if this role is maintained upon the interaction of *C. glabrata* with human monocytes. In the case of CgTpo4, further studies should be performed to assess its role in virulence and biofilm formation, in a vaginal/urogenital and oral models of infection, where polyamines and antimicrobial peptides are usually found, and encountered by this pathogenic

yeast *in vivo* [426], [481]. It would also enhance this work, the testing of the importance of CgTpo4 against more human AMPs, and observe their effect upon *C. glabrata* biofilm formation. These complementary works would link undoubtedly the role of these transporters to the virulence and biofilm formation of *C. glabrata.*

Regarding Chapter III, it would be important to ascertain if the upregulation of these new determinants is also present in resistant clinical isolates to validate their importance in the clinical setting. Specifically, in Subchapter III.2, the sphingolipid and ergosterol distribution results should be complemented with the quantification of the signal-staining by flow cytometry, for the *C. glabrata* wild-type and *Δcgpil2* deletion mutant. It would be important to overexpress *CgCDR1* and *CgQDR2* genes in the *Δcgpil2* deletion mutant, so that we could observe if these transporters also suffer changes in their localization upon the absence of *CgPIL2* in *C. glabrata*, as was observed in *S. cerevisiae* upon the absence of ScPil1. In addition, a western-blot analysis should be performed to quantify the expression of these transporters, CgCdr1 and CgQdr2, on the plasma membrane, upon the loss of this eisosome component, in *C. glabrata*. These experiments would confirm our hypothesis that CgPil2 influences azole resistance and biofilm formation, by influencing the correct localization and, eventually, expression of MDR transporters. Moreover, given that the upregulation of *CgPIL2* in the resistant evolved strain was accompanied by a possible GOF mutation in CgPdr1, it would be interesting to assess the possible role of this regulator in the control of expression of *CgPIL2* gene. Given the importance of both CgEpa3 and CgPil1 in biofilm formation, it would be relevant to assess if these determinants may also play a role in *C. glabrata* virulence, which would turn them in even more promising drug targets. This could be initially evaluated in the *G. mellonella* model of infection and further confirmed on mouse models.

Overall, this thesis presents the identification of two new regulators of biofilm formation, CgEfg1 and CgTec1, as well as four new effectors in biofilm formation: CgDtr1, CgTpo4, CgEpa3 and CgPil1, the first two involved in virulence, and the last two implicated in azole resistance. It is fascinating to observe that all new players from both Chapter II and Chapter III studied herein are involved in biofilm formation. Besides highlighting this process as a key function for *C. glabrata* success, this thesis also indicates that still a lot is yet to be uncovered regarding biofilm formation in this pathogen. Furthermore, this thesis gives support to the notion that there are central mechanisms that allow the success of this pathogenic yeast infecting the human host and that such molecular mechanisms contribute to understand how *C. glabrata* is effective in responding to different situations, using the same effectors. This effectiveness should be used against it, designing new therapeutic strategies to target these vital central mechanisms.

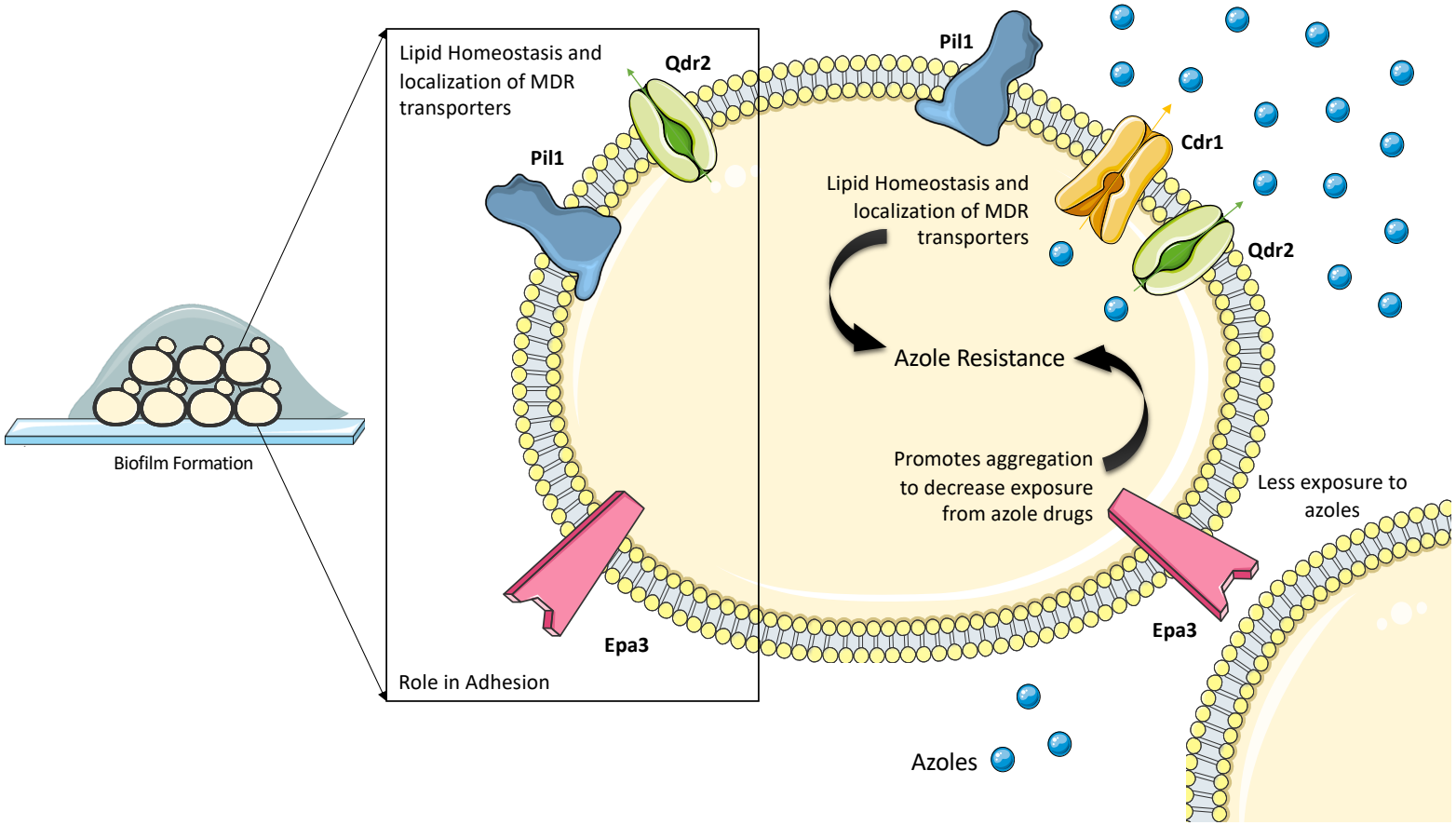

Figure IV.4. Role of CgEpa3 and CgPil1 in biofilm formation and azole resistance. CgEpa3 allows adhesion for biofilm formation and promotes aggregation which is believed to decrease the exposure to azole drugs. CgPil1 controls lipid homeostasis influencing the localization of MDR transporters important for both biofilm formation and azole resistance, like CgQdr2.

List of Publications and Communications

Peer-reviewed scientific publications:

Santos R, Cavalheiro M, Costa C, Takahashi-Nakaguchi A, Okamoto M, Chibana H, Teixeira MC (2020) Screening the Drug:H+ Antiporter family for a role in biofilm formation in *Candida glabrata*. Front Cell Infect Microbiol. 10(29).

Monteiro PT, Oliveira J, Pais P, Antunes M, Palma M, Cavalheiro M, Galocha M, Godinho CP, Martins LC, Bourbon N, Mota MN, Ribeiro RA, Viana R, Sá-Correia I, Teixeira MC (2019) YEASTRACT+: a portal for cross-species comparative genomics of transcription regulation in yeasts. Nucleic Acids Res. gkz859

Galocha M, Pais P, Cavalheiro M, Pereira D, Viana R, Teixeira MC (2019) Divergent Approaches to Virulence in *C. albicans* and *C. glabrata*: Two Sides of the Same Coin. Int J Mol Sci. 20(9).

Pais P, Galocha M, Viana R, Cavalheiro M, Pereira D, Teixeira MC (2019) Microevolution of the pathogenic yeasts *Candida albicans* and *Candida glabrata* during antifungal therapy and host infection. Microb Cell. 6(3).

Cavalheiro M, Costa C, Silva-Dias A, Miranda IM, Wang C, Pais P, Pinto SN, Mil-Homens D, Sato-Okamoto M, Takahashi-Nakaguchi A, Silva RM, Mira NP, Fialho AM, Chibana H, Rodrigues AG, Butler G, Teixeira MC (2018) A transcriptomics approach to unveiling the mechanisms of *in vitro* evolution towards fluconazole resistance of *a Candida glabrata* clinical isolate. Antimicrob Agents Chemother. 63(1).

Cavalheiro M, Pais P, Galocha M, Teixeira MC (2018) Host-pathogen interactions mediated by MDR transporters in fungi: as pleiotropic as it gets! Genes. 9:332.

Cavalheiro M, Teixeira MC (2018) *Candida* biofilms: threats, challenges, and promising strategies. Front Med (Lausanne). 5:28.

Romão D, Cavalheiro M, Mil-Homens D, Santos R, Pais P, Costa C, Takahashi-Nakaguchi A, Fialho AM, Chibana H, Teixeira MC (2017) A new determinant of *Candida glabrata* virulence: the acetate exporter CgDtr1. Front Cell Infect Microbiol. 7:473.

Teixeira MC, Monteiro P, Palma M, Costa C, Godinho CP, Pais P, Cavalheiro M, Antunes M, Lemos A, Pedreira T, Sá-Correia I (2017) YEASTRACT: an upgraded database for the analysis of transcription regulatory networks in *Saccharomyces cerevisiae*. Nucleic Acids Res. gkx842

Pais P, Costa C, Cavalheiro M, Romão D, Teixeira MC (2016) Transcriptional control of drug resistance, virulence and immune system evasion in pathogenic fungi: a cross-species comparison. Front. Cell. Infect. Microbiol. 6:131.

Costa C, Ribeiro J, Miranda IM, Silva-dias AI, Cavalheiro M, Costa-de-oliveira S, Rodrigues AG and Teixeira MC (2016) Clotrimazole drug resistance in *Candida glabrata* clinical isolates correlates with increased expression of the drug:H+ antiporters CgAqr1, CgTpo1_1, CgTpo3 and CgQdr2. Front. Microbiol. 7:526.

Costa C, Ponte A, Pais, P, Santos R, Cavalheiro M, Takashi Y, Chibana H, Teixeira MC (2015), "New mechanisms of flucytosine resistance in *C. glabrata* unveiled by a chemogenomics analysis in *S. cerevisiae*", PLoS ONE, 10(8):e0135110.

Submitted:

Mafalda Cavalheiro, Daniela Romão, Rui Santos, Dalila Mil-Homens, Pedro Pais, Catarina Costa, Mónica Galocha, Diana Pereira, Azusa Takahashi-Nakaguchi, Hiroji Chibana, Arsénio M. Fialho, Miguel C. Teixeira, Role of CgTpo4 in polyamine and antimicrobial peptide resistance: determining virulence in *Candida glabrata* (submitted to Scientific Reports).

Mafalda Cavalheiro, Diana Pereira, Carolina Leitão, Pedro Pais, Easter Ndlovu, Andreia I. Pimenta, Rui Santos, Azusa Takahashi-Nakaguchi, Michiyo Okamoto, Mihaela Ola, Hiroji Chibana, Arsénio M. Fialho, Geraldine Butler, Etienne Dague, Miguel Cacho Teixeira, From the first touch to biofilm establishment by the human pathogen *Candida glabrata*: a genome-wide to nanoscale view (submitted to Communications Biology).

In preparation:

Mafalda Cavalheiro, Pedro Pais, Catarina Costa, Rui Santos, Michiyo Okamoto, Azusa Takahashi-Nakaguchi, Hiroji Chibana, Miguel Cacho Teixeira, Eisosome component Pil2 participates in azole drug resistance and biofilm formation in *Candida glabrata* (in preparation).

Book Chapters:

Cavalheiro M, Teixeira MC (2018) In the crossroad between drug resistance and virulence in Fungal Pathogens, In: Skoneczny M. (eds) Stress response mechanisms in fungi. Springer, Cham.
Cavalheiro M, Costa C, Pais P, Teixeira MC (2016) Acquisition of resistance to azole antifungal drugs in *Candida* species: imidazoles versus triazoles, In: Ketoconazole: Clinical Pharmacokinetics, Uses and Potential Side Effects. Nova Science Publishers, Inc., NY, USA.

Oral communications in national or international meetings:

Cavalheiro M, Costa C, Wang C, Silva-Dias A, Miranda IM, Rodrigues AG, Butler G, Teixeira MC, Transcriptomic analysis of the *in vitro* evolution of a susceptible *Candida glabrata* clinical isolate towards azole resistance, oral presentation at the anual meeting 2018 of Portuguese Society of Genetics, 14-15 June 2018, Porto, Portugal.

Poster communications in national or international meetings:

Cavalheiro M, Costa C, Silva-Dias A, Miranda IM, Chibana H, Rodrigues AG, Butler G, Teixeira MC, New insights into the clinical acquisition of azole resistance: witnessing *Candida glabrata* evolution, poster presentation at 29th European Congress of Clinical Microbiology and Infectious Diseases (ECCMID), 13-16 April 2019, Amesterdam, Netherlands.

Cavalheiro M, Costa, C, Wang C, Silva-Dias A, Miranda IM, Rodrigues AG, Butler G, Teixeira MC, Determining the molecular mechanisms behind the *in vitro* evolution of a susceptible *Candida glabrata* clinical isolate towards azole resistance, poster presentation at 14th ASM Conference on *Candida* and Candidiasis, 15-19 April 2018, Providence, RI, EUA.

Cavalheiro M, Santos R, Romão D, Mil-Homens D, Pais P, Costa C, Viana R, Vagueiro S, Fialho A, Teixeira MC, Determining virulence by protecting the cell from host induced stresses: the unexpected role of *C. glabrata* multidrug transportes, poster presentation at MICROBIOTEC'17, 7-9 December 2017, Porto, Portugal.

Cavalheiro M, Santos R, Romão D, Mil-Homens D, Pais P, Costa C, Galocha M, Fialho A, Teixeira MC, A new role for *C. glabrata* drug:H+ antiporters: in the crossroad between drug resistance and virulence, poster presentation at HFP2017 – Advanced Lecture Course, Molecular Mechanisms of Host-Pathogens Interactions and Virulence in Human Fungal Pathogens, 13-19 May 2017, La Colle sur Loup, France.

Cavalheiro M, Costa C, Wang C, Miranda IM, Silva-Dias A, Rodrigues AG, Butler G, Teixeira MC, Unveiling the mechanisms of azole drug resistance acquisition in a clinical isolate: a transcriptomics approach, poster presentation at PYFF6 – 6th Conference on Physiology of Yeasts and Filamentous Fungi, 11 -14 July 2016, Lisbon, Portugal.

Awards:

Travel Grant Award given by the Microbiology Society, at *Candida* and Candidiasis 2020 conference, Montreal, Canada.

Travel Grant Award given by the American Society for Microbiology, at 14th ASM Conference on *Candida* and Candidiasis, 15-19 April 2018, Providence, RI, EUA.

Best Poster Communication in the Symposium Cellular Microbiology and Pathogenesis given by the Portuguese Society of Microbiology, at MICROBIOTEC'17, 7-9 December 2017, Porto, Portugal.

References

[1] A. Casadevall, “Fungal Diseases in the 21st Century: The Near and Far Horizons,” *Pathog. Immun.*, vol. 3, no. 2, p. 183, 2018, doi: 10.20411/pai.v3i2.249.

[2] A. Fausto, M. L. Rodrigues, and C. Coelho, “The still underestimated problem of fungal diseases worldwide,” *Front. Microbiol.*, vol. 10, no. 214, pp. 1–5, 2019, doi: 10.3389/fmicb.2019.00214.

[3] A. Casadevall, “Don’t Forget the Fungi When Considering Global Catastrophic Biorisks,” *Heal. Secur.*, vol. 15, no. 4, pp. 341–342, 2017, doi: 10.1089/hs.2017.0048.

[4] M. A. Garcia-Solache and A. Casadevall, “Global warming will bring new fungal diseases for mammals,” *MBio*, vol. 1, no. 1, pp. 1–3, 2010, doi: 10.1128/mBio.00061-10.

[5] G. D. Brown, D. W. Denning, N. A. R. Gow, S. M. Levitz, M. G. Netea, and T. C. White, “Hidden Killers: Human Fungal Infections,” *Sci. Transl. Med.*, vol. 4, no. 165, pp. 1–9, 2012, doi: 10.1126/scitranslmed.3004404.

[6] G. Suleyman and G. J. Alangaden, “Nosocomial Fungal Infections: Epidemiology, Infection Control, and Prevention,” *Infect. Dis. Clin. North Am.*, vol. 30, no. 4, pp. 1023–1052, 2016, doi: 10.1016/j.idc.2016.07.008.

[7] F. C. Odds, “*Candida* Infections: an overview,” *CRC, Crit. Rev. Microbiol.*, vol. 15, no. 1, pp. 1–5, 1987.

[8] B. Gonçalves, C. Ferreira, C. T. Alves, M. Henriques, J. Azeredo, and S. Silva, “Vulvovaginal candidiasis: Epidemiology, microbiology and risk factors,” *Crit. Rev. Microbiol.*, vol. 42, no. 6, pp. 905–927, 2016, doi: 10.3109/1040841X.2015.1091805.

[9] M. F. Mushi, O. Bader, L. Taverne-Ghadwal, C. Bii, U. Groß, and S. E. Mshana, “Oral candidiasis among African human immunodeficiency virus-infected individuals: 10 years of systematic review and meta-analysis from sub-Saharan Africa,” *J. Oral Microbiol.*, vol. 9, no. 1, p. 1317579, Jan. 2017, doi: 10.1080/20002297.2017.1317579.

[10] T. Muadcheingka and P. Tantivitayakul, “Distribution of *Candida albicans* and non-albicans *Candida* species in oral candidiasis patients: Correlation between cell surface hydrophobicity and biofilm forming activities,” *Arch. Oral Biol.*, vol. 60, no. 6, pp. 894–901, Jun. 2015, doi: 10.1016/j.archoralbio.2015.03.002.

[11] S. Patil, B. Majumdar, S. C. Sarode, G. S. Sarode, and K. H. Awan, “Oropharyngeal Candidosis in HIV-Infected Patients—An Update,” *Front. Microbiol.*, vol. 9, no. 980, May 2018, doi: 10.3389/fmicb.2018.00980.

[12] S. Ghazi *et al.*, “The epidemiology of *Candida* species in the Middle East and North Africa,” *J. Mycol. Med.*, vol. 29, no. 3, pp. 245–252, 2019, doi: 10.1016/j.mycmed.2019.07.006.

[13] C. F. Rodrigues, S. Silva, and M. Henriques, “*Candida glabrata*: A review of its features and resistance,” *Eur. J. Clin. Microbiol. Infect. Dis.*, vol. 33, no. 5, pp. 673–688, 2014, doi: 10.1007/s10096-013-2009-3.

[14] M. Kothalawala, J. A. A. S. Jayaweera, S. Arunan, and A. Jayathilake, “The emergence of non-albicans candidemia and evaluation of HiChrome Candida differential agar and VITEK2 YST® platform for differentiation of *Candida* bloodstream isolates in teaching hospital Kandy, Sri Lanka,” *BMC Microbiol.*, vol. 19, no. 1, p. 136, Dec. 2019, doi: 10.1186/s12866-019-1518-3.

[15] M. A. Pfaller, D. J. Diekema, J. D. Turnidge, M. Castanheira, and R. N. Jones, “Twenty Years of the SENTRY Antifungal Surveillance Program: Results for *Candida* Species From 1997–2016,” *Open Forum Infect. Dis.*, vol. 6, no. Supplement_1, pp. S79–S94, Mar. 2019, doi: 10.1093/ofid/ofy358.

[16] M. Sanguinetti, B. Posteraro, and C. Lass-Flörl, “Antifungal drug resistance among *Candida* species: mechanisms and clinical impact,” *Mycoses*, vol. 58, pp. 2–13, Jun. 2015, doi: 10.1111/myc.12330.

[17] A.-H. Mari, M. Valkonen, E. Kolho, N. Friberg, and V.-J. Anttila, “Clinical and microbiological factors associated with mortality in candidemia in adult patients 2007–2016,” *Infect. Dis. (Auckl).*, pp. 1–7, Sep. 2019, doi: 10.1080/23744235.2019.1662941.

[18] J. Fuller *et al.*, “Species distribution and antifungal susceptibility of invasive *Candida* isolates from Canadian hospitals: results of the CANWARD 2011–16 study,” *J. Antimicrob. Chemother.*, vol. 74, no. Supplement_4, pp. iv48–iv54, Aug. 2019, doi: 10.1093/jac/dkz287.

[19] M. A. Pfaller and D. J. Diekema, “Epidemiology of invasive candidiasis: A persistent public health problem,” *Clin. Microbiol. Rev.*, vol. 20, no. 1, pp. 133–163, 2007, doi: 10.1128/CMR.00029-06.

[20] R. Khatib, L. B. Johnson, M. G. Fakih, K. Riederer, and L. Briski, “Current trends in candidemia and species distribution among adults: *Candida glabrata* surpasses *C. albicans* in diabetic patients and abdominal sources,” *Mycoses*, vol. 59, no. 12, pp. 781–786, Dec. 2016, doi: 10.1111/myc.12531.

[21] Z. Zeng, G. Tian, Y. Ding, K. Yang, J. Liu, and J. Deng, “Surveillance study of the prevalence, species distribution, antifungal susceptibility, risk factors and mortality of invasive candidiasis in a tertiary teaching hospital in Southwest China,” *BMC Infect. Dis.*, vol. 19, no. 1, p. 939, Dec. 2019, doi: 10.1186/s12879-019-4588-9.

[22] N. Ghaddar, A. El Roz, G. Ghssein, and J.-N. Ibrahim, “Emergence of Vulvovaginal Candidiasis among Lebanese Pregnant Women: Prevalence, Risk Factors, and Species Distribution,” *Infect. Dis. Obstet. Gynecol.*, vol. 2019, pp. 1–8, Jul. 2019, doi: 10.1155/2019/5016810.

[23] J. C. O. Sardi, L. Scorzoni, T. Bernardi, A. M. Fusco-Almeida, and M. J. S. Mendes Giannini, “*Candida* species: current epidemiology, pathogenicity, biofilm formation, natural antifungal products and new therapeutic options,” *J. Med. Microbiol.*, vol. 62, no. 1, pp. 10–24, Jan. 2013, doi: 10.1099/jmm.0.045054-0.

[24] R. Kaur, R. Domergue, M. L. Zupancic, and B. P. Cormack, “A yeast by any other name: *Candida glabrata* and its interaction with the host,” *Curr. Opin. Microbiol.*, vol. 8, no. 4, pp. 378–384, 2005, doi: 10.1016/j.mib.2005.06.012.

[25] S. Wong, M. A. Fares, W. Zimmermann, G. Butler, and K. H. Wolfe, “Evidence from comparative genomics for a complete sexual cycle in the ‘asexual’ pathogenic yeast *Candida glabrata*.,” *Genome Biol.*, vol. 4, no. 2, p. R10, 2003, doi: 10.1186/gb-2003-4-2-r10.

[26] M. T. Yassin, A. A. Mostafa, A. A. Al-Askar, and R. Bdeer, “*In vitro* antifungal resistance profile of *Candida* strains isolated from Saudi women suffering from vulvovaginitis,” *Eur. J. Med. Res.*, vol. 25, no. 1, p. 1, Dec. 2020, doi: 10.1186/s40001-019-0399-0.

[27] M. A. Pfaller, M. Castanheira, S. R. Lockhart, A. M. Ahlquist, S. A. Messer, and R. N. Jones, “Frequency of decreased susceptibility and resistance to echinocandins among fluconazole-resistant bloodstream isolates of *Candida glabrata*,” *J. Clin. Microbiol.*, vol. 50, no. 4, pp. 1199–1203, 2012, doi: 10.1128/JCM.06112-11.

[28] M. A. Pfaller, S. A. Messer, L. N. Woosley, R. N. Jones, and M. Castanheira, “Echinocandin and Triazole Antifungal Susceptibility Profiles for Clinical Opportunistic Yeast and Mold Isolates Collected from 2010 to 2011 : Application of New CLSI Clinical Breakpoints and Epidemiological Cutoff Values for Characterization of Geographic,” vol. 51, no. 8, pp. 2571–2581, 2013, doi: 10.1128/JCM.00308-13.

[29] D. Farmakiotis, J. J. Tarrand, and D. P. Kontoyiannis, “Drug-Resistant *Candida glabrata* Infection in Cancer Patients,” *Emerg. Infect. Dis.*, vol. 20, no. 11, pp. 1833–1840, Nov. 2014, doi: 10.3201/eid2011.140685.

[30] A. Persyn *et al.*, “Monitoring of Fluconazole and Caspofungin Activity against *In Vivo Candida glabrata* Biofilms by Bioluminescence Imaging,” *Antimicrob. Agents Chemother.*, vol. 63, no. 2, pp. e01555-18, Nov. 2018, doi: 10.1128/AAC.01555-18.

[31] S. P. Hawser and L. J. Douglas, “Biofilm formation by *Candida* species on the surface of catheter materials *in vitro*,” *Infect. Immun.*, vol. 62, no. 3, pp. 915–921, 1994.

[32] M. Cuéllar-Cruz, E. López-Romero, J. C. Villagómez-Castro, and E. Ruiz-Baca, "*Candida* species: New insights into biofilm formation," *Future Microbiol.*, vol. 7, no. 6, pp. 755–771, 2012, doi: 10.2217/fmb.12.48.

[33] M. Henriques, J. Azeredo, and R. Oliveira, "*Candida* Species Adhesion to Oral Epithelium: Factors Involved and Experimental Methodology Used," *Crit. Rev. Microbiol.*, vol. 32, no. 4, pp. 217–226, 2006, doi: 10.1080/10408410601023524.

[34] E. Vitális *et al.*, "*Candida* biofilm production is associated with higher mortality in patients with candidaemia," *Mycoses*, p. myc.13049, Jan. 2020, doi: 10.1111/myc.13049.

[35] K. Kumar, F. Askari, M. Sahu, and R. Kaur, "*Candida glabrata*: A Lot More Than Meets the Eye," *Microorganisms*, vol. 7, no. 2, p. 39, 2019, doi: 10.3390/microorganisms7020039.

[36] K. F. Mitchell, H. T. Taff, M. A. Cuevas, E. L. Reinicke, H. Sanchez, and D. R. Andes, "Role of Matrix β-1,3 Glucan in Antifungal Resistance of Non-*albicans Candida* Biofilms," *Antimicrob. Agents Chemother.*, vol. 57, no. 4, pp. 1918–1920, Apr. 2013, doi: 10.1128/AAC.02378-12.

[37] G. Ramage, J. P. Martínez, and J. L. López-Ribot, "*Candida* biofilms on implanted biomaterials: A clinically significant problem," *FEMS Yeast Res.*, vol. 6, no. 7, pp. 979–986, 2006, doi: 10.1111/j.1567-1364.2006.00117.x.

[38] M. Galocha, P. Pais, M. Cavalheiro, D. Pereira, R. Viana, and M. C. Teixeira, "Divergent Approaches to Virulence in *C. albicans* and *C. glabrata*: Two Sides of the Same Coin," *Int. J. Mol. Sci.*, vol. 20, no. 2345, 2019.

[39] A. Roetzer *et al.*, "*Candida glabrata* environmental stress response involves *Saccharomyces cerevisiae* Msn2/4 orthologous transcription factors," *Mol. Microbiol.*, vol. 69, no. 3, pp. 603–620, 2008, doi: 10.1111/j.1365-2958.2008.06301.x.

[40] M. Cuéllar-Cruz *et al.*, "High resistance to oxidative stress in the fungal pathogen *Candida glabrata* is mediated by a single catalase, Cta1p, and is controlled by the transcription factors Yap1p, Skn7p, Msn2p, and Msn4p," *Eukaryot. Cell*, vol. 7, no. 5, pp. 814–825, 2008, doi: 10.1128/EC.00011-08.

[41] M. Briones-Martin-del-Campo *et al.*, "The superoxide dismutases of *Candida glabrata* protect against oxidative damage and are required for lysine biosynthesis, DNA integrity and chronological life survival," *Microbiology*, vol. 161, no. 2, pp. 300–310, Feb. 2015, doi: 10.1099/mic.0.000006.

[42] G. Gutiérrez-Escobedo, E. Orta-Zavalza, I. Castaño, and A. De Las Peñas, "Role of glutathione in the oxidative stress response in the fungal pathogen *Candida glabrata*," *Curr. Genet.*, vol. 59, no. 3, pp. 91–106, Aug. 2013, doi: 10.1007/s00294-013-0390-1.

[43] Y.-L. Chen *et al.*, "Convergent Evolution of Calcineurin Pathway Roles in Thermotolerance and Virulence in *Candida glabrata*," *G3*, vol. 2, no. 6, pp. 675–691, Jun. 2012, doi: 10.1534/g3.112.002279.

[44] T. Miyazaki, H. Nakayama, Y. Nagayoshi, H. Kakeya, and S. Kohno, "Dissection of Ire1 Functions Reveals Stress Response Mechanisms Uniquely Evolved in *Candida glabrata*," *PLoS Pathog.*, vol. 9, no. 1, p. e1003160, Jan. 2013, doi: 10.1371/journal.ppat.1003160.

[45] K. I. M. Lewis, "Riddle of Biofilm Resistance," *Antimicrob. Agents Chemother.*, vol. 45, no. 4, pp. 999–1007, 2001, doi: 10.1128/AAC.45.4.999.

[46] R. M. Donlan, "Biofilms and Device-Associated Infections," *Emerg. Infect. Dis.*, vol. 7, no. 2, pp. 277–281, 2001.

[47] L. J. Douglas, "*Candida* biofilms and their role in infection," *Trends Microbiol.*, vol. 11, no. 1, pp. 30–36, 2003.

[48] C. Potera, "Forging a Link Between Biofilms and Disease," *Science (80-.).*, vol. 283, no. 5409, pp. 1837–1839, 1999, doi: 10.1126/science.283.5409.1837.

[49] G. O'Toole, H. B. Kaplan, and R. Kolter, "Biofilm Formation as Microbial Development," *Annu.*

Rev. Microbiol., vol. 54, pp. 49–79, 2000.

[50] C. Enfert and G. Janbon, “Biofilm formation in *Candida glabrata*: What have we learnt from functional genomics approaches?,” *FEMS Yeast Res.*, vol. 16, no. 1, pp. 1–13, 2016, doi: 10.1093/femsyr/fov111.

[51] C. R. Sims, L. Ostrosky-zeichner, and J. H. Rex, “Invasive Candidiasis in Immunocompromised Hospitalized Patients,” *Arch. Med. Res.*, vol. 36, pp. 660–671, 2005, doi: 10.1016/j.arcmed.2005.05.015.

[52] S. Ganguly and A. P. Mitchell, “Mucosal biofilms of *Candida albicans*,” *Curr. Opin. Microbiol.*, vol. 14, no. 4, pp. 380–385, 2011, doi: 10.1016/j.mib.2011.06.001.Mucosal.

[53] A. Dongari-bagtzoglou, H. Kashleva, P. Dwivedi, P. Diaz, and J. Vasilakos, “Characterization of Mucosal *Candida albicans* Biofilms,” *PLoS One*, vol. 4, no. 11, pp. 1–9, 2009, doi: 10.1371/journal.pone.0007967.

[54] C. Geffers and P. Gastmeier, “Nosocomial Infections and Multidrug-resistant Organisms in Germany : Epidemiological Data From KISS (The Hospital Infection Surveillance System),” *Medicine (Baltimore)*., vol. 108, no. 18, p. 320, 2011, doi: 10.3238/arztebl.2011.0320a.

[55] R. P. Wenzel and C. Gennings, “Bloodstream Infections Due to *Candida* Species in the Intensive Care Unit : Identifying Especially High-Risk Patients to Determine Prevention Strategies,” *Clin. Infect. Dis.*, vol. 41, no. Suppl 6, pp. 389–393, 2005.

[56] G. J. Elving, H. C. Van Der Mei, H. J. Busscher, R. Van Weissenbruch, and F. W. J. Albers, “Comparison of the microbial composition of voice prosthesis biofilms from patients requiring frequent versus infrequent replacement,” *Ann. Otol. Rhinol. Laryngol.*, vol. 111, no. 3, pp. 200–203, 2002, doi: 10.1177/000348940211100302.

[57] E. M. Kojic and R. O. Darouiche, “*Candida* Infections of Medical Devices,” *Clin. Microbiol. Revi*, vol. 17, no. 2, pp. 255–267, 2004, doi: 10.1128/CMR.17.2.255.

[58] M. Tscherner, T. Schwarzmüller, and K. Kuchler, “Pathogenesis and Antifungal Drug Resistance of the Human Fungal Pathogen *Candida glabrata*,” *Pharmaceuticals*, vol. 4, no. 12, pp. 169–186, Jan. 2011, doi: 10.3390/ph4010169.

[59] J. Rho *et al.*, “Molecular investigation of two consecutive nosocomial clusters of *Candida tropicalis* candiduria using pulsed-field gel electrophoresis.,” *J. Microbiol.*, vol. 42, no. 2, pp. 80–6, 2004.

[60] L. A. Bonassoli, M. Bertoli, and T. I. E. Svidzinski, “High frequency of *Candida parapsilosis* on the hands of healthy hosts,” *J. Hosp. Infect.*, vol. 59, no. 2, pp. 159–162, 2005, doi: 10.1016/j.jhin.2004.06.033.

[61] N. Yapar, “Epidemiology and risk factors for invasive candidiasis,” *Ther. Clin. Risk Manag.*, vol. 10, no. 1, pp. 95–105, 2014, doi: 10.2147/TCRM.S40160.

[62] C. J. Seneviratne, L. Jin, and L. P. Samaranayake, “Biofilm lifestyle of *Candida*: a mini review,” *Oral Diseasis*, vol. 14, pp. 582–590, 2008, doi: 10.1111/j.1601-0825.2007.01424.x.

[63] J. Chandra, D. M. Kuhn, P. K. Mukherjee, L. L. Hoyer, T. M. C. Cormick, and M. A. Ghannoum, “Biofilm Formation by the Fungal Pathogen *Candida albicans*: Development, Architecture, and Drug Resistance,” *J. Bacteriol.*, vol. 183, no. 18, pp. 5385–5394, 2001, doi: 10.1128/JB.183.18.5385.

[64] K. F. Mitchell, R. Zarnowski, and D. R. Andes, “The Extracellular Matrix of Fungal Biofilms,” *Adv. Microbiol. , Infect. Dis. Public Heal.*, vol. 931, pp. 21–35, 2016, doi: 10.1007/5584.

[65] G. Ramage, K. Vande Walle, B. L. Wickes, and J. L. Lopez-ribot, “Biofilm Formation by *Candida dubliniensis*,” *J. Clin. Microbiol.*, vol. 39, no. 9, pp. 3234–3240, 2001, doi: 10.1128/JCM.39.9.3234.

[66] S. Silva, M. Henriques, A. Martins, R. Oliveira, D. Williams, and J. Azeredo, “Biofilms of non-*Candida albicans Candida* species: quantification, structure and matrix composition,” *Med.*

Mycol., vol. 47, no. 7, pp. 681–689, 2009, doi: 10.3109/13693780802549594.

[67] F. C. Bizerra *et al.*, “Characteristics of biofilm formation by *Candida tropicalis* and antifungal resistance,” *FEMS Yeast Res.*, vol. 8, no. 3, pp. 442–450, 2008, doi: 10.1111/j.1567-1364.2007.00347.x.

[68] A. A. Lattif *et al.*, “Characterization of biofilms formed by *Candida parapsilosis, C. metapsilosis*, and *C. orthopsilosis*,” *Int. J. Med. Microbiol.*, vol. 300, no. 4, pp. 265–270, 2010, doi: 10.1016/j.ijmm.2009.09.001.

[69] J. Nett, “The Host’s Reply to *Candida* Biofilm,” *Pathogens*, vol. 5, no. 33, pp. 1–10, 2016, doi: 10.3390/pathogens5010033.

[70] L. A. Mermel *et al.*, “Guidelines for the Management of Intravascular Catheter – Related Infections,” *Clin. Infect. Dis.*, vol. 32, pp. 1249–1272, 2001.

[71] J. Chandra and P. Mukherjee, “*Candida* Biofilms: Development, Architecture, and Resistance,” *Microbiol Spectr.*, vol. 3, no. 4, pp. 157–176, 2015, doi: 10.1161/CIRCRESAHA.116.303790.The.

[72] J. R. Blankenship and A. P. Mitchell, “How to build a biofilm: a fungal perspective,” *Curr. Opin. Microbiol.*, vol. 9, pp. 588–594, 2006, doi: 10.1016/j.mib.2006.10.003.

[73] D. Andes, J. Nett, and P. Oschel, “Development and characterization of an *in vivo* central venous catheter *Candida albicans* biofilm model,” *Infect. Immun.*, vol. 72, no. 10, pp. 6023–6031, 2004, doi: 10.1128/IAI.72.10.6023.

[74] M. Ricicova *et al.*, “*Candida albicans* biofilm formation in a new *in vivo* rat model,” *Microbiology*, vol. 156, no. 3, pp. 909–919, 2010, doi: 10.1099/mic.0.033530-0.

[75] S. Kucharíková *et al.*, “*In vivo Candida glabrata* biofilm development on foreign bodies in a rat subcutaneous model,” *J. Antimicrob. Chemother.*, vol. 70, no. 3, pp. 846–856, 2014, doi: 10.1093/jac/dku447.

[76] K. J. Verstrepen and F. M. Klis, “Flocculation, adhesion and biofilm formation in yeasts,” *Mol. Microbiol.*, vol. 60, no. 1, pp. 5–15, 2006, doi: 10.1111/j.1365-2958.2006.05072.x.

[77] C. J. Nobile *et al.*, “Critical Role of Bcr1-Dependent Adhesins in *C. albicans* Biofilm Formation *In Vitro* and *In Vivo*,” *PLoS Pathog.*, vol. 2, no. 7, pp. 0636–0649, 2006, doi: 10.1371/journal.ppat.0020063.

[78] P. W. J. de Groot, O. Bader, A. D. de Boer, M. Weig, and N. Chauhan, “Adhesins in human fungal pathogens: Glue with plenty of stick,” *Eukaryot. Cell*, vol. 12, no. 4, pp. 470–481, 2013, doi: 10.1128/EC.00364-12.

[79] B. Modrezewka and P. Kurnatowski, “Adherence of *Candida* sp. to host tissues and cells as one of its pathogenicity features,” *Ann. Parasitol.*, vol. 61, no. 1, pp. 3–9, 2015, doi: 10.1093/cid/cis290.

[80] A. D. Las Peñas *et al.*, “Virulence-related surface glycoproteins in the yeast pathogen *Candida glabrata* are encoded in subtelomeric clusters and subject to </i>RAP1</i> - and *SIR* -dependent transcriptional silencing,” *Genes Dev.*, vol. 17, no. 18, pp. 2245–2258, 2003, doi: 10.1101/gad.1121003.cans.

[81] G. Ramage, S. Bachmann, T. F. Patterson, B. L. Wickes, and J. L. López-ribot, “Investigation of multidrug efflux pumps in relation to fluconazole resistance in *Candida albicans* biofilms,” *J. Antimicrob. Chemother.*, vol. 49, pp. 973–980, 2002, doi: 10.1093/jac/dkf049.

[82] D. M. Kuhn, J. Chandra, P. K. Mukherjee, and M. A. Ghannoum, “Comparison of Biofilms Formed by *Candida albicans* and *Candida parapsilosis* on Bioprosthetic Surfaces,” *Infect. Immun.*, vol. 70, no. 2, pp. 878–888, 2002, doi: 10.1128/IAI.70.2.878.

[83] M. A. Al-Fattani and L. J. Douglas, “Biofilm matrix of *Candida albicans* and *Candida tropicalis*: Chemical composition and role in drug resistance,” *J. Med. Microbiol.*, vol. 55, no. 8, pp. 999–1008, 2006, doi: 10.1099/jmm.0.46569-0.

[84] H. Flemming and J. Wingender, “The biofilm matrix,” *Nat. Rev. Microbiol.*, vol. 8, no. 9, pp. 623–33, 2010, doi: 10.1038/nrmicro2415.

[85] R. Zarnowski *et al.*, “Novel entries in a fungal biofilm matrix encyclopedia,” *MBio*, vol. 5, no. 4, pp. e01333–e01314, 2014, doi: 10.1128/mBio.01333-14.

[86] K. F. Mitchell *et al.*, “Community participation in biofilm matrix assembly and function,” *Proc. Natl. Acad. Sci.*, vol. 112, no. 13, pp. 4092–4097, 2015, doi: 10.1073/pnas.1421437112.

[87] Y. Jin, L. P. Samaranayake, Y. Samaranayake, and H. K. Yip, “Biofilm formation of *Candida albicans* is variably affected by saliva and dietary sugars,” *Arch. Oral Biol.*, vol. 49, no. 10, pp. 789–798, 2004, doi: 10.1016/j.archoralbio.2004.04.011.

[88] G. S. Baillie and L. J. Douglas, “Role of dimorphism in the development of *Candida albicans* biofilms.,” *J. Med. Microbiol.*, vol. 48, no. 7, pp. 671–679, 1999, doi: 10.1099/00222615-48-7-671.

[89] H. Nikawa, H. Nishimura, T. Yamamoto, T. Hamada, and L. P. Samaranayake, “The role of saliva and serum in *Candida albicans* biofilm formation on denture acrylic surfaces,” *Microb. Ecol. Health Dis.*, vol. 9, pp. 35–48, 1996, doi: 10.3109/08910609609167727.

[90] S. Susewind, R. Lang, and S. Hahnel, “Biofilm formation and *Candida albicans* morphology on the surface of denture base materials,” *Mycoses*, vol. 58, no. 12, pp. 719–727, 2015, doi: 10.1111/myc.12420.

[91] D. R. Radford, S. P. Sweet, S. J. Challacombe, and J. D. Walter, “Adherence of *Candida albicans* to denture-base materials with different surface finishes.,” *J. Dent.*, vol. 26, no. 7, pp. 577–583, 1998, doi: 10.1016/S0300-5712(97)00034-1.

[92] J. Chandra *et al.*, “Modification of Surface Properties of Biomaterials Influences the Ability of *Candida albicans* to Form Biofilms,” *Appl. Environ. Microbiol.*, vol. 71, no. 12, pp. 8795–8801, 2005, doi: 10.1128/AEM.71.12.8795.

[93] D. Estivill, A. Arias, A. Torres-Lana, A. J. Carrillo-Muñoz, and M. P. Arévalo, “Biofilm formation by five species of *Candida* on three clinical materials,” *J. Microbiol. Methods*, vol. 86, no. 2, pp. 238–242, 2011, doi: 10.1016/j.mimet.2011.05.019.

[94] T. Pereira-cenci *et al.*, “The effect of *Streptococcus mutans* and *Candida glabrata* on *Candida albicans* biofilms formed on different surfaces,” *Arch. Oral Biol.*, vol. 53, pp. 755–764, 2008, doi: 10.1016/j.archoralbio.2008.02.015.

[95] T. S. Ng, M. N. M. Desa, D. Sandai, P. P. Chong, and L. T. L. Than, “Growth, biofilm formation, antifungal susceptibility and oxidative stress resistance of *Candida glabrata* are affected by different glucose concentrations,” *Infect. Genet. Evol.*, vol. 40, pp. 331–338, 2016, doi: 10.1016/j.meegid.2015.09.004.

[96] P. A. Queiroz, J. S. R. Godoy, P. de S. B. Mendonça, R. B. Pedroso, T. I. E. Svidzinski, and M. Negri, “Adhesion and biofilm formation in artificial saliva and susceptibility of yeasts isolated from chronic kidney patients undergoing haemodialysis,” *J. Med. Microbiol.*, vol. 64, no. 9, pp. 960–966, 2015, doi: 10.1099/jmm.0.000122.

[97] S. P. Hawser, G. S. Baillie, and L. J. Douglas, “Production of extracellular matrix by *Candida albicans* biofilms.,” *J Med Microbiol.*, vol. 47, pp. 253–256., 1998.

[98] P. K. Mukherjee, D. V. Chand, J. Chandra, J. M. Anderson, and M. A. Ghannoum, “Shear stress modulates the thickness and architecture of *Candida albicans* biofilms in a phase-dependent manner,” *Mycoses*, vol. 52, no. 5, pp. 440–446, 2009, doi: 10.1038/jid.2014.371.

[99] C. J. Nobile *et al.*, “A Recently Evolved Transcriptional Network Controls Biofilm Development in *Candida albicans*,” *Cell*, vol. 148, no. 1–2, pp. 126–138, Jan. 2012, doi: 10.1016/j.cell.2011.10.048.

[100] C. E. Birse, M. Y. Irwin, W. A. Fonzi, and P. S. Sypherdt, “Cloning and Characterization of *ECE1*, a Gene Expressed in Association with Cell Elongation of the Dimorphic Pathogen *Candida albicans*,” *Infect. Immun.*, vol. 61, no. 9, pp. 3648–3655, 1993.

[101] D. A. Bailey, P. J. F. Feldmann, M. Bovey, N. A. R. Gow, and A. J. P. Brown, “The *Candida albicans HYR1* Gene , Which Is Activated in Response to Hyphal Development , Belongs to a Gene Family Encoding Yeast Cell Wall Proteins,” *J. Bacteriol.*, vol. 178, no. 18, pp. 5353–5360, 1996.

[102] J. F. Staab, C. A. Ferrer, and P. Sundstrom, “Developmental Expression of a Tandemly Repeated, Proline- and Glutamine-rich Amino Acid Motif on Hyphal Surfaces of *Candida albicans*,” *J. Biol. Chem.*, vol. 271, no. 11, pp. 6298–6305, 1996.

[103] L. L. Hoyer, T. L. Payne, M. Bell, A. M. Myers, and S. Scherer, “*Candida albicans ALS3* and insights into the nature of the ALS gene family,” *Curr. Genet.*, vol. 33, pp. 451–459, 1998.

[104] P. Maiti, P. Ghorai, S. Ghosh, M. Kamthan, R. Kumar, and A. Datta, “Mapping of functional domains and characterization of the transcription factor Cph1 that mediate morphogenesis in *Candida albicans*,” *Fungal Genet. Biol.*, vol. 83, pp. 45–57, 2015, doi: 10.1016/j.fgb.2015.08.004.

[105] W. L. Chaffin, J. L. López-Ribot, M. Casanova, D. Gozalbo, and J. P. Martinez, “Cell Wall and Secreted Proteins of *Candida albicans*: Identification, Function, and Expression,” *Microbiol. Immunol.*, vol. 62, no. 1, pp. 130–180, 1998.

[106] K. Sohn, C. Urban, H. Brunner, and S. Rupp, “*EFG1* is a major regulator of cell wall dynamics in *Candida albicans* as revealed by DNA microarrays,” *Mol. Microbiol.*, vol. 47, no. 1, pp. 89–102, 2003.

[107] G. Ramage, K. VandeWalle, J. L. López-Ribot, and B. L. Wickes, “The filamentation pathway controlled by the Efg1 regulator protein is required for normal biofilm formation and development in *Candida albicans*,” *FEMS Microbiol. Lett.*, vol. 214, pp. 95–100, 2002.

[108] T. Doedt *et al.*, “APSES Proteins Regulate Morphogenesis and Metabolism in *Candida albicans*,” *Mol. Biol. Cell*, vol. 15, pp. 3167–3180, 2004, doi: 10.1091/10.1091/mbc.E03.

[109] L. A. Connolly *et al.*, “The APSES transcription factor Efg1 is a global regulator that controls morphogenesis and biofilm formation in *Candida parapsilosis*,” *Mol. Microbiol.*, vol. 90, no. 1, pp. 36–53, 2013, doi: 10.1111/mmi.12345.

[110] L. M. Holland *et al.*, “Comparative Phenotypic Analysis of the Major Fungal Pathogens *Candida parapsilosis* and *Candida albicans*,” *PLoS Pathog.*, vol. 10, no. 9, pp. 1–18, 2014, doi: 10.1371/journal.ppat.1004365.

[111] P. Pais, C. Costa, M. Cavalheiro, D. Romão, and M. C. Teixeira, “Transcriptional Control of Drug Resistance, Virulence and Immune System Evasion in Pathogenic Fungi: A Cross-Species Comparison,” *Front. Cell. Infect. Microbiol.*, vol. 6, no. 131, pp. 1–26, 2016, doi: 10.3389/fcimb.2016.00131.

[112] A. Calcagno *et al.*, “*Candida glabrata STE12* is required for wild-type levels of virulence and nitrogen starvation induced filamentation,” *Mol. Microbiol.*, vol. 50, no. 4, pp. 1309–1318, 2003, doi: 10.1046/j.1365-2958.2003.03755.x.

[113] A. Sellam, F. Tebbji, and A. Nantel, “Role of Ndt80p in sterol metabolism regulation and azole resistance in *Candida albicans*,” *Eukaryot. Cell*, vol. 8, no. 8, pp. 1174–1183, 2009, doi: 10.1128/EC.00074-09.

[114] A. Sellam *et al.*, “Role of transcription factor CaNdt80p in cell separation, hyphal growth, and virulence in *Candida albicans*,” *Eukaryot. Cell*, vol. 9, no. 4, pp. 634–644, 2010, doi: 10.1128/EC.00325-09.

[115] I. A. Cleary, A. L. Lazzell, C. Monteagudo, D. P. Thomas, and P. Stephen, “*BRG1* and *NRG1* form a novel feedback circuit regulating *C. albicans* hyphal formation and virulence,” *Mol. Microbiol.*, vol. 85, no. 3, pp. 557–573, 2012, doi: 10.1111/j.1365-2958.2012.08127.x.BRG1.

[116] B. R. Braun, D. Kadosh, and A. D. Johnson, “*NRG1*, a repressor of filamentous growth in *C.albicans*, is down-regulated during filament induction,” *EMBO J.*, vol. 20, no. 17, pp. 4753–4761, 2001, doi: 10.1093/emboj/20.17.4753.

[117] Q. Zhang *et al.*, “Regulation of filamentation in the human fungal pathogen *Candida tropicalis*,”

Mol. Microbiol., vol. 99, no. 3, pp. 528–545, 2016, doi: 10.1111/mmi.13247.

[118] A. M. A. Murad *et al.*, "Transcript profiling in *Candida albicans* reveals new cellular functions for the transcriptional repressors CaTup1, CaMig1 and CaNrg1," *Mol. Microbiol.*, vol. 42, no. 4, pp. 981–993, 2001, doi: 10.1046/j.1365-2958.2001.02713.x.

[119] R. A. Khalaf and R. S. Zitomer, "The DNA binding protein Rfg1 is a repressor of filamentation in *Candida albicans*," *Genetics*, vol. 157, no. 4, pp. 1503–1512, 2001.

[120] D. Kadosh and A. D. Johnson, "Induction of the *Candida albicans* filamentous growth program by relief of transcriptional repression: a genome-wide analysis," *Mol. Biol. Cell*, vol. 16, no. 2, pp. 2903–2912, 2005, doi: 10.1091/mbc.E05.

[121] D. Kadosh and A. D. Johnson, "Rfg1, a Protein Related to the to the *Saccharomyces cerevisiae* Hypoxic Regulator Rox1, Controls Filamentous Growth and Virulence in *Candida albicans*," *Mol. Cell. Biol.*, vol. 21, no. 7, pp. 2496–2505, 2001, doi: 10.1128/MCB.21.7.2496.

[122] C. J. Nobile and A. P. Mitchell, "Regulation of Cell-Surface Genes and Biofilm Formation by the *C. albicans* Transcription Factor Bcr1p," *Curr. Biol.*, vol. 15, pp. 1150–1155, 2005, doi: 10.1016/j.cub.2005.05.047.

[123] C. Ding and G. Butler, "Development of a Gene Knockout System in *Candida parapsilosis* Reveals a Conserved Role for *BCR1* in Biofilm Formation," *Eukaryot. Cell*, vol. 6, no. 8, pp. 1310–1319, 2007, doi: 10.1128/EC.00136-07.

[124] C. Ding *et al.*, "Conserved and Divergent Roles of Bcr1 and CFEM Proteins in *Candida parapsilosis* and *Candida albicans*," *PLoS One*, vol. 6, no. 12, pp. 1–11, 2011, doi: 10.1371/journal.pone.0028151.

[125] A. Schweizer *et al.*, "The TEA/ATTS transcription factor CaTec1p regulates hyphal development and virulence in *Candida albicans*," *Mol. Microbiol.*, vol. 38, no. 3, pp. 2–12, 2000, doi: 10.1046/j.1365-2958.2000.02132.x.

[126] S. Lane, C. Birse, S. Zhou, R. Matson, and H. Liu, "DNA Array Studies Demonstrate Convergent Regulation of Virulence Factors by Cph1, Cph2, and Efg1 in *Candida albicans*," *J. Biol. Chem.*, vol. 276, no. 52, pp. 48988–96, Dec. 2001, doi: 10.1074/jbc.M104484200.

[127] S. Lane, S. Zhou, T. Pan, Q. Dai, and H. Liu, "The Basic Helix-Loop-Helix Transcription Factor Cph2 Regulates Hyphal Development in *Candida albicans* Partly via Tec1," *Mol. Cell. Biol.*, vol. 21, no. 19, pp. 6418–6428, 2001, doi: 10.1128/MCB.21.19.6418.

[128] J. S. Finkel *et al.*, "Portrait of *Candida albicans* adherence regulators," *PLoS Pathog.*, vol. 8, no. 2, pp. 1–14, 2012, doi: 10.1371/journal.ppat.1002525.

[129] C. J. Nobile *et al.*, "Biofilm matrix regulation by *Candida albicans* Zap1," *PLoS Biol.*, vol. 7, no. 6, pp. 1–15, 2009, doi: 10.1371/journal.pbio.1000133.

[130] J. Bonhomme *et al.*, "Contribution of the glycolytic flux and hypoxia adaptation to efficient biofilm formation by *Candida albicans*," *Mol. Microbiol.*, vol. 80, no. 4, pp. 995–1013, 2011, doi: 10.1111/j.1365-2958.2011.07626.x.

[131] P. Vandeputte *et al.*, "Identification and functional characterization of Rca1, a transcription factor involved in both antifungal susceptibility and host response in *Candida albicans*," *Eukaryot. Cell*, vol. 11, no. 7, pp. 916–931, 2012, doi: 10.1128/EC.00134-12.

[132] M. Riera, E. Mogensen, C. D'Enfert, and G. Janbon, "New regulators of biofilm development in *Candida glabrata*," *Res. Microbiol.*, vol. 163, no. 4, pp. 297–307, May 2012, doi: 10.1016/j.resmic.2012.02.005.

[133] M. T. Kelly, D. M. MacCallum, S. D. Clancy, F. C. Odds, A. J. P. Brown, and G. Butler, "The *Candida albicans CaACE2* gene affects morphogenesis, adherence and virulence," *Mol. Microbiol.*, vol. 53, no. 3, pp. 969–983, 2004, doi: 10.1111/j.1365-2958.2004.04185.x.

[134] D. M. MacCallum, H. Findon, C. C. Kenny, G. Butler, K. Haynes, and F. C. Odds, "Different consequences of *ACE2* and *SWI5* gene disruptions for virulence of pathogenic and

nonpathogenic yeasts," *Infect. Immun.*, vol. 74, no. 9, pp. 5244–5248, 2006, doi: 10.1128/IAI.00817-06.

[135] C. Stichternoth and J. F. Ernst, "Hypoxic adaptation by Efg1 regulates biofilm formation by *Candida albicans*," *Appl. Environ. Microbiol.*, vol. 75, no. 11, pp. 3663–3672, 2009, doi: 10.1128/AEM.00098-09.

[136] S. M. Mulhern, M. E. Logue, and G. Butler, "*Candida albicans* transcription factor Ace2 regulates metabolism and is required for filamentation in hypoxic conditions," *Eukaryot. Cell*, vol. 5, no. 12, pp. 2001–2013, 2006, doi: 10.1128/EC.00155-06.

[137] D. A. Stead *et al.*, "Impact of the transcriptional regulator, Ace2, on the *Candida glabrata* secretome," *Proteomics*, vol. 10, no. 2, pp. 212–223, 2009, doi: 10.1002/pmic.200800706.

[138] V. Gallegos-García *et al.*, "A novel downstream regulatory element cooperates with the silencing machinery to repress *EPA1* expression in *Candida glabrata*," *Genetics*, vol. 190, no. 4, pp. 1285–1297, 2012, doi: 10.1534/genetics.111.138099.

[139] S. P. Hawser and L. J. Douglas, "Resistance of *Candida albicans* biofilms to antifungal agents *in vitro*," *Antimicrob. Agents Chemother.*, vol. 39, no. 9, pp. 2128–2131, 1995, doi: 10.1128/AAC.39.9.2128.

[140] D. M. Kuhn, T. George, J. Chandra, P. K. Mukherjee, and M. A. Ghannoum, "Antifungal Susceptibility of *Candida* biofilms: Unique Efficacy of Amphotericin B Lipid Formulations and Echinocandins," *Antimicrob. Agents Chemother.*, vol. 46, no. 6, pp. 1773–1780, 2002, doi: 10.1128/AAC.46.6.1773.

[141] J. Nett *et al.*, "Putative role of β-1,3 glucans in *Candida albicans* biofilm resistance," *Antimicrob. Agents Chemother.*, vol. 51, no. 2, pp. 510–520, 2007, doi: 10.1128/AAC.01056-06.

[142] J. W. Song *et al.*, "Expression of *CgCDR1, CgCDR2,* and *CgERG11* in *Candida glabrata* biofilms formed by bloodstream isolates," *Med. Mycol.*, vol. 47, no. 5, pp. 545–548, 2009, doi: 10.1080/13693780802210726.

[143] R. Santos *et al.*, "The multidrug resistance transporters CgTpo1_1 and CgTpo1_2 play a role in virulence and biofilm formation in the human pathogen *Candida glabrata*," *Cell. Microbiol.*, vol. 19, no. 5, pp. 1–13, 2017, doi: 10.1111/cmi.12686.

[144] P. Pais, C. Costa, C. Pires, K. Shimizu, H. Chibana, and M. C. Teixeira, "Membrane Proteome-Wide Response to the Antifungal Drug Clotrimazole in *Candida glabrata*: Role of the Transcription Factor CgPdr1 and the Drug:H+ Antiporters CgTpo1_1 and CgTpo1_2," *Mol. Cell. Proteomics*, vol. 15, no. 1, pp. 57–72, 2016, doi: 10.1074/mcp.M114.045344.

[145] C. J. Seneviratne, Y. Wang, L. Jin, Y. Abiko, and L. P. Samaranayake, "Proteomics of drug resistance in *Candida glabrata* biofilms," *Proteomics*, vol. 10, no. 7, pp. 1444–1454, 2010, doi: 10.1002/pmic.200900611.

[146] G. Vediyappan, T. Rossignol, and C. D'Enfert, "Interaction of *Candida albicans* biofilms with antifungals: Transcriptional response and binding of antifungals to beta-glucans," *Antimicrob. Agents Chemother.*, vol. 54, no. 5, pp. 2096–2111, 2010, doi: 10.1128/AAC.01638-09.

[147] K. Lewis, "Persister cells , dormancy and infectious disease," *Nat. Revies Microbiol.*, vol. 5, pp. 48–56, 2007, doi: 10.1038/nrmicro1557.

[148] M. D. Lafleur, C. A. Kumamoto, and K. Lewis, "*Candida albicans* Biofilms Produce Antifungal-Tolerant Persister Cells," *Antimicrob. Agents Chemother.*, vol. 50, no. 11, pp. 3839–3846, 2006, doi: 10.1128/AAC.00684-06.

[149] S. Elias and E. Banin, "Multi-species biofilms: Living with friendly neighbors," *FEMS Microbiol. Rev.*, vol. 36, no. 5, pp. 990–1004, 2012, doi: 10.1111/j.1574-6976.2012.00325.x.

[150] A. K. Pathak, S. Sharma, and P. Shrivastva, "Multi-species biofilm of *Candida albicans* and non-*Candida albicans Candida* species on acrylic substrate," *J. Appl Oral Sci.*, vol. 20, no. 1, pp. 70–75, 2012.

[151] Y. W. Cavalcanti *et al.*, “Virulence and pathogenicity of *Candida albicans* is enhanced in biofilms containing oral bacteria.,” *Biofouling*, vol. 31, no. 1, pp. 27–38, 2015, doi: 10.1080/08927014.2014.996143.

[152] K. Zhang *et al.*, “Effect of Antimicrobial Denture Base Resin on Multi-Species Biofilm Formation,” *Int. J. Mol. Sci.*, vol. 17, no. 7, pp. 1–13, 2016, doi: 10.3390/ijms17071033.

[153] M. M. Harriott and M. C. Noverr, “*Candida albicans* and *Staphylococcus aureus* form polymicrobial biofilms: Effects on antimicrobial resistance,” *Antimicrob. Agents Chemother.*, vol. 53, no. 9, pp. 3914–3922, 2009, doi: 10.1128/AAC.00657-09.

[154] M. M. Harriott and M. C. Noverr, “Ability of *Candida albicans* mutants to induce *Staphylococcus aureus* vancomycin resistance during polymicrobial biofilm formation,” *Antimicrob. Agents Chemother.*, vol. 54, no. 9, pp. 3746–3755, 2010, doi: 10.1128/AAC.00573-10.

[155] B. Adam, G. S. Baillie, and L. J. Douglas, “Mixed species biofilms of *Candida albicans* and *Staphylococcus epidermidis*,” *J. Med. Microbiol*, vol. 51, pp. 344–349, 2002, doi: 10.1099/0022-1317-51-4-344.

[156] C. V. Bamford, A. D’Mello, A. H. Nobbs, L. C. Dutton, M. M. Vickerman, and H. F. Jenkinson, “*Streptococcus gordonii* modulates *Candida albicans* biofilm formation through intergeneric communication,” *Infect. Immun.*, vol. 77, no. 9, pp. 3696–3704, 2009, doi: 10.1128/IAI.00438-09.

[157] H. F. Jenkinson, H. C. Lala, and M. G. Shepherd, “Coaggregation of *Streptococcus sanguis* and other *Streptococci* with *Candida albicans*,” *Infect. Immun.*, vol. 58, no. 5, pp. 1429–1436, 1990.

[158] R. J. Silverman, A. H. Nobbs, M. M. Vickerman, M. E. Barbour, and H. F. Jenkinson, “Interaction of *Candida albicans* cell wall Als3 Protein with *Streptococcus gordonii* SspB adhesin promotes development of mixed-species communities,” *Infect. Immun.*, vol. 78, no. 11, pp. 4644–4652, 2010, doi: 10.1128/IAI.00685-10.

[159] S. C. J. De Keersmaecker, K. Sonck, and J. Vanderleyden, “Let LuxS speak up in AI-2 signaling,” *Trends Microbiol.*, vol. 14, no. 3, pp. 114–119, 2006, doi: 10.1016/j.tim.2006.01.003.

[160] J. M. Hornby *et al.*, “Quorum Sensing in the Dimorphic Fungus *Candida albicans* Is Mediated by Farnesol,” *Appl. Environ. Microbiol.*, vol. 67, no. 7, pp. 2982–2992, 2001, doi: 10.1128/AEM.67.7.2982.

[161] W. R. Riekhof and K. W. Nickerson, “Quorum sensing in *Candida albicans*: farnesol versus farnesoic acid,” *FEBS Lett.*, vol. 591, pp. 1637–1640, 2017, doi: 10.1002/1873-3468.12694.

[162] M. Polke, I. Leonhardt, O. Kurzai, and I. D. Jacobsen, “Farnesol signalling in *Candida albicans* – more than just communication,” *Crit. Rev. Microbiol.*, vol. 0, no. 0, pp. 1–14, 2017, doi: 10.1080/1040841X.2017.1337711.

[163] G. Ramage, S. P. Saville, B. L. Wickes, and J. L. López-Ribot, “Inhibition of *Candida albicans* Biofilm Formation by Farnesol, a Quorum-Sensing Molecule,” *Appl. Environ. Microbiol.*, vol. 68, no. 11, pp. 5459–5463, 2002, doi: 10.1128/AEM.68.11.5459.

[164] M. A. S. Alem, M. D. Y. Oteef, T. H. Flowers, and L. J. Douglas, “Production of tyrosol by *Candida albicans* biofilms and its role in quorum sensing and biofilm development,” *Eukaryot. Cell*, vol. 5, no. 10, pp. 1770–1779, 2006, doi: 10.1128/EC.00219-06.

[165] K. Weber, B. Schulz, and M. Ruhnke, “The quorum-sensing molecule E,E-farnesol—its variable secretion and its impact on the growth and metabolism of *Candida* species,” *Yeast*, vol. 27, pp. 727–739, 2010, doi: 10.1002/yea.

[166] A. Katragkou *et al.*, “*In vitro* interactions between farnesol and fluconazole, amphotericin B or micafungin against *Candida albicans* biofilms,” *J. Antimicrob. Chemother.*, vol. 70, pp. 470–478, 2015, doi: 10.1093/jac/dku374.

[167] T. Rossignol, M. E. Logue, K. Reynolds, M. Grenon, N. F. Lowndes, and G. Butler, “Transcriptional Response of *Candida parapsilosis* following Exposure to Farnesol,” *Antimicrob. Agents Chemother.*, vol. 51, no. 7, pp. 2304–2312, 2007, doi: 10.1128/AAC.01438-06.

[168] S. F. Laffey and G. Butler, “Phenotype switching affects biofilm formation by *Candida parapsilosis*,” *Microbiology*, vol. 151, pp. 1073–1081, 2005, doi: 10.1099/mic.0.27739-0.

[169] M. Kruppa, “Quorum sensing and *Candida albicans*,” *Mycoses*, vol. 52, no. 1, pp. 1–10, 2008, doi: 10.1111/j.1439-0507.2008.01626.x.

[170] H. Chen, M. Fujita, Q. Feng, J. Clardy, and G. R. Fink, “Tyrosol is a quorum-sensing molecule in *Candida albicans*,” *Proc. Natl. Acad. Sci.*, vol. 101, no. 14, pp. 5048–5052, 2004, doi: 10.1073/pnas.0401416101.

[171] C. P. Semighini, J. M. Hornby, R. Dumitru, K. W. Nickerson, and S. D. Harris, “Farnesol-induced apoptosis in *Aspergillus nidulans* reveals a possible mechanism for antagonistic interactions between fungi,” *Mol. Microbiol.*, vol. 59, no. 3, pp. 753–764, 2006, doi: 10.1111/j.1365-2958.2005.04976.x.

[172] D. A. Hogan and R. Kolter, “*Pseudomonas-Candida* Interactions: An Ecological Role for Virulence Factors,” *Science (80-.).*, vol. 296, no. 5576, pp. 2229–2232, 2002.

[173] L. J. Holcombe *et al.*, “*Pseudomonas aeruginosa* secreted factors impair biofilm development in *Candida albicans*,” *Microbiology*, vol. 156, no. 5, pp. 1476–1485, 2010, doi: 10.1099/mic.0.037549-0.

[174] D. A. Hogan, Å.˚ Vik, and R. Kolter, “A *Pseudomonas aeruginosa* quorum-sensing molecule influences *Candida albicans* morphology,” *Mol. Microbiol.*, vol. 54, no. 5, pp. 1212–1223, 2004, doi: 10.1111/j.1365-2958.2004.04349.x.

[175] C. Cugini, M. W. Calfee, J. M. Farrow, D. K. Morales, E. C. Pesci, and D. A. Hogan, “Farnesol, a common sesquiterpene, inhibits PQS production in *Pseudomonas aeruginosa*,” *Mol. Microbiol.*, vol. 65, no. 4, pp. 896–906, 2007, doi: 10.1111/j.1365-2958.2007.05840.x.

[176] H. Bandara, J. Y. Y. Yau, R. M. Watt, L. J. Jin, and L. P. Samaranayake, “*Pseudomonas aeruginosa* inhibits *in-vitro Candida* biofilm development,” *BMC Microbiol.*, vol. 10, no. 125, pp. 1–9, 2010.

[177] J. R. Kerr, “Suppression of fungal growth exhibited by *Pseudomonas aeruginosa*,” *J. Clin. Microbiol.*, vol. 32, no. 2, pp. 525–527, 1994.

[178] I. Kaleli, N. Cevahir, M. Demir, U. Yildirim, and R. Sahin, “Anticandidal activity of *Pseudomonas aeruginosa* strains isolated from clinical specimens,” *Mycoses*, vol. 50, pp. 74–78, 2006, doi: 10.1111/j.0933-7407.2006.01322.x.

[179] J. Carratalà, “The antibiotic-lock technique for therapy of ‘highly needed’ infected catheters,” *Clin. Microbiol. Infect.*, vol. 8, no. 5, pp. 282–289, 2002, doi: 10.1046/j.1469-0691.2002.00388.x.

[180] E. Cateau, J. M. Berjeaud, and C. Imbert, “Possible role of azole and echinocandin lock solutions in the control of *Candida* biofilms associated with silicone,” *Int. J. Antimicrob. Agents*, vol. 37, no. 4, pp. 380–384, 2011, doi: 10.1016/j.ijantimicag.2010.12.016.

[181] D. Toulet, C. Debarre, and C. Imbert, “Could liposomal amphotericin B (L-AMB) lock solutions be useful to inhibit *Candida* spp. biofilms on silicone biomaterials?,” *J. Antimicrob. Chemother.*, vol. 67, no. 2, pp. 430–432, 2012, doi: 10.1093/jac/dkr473.

[182] F. Piersigilli *et al.*, “Antifungal Lock Therapy With Combined 70% Ethanol and Micafungin in a Critically Ill Infant,” *Pediatr. Infect. Dis. J.*, vol. 33, no. 4, pp. 419–420, 2014, doi: 10.1097/INF.0000000000000116.

[183] S. Bonne *et al.*, “Effectiveness of Minocycline and Rifampin vs Chlorhexidine and Silver Sulfadiazine-Impregnated Central Venous Catheters in Preventing Central Line-Associated Bloodstream Infection in a High-Volume Academic Intensive Care Unit: A before and after Trial,” *J. Am. Coll. Surg.*, vol. 221, no. 3, pp. 739–747, 2015, doi: 10.1016/j.jamcollsurg.2015.05.013.

[184] N. Villard, C. Seneviratne, J. K. H. Tsoi, M. Heinonen, and J. Matinlinna, “*Candida albicans* aspects of novel silane system-coated titanium and zirconia implant surfaces,” *Clin. Oral Implants Res.*, vol. 26, no. 3, pp. 332–341, 2015, doi: 10.1111/clr.12338.

[185] J. S. Raut, R. B. Shinde, N. M. Chauhan, and S. M. Karuppayil, “Phenylpropanoids of plant origin as inhibitors of biofilm formation by *Candida albicans*,” *J. Microbiol. Biotechnol.*, vol. 24, no. 9, pp. 1216–1225, 2014, doi: 10.4014/jmb.1402.02056.

[186] J. S. Raut, R. B. Shinde, N. M. Chauhan, and S. Mohan Karuppayil, “Terpenoids of plant origin inhibit morphogenesis, adhesion, and biofilm formation by *Candida albicans*,” *Biofouling*, vol. 29, no. 1, pp. 87–96, 2013, doi: 10.1080/08927014.2012.749398.

[187] D. K. Morales, N. Grahl, C. Okegbe, L. E. P. Dietrich, N. J. Jacobs, and D. A. Hogan, “Control of *Candida albicans* metabolism and biofilm formation by *Pseudomonas aeruginosa* phenazines.,” *MBio*, vol. 4, no. 1, pp. 1–9, 2013, doi: 10.1128/mBio.00526-12.

[188] S. S. W. Wong *et al.*, “*In vitro* and *in vivo* activity of a novel antifungal small molecule against *Candida* infections,” *PLoS One*, vol. 9, no. 1, pp. 1–17, 2014, doi: 10.1371/journal.pone.0085836.

[189] S. Theberge, A. Semlali, A. Alamri, K. P. Leung, and M. Rouabhia, “*C. albicans* growth, transition, biofilm formation, and gene expression modulation by antimicrobial decapeptide KSL-W,” *BMC Microbiol.*, vol. 13, no. 246, pp. 1–14, 2013, doi: 10.1186/1471-2180-13-246.

[190] A. J. Karlsson, R. M. Flessner, S. H. Gellman, D. M. Lynn, and S. P. Palecek, “Polyelectrolyte Multilayers Fabricated from Antifungal β-Peptides: Design of Surfaces that Exhibit Antifungal Activity Against *Candida albicans*,” *Biomacromolecules*, vol. 11, no. 9, pp. 2321–2328, 2010, doi: 10.1002/nbm.3066.Non-invasive.

[191] J. Hoque *et al.*, “Broad spectrum antibacterial and antifungal polymeric paint materials: Synthesis, structure-activity relationship, and membrane-active mode of action,” *ACS Appl. Mater. Interfaces*, vol. 7, no. 3, pp. 1804–1815, 2015, doi: 10.1021/am507482y.

[192] A. Silva-Dias *et al.*, “Anti-biofilm activity of low-molecular weight chitosan hydrogel against *Candida* species,” *Med. Microbiol. Immunol.*, vol. 203, no. 1, pp. 25–33, 2014, doi: 10.1007/s00430-013-0311-4.

[193] S. Stepanovic, D. Vukovic, M. Jesic, and L. Ranin, “Influence of Acetylsalicylic Acid (Aspirin) on Biofilm Production by *Candida* Species,” *J. Chemother.*, vol. 16, no. 3, pp. 134–138, 2004.

[194] I. B. Rosseti, L. R. Chagas, and M. S. Costa, “Photodynamic antimicrobial chemotherapy (PACT) inhibits biofilm formation by *Candida albicans*, increasing both ROS production and membrane permeability,” *Lasers Med. Sci.*, vol. 29, no. 3, pp. 1059–1064, 2014, doi: 10.1007/s10103-013-1473-4.

[195] L. Černáková, J. Chupáčová, K. Židlíková, and H. Bujdáková, “Effectiveness of the Photoactive Dye Methylene Blue versus Caspofungin on the *Candida parapsilosis* Biofilm *in vitro* and *ex vivo*,” *Photochem. Photobiol.*, vol. 91, no. 5, pp. 1181–1190, 2015, doi: 10.1111/php.12480.

[196] H. F. Chien, C. P. Chen, Y. C. Chen, P. H. Chang, T. Tsai, and C. T. Chen, “The use of chitosan to enhance photodynamic inactivation against *Candida albicans* and its drug-resistant clinical isolates,” *Int. J. Mol. Sci.*, vol. 14, no. 4, pp. 7445–7456, 2013, doi: 10.3390/ijms14047445.

[197] H. Bujdáková, “Management of *Candida* biofilms: state of knowledge and new options for prevention and eradication,” *Future Microbiol.*, vol. 11, no. 2, pp. 235–251, 2016, doi: 10.2217/fmb.15.139.

[198] D. S. Perlin, R. Rautemaa-Richardson, and A. Alastruey-Izquierdo, “The global problem of antifungal resistance: prevalence, mechanisms, and management,” *Lancet Infect. Dis.*, vol. 17, no. 12, pp. e383–e392, 2017, doi: 10.1016/S1473-3099(17)30316-X.

[199] J. E. Bennett, K. Izumikawa, and K. A. Marr, “Mechanism of Increased Fluconazole Resistance in *Candida glabrata* during Prophylaxis,” *Antimicrob. Agents Chemother.*, vol. 48, no. 5, pp. 1773–1777, 2004, doi: 10.1128/AAC.48.5.1773.

[200] F. C. Bizerra *et al.*, “Breakthrough Candidemia Due to Multidrug-Resistant *Candida glabrata* during Prophylaxis with a Low Dose of Micafungin,” *Antimicrob. Agents Chemother.*, vol. 58, no. 4, pp. 2438–2440, Apr. 2014, doi: 10.1128/AAC.02189-13.

[201] K. E. Pristov and M. A. Ghannoum, “Resistance of *Candida* to azoles and echinocandins worldwide,” *Clin. Microbiol. Infect.*, vol. 25, no. 7, pp. 792–798, 2019, doi: 10.1016/j.cmi.2019.03.028.

[202] P. L. Fidel, J. A. Vazquez, and J. D. Sobel, “*Candida glabrata*: Review of Epidemiology , Pathogenesis , and Clinical Disease with Comparison to *C. albicans*,” *Clin. Microbiol. Rev.*, vol. 12, no. 1, pp. 80–96, Jan. 1999.

[203] A. Espinel-Ingroff *et al.*, “Interlaboratory Variability of Caspofungin MICs for *Candida* spp. Using CLSI and EUCAST Methods: Should the Clinical Laboratory Be Testing This Agent?,” *Antimicrob. Agents Chemother.*, vol. 57, no. 12, pp. 5836–5842, Dec. 2013, doi: 10.1128/AAC.01519-13.

[204] P. G. Pappas *et al.*, “Clinical Practice Guideline for the Management of Candidiasis: 2016 Update by the Infectious Diseases Society of America,” *Clin. Infect. Dis.*, vol. 62, no. 4, pp. e1–e50, 2015, doi: 10.1093/cid/civ933.

[205] F. C. Odds, “Resistance of clinically important yeasts to antifungal agents,” *Int. J. Antimicrob. Agents*, vol. 6, no. 3, pp. 145–147, Feb. 1996, doi: 10.1016/0924-8579(95)00048-8.

[206] S. L. Kelly, D. C. Lamb, A. J. Corran, B. C. Baldwin, and D. E. Kelly, “Mode of Action and Resistance to Azole Antifungals Associated with the Formation of 14α-Methylergosta-8,24(28)-dien-3β,6α-diol,” *Biochem. Biophys. Res. Commun.*, vol. 207, no. 3, pp. 910–915, Feb. 1995, doi: 10.1006/bbrc.1995.1272.

[207] S. G. Whaley and P. D. Rogers, “Azole Resistance in *Candida glabrata*,” *Curr. Infect. Dis. Rep.*, vol. 18, no. 12, pp. 19–21, 2016, doi: 10.1007/s11908-016-0554-5.

[208] H. Jungwirth and K. Kuchler, “Yeast ABC transporters - A tale of sex, stress, drugs and aging,” *FEBS Lett.*, vol. 580, no. 4, pp. 1131–1138, Feb. 2006, doi: 10.1016/j.febslet.2005.12.050.

[209] C. F. Higgins, “Multiple molecular mechanisms for multidrug resistance transporters,” *Nature*, vol. 446, no. 7137, pp. 749–757, Apr. 2007, doi: 10.1038/nature05630.

[210] S. Kumari *et al.*, “ABC transportome inventory of human pathogenic yeast *Candida glabrata*: Phylogenetic and expression analysis,” *PLoS One*, vol. 13, no. 8, p. e0202993, Aug. 2018, doi: 10.1371/journal.pone.0202993.

[211] D. Sanglard *et al.*, “The ATP binding cassette transporter gene *CgCDR1* from *Candida glabrata* is involved in the resistance of clinical isolates to azole antifungal agents.,” *Antimicrob. Agents Chemother.*, vol. 43, no. 11, pp. 2753–2765, 1999.

[212] D. Sanglard, F. Ischer, and J. Bille, “Role of ATP-binding-cassette transporter genes in high-frequency acquisition of resistance to azole antifungals in *Candida glabrata*,” *Antimicrob. Agents Chemother.*, vol. 45, no. 4, pp. 1174–1183, Apr. 2001, doi: 10.1128/AAC.45.4.1174-1183.2001.

[213] R. Torelli *et al.*, “The ATP-binding cassette transporter – encoding gene *CgSNQ2* is contributing to the *CgPDR1*-dependent azole resistance of *Candida glabrata*,” *Mol. Microbiol.*, vol. 68, no. 1, pp. 186–201, Apr. 2008, doi: 10.1111/j.1365-2958.2008.06143.x.

[214] J.-P. Vermitsky and T. D. Edlind, “Azole Resistance in *Candida glabrata*: Coordinate Upregulation of Multidrug Transporters and Evidence for a Pdr1-Like Transcription Factor,” *Antimicrob. Agents Chemother.*, vol. 48, no. 10, pp. 3773–3781, Oct. 2004, doi: 10.1128/AAC.48.10.3773.

[215] J.-P. Vermitsky, K. D. Earhart, W. L. Smith, R. Homayouni, T. D. Edlind, and P. D. Rogers, “Pdr1 regulates multidrug resistance in *Candida glabrata*: gene disruption and genome-wide expression studies,” *Mol. Microbiol.*, vol. 61, no. 3, pp. 704–722, Aug. 2006, doi: 10.1111/j.1365-2958.2006.05235.x.

[216] H.-F. H.-F. Tsai *et al.*, “Microarray and Molecular Analyses of the Azole Resistance Mechanism in *Candida glabrata* Oropharyngeal Isolates,” *Antimicrob. Agents Chemother.*, vol. 54, no. 8, pp. 3308–3317, Aug. 2010, doi: 10.1128/AAC.00535-10.

[217] I. Sá-Correia, S. C. dos Santos, M. C. Teixeira, T. R. Cabrito, and N. P. Mira, “Drug:H+

antiporters in chemical stress response in yeast," *Trends Microbiol.*, vol. 17, no. 1, pp. 22–31, 2008, doi: 10.1016/j.tim.2008.09.007.

[218] C. Costa *et al.*, "The dual role of *Candida glabrata* drug:H+ antiporter CgAqr1 (ORF CAGL0J09944g) in antifungal drug and acetic acid resistance.," *Front. Microbiol.*, vol. 4, no. 170, pp. 1–13, Jan. 2013, doi: 10.3389/fmicb.2013.00170.

[219] C. Costa *et al.*, "*Candida glabrata* drug:H+ antiporter CgQdr2 confers imidazole drug resistance, being activated by transcription factor CgPdr1.," *Antimicrob. Agents Chemother.*, vol. 57, no. 7, pp. 3159–67, Jul. 2013, doi: 10.1128/AAC.00811-12.

[220] C. Costa *et al.*, "*Candida glabrata* drug:H+ antiporter CgTpo3 (ORF CAGL0I10384g): role in azole drug resistance and polyamine homeostasis.," *J. Antimicrob. Chemother.*, vol. 69, no. 7, pp. 1767–76, Jul. 2014, doi: 10.1093/jac/dku044.

[221] P. Pais, C. Pires, C. Costa, M. Okamoto, H. Chibana, and M. C. Teixeira, "Membrane proteomics analysis of the *Candida glabrata* response to 5-flucytosine: Unveiling the role and regulation of the drug efflux transporters CgFlr1 and CgFlr2," *Front. Microbiol.*, vol. 7, no. 2045, pp. 1–14, 2016, doi: 10.3389/fmicb.2016.02045.

[222] C. Costa *et al.*, "Clotrimazole drug resistance in *Candida glabrata* clinical isolates correlates with increased expression of the drug:H+ antiporters CgAqr1, CgTpo1_1, CgTpo3 and CgQdr2," *Front. Microbiol.*, vol. 7, pp. 1–11, 2016, doi: 10.3389/fmicb.2016.00526.

[223] H.-F. Tsai, A. A. Krol, K. E. Sarti, and J. E. Bennett, "*Candida glabrata PDR1*, a transcriptional regulator of a pleiotropic drug resistance network, mediates azole resistance in clinical isolates and petite mutants.," *Antimicrob. Agents Chemother.*, vol. 50, no. 4, pp. 1384–92, Apr. 2006, doi: 10.1128/AAC.50.4.1384-1392.2006.

[224] S. Ferrari *et al.*, "Gain of function mutations in *CgPDR1* of *Candida glabrata* not only mediate antifungal resistance but also enhance virulence," *PLoS Pathog.*, vol. 5, no. 1, pp. 1–17, 2009, doi: 10.1371/journal.ppat.1000268.

[225] K. Spettel *et al.*, "Analysis of antifungal resistance genes in *Candida albicans* and *Candida glabrata* using next generation sequencing," *PLoS One*, vol. 14, no. 1, p. e0210397, Jan. 2019, doi: 10.1371/journal.pone.0210397.

[226] S. Khakhina, L. Simonicova, and W. S. Moye-Rowley, "Positive autoregulation and repression of transactivation are key regulatory features of the *Candida glabrata* Pdr1 transcription factor," *Mol. Microbiol.*, vol. 107, no. 6, pp. 747–764, Mar. 2018, doi: 10.1111/mmi.13913.

[227] S. Ferrari, M. Sanguinetti, R. Torelli, B. Posteraro, and D. Sanglard, "Contribution of *CgPDR1*-regulated genes in enhanced virulence of azole-resistant *Candida glabrata*," *PLoS One*, vol. 6, no. 3, pp. 1–16, Jan. 2011, doi: 10.1371/journal.pone.0017589.

[228] G. Epa *et al.*, "Upregulation of the Adhesin Gene *EPA1* Mediated by *PDR1* in *Candida glabrata* Leads to Enhanced Host Colonization," *mSphere*, vol. 1, no. 2, pp. 1–16, 2016, doi: 10.1128/mSphere.00065-15.Editor.

[229] J. A. Noble, H.-F. Tsai, S. D. Suffis, Q. Su, T. G. Myers, and J. E. Bennett, "STB5 is a negative regulator of azole resistance in *Candida glabrata*.," *Antimicrob. Agents Chemother.*, vol. 57, no. 2, pp. 959–67, Feb. 2013, doi: 10.1128/AAC.01278-12.

[230] M. Sanguinetti, B. Posteraro, B. Fiori, S. Ranno, R. Torelli, and G. Fadda, "Mechanisms of Azole Resistance in Clinical Isolates of *Candida glabrata* Collected during a Hospital Survey of Antifungal Resistance," *Antimicrob. Agents Chemother.*, vol. 49, no. 2, pp. 668–679, Feb. 2005, doi: 10.1128/AAC.49.2.668-679.2005.

[231] K. W. Henry, J. T. Nickels, T. D. Edlind, and H. E. T. Al, "Upregulation of *ERG* Genes in *Candida* Species by Azoles and Other Sterol Biosynthesis Inhibitors," *Antimicrob. Agents Chemother.*, vol. 44, no. 10, pp. 2693–700, Oct. 2000, doi: 10.1128/AAC.44.10.2693-2700.2000.Updated.

[232] S. W. Redding *et al.*, "Multiple Patterns of Resistance to Fluconazole in *Candida glabrata* Isolates from a Patient with Oropharyngeal Candidiasis Receiving Head and Neck Radiation," *J. Clin.*

Microbiol., vol. 41, no. 2, pp. 619–622, Feb. 2003, doi: 10.1128/JCM.41.2.619.

[233] C. M. Hull *et al.*, “Facultative sterol uptake in an ergosterol-deficient clinical isolate of *Candida glabrata* harboring a missense mutation in *ERG11* and exhibiting cross-resistance to azoles and amphotericin B,” *Antimicrob. Agents Chemother.*, vol. 56, no. 8, pp. 4223–4232, Aug. 2012, doi: 10.1128/AAC.06253-11.

[234] J. Il Yoo, C. W. Choi, K. M. Lee, and Y. S. Lee, “Gene Expression and Identification Related to Fluconazole Resistance of *Candida glabrata* Strains,” *Osong public Heal. Res. Perspect.*, vol. 1, no. 1, pp. 36–41, Dec. 2010, doi: 10.1016/j.phrp.2010.12.009.

[235] Q. Q. Li *et al.*, “Sterol uptake and sterol biosynthesis act coordinately to mediate antifungal resistance in *Candida glabrata* under azole and hypoxic stress,” *Mol. Med. Rep.*, vol. 17, no. 5, pp. 6585–6597, 2018, doi: 10.3892/mmr.2018.8716.

[236] S. G. Whaley *et al.*, “*UPC2A* is required for high-level azole antifungal resistance in *Candida glabrata*,” *Antimicrob. Agents Chemother.*, vol. 58, no. 8, pp. 4543–4554, 2014, doi: 10.1128/AAC.02217-13.

[237] M. Nagi *et al.*, “Transcription factors *CgUPC2A* and *CgUPC2B* regulate ergosterol biosynthetic genes in *Candida glabrata*,” *Genes to Cells*, vol. 16, no. 1, pp. 80–89, Jan. 2011, doi: 10.1111/j.1365-2443.2010.01470.x.

[238] S. Brun *et al.*, “Mechanisms of Azole Resistance in *Petite* Mutants of *Candida glabrata*,” *Antimicrob. Agents Chemother.*, vol. 48, no. 5, pp. 1788–96, May 2004, doi: 10.1128/AAC.48.5.1788.

[239] S. Ferrari *et al.*, “Loss of mitochondrial functions associated with azole resistance in *Candida glabrata* results in enhanced virulence in mice,” *Antimicrob. Agents Chemother.*, vol. 55, no. 5, pp. 1852–1860, May 2011, doi: 10.1128/AAC.01271-10.

[240] A. Defontaine, J. P. Bouchara, P. Declerk, C. Planchenault, D. Chabasse, and J. N. Hallet, “*In-vivo* selection of an azole-resistant petite mutant of *Candida glabrata*,” *J. Med. Microbiol.*, vol. 48, pp. 663–670, 1999.

[241] L. Demuyser, E. Swinnen, A. Fiori, B. Herrera-Malaver, K. Vestrepen, and P. Van Dijck, “Mitochondrial Cochaperone Mge1 Is Involved in Regulating Susceptibility to Fluconazole in *Saccharomyces cerevisiae* and *Candida* Species,” *MBio*, vol. 8, no. 4, Sep. 2017, doi: 10.1128/mBio.00201-17.

[242] R. Alves *et al.*, “Transcriptional responses of *Candida glabrata* biofilm cells to fluconazole are modulated by the carbon source,” *npj Biofilms Microbiomes*, vol. 6, no. 1, pp. 1–11, 2020, doi: 10.1038/s41522-020-0114-5.

[243] N. A. Kartsonis, J. Nielsen, and C. M. Douglas, “Caspofungin: the first in a new class of antifungal agents,” *Drug Resist. Updat.*, vol. 6, no. 4, pp. 197–218, Aug. 2003, doi: 10.1016/S1368-7646(03)00064-5.

[244] B. D. Alexander *et al.*, “Increasing Echinocandin Resistance in *Candida glabrata*: Clinical Failure Correlates With Presence of FKS Mutations and Elevated Minimum Inhibitory Concentrations,” *Clin. Infect. Dis.*, vol. 56, no. 12, pp. 1724–1732, Jun. 2013, doi: 10.1093/cid/cit136.

[245] G. Garcia-Effron, S. Lee, S. Park, J. D. Cleary, and D. S. Perlin, “Effect of *Candida glabrata FKS1* and *FKS2* Mutations on Echinocandin Sensitivity and Kinetics of 1,3-β-D-Glucan Synthase: Implication for the Existing Susceptibility Breakpoint,” *Antimicrob. Agents Chemother.*, vol. 53, no. 9, pp. 3690–3699, Sep. 2009, doi: 10.1128/AAC.00443-09.

[246] J. D. Cleary, G. Garcia-Effron, S. W. Chapman, and D. S. Perlin, “Reduced *Candida glabrata* Susceptibility Secondary to an *FKS1* Mutation Developed during Candidemia Treatment,” *Antimicrob. Agents Chemother.*, vol. 52, no. 6, pp. 2263–2265, Jun. 2008, doi: 10.1128/AAC.01568-07.

[247] S. Katiyar, M. Pfaller, and T. Edlind, “*Candida albicans* and *Candida glabrata* Clinical Isolates Exhibiting Reduced Echinocandin Susceptibility,” *Antimicrob. Agents Chemother.*, vol. 50, no. 8,

pp. 2892–2894, Aug. 2006, doi: 10.1128/AAC.00349-06.

[248] G. R. Thompson, N. P. Wiederhold, A. C. Vallor, N. C. Villareal, J. S. Lewis, and T. F. Patterson, “Development of Caspofungin Resistance following Prolonged Therapy for Invasive Candidiasis Secondary to *Candida glabrata* Infection,” *Antimicrob. Agents Chemother.*, vol. 52, no. 10, pp. 3783–3785, Oct. 2008, doi: 10.1128/AAC.00473-08.

[249] X. Hou *et al.*, “Novel *FKS1* and *FKS2* modifications in a high-level echinocandin resistant clinical isolate of *Candida glabrata*,” *Emerg. Microbes Infect.*, vol. 8, no. 1, pp. 1619–1625, Jan. 2019, doi: 10.1080/22221751.2019.1684209.

[250] Y. Zhao *et al.*, “Rapid Detection of *FKS* -Associated Echinocandin Resistance in *Candida glabrata*,” *Antimicrob. Agents Chemother.*, vol. 60, no. 11, pp. 6573–6577, Nov. 2016, doi: 10.1128/AAC.01574-16.

[251] D. Ellis, “Amphotericin B: spectrum and resistance,” *J. Antimicrob. Chemother.*, vol. 49, no. suppl_1, pp. 7–10, Jan. 2002, doi: 10.1093/jac/49.suppl_1.7.

[252] P. Vandeputte *et al.*, “A Nonsense Mutation in the *ERG6* Gene Leads to Reduced Susceptibility to Polyenes in a Clinical Isolate of *Candida glabrata*,” *Antimicrob. Agents Chemother.*, vol. 52, no. 10, pp. 3701–3709, Oct. 2008, doi: 10.1128/AAC.00423-08.

[253] P. Vandeputte, G. Tronchin, T. Berges, C. Hennequin, D. Chabasse, and J.-P. Bouchara, “Reduced Susceptibility to Polyenes Associated with a Missense Mutation in the *ERG6* Gene in a Clinical Isolate of *Candida glabrata* with Pseudohyphal Growth,” *Antimicrob. Agents Chemother.*, vol. 51, no. 3, pp. 982–990, Mar. 2007, doi: 10.1128/AAC.01510-06.

[254] A. Vermes, H.-J. Guchelaar, and J. Dankert, “Flucytosine: a review of its pharmacology, clinical indications, pharmacokinetics, toxicity and drug interactions,” *J. Antimicrob. Chemother.*, vol. 46, no. 2, pp. 171–179, Aug. 2000, doi: 10.1093/jac/46.2.171.

[255] A. Polak and H. J. Scholer, “Mode of Action of 5-fluorocytosine and Mechanisms of Resistance,” *Chemotherapy*, vol. 21, pp. 113–130, 1975.

[256] P. Vandeputte *et al.*, “Molecular Mechanisms of Resistance to 5-Fluorocytosine in Laboratory Mutants of *Candida glabrata*,” *Mycopathologia*, vol. 171, no. 1, pp. 11–21, Jan. 2011, doi: 10.1007/s11046-010-9342-1.

[257] W. W. Hope, L. Tabernero, D. W. Denning, and M. J. Anderson, “Molecular Mechanisms of Primary Resistance to Flucytosine in *Candida albicans*,” *Antimicrob. Agents Chemother.*, vol. 48, no. 11, pp. 4377–4386, Nov. 2004, doi: 10.1128/AAC.48.11.4377-4386.2004.

[258] A. R. Dodgson, K. J. Dodgson, C. Pujol, M. A. Pfaller, and D. R. Soll, “Clade-Specific Flucytosine Resistance Is Due to a Single Nucleotide Change in the *FUR1* Gene of *Candida albicans*,” *Antimicrob. Agents Chemother.*, vol. 48, no. 6, pp. 2223–2227, Jun. 2004, doi: 10.1128/AAC.48.6.2223-2227.2004.

[259] T. D. Edlind and S. K. Katiyar, “Mutational Analysis of Flucytosine Resistance in *Candida glabrata*,” *Antimicrob. Agents Chemother.*, vol. 54, no. 11, pp. 4733–4738, Nov. 2010, doi: 10.1128/AAC.00605-10.

[260] S. Normark and J. Schonebeck, “*In Vitro* Studies of 5-Fluorocytosine Resistance in *Candida albicans* and *Torulopsis glabrata*,” *Antimicrob. Agents Chemother.*, vol. 2, no. 3, pp. 114–121, Sep. 1972, doi: 10.1128/AAC.2.3.114.

[261] C. Costa *et al.*, “New Mechanisms of Flucytosine Resistance in *C. glabrata* Unveiled by a Chemogenomics Analysis in *S. cerevisiae*,” *PLoS One*, vol. 10, no. 8, p. e0135110, Aug. 2015, doi: 10.1371/journal.pone.0135110.

[262] M. Pfaller, S. Messer, L. Boyken, H. Huynh, R. Hollis, and D. Diekema, “*In vitro* activities of 5-fluorocytosine against 8,803 clinical isolates of *Candida* spp.: global assessment of primary resistance using National Committee for Clinical Laboratory Standards susceptibility testing methods,” *Antimicrob Agents Chemother*, vol. 46, no. 11, pp. 3518–3521, 2002.

[263] K. R. Healey *et al.*, “Prevalent mutator genotype identified in fungal pathogen *Candida glabrata*

promotes multi-drug resistance," *Nat. Commun.*, vol. 7, no. 1, p. 11128, Sep. 2016, doi: 10.1038/ncomms11128.

[264] B. P. Cormack, N. Ghori, and S. Falkow, "An adhesin of the yeast pathogen Candida glabrata mediating adherence to human epithelial cells.," *Science (80-.).*, vol. 285, no. 5427, pp. 578–582, 1999, doi: 10.1126/science.285.5427.578.

[265] V. Martínez-Jiménez *et al.*, "Sir3 Polymorphisms in *Candida glabrata* Clinical Isolates," *Mycopathologia*, vol. 175, no. 3–4, pp. 207–219, Apr. 2013, doi: 10.1007/s11046-013-9627-2.

[266] L. Vale-Silva, F. Ischer, S. Leibundgut-Landmann, and D. Sanglard, "Gain-of-function mutations in *PDR1*, a regulator of antifungal drug resistance in *Candida glabrata*, control adherence to host cells," *Infect. Immun.*, vol. 81, no. 5, pp. 1709–1720, 2013, doi: 10.1128/IAI.00074-13.

[267] C. Desai, J. Mavrianos, and N. Chauhan, "*Candida glabrata* Pwp7p and Aed1p are required for adherence to human endothelial cells," *FEMS Yeast Res.*, vol. 11, no. 7, pp. 595–601, Nov. 2011, doi: 10.1111/j.1567-1364.2011.00743.x.

[268] D. M. Kuhn and V. K. Vyas, "The *Candida glabrata* adhesin Epa1p causes adhesion, phagocytosis, and cytokine secretion by innate immune cells," *FEMS Yeast Res.*, vol. 12, no. 4, pp. 398–414, 2012, doi: 10.1111/j.1567-1364.2011.00785.x.

[269] G. Santonp, P. Birarelli, L. Jin Hong, A. Gamero, J. Y. Djeu, and M. Piccoli, "An α5β1 -like integrin receptor mediates the binding of less pathogenic *Candida* species to fibronectin," *J. Med. Microbiol.*, vol. 43, no. 5, pp. 360–367, Nov. 1995, doi: 10.1099/00222615-43-5-360.

[270] P. W. J. De Groot *et al.*, "The cell wall of the human pathogen *Candida glabrata*: Differential incorporation of novel adhesin-like wall proteins," *Eukaryot. Cell*, vol. 7, no. 11, pp. 1951–1964, 2008, doi: 10.1128/EC.00284-08.

[271] B. Timmermans, A. De Las Peñas, I. Castaño, and P. Van Dijck, "Adhesins in *Candida glabrata*," *J. Fungi*, vol. 4, no. 2, p. 60, May 2018, doi: 10.3390/jof4020060.

[272] E. López-Fuentes, G. Gutiérrez-Escobedo, B. Timmermans, P. Van Dijck, A. De Las Peñas, and I. Castaño, "*Candida glabrata's* Genome Plasticity Confers a Unique Pattern of Expressed Cell Wall Proteins.," *J. fungi (Basel, Switzerland)*, vol. 4, no. 2, Jun. 2018, doi: 10.3390/jof4020067.

[273] M. Maestre-Reyna *et al.*, "Structural basis for promiscuity and specificity during *Candida glabrata* invasion of host epithelia," *Proc. Natl. Acad. Sci.*, vol. 109, no. 42, pp. 16864–16869, Oct. 2012, doi: 10.1073/pnas.1207653109.

[274] F. S. Ielasi, K. Decanniere, and R. G. Willaert, "The epithelial adhesin 1 (Epa1p) from the human-pathogenic yeast *Candida glabrata*: structural and functional study of the carbohydrate-binding domain," *Acta Crystallogr. Sect. D Biol. Crystallogr.*, vol. 68, no. 3, pp. 210–217, Mar. 2012, doi: 10.1107/S0907444911054898.

[275] I. Castaño, S. J. Pan, M. Zupancic, C. Hennequin, B. Dujon, and B. P. Cormack, "Telomere length control and transcriptional regulation of subtelomeric adhesins in *Candida glabrata*," *Mol. Microbiol.*, vol. 55, no. 4, pp. 1246–1258, 2005, doi: 10.1111/j.1365-2958.2004.04465.x.

[276] R. Domergue *et al.*, "Nicotinic acid limitation regulates silencing of *Candida* adhesins during UTI.," *Science*, vol. 308, no. 5723, pp. 866–870, 2005, doi: 10.1126/science.1108640.

[277] A. Vitenshtein *et al.*, "NK Cell Recognition of *Candida glabrata* through Binding of NKp46 and NCR1 to Fungal Ligands Epa1, Epa6, and Epa7," *Cell Host Microbe*, vol. 20, no. 4, pp. 527–534, Oct. 2016, doi: 10.1016/j.chom.2016.09.008.

[278] J. Juárez-Cepeda *et al.*, "The *EPA2* adhesin encoding gene is responsive to oxidative stress in the opportunistic fungal pathogen *Candida glabrata*," *Curr. Genet.*, vol. 61, no. 4, pp. 529–544, Nov. 2015, doi: 10.1007/s00294-015-0473-2.

[279] M. L. Zupancic, M. Frieman, D. Smith, R. A. Alvarez, R. D. Cummings, and B. P. Cormack, "Glycan microarray analysis of *Candida glabrata* adhesin ligand specificity," *Mol. Microbiol.*, vol. 68, no. 3, pp. 547–559, May 2008, doi: 10.1111/j.1365-2958.2008.06184.x.

[280] F. S. Ielasi *et al.*, “Lectin-Glycan Interaction Network-Based Identification of Host Receptors of Microbial Pathogenic Adhesins,” *MBio*, vol. 7, no. 4, Sep. 2016, doi: 10.1128/mBio.00584-16.

[281] R. D. Mundy and B. Cormack, “Expression of *Candida glabrata* Adhesins after Exposure to Chemical Preservatives,” *J. Infect. Dis.*, vol. 199, no. 12, pp. 1891–1898, Jun. 2009, doi: 10.1086/599120.

[282] E. Gómez-Molero *et al.*, “Proteomic analysis of hyperadhesive *Candida glabrata* clinical isolates reveals a core wall proteome and differential incorporation of adhesins,” *FEMS Yeast Res.*, vol. 15, no. 8, p. fov098, Dec. 2015, doi: 10.1093/femsyr/fov098.

[283] L. Vale-Silva, E. Beaudoing, V. D. T. Tran, and D. Sanglard, “Comparative Genomics of Two Sequential *Candida glabrata* Clinical Isolates,” *G3: Genes|Genomes|Genetics*, vol. 7, no. 8, pp. 2413–2426, 2017, doi: 10.1534/g3.117.042887.

[284] R. Kaur, B. Ma, and B. P. Cormack, “A family of glycosylphosphatidylinositol-linked aspartyl proteases is required for virulence of *Candida glabrata.*,” *Proc. Natl. Acad. Sci. U. S. A.*, vol. 104, no. 18, pp. 7628–7633, 2007, doi: 10.1073/pnas.0611195104.

[285] S. A. Lachke, T. Srikantha, L. K. Tsai, K. Daniels, and D. R. Soll, “Phenotypic Switching in *Candida glabrata* Involves Phase-Specific Regulation of the Metallothionein Gene *MT-II* and the Newly Discovered Hemolysin Gene *HLP*,” *Infect. Immun.*, vol. 68, no. 2, pp. 884–895, 2000.

[286] P. J. Brockert, S. A. Lachke, T. Srikantha, C. Pujol, R. Galask, and D. R. Soll, “Phenotypic Switching and Mating Type Switching of *Candida glabrata* at Sites of Colonization,” *Infect. Immun.*, vol. 71, no. 12, pp. 7109–7118, Dec. 2003, doi: 10.1128/IAI.71.12.7109-7118.2003.

[287] T. Srikantha *et al.*, “Dark brown is the more virulent of the switch phenotypes of *Candida glabrata*,” *Microbiology*, vol. 154, no. 11, pp. 3309–3318, Nov. 2008, doi: 10.1099/mic.0.2008/020578-0.

[288] T. Srikantha, R. Zhao, K. Daniels, J. Radke, and D. R. Soll, “Phenotypic Switching in *Candida glabrata* Accompanied by Changes in Expression of Genes with Deduced Functions in Copper Detoxification and Stress,” *Eukaryot. Cell*, vol. 4, no. 8, pp. 1434–1445, Aug. 2005, doi: 10.1128/EC.4.8.1434-1445.2005.

[289] A. Roetzer, N. Gratz, P. Kovarik, and C. Schüller, “Autophagy supports *Candida glabrata* survival during phagocytosis,” *Cell. Microbiol.*, vol. 12, no. 2, pp. 199–216, 2010, doi: 10.1111/j.1462-5822.2009.01391.x.

[290] O. V. Vieira, R. J. Botelho, and S. Grinstein, “Phagosome maturation: aging gracefully,” *Biochem. J.*, vol. 366, no. 3, pp. 689–704, Sep. 2002, doi: 10.1042/bj20020691.

[291] K. Seider *et al.*, “The Facultative Intracellular Pathogen *Candida glabrata* Subverts Macrophage Cytokine Production and Phagolysosome Maturation,” *J. Immunol.*, vol. 187, no. 6, pp. 3072–3086, 2011, doi: 10.4049/jimmunol.1003730.

[292] K. Seider *et al.*, “Immune evasion, stress resistance, and efficient nutrient acquisition are crucial for intracellular survival of *Candida glabrata* within macrophages,” *Eukaryot. Cell*, vol. 13, no. 1, pp. 170–183, 2014, doi: 10.1128/EC.00262-13.

[293] M. N. Rai, S. Balusu, N. Gorityala, L. Dandu, and R. Kaur, “Functional Genomic Analysis of *Candida glabrata*-Macrophage Interaction: Role of Chromatin Remodeling in Virulence,” *PLoS Pathog.*, vol. 8, no. 8, 2012, doi: 10.1371/journal.ppat.1002863.

[294] L. Kasper *et al.*, “Identification of *Candida glabrata* Genes Involved in pH Modulation and Modification of the Phagosomal Environment in Macrophages,” *PLoS One*, vol. 9, no. 5, p. e96015, May 2014, doi: 10.1371/journal.pone.0096015.

[295] B. Hube, “Possible role of secreted proteinases in *Candida albicans* infections.,” *Rev. Iberoam. Micol.*, vol. 15, no. 2, pp. 65–8, Jun. 1998.

[296] A. S. Ibrahim *et al.*, “Evidence implicating phospholipase as a virulence factor of *Candida albicans*.,” *Infect. Immun.*, vol. 63, no. 5, pp. 1993–8, May 1995.

[297] M. A. Ghannoum, “Potential Role of Phospholipases in Virulence and Fungal Pathogenesis,” *Clin. Microbiol. Rev.*, vol. 13, no. 1, pp. 122–143, Jan. 2000, doi: 10.1128/CMR.13.1.122-143.2000.

[298] C. Marcos-Arias, E. Eraso, L. Madariaga, J. M. Aguirre, and G. Quindós, “Phospholipase and proteinase activities of *Candida* isolates from denture wearers,” *Mycoses*, vol. 54, no. 4, pp. e10–e16, Jul. 2011, doi: 10.1111/j.1439-0507.2009.01812.x.

[299] V. Mohan Das and M. Ballal, “Proteinase and phospholipase activity as virulence factors in *Candida* species isolated from blood.,” *Rev. Iberoam. Micol.*, vol. 25, no. 4, pp. 208–210, Dec. 2008, doi: 10.1016/S1130-1406(08)70050-0.

[300] N. Berila, P. Hyroššová, and J. Šubík, “Oxidative stress response and virulence factors in *Candida glabrata* clinical isolates,” *Folia Microbiol. (Praha).*, vol. 56, no. 2, pp. 116–121, Mar. 2011, doi: 10.1007/s12223-011-0016-2.

[301] M. Fatahinia, M. Halvaeezadeh, and A. Rezaei-Matehkolaei, “Comparison of enzymatic activities in different *Candida* species isolated from women with vulvovaginitis,” *J. Mycol. Med.*, vol. 27, no. 2, pp. 188–194, Jun. 2017, doi: 10.1016/j.mycmed.2017.01.009.

[302] É. B. de M. Riceto, R. de P. Menezes, M. P. A. Penatti, and R. dos S. Pedroso, “Enzymatic and hemolytic activity in different *Candida* species,” *Rev. Iberoam. Micol.*, vol. 32, no. 2, pp. 79–82, Apr. 2015, doi: 10.1016/j.riam.2013.11.003.

[303] G. Luo, L. P. Samaranayake, B. P. K. Cheung, and G. Tand, “Reverse transcriptase polymerase chain reaction (RT-PCR) detection of *HLP* gene expression in *Candida glabrata* and its possible role in i*n vitro* haemolysin production,” *APMIS*, vol. 112, no. 4–5, pp. 283–290, Apr. 2004, doi: 10.1111/j.1600-0463.2004.apm11204-0509.x.

[304] M. Kamran *et al.*, “Inactivation of Transcription Factor Gene *ACE2* in the Fungal Pathogen *Candida glabrata* Results in Hypervirulence,” *Eukaryot. Cell*, vol. 3, no. 2, pp. 546–552, 2004, doi: 10.1128/EC.3.2.546.

[305] T. L. Laabs, D. D. Markwardt, M. G. Slattery, L. L. Newcomb, D. J. Stillman, and W. Heideman, “*ACE2* is required for daughter cell-specific G1 delay in *Saccharomyces cerevisiae*,” *Proc. Natl. Acad. Sci.*, vol. 100, no. 18, pp. 10275–10280, Sep. 2003, doi: 10.1073/pnas.1833999100.

[306] D. Stead *et al.*, “Proteomic changes associated with inactivation of the *Candida glabrata ACE2* virulence-moderating gene.,” *Proteomics*, vol. 5, no. 7, pp. 1838–48, May 2005, doi: 10.1002/pmic.200401064.

[307] P. Mayser, M. Wenzel, H.-J. Krämer, B. L. J. Kindler, P. Spiteller, and G. Haase, “Production of indole pigments by *Candida glabrata*,” *Med. Mycol.*, vol. 45, no. 6, pp. 519–524, Jan. 2007, doi: 10.1080/13693780701411557.

[308] S. Brunke *et al.*, “*Candida glabrata* tryptophan-based pigment production via the Ehrlich pathway,” *Mol. Microbiol.*, vol. 76, no. 1, pp. 25–47, Apr. 2010, doi: 10.1111/j.1365-2958.2010.07052.x.

[309] S. D. Salas, J. E. Bennett, K. J. Kwon-Chung, J. R. Perfect, and P. R. Williamson, “Effect of the laccase gene *CNLAC1*, on virulence of *Cryptococcus neoformans.*,” *J. Exp. Med.*, vol. 184, no. 2, pp. 377–386, Aug. 1996, doi: 10.1084/jem.184.2.377.

[310] M. Cavalheiro and M. C. Teixeira, “In the Crossroad Between Drug Resistance and Virulence in Fungal Pathogens,” in *Stress Response Mechanisms in Fungi*, Cham: Springer International Publishing, 2018, pp. 223–259.

[311] C. Valotteau, V. Prystopiuk, B. P. Cormack, and Y. F. Dufrêne, “Atomic Force Microscopy Demonstrates that *Candida glabrata* Uses Three Epa Proteins To Mediate Adhesion to Abiotic Surfaces,” *mSphere*, vol. 4, no. 3, pp. 1–9, 2019.

[312] E. a. Kraneveld *et al.*, “Identification and Differential Gene Expression of Adhesin-Like Wall Proteins in *Candida glabrata* Biofilms,” *Mycopathologia*, vol. 172, no. 6, pp. 415–427, 2011, doi: 10.1007/s11046-011-9446-2.

[313] M. Cavalheiro *et al.*, “A Transcriptomics Approach To Unveiling the Mechanisms of *In Vitro* Evolution towards Fluconazole Resistance of a *Candida glabrata* Clinical Isolate,” *Antimicrob. Agents Chemother.*, vol. 63, no. 1, pp. 1–17, 2019.

[314] S. Brun *et al.*, “Biological consequences of *petite* mutations in *Candida glabrata*,” *J. Antimicrob. Chemother.*, vol. 56, no. 2, pp. 307–314, 2005, doi: 10.1093/jac/dki200.

[315] J. Verma-Gaur *et al.*, “Integration of Posttranscriptional Gene Networks into Metabolic Adaptation and Biofilm Maturation in *Candida albicans*,” *PLOS Genet.*, vol. 11, no. 10, p. e1005590, Oct. 2015, doi: 10.1371/journal.pgen.1005590.

[316] R. Santos *et al.*, “Screening the Drug:H+ Antiporter Family for a Role in Biofilm Formation in *Candida glabrata*,” *Front. Cell. Infect. Microbiol.*, vol. 10, no. 29, 2020, doi: doi: 10.3389/fcimb.2020.00029.

[317] T. Widiasih Widiyanto, X. Chen, S. Iwatani, H. Chibana, and S. Kajiwara, “Role of major facilitator superfamily transporter Qdr2p in biofilm formation by *Candida glabrata*,” *Mycoses*, vol. 62, no. 12, pp. 1154–1163, Dec. 2019, doi: 10.1111/myc.13005.

[318] S. Liu, Y. Hou, W. Liu, C. Lu, W. Wang, and S. Sun, “Components of the calcium-calcineurin signaling pathway in fungal cells and their potential as antifungal targets,” *Eukaryot. Cell*, vol. 14, no. 4, pp. 324–334, 2015, doi: 10.1128/EC.00271-14.

[319] T. Miyazaki *et al.*, “Roles of calcineurin and Crz1 in antifungal susceptibility and virulence of *Candida glabrata*,” *Antimicrob. Agents Chemother.*, vol. 54, no. 4, pp. 1639–1643, 2010, doi: 10.1128/AAC.01364-09.

[320] A. Ceballos Garzon, D. Amado, E. Robert, C. M. Parra Giraldo, and P. Le Pape, “Impact of calmodulin inhibition by fluphenazine on susceptibility, biofilm formation and pathogenicity of caspofungin-resistant *Candida glabrata*,” *J. Antimicrob. Chemother.*, vol. dkz565, pp. 1–7, 2020, doi: 10.1093/jac/dkz565.

[321] T. Schwarzmüller *et al.*, “Systematic Phenotyping of a Large-Scale *Candida glabrata* Deletion Collection Reveals Novel Antifungal Tolerance Genes,” *PLoS Pathog.*, vol. 10, no. 6, 2014, doi: 10.1371/journal.ppat.1004211.

[322] C. Onyewu, J. R. Blankenship, M. Del Poeta, and J. Heitman, “Ergosterol Biosynthesis Inhibitors Become Fungicidal when Combined with Calcineurin Inhibitors against *Candida albicans, Candida glabrata*, and *Candida krusei*,” *Antimicrob. Agents Chemother.*, vol. 47, no. 3, pp. 956–964, Mar. 2003, doi: 10.1128/AAC.47.3.956-964.2003.

[323] T. Miyazaki *et al.*, “Functional characterization of the regulators of calcineurin in *Candida glabrata*,” *FEMS Yeast Res.*, vol. 11, no. 8, pp. 621–630, 2011, doi: 10.1111/j.1567-1364.2011.00751.x.

[324] R. Kaur, I. Castaño, and B. P. Cormack, “Functional genomic analysis of fluconazole susceptibility in the pathogenic yeast *Candida glabrata*: roles of calcium signaling and mitochondria.,” *Antimicrob. Agents Chemother.*, vol. 48, no. 5, pp. 1600–13, May 2004, doi: 10.1128/AAC.48.5.1600.

[325] J. M. Cota *et al.*, “Increases in *SLT2* Expression and Chitin Content Are Associated with Incomplete Killing of *Candida glabrata* by Caspofungin,” *Antimicrob. Agents Chemother.*, vol. 52, no. 3, pp. 1144–1146, Mar. 2008, doi: 10.1128/AAC.01542-07.

[326] T. Miyazaki *et al.*, “Role of the Slt2 mitogen-activated protein kinase pathway in cell wall integrity and virulence in *Candida glabrata*,” *FEMS Yeast Res.*, vol. 10, no. 3, pp. 343–352, Apr. 2010, doi: 10.1111/j.1567-1364.2010.00611.x.

[327] T. Saijo *et al.*, “Skn7p Is Involved in Oxidative Stress Response and Virulence of *Candida glabrata*,” *Mycopathologia*, vol. 169, no. 2, pp. 81–90, Feb. 2010, doi: 10.1007/s11046-009-9233-5.

[328] A.-M. Calcagno, E. Bignell, T. R. Rogers, M. Canedo, F. A. Mühlschlegel, and K. Haynes, “*Candida glabrata* Ste20 is involved in maintaining cell wall integrity and adaptation to hypertonic

stress, and is required for wild-type levels of virulence," *Yeast*, vol. 21, no. 7, pp. 557–568, May 2004, doi: 10.1002/yea.1125.

[329] S. Poláková *et al.*, "Formation of new chromosomes as a virulence mechanism in yeast *Candida glabrata*," *Proc. Natl. Acad. Sci.*, vol. 106, no. 8, pp. 2688–2693, Feb. 2009, doi: 10.1073/pnas.0809793106.

[330] O. Bader *et al.*, "Gross Karyotypic and Phenotypic Alterations among Different Progenies of the *Candida glabrata* CBS138/ATCC2001 Reference Strain," *PLoS One*, vol. 7, no. 12, p. e52218, Dec. 2012, doi: 10.1371/journal.pone.0052218.

[331] K. M. Ahmad *et al.*, "Small chromosomes among Danish *Candida glabrata* isolates originated through different mechanisms," *Antonie van Leeuwenhoek, Int. J. Gen. Mol. Microbiol.*, vol. 104, no. 1, pp. 111–122, 2013, doi: 10.1007/s10482-013-9931-3.

[332] J. H. Ch'ng, K. K. L. Chong, L. N. Lam, J. J. Wong, and K. A. Kline, "Biofilm-associated infection by enterococci," *Nat. Rev. Microbiol.*, vol. 17, no. 2, pp. 82–94, 2019, doi: 10.1038/s41579-018-0107-z.

[333] A. S. Lynch and G. T. Robertson, "Bacterial and Fungal Biofilm Infections," *Annu. Rev. Med.*, vol. 59, no. 1, pp. 415–428, 2008, doi: 10.1146/annurev.med.59.110106.132000.

[334] C. J. Nobile and A. D. Johnson, "*Candida albicans* Biofilms and Human Disease," *Annu. Rev. Microbiol.*, vol. 69, no. 1, pp. 71–92, Oct. 2015, doi: 10.1146/annurev-micro-091014-104330.

[335] M. Cavalheiro and M. C. Teixeira, "*Candida* Biofilms: Threats, Challenges, and Promising Strategies," *Front. Med.*, vol. 5, no. 28, pp. 1–15, 2018, doi: 10.3389/fmed.2018.00028.

[336] L. Li, S. Redding, and A. Dongari-Bagtzoglou, "*Candida glabrata*: an emerging oral opportunistic pathogen.," *J. Dent. Res.*, vol. 86, no. 3, pp. 204–215, 2007, doi: 10.1177/154405910708600304.

[337] G. Luo and L. P. Samaranayake, "*Candida glabrata*, an emerging fungal pathogen, exhibits superior relative cell surface hydrophobicity and adhesion to denture acrylic surfaces compared with *Candida albicans*.," *APMIS*, vol. 110, no. 9, pp. 601–10, Sep. 2002.

[338] S. Silva, M. Negri, M. Henriques, R. Oliveira, D. Williams, and J. Azeredo, "Silicone colonization by non-*Candida albicans Candida* species in the presence of urine," *J. Med. Microbiol.*, vol. 59, no. 7, pp. 747–754, 2010, doi: 10.1099/jmm.0.017517-0.

[339] K. Ueno, J. Uno, H. Nakayama, K. Sasamoto, Y. Mikami, and H. Chibana, "Development of a Highly Efficient Gene Targeting System Induced by Transient Repression of *YKU80* Expression in *Candida glabrata*," *Eukaryot. Cell*, vol. 6, no. 7, pp. 1239–1247, Jul. 2007, doi: 10.1128/EC.00414-06.

[340] K.-H. H. Chen, T. Miyazaki, H.-F. F. Tsai, and J. E. Bennett, "The bZip transcription factor Cgap1p is involved in multidrug resistance and required for activation of multidrug transporter gene *CgFLR1* in *Candida glabrata*.," *Gene*, vol. 386, no. 1–2, pp. 63–72, Jan. 2007, doi: 10.1016/j.gene.2006.08.010.

[341] G. Jansen, C. Wu, B. Schade, D. Y. Thomas, and M. Whiteway, "Drag&Drop cloning in yeast," *Gene*, vol. 344, pp. 43–51, Jan. 2005, doi: 10.1016/j.gene.2004.10.016.

[342] T. R. Cabrito, M. C. Teixeira, A. A. Duarte, P. Duque, and I. Sá-Correia, "Heterologous expression of a Tpo1 homolog from Arabidopsis thaliana confers resistance to the herbicide 2,4-D and other chemical stresses in yeast," *Appl. Microbiol. Biotechnol.*, vol. 84, no. 5, pp. 927–936, 2009, doi: 10.1007/s00253-009-2025-5.

[343] H. Jiang, R. Lei, S. Ding, and S. Zhu, "Skewer : a fast and accurate adapter trimmer for next-generation sequencing paired-end reads," *BMC Bioinformatics*, vol. 15, no. 182, pp. 1–12, 2014.

[344] M. S. Skrzypek, J. Binkley, G. Binkley, S. R. Miyasato, M. Simison, and G. Sherlock, "The *Candida* Genome Database (CGD): incorporation of Assembly 22 , systematic identifiers and visualization of high throughput sequencing data," *Nucleic Acids Res.*, vol. 45, pp. 592–596, 2017, doi: 10.1093/nar/gkw924.

[345] C. Trapnell, L. Pachter, and S. L. Salzberg, “TopHat : discovering splice junctions with RNA-Seq,” *Bioinformatics*, vol. 25, no. 9, pp. 1105–1111, 2009, doi: 10.1093/bioinformatics/btp120.

[346] S. Anders and W. Huber, “Differential expression analysis for sequence count data,” *Genome Biol.*, vol. 11, no. 10, p. R106.1-12, 2010, doi: 10.1186/gb-2010-11-10-r106.

[347] M. I. Love, W. Huber, and S. Anders, “Moderated estimation of fold change and dispersion for RNA-seq data with DESeq2,” *Genome Biol.*, vol. 15, no. 550, pp. 1–21, 2014, doi: 10.1186/s13059-014-0550-8.

[348] R. C. Gentleman *et al.*, “Bioconductor: open software development for computational biology and bioinformatics,” *Genome Biol.*, vol. 5, no. 10, p. R80.1-15, 2004.

[349] J. M. Cherry *et al.*, “*Saccharomyces* Genome Database : the genomics resource of budding yeast,” *Nucleic Acids Res.*, vol. 40, pp. 700–705, 2012, doi: 10.1093/nar/gkr1029.

[350] D. Martin, C. Brun, E. Remy, P. Mouren, D. Thieffry, and B. Jacq, “GOToolBox: functional analysis of gene datasets based on Gene Ontology.,” *Genome Biol.*, vol. 5, no. 12, p. R101, 2004, doi: 10.1186/gb-2004-5-12-r101.

[351] L. Chopinet, C. Formosa, M. P. Rols, R. E. Duval, and E. Dague, “Imaging living cells surface and quantifying its properties at high resolution using AFM in QI™ mode,” *Micron*, vol. 48, pp. 26–33, 2013, doi: 10.1016/j.micron.2013.02.003.

[352] L. W. McKeen, “Plastics Used in Medical Devices,” in *Handbook of Polymer Applications in Medicine and Medical Devices*, Elsevier, 2014, pp. 21–53.

[353] E. Dague *et al.*, “Chemical force microscopy of single live cells,” *Nano Lett.*, vol. 7, no. 10, pp. 3026–3030, 2007, doi: 10.1021/nl071476k.

[354] F. Ahimou, F. A. Denis, A. Touhami, and Y. F. Dufrêne, “Probing microbial cell surface charges by atomic force microscopy,” *Langmuir*, vol. 18, no. 25, pp. 9937–9941, 2002, doi: 10.1021/la026273k.

[355] D. T. L. Le, Y. Guérardel, P. Loubire, M. Mercier-Bonin, and E. Dague, “Measuring kinetic dissociation/association constants between *Lactococcus lactis* bacteria and mucins using living cell probes,” *Biophys. J.*, vol. 101, no. 11, pp. 2843–2853, 2011, doi: 10.1016/j.bpj.2011.10.034.

[356] S. S. Nakamura-Vasconcelos *et al.*, “Emergence of *Candida glabrata* in vulvovaginal candidiasis should be attributed to selective pressure or virulence ability?,” *Arch. Gynecol. Obstet.*, vol. 296, no. 3, pp. 519–526, Sep. 2017, doi: 10.1007/s00404-017-4465-y.

[357] G. Smolyakov, C. Formosa-Dague, C. Severac, R. E. Duval, and E. Dague, “High speed indentation measures by FV, QI and QNM introduce a new understanding of bionanomechanical experiments,” *Micron*, vol. 85, pp. 8–14, Jun. 2016, doi: 10.1016/j.micron.2016.03.002.

[358] M. Tulla, J. Helenius, J. Jokinen, A. Taubenberger, D. J. Müller, and J. Heino, “TPA primes α2β1 integrins for cell adhesion,” *FEBS Lett.*, vol. 582, no. 23–24, pp. 3520–3524, Oct. 2008, doi: 10.1016/j.febslet.2008.09.022.

[359] M. Sun *et al.*, “Multiple membrane tethers probed by atomic force microscopy,” *Biophys. J.*, vol. 89, no. 6, pp. 4320–4329, 2005, doi: 10.1529/biophysj.104.058180.

[360] D. Raucher and M. P. Sheetz, “Characteristics of a Membrane Reservoir Buffering Membrane Tension,” *Biophys. J.*, vol. 77, no. 4, pp. 1992–2002, Oct. 1999, doi: 10.1016/S0006-3495(99)77040-2.

[361] J. Schmitz, M. Benoit, and K. E. Gottschalk, “The viscoelasticity of membrane tethers and its importance for cell adhesion,” *Biophys. J.*, vol. 95, no. 3, pp. 1448–1459, 2008, doi: 10.1529/biophysj.107.124289.

[362] G. Smolyakov *et al.*, “Elasticity, Adhesion, and Tether Extrusion on Breast Cancer Cells Provide a Signature of Their Invasive Potential,” *ACS Appl. Mater. Interfaces*, vol. 8, no. 41, pp. 27426–27431, Oct. 2016, doi: 10.1021/acsami.6b07698.

[363] J. Dai and M. P. Sheetz, “Membrane Tether Formation from Blebbing Cells,” *Biophys. J.*, vol. 77, no. 6, pp. 3363–3370, Dec. 1999, doi: 10.1016/S0006-3495(99)77168-7.

[364] D. W. Schmidtke and S. L. Diamond, “Direct observation of membrane tethers formed during neutrophil attachment to platelets or P-selectin under physiological flow.,” *J. Cell Biol.*, vol. 149, no. 3, pp. 719–30, May 2000, doi: 10.1083/jcb.149.3.719.

[365] A. Iglič, H. Hägerstrand, M. Bobrowska-Hägerstrand, V. Arrigler, and V. Kralj-Iglič, “Possible role of phospholipid nanotubes in directed transport of membrane vesicles,” *Phys. Lett. Sect. A Gen. At. Solid State Phys.*, vol. 310, no. 5–6, pp. 493–497, 2003, doi: 10.1016/S0375-9601(03)00449-3.

[366] C. Dieterich *et al.*, “*In vitro* reconstructed human epithelia reveal contributions of *Candida albicans EFG1* and *CPH1* to adhesion and invasion,” *Microbiology*, vol. 148, no. 2, pp. 497–506, 2002, doi: 10.1099/00221287-148-2-497.

[367] E. Preedy, S. Perni, D. Nipiĉ, K. Bohinc, and P. Prokopovich, “Surface roughness mediated adhesion forces between borosilicate glass and gram-positive bacteria,” *Langmuir*, vol. 30, no. 31, pp. 9466–9476, 2014, doi: 10.1021/la501711t.

[368] S. El-kirat-chatel *et al.*, “Force Nanoscopy of Hydrophobic Interactions in the Fungal Pathogen *Candida glabrata*,” *ASC Nano*, vol. 9, no. 2, pp. 1648–55, 2015.

[369] E. Potthoff *et al.*, “Rapid and Serial Quantification of Adhesion Forces of Yeast and Mammalian Cells,” *PLoS One*, vol. 7, no. 12, 2012, doi: 10.1371/journal.pone.0052712.

[370] S. El-Kirat-Chatel and Y. F. Dufrêne, “Nanoscale adhesion forces between the fungal pathogen: *Candida albicans* and macrophages,” *Nanoscale Horizons*, vol. 1, no. 1, pp. 69–74, 2016, doi: 10.1039/c5nh00049a.

[371] F. Zuttion *et al.*, “The anti-adhesive effect of glycoclusters on: *Pseudomonas aeruginosa* bacteria adhesion to epithelial cells studied by AFM single cell force spectroscopy,” *Nanoscale*, vol. 10, no. 26, pp. 12771–12778, 2018, doi: 10.1039/c8nr03285h.

[372] E. P. Fox *et al.*, “An expanded regulatory network temporally controls *Candida albicans* biofilm formation.,” *Mol. Microbiol.*, vol. 96, no. 6, pp. 1226–39, Jun. 2015, doi: 10.1111/mmi.13002.

[373] H. Wisplinghoff, T. Bischoff, S. M. Tallent, H. Seifert, R. P. Wenzel, and M. B. Edmond, “Nosocomial bloodstream infections in US hospitals: analysis of 24,179 cases from a prospective nationwide surveillance study.,” *Clin. Infect. Dis.*, vol. 39, no. 3, pp. 309–317, Aug. 2004, doi: 10.1086/421946.

[374] D. W. Denning and M. J. Bromley, “How to bolster the antifungal pipeline,” *Science (80-.).*, vol. 347, no. 6229, pp. 1414–1416, Mar. 2015, doi: 10.1126/science.aaa6097.

[375] M. a. Pfaller *et al.*, “Epidemiology and outcomes of invasive candidiasis due to non-albicans species of *Candida* in 2,496 patients: Data from the Prospective Antifungal Therapy (PATH) registry 2004-2008,” *PLoS One*, vol. 9, no. 7, 2014, doi: 10.1371/journal.pone.0101510.

[376] A. Kramer, I. Schwebke, and G. Kampf, “How long do nosocomial pathogens persist on inanimate surfaces? A systematic review.,” *BMC Infect. Dis.*, vol. 6, p. 130, 2006, doi: 10.1186/1471-2334-6-130.

[377] T. Felder, E. Bogengruber, S. Tenreiro, A. Ellinger, I. Sá-Correia, and P. Briza, “Dtr1p, a Multidrug Resistance Transporter of the Major Facilitator Superfamily, Plays an Essential Role in Spore Wall Maturation in *Saccharomyces cerevisiae*,” *Eukaryot. Cell*, vol. 1, no. 5, pp. 799–810, Oct. 2002, doi: 10.1128/EC.1.5.799-810.2002.

[378] C. Costa, P. J. Dias, I. Sá-Correia, and M. C. Teixeira, “MFS multidrug transporters in pathogenic fungi: Do they have real clinical impact?,” *Front. Physiol.*, vol. 5 MAY, no. May, pp. 1–8, Jan. 2014, doi: 10.3389/fphys.2014.00197.

[379] J. M. Becker, L. K. Henry, W. Jiang, and Y. Koltin, “Reduced virulence of *Candida albicans* mutants affected in multidrug resistance,” *Infect. Immun.*, vol. 63, no. 11, pp. 4515–4518, 1995.

[380] T. Yamada-Okabe, H. Yamada-Okabe, Yamada-OkabeT., and H. Yamada-Okabe, “Characterization of the *CaNAG3, CaNAG4*, and *CaNAG6* genes of the pathogenic fungus *Candida albicans*: Possible involvement of these genes in the susceptibilities of cytotoxic agents,” *FEMS Microbiol. Lett.*, vol. 212, no. 1, pp. 15–21, 2002, doi: 10.1016/S0378-1097(02)00726-7.

[381] A. H. Shah *et al.*, “Novel role of a family of major facilitator transporters in biofilm development and virulence of *Candida albicans*.,” *Biochem. J.*, vol. 460, no. 2, pp. 223–235, 2014, doi: 10.1042/BJ20140010.

[382] G. Cotter, S. Doyle, and K. Kavanagh, “Development of an insect model for the *in vivo* pathogenicity testing of yeasts,” *FEMS Immunol. Med. Microbiol.*, vol. 27, no. 2, pp. 163–169, Feb. 2000, doi: 10.1111/j.1574-695X.2000.tb01427.x.

[383] D. Mil-Homens and A. M. Fialho, “A BCAM0223 Mutant of *Burkholderia cenocepacia* Is Deficient in Hemagglutination, Serum Resistance, Adhesion to Epithelial Cells and Virulence,” *PLoS One*, vol. 7, no. 7, p. e41747, Jul. 2012, doi: 10.1371/journal.pone.0041747.

[384] M. F. Brivio, M. Mastore, and A. J. Nappi, “A pathogenic parasite interferes with phagocytosis of insect immunocompetent cells,” *Dev. Comp. Immunol.*, vol. 34, no. 9, pp. 991–998, Sep. 2010, doi: 10.1016/j.dci.2010.05.002.

[385] K. Köhrer and H. Domdey, “Preparation of high molecular weight RNA,” *Methods Enzymol.*, vol. 194, pp. 398–405, 1991.

[386] A. Y. Peleg, D. A. Hogan, and E. Mylonakis, “Medically important bacterial–fungal interactions,” *Nat. Rev. Microbiol.*, vol. 8, no. 5, pp. 340–349, May 2010, doi: 10.1038/nrmicro2313.

[387] I. D. Jacobsen, “*Galleria mellonella* as a model host to study virulence of *Candida*.,” *Virulence*, vol. 5, no. 2, pp. 237–9, Feb. 2014, doi: 10.4161/viru.27434.

[388] I. D. Jacobsen *et al.*, “*Candida glabrata* persistence in mice does not depend on host immunosuppression and is unaffected by fungal amino acid auxotrophy,” *Infect. Immun.*, vol. 78, no. 3, pp. 1066–1077, 2010, doi: 10.1128/IAI.01244-09.

[389] C. Ribeiro and M. Brehélin, “Insect haemocytes: what type of cell is that?,” *J. Insect Physiol.*, vol. 52, no. 5, pp. 417–29, May 2006, doi: 10.1016/j.jinsphys.2006.01.005.

[390] P. Piper, C. O. Calderon, K. Hatzixanthis, and M. Mollapour, “Weak acid adaptation: the stress response that confers yeasts with resistance to organic acid food preservatives,” *Microbiology*, vol. 147, no. 10, pp. 2635–2642, Oct. 2001, doi: 10.1099/00221287-147-10-2635.

[391] M. C. Teixeira, P. Duque, and I. Sá-Correia, “Environmental genomics: mechanistic insights into toxicity of and resistance to the herbicide 2,4-D,” *Trends Biotechnol.*, vol. 25, no. 8, pp. 363–370, Aug. 2007, doi: 10.1016/j.tibtech.2007.06.002.

[392] S. Tenreiro, P. C. Rosa, C. A. Viegas, and I. Sá-Correia, “Expression of the *AZR1* gene (ORF YGR224w), encoding a plasma membrane transporter of the major facilitator superfamily, is required for adaptation to acetic acid and resistance to azoles in *Saccharomyces cerevisiae*,” *Yeast*, vol. 16, no. 16, pp. 1469–1481, Dec. 2000, doi: 10.1002/1097-0061(200012)16:16<1469::AID-YEA640>3.0.CO;2-A.

[393] S. Tenreiro *et al.*, “*AQR1* gene (ORF YNL065w) encodes a plasma membrane transporter of the major facilitator superfamily that confers resistance to short-chain monocarboxylic acids and quinidine in *Saccharomyces cerevisiae*,” *Biochem. Biophys. Res. Commun.*, vol. 292, no. 3, pp. 741–748, 2002, doi: 10.1006/bbrc.2002.6703.

[394] A. R. Fernandes, N. P. Mira, R. C. Vargas, I. Canelhas, and I. Sá-Correia, “*Saccharomyces cerevisiae* adaptation to weak acids involves the transcription factor Haa1p and Haa1p-regulated genes,” *Biochem. Biophys. Res. Commun.*, vol. 337, no. 1, pp. 95–103, Nov. 2005, doi: 10.1016/j.bbrc.2005.09.010.

[395] C. P. Godinho *et al.*, “Yeast response and tolerance to benzoic acid involves the Gcn4- and Stp1-regulated multidrug/multixenobiotic resistance transporter Tpo1,” *Appl. Microbiol. Biotechnol.*,

vol. 101, no. 12, pp. 5005–5018, Jun. 2017, doi: 10.1007/s00253-017-8277-6.

[396] D. A. Davis, “How human pathogenic fungi sense and adapt to pH: the link to virulence,” *Curr. Opin. Microbiol.*, vol. 12, no. 4, pp. 365–370, 2009, doi: 10.1016/j.mib.2009.05.006.

[397] L. Kasper, K. Seider, and B. Hube, “Intracellular survival of *Candida glabrata* in macrophages: immune evasion and persistence,” *FEMS Yeast Res.*, vol. 15, no. 5, p. fov042, Aug. 2015, doi: 10.1093/femsyr/fov042.

[398] M. C. Arendrup *et al.*, “Echinocandin Susceptibility Testing of *Candida* Species: Comparison of EUCAST EDef 7.1, CLSI M27-A3, Etest, Disk Diffusion, and Agar Dilution Methods with RPMI and IsoSensitest Media,” *Antimicrob. Agents Chemother.*, vol. 54, no. 1, pp. 426–439, Jan. 2010, doi: 10.1128/AAC.01256-09.

[399] J. Perlroth, B. Choi, and B. Spellberg, “Nosocomial fungal infections: epidemiology, diagnosis, and treatment,” *Med. Mycol.*, vol. 45, no. 4, pp. 321–346, 2007, doi: 10.1080/13693780701218689.

[400] P. L. Fidel, J. A. Vazquez, and J. D. Sobel, “*Candida glabrata*: review of epidemiology, pathogenesis, and clinical disease with comparison to *C. albicans*.,” *Clin. Microbiol. Rev.*, vol. 12, no. 1, pp. 80–96, Jan. 1999.

[401] N. Mishra *et al.*, “Pathogenicity and drug resistance in *Candida albicans* and other yeast species,” *Acta Microbiol. Immunol. Hung.*, vol. 54, no. 3, pp. 201–235, Sep. 2007, doi: 10.1556/AMicr.54.2007.3.1.

[402] S. Silva, M. Negri, M. Henriques, R. Oliveira, D. W. Williams, and J. Azeredo, “*Candida glabrata, Candida parapsilosis* and *Candida tropicalis*: biology, epidemiology, pathogenicity and antifungal resistance,” *FEMS Microbiol. Rev.*, vol. 36, no. 2, pp. 288–305, Mar. 2012, doi: 10.1111/j.1574-6976.2011.00278.x.

[403] B. M. Peters, M. E. Shirtliff, and M. A. Jabra-Rizk, “Antimicrobial peptides: primeval molecules or future drugs?,” *PLoS Pathog.*, vol. 6, no. 10, p. e1001067, Oct. 2010, doi: 10.1371/journal.ppat.1001067.

[404] P. Tam, K. Gee, M. Piechocinski, and I. Macreadie, “*Candida glabrata*, Friend and Foe,” *J. Fungi*, vol. 1, no. 2, pp. 277–292, Sep. 2015, doi: 10.3390/jof1020277.

[405] R. S. Shapiro, N. Robbins, and L. E. Cowen, “Regulatory Circuitry Governing Fungal Development, Drug Resistance, and Disease,” *Microbiol. Mol. Biol. Rev.*, vol. 75, no. 2, pp. 213–267, Jun. 2011, doi: 10.1128/MMBR.00045-10.

[406] H. Tomitori, K. Kashiwagi, T. Asakawa, Y. Kakinuma, A. J. Michael, and K. Igarashi, “Multiple polyamine transport systems on the vacuolar membrane in yeast.,” *Biochem. J.*, vol. 353, no. Pt 3, pp. 681–8, Feb. 2001.

[407] D. Romão *et al.*, “A New Determinant of *Candida glabrata* Virulence: The Acetate Exporter CgDtr1,” *Front. Cell. Infect. Microbiol.*, vol. 7, no. 473, pp. 1–10, 2017, doi: 10.3389/fcimb.2017.00473.

[408] M. Cavalheiro, P. Pais, M. Galocha, and M. C. Teixeira, “Host-pathogen interactions mediated by MDR transporters in fungi: As pleiotropic as it gets!,” *Genes (Basel).*, vol. 9, no. 7, p. 332, 2018, doi: 10.3390/genes9070332.

[409] C. J.-Y. Tsai, J. M. S. Loh, and T. Proft, “*Galleria mellonella* infection models for the study of bacterial diseases and for antimicrobial drug testing,” *Virulence*, vol. 7, no. 3, pp. 214–229, Apr. 2016, doi: 10.1080/21505594.2015.1135289.

[410] V. Carmelo, H. Santos, and I. Sá-Correia, “Effect of extracellular acidification on the activity of plasma membrane ATPase and on the cytosolic and vacuolar pH of *Saccharomyces cerevisiae*.,” *Biochim. Biophys. Acta*, vol. 1325, no. 1, pp. 63–70, Apr. 1997.

[411] T. R. Cabrito, M. C. Teixeira, A. Singh, R. Prasad, and I. Sá-Correia, “The yeast ABC transporter Pdr18 (ORF *YNR070w*) controls plasma membrane sterol composition, playing a role in multidrug resistance,” *Biochem. J.*, vol. 440, no. 2, pp. 195–202, 2011, doi:

10.1042/BJ20110876.

[412] B. Altincicek and A. Vilcinskas, “Metamorphosis and collagen-IV-fragments stimulate innate immune response in the greater wax moth, *Galleria mellonella*,” *Dev. Comp. Immunol.*, vol. 30, no. 12, pp. 1108–1118, Jan. 2006, doi: 10.1016/j.dci.2006.03.002.

[413] I. Wojda, P. Kowalski, and T. Jakubowicz, “Humoral immune response of *Galleria mellonella* larvae after infection by *Beauveria bassiana* under optimal and heat-shock conditions,” *J. Insect Physiol.*, vol. 55, no. 6, pp. 525–531, Jun. 2009, doi: 10.1016/j.jinsphys.2009.01.014.

[414] G. Wu, L. Xu, and Y. Yi, “*Galleria mellonella* larvae are capable of sensing the extent of priming agent and mounting proportionatal cellular and humoral immune responses,” *Immunol. Lett.*, vol. 174, pp. 45–52, 2016, doi: 10.1016/j.imlet.2016.04.013.

[415] M. Edgerton, S. E. Koshlukova, T. E. Lo, B. G. Chrzan, R. M. Straubinger, and P. A. Raj, “Candidacidal activity of salivary histatins. Identification of a histatin 5-binding protein on *Candida albicans*.,” *J. Biol. Chem.*, vol. 273, no. 32, pp. 20438–47, Aug. 1998.

[416] M. Albertsen, I. Bellahn, R. Krämer, and S. Waffenschmidt, “Localization and function of the yeast multidrug transporter Tpo1p,” *J. Biol. Chem.*, vol. 278, no. 15, pp. 12820–12825, 2003, doi: 10.1074/jbc.M210715200.

[417] R. Kumar *et al.*, “Histatin 5 Uptake by *Candida albicans* Utilizes Polyamine Transporters Dur3 and Dur31 Proteins,” *J. Biol. Chem.*, vol. 286, no. 51, pp. 43748–43758, Dec. 2011, doi: 10.1074/jbc.M111.311175.

[418] D. Bergin, E. P. Reeves, J. Renwick, F. B. Wientjes, and K. Kavanagh, “Superoxide Production in *Galleria mellonella* Hemocytes: Identification of Proteins Homologous to the NADPH Oxidase Complex of Human Neutrophils,” *Infect. Immun.*, vol. 73, no. 7, pp. 4161–4170, Jul. 2005, doi: 10.1128/IAI.73.7.4161-4170.2005.

[419] M. J. Spiering, “Primer on the Immune System.,” *Alcohol Res.*, vol. 37, no. 2, pp. 171–5, 2015.

[420] S. C. Viegas, D. Mil-Homens, A. M. Fialho, and C. M. Arraiano, “The virulence of *Salmonella enterica Serovar Typhimurium* in the insect model *Galleria mellonella* is impaired by mutations in RNase E and RNase III.,” *Appl. Environ. Microbiol.*, vol. 79, no. 19, pp. 6124–33, Oct. 2013, doi: 10.1128/AEM.02044-13.

[421] C. R. Harding *et al.*, “*Legionella pneumophila* Pathogenesis in the *Galleria mellonella* Infection Model,” *Infect. Immun.*, vol. 80, no. 8, pp. 2780–2790, Aug. 2012, doi: 10.1128/IAI.00510-12.

[422] P. Mak, A. Zdybicka-Barabas, and M. Cytryńska, “A different repertoire of *Galleria mellonella* antimicrobial peptides in larvae challenged with bacteria and fungi,” *Dev. Comp. Immunol.*, vol. 34, no. 10, pp. 1129–1136, Oct. 2010, doi: 10.1016/j.dci.2010.06.005.

[423] A. Sowa-Jasiłek *et al.*, “*Galleria mellonella* lysozyme induces apoptotic changes in *Candida albicans* cells.,” *Microbiol. Res.*, vol. 193, pp. 121–131, Dec. 2016, doi: 10.1016/j.micres.2016.10.003.

[424] B. Schuhmann, V. Seitz, A. Vilcinskas, and L. Podsiadlowski, “Cloning and expression of gallerimycin, an antifungal peptide expressed in immune response of greater wax moth larvae, *Galleria mellonella*,” *Arch. Insect Biochem. Physiol.*, vol. 53, no. 3, pp. 125–133, Jul. 2003, doi: 10.1002/arch.10091.

[425] G. Langen, J. Imani, B. Altincicek, G. Kieseritzky, K.-H. Kogel, and A. Vilcinskas, “Transgenic expression of gallerimycin, a novel antifungal insect defensin from the greater wax moth *Galleria mellonella*, confers resistance to pathogenic fungi in tobacco,” *Biol. Chem.*, vol. 387, no. 5, pp. 549–57, Jan. 2006, doi: 10.1515/BC.2006.071.

[426] E. J. Helmerhorst, A. S. Alagl, W. L. Siqueira, and F. G. Oppenheim, “Oral fluid proteolytic effects on histatin 5 structure and function,” *Arch. Oral Biol.*, vol. 51, no. 12, pp. 1061–1070, Dec. 2006, doi: 10.1016/j.archoralbio.2006.06.005.

[427] R. Li, R. Kumar, S. Tati, S. Puri, and M. Edgerton, “*Candida albicans* Flu1-Mediated Efflux of Salivary Histatin 5 Reduces Its Cytosolic Concentration and Fungicidal Activity,” *Antimicrob.*

Agents Chemother., vol. 57, no. 4, pp. 1832–1839, Apr. 2013, doi: 10.1128/AAC.02295-12.

[428] R. C. Vargas *et al.*, "*Saccharomyces cerevisiae* multidrug resistance transporter Qdr2 is implicated in potassium uptake, providing a physiological advantage to quinidine-stressed cells," *Eukaryot. Cell*, vol. 6, no. 2, pp. 134–142, 2007, doi: 10.1128/EC.00290-06.

[429] M. C. Teixeira, R. Cabrito, Z. M. Hanif, R. C. Vargas, S. Tenreiro, and I. Sá-Correia, "Yeast response and tolerance to polyamine toxicity involving the drug: H+ antiporter Qdr3 and the transcription factors Yap1 and Gcn4," *Microbiology*, vol. 157, pp. 945–956, 2011, doi: 10.1099/mic.0.043661-0.

[430] Y. Asai *et al.*, "Elevated polyamines in saliva of pancreatic cancer," *Cancers (Basel).*, vol. 10, no. 43, pp. 1–11, 2018, doi: 10.3390/cancers10020043.

[431] N. Papon, V. Courdavault, M. Clastre, and R. J. Bennett, "Emerging and Emerged Pathogenic *Candida* Species: Beyond the *Candida albicans* Paradigm," *PLoS Pathog.*, vol. 9, no. 9, pp. 1–4, 2013, doi: 10.1371/journal.ppat.1003550.

[432] P. D. Crowley and H. C. Gallagher, "Clotrimazole as a pharmaceutical: Past, present and future.," *J. Appl. Microbiol.*, vol. 117, pp. 611–617, 2014, doi: 10.1111/jam.12554.

[433] S. Abbes, C. Mary, H. Sellami, A. Michel-Nguyen, A. Ayadi, and S. Ranque, "Interactions between copy number and expression level of genes involved in fluconazole resistance in *Candida glabrata*.," *Front. Cell. Infect. Microbiol.*, vol. 3, no. 74, pp. 1–8, Jan. 2013, doi: 10.3389/fcimb.2013.00074.

[434] R. A. Calderone and C. J. Clancy, *Candida and Candidiasis*, Second Edi. ASM Press, 2012.

[435] M. . Pfaller *et al.*, "*In vitro* activities of voriconazole, posaconazole, and fluconazole against 4,169 clinical isolates of *Candida* spp. and *Cryptococcus neoformans* collected during 2001 and 2002 in the ARTEMIS global antifungal surveillance program," *Diagn. Microbiol. Infect. Dis.*, vol. 48, no. 3, pp. 201–205, Mar. 2004, doi: 10.1016/j.diagmicrobio.2003.09.008.

[436] X. Li *et al.*, "Changes in susceptibility to posaconazole in clinical isolates of *Candida albicans*.," *J. Antimicrob. Chemother.*, vol. 53, no. 1, pp. 74–80, Jan. 2004, doi: 10.1093/jac/dkh027.

[437] B. Favre, M. Didmon, and N. S. Ryder, "Multiple amino acid substitutions in lanosterol 14alpha-demethylase contribute to azole resistance in *Candida albicans*.," *Microbiology*, vol. 145, pp. 2715–2725, 1999, doi: 10.1099/00221287-145-10-2715.

[438] P. Marichal *et al.*, "Molecular Biological Characterization of an Azole-Resistant *Candida glabrata* Isolate," *Antimicrob. Agents Chemother.*, vol. 41, no. 10, pp. 2229–2237, 1997.

[439] S. B. Salazar *et al.*, "Comparative genomic and transcriptomic analyses unveil novel features of azole resistance and adaptation to the human host in *Candida glabrata*," *FEMS Yeast Res.*, vol. 18, no. 1, 2018, doi: 10.1093/femsyr/fox079.

[440] J. Branco *et al.*, "Impact of *ERG3* mutations and expression of ergosterol genes controlled by *UPC2* and *NDT80* in *Candida parapsilosis* azole resistance," *Clin. Microbiol. Infect.*, vol. 23, no. 8, pp. 575.e1-575.e8, 2017, doi: 10.1016/j.cmi.2017.02.002.

[441] A. Geber *et al.*, "Deletion of the *Candida glabrata ERG3* and *ERG11* genes: effect on cell viability, cell growth, sterol composition, and antifungal susceptibility," *Antimicrob. Agents Chemother.*, vol. 39, no. 12, pp. 2708–2717, Dec. 1995, doi: 10.1128/AAC.39.12.2708.

[442] E. Cantón *et al.*, "Epidemiological cutoff values for fluconazole, itraconazole, posaconazole, and voriconazole for six *Candida* species as determined by the colorimetric Sensititre YeastOne method.," *J. Clin. Microbiol.*, vol. 51, no. 8, pp. 2691–5, Aug. 2013, doi: 10.1128/JCM.01230-13.

[443] R. Ben-Ami, Y. Hilerowicz, A. Novikov, and M. Giladi, "The impact of new epidemiological cutoff values on *Candida glabrata* resistance rates and concordance between testing methods," *Diagn. Microbiol. Infect. Dis.*, vol. 79, no. 2, pp. 209–213, Jun. 2014, doi: 10.1016/j.diagmicrobio.2014.02.008.

[444] J. R. Azanza, E. García-quetglas, and B. Sádaba, "Farmacología de los azoles," *Rev Iberoam*

Micol, vol. 24, pp. 223–227, 2007.

[445] J. H. Rex *et al.*, “Reference method for broth dilution antifungal susceptibility testing of yeasts: approved standard - third edition,” *Clin. Lab. Stand. Inst.*, vol. 28, no. 14, 2008, doi: 10.1007/SpringerReference_5244.

[446] M. A. Pfaller *et al.*, “International Surveillance of Bloodstream Infections Due to *Candida* Species : Frequency of Occurrence and *In Vitro* Susceptibilities to Fluconazole , Ravuconazole , and Voriconazole of Isolates Collected from 1997 through 1999 in the SENTRY A,” *J. Clin. Microbiol.*, vol. 39, no. 9, pp. 3254–3259, 2001, doi: 10.1128/JCM.39.9.3254.

[447] M. A. Pfaller, D. J. Diekema, S. A. Messer, R. J. Hollis, and R. N. Jones, “*In Vitro* Activities of Caspofungin Compared with Those of Fluconazole and Itraconazole against 3 , 959 Clinical Isolates of *Candida* spp ., Including 157 Fluconazole-Resistant Isolates,” *Antimicrob. Agents Chemother.*, vol. 47, no. 3, pp. 1068–1071, 2003, doi: 10.1128/AAC.47.3.1068.

[448] R. T. Bernardo *et al.*, “The CgHaa1-Regulon Mediates Response and Tolerance to Acetic Acid Stress in the Human Pathogen *Candida glabrata*,” *G3: Genes|Genomes|Genetics*, vol. 7, no. 1, pp. 1–18, 2017, doi: 10.1534/g3.116.034660.

[449] K. P. Byrne, “The Yeast Gene Order Browser: Combining curated homology and syntenic context reveals gene fate in polyploid species,” *Genome Res.*, vol. 15, no. 10, pp. 1456–1461, Sep. 2005, doi: 10.1101/gr.3672305.

[450] P. T. Monteiro, P. Pais, C. Costa, S. Manna, I. Sa-Correia, and M. C. Teixeira, “The PathoYeastract database: An information system for the analysis of gene and genomic transcription regulation in pathogenic yeasts,” *Nucleic Acids Res.*, vol. 45, no. D1, pp. D597–D603, 2017, doi: 10.1093/nar/gkw817.

[451] O. Reuss *et al.*, “The *SAT1* flipper, an optimized tool for gene disruption in *Candida albicans*.,” *Gene*, vol. 341, pp. 119–27, Oct. 2004, doi: 10.1016/j.gene.2004.06.021.

[452] M. F. Rosa and I. Sá-Correia, “Intracellular acidification does not account for inhibition of *Saccharomyces cerevisiae* growth in the presence of ethanol,” *FEMS Microbiol. Lett.*, vol. 135, no. 2–3, pp. 271–274, 1996, doi: 10.1016/0378-1097(95)00465-3.

[453] P. Gong, X. Guan, and E. Witter, “Short communication A rapid method to extract ergosterol from soil by physical disruption,” *Appl. Soil Ecol.*, vol. 17, pp. 285–289, 2001, doi: 10.1016/S0929-1393(01)00141-X.

[454] K. Mukhopadhyay, T. Prasad, P. Saini, T. J. Pucadyil, A. Chattopadhyay, and R. Prasad, “Membrane Sphingolipid-Ergosterol Interactions Are Important Determinants of Multidrug Resistance in *Candida albicans*,” *Antimicrob. Agents Chemother.*, vol. 48, no. 5, pp. 1778–1787, 2004, doi: 10.1128/AAC.48.5.1778.

[455] Y. Q. Zhang, S. Gamarra, G. Garcia-Effron, S. Park, D. S. Perlin, and R. Rao, “Requirement for ergosterol in V-ATPase function underlies antifungal activity of azole drugs,” *PLoS Pathog.*, vol. 6, no. 6, 2010, doi: 10.1371/journal.ppat.1000939.

[456] A. Singh, V. Yadav, and R. Prasad, “Comparative lipidomics in clinical isolates of *Candida albicans* reveal crosstalk between mitochondria, cell wall integrity and azole resistance,” *PLoS One*, vol. 7, no. 6, pp. 1–13, 2012, doi: 10.1371/journal.pone.0039812.

[457] J. Cernicka and J. Subik, “Resistance mechanisms in fluconazole-resistant *Candida albicans* isolates from vaginal candidiasis.,” *Int. J. Antimicrob. Agents*, vol. 27, no. 5, pp. 403–8, May 2006, doi: 10.1016/j.ijantimicag.2005.12.005.

[458] P. Szweda *et al.*, “Mechanisms of azole resistance among clinical isolates of *Candida glabrata* in Poland,” *J. Med. Microbiol.*, vol. 64, no. 6, pp. 610–9, Jun. 2015, doi: 10.1099/jmm.0.000062.

[459] S.-Y. Ruan, L.-N. Lee, J.-S. Jerng, C.-J. Yu, and P.-R. Hsueh, “*Candida glabrata* fungaemia in intensive care units,” *Clin. Microbiol. Infect.*, vol. 14, no. 2, pp. 136–140, Feb. 2008, doi: 10.1111/j.1469-0691.2007.01892.x.

[460] P. Pais, M. Galocha, R. Viana, M. Cavalheiro, D. Pereira, and M. C. Teixeira, “Microevolution of

the pathogenic yeasts *Candida albicans* and *Candida glabrata* during antifungal therapy and host infection," *Microb. Cell*, vol. 6, no. 3, pp. 142–159, 2019, doi: 10.15698/mic2019.03.670.

[461] S. G. Whaley, Q. Zhang, K. E. Caudle, and P. D. Rogers, "Relative Contribution of the ABC Transporters Cdr1, Pdh1, and Snq2 to Azole Resistance in *Candida glabrata*," *Antimicrob. Agents Chemother.*, vol. 62, no. 10, Jul. 2018, doi: 10.1128/AAC.01070-18.

[462] M. Shingu-Vazquez and A. Traven, "Mitochondria and fungal pathogenesis: Drug tolerance, virulence, and potential for antifungal therapy," *Eukaryot. Cell*, vol. 10, no. 11, pp. 1376–1383, 2011, doi: 10.1128/EC.05184-11.

[463] P. Pais, M. Galocha, and M. C. Teixeira, "Genome-Wide Response to Drugs and Stress in the Pathogenic Yeast *Candida glabrata*," in *Progress in Molecular and Subcellular Biology 58,* vol. 58, Springer International Publishing, 2019, pp. 155–193.

[464] C. J. Seneviratne, W. J. Silva, L. J. Jin, Y. H. Samaranayake, and L. P. Samaranayake, "Architectural analysis, viability assessment and growth kinetics of *Candida albicans* and *Candida glabrata* biofilms," *Arch. Oral Biol.*, vol. 54, no. 11, pp. 1052–1060, 2009, doi: 10.1016/j.archoralbio.2009.08.002.

[465] T. C. Walther, J. H. Brickner, P. S. Aguilar, S. Bernales, C. Pantoja, and P. Walter, "Eisosomes mark static sites of endocytosis.," *Nature*, vol. 439, no. 7079, pp. 998–1003, Feb. 2006, doi: 10.1038/nature04472.

[466] H. Moor and K. Mühlethaler, "Fine structure in frozen-etched yeast cells," *J. Cell Biol.*, vol. 17, no. 3, pp. 609–628, Jun. 1963, doi: 10.1083/jcb.17.3.609.

[467] A. Olivera-Couto, M. Graña, L. Harispe, and P. S. Aguilar, "The eisosome core is composed of BAR domain proteins," *Mol. Biol. Cell*, vol. 22, no. 13, pp. 2360–2372, Jul. 2011, doi: 10.1091/mbc.e10-12-1021.

[468] N. E. Ziółkowska, L. Karotki, M. Rehman, J. T. Huiskonen, and T. C. Walther, "Eisosome-driven plasma membrane organization is mediated by BAR domains," *Nat. Struct. Mol. Biol.*, vol. 18, no. 7, pp. 854–856, Jul. 2011, doi: 10.1038/nsmb.2080.

[469] K. E. Moreira *et al.*, "Seg1 controls eisosome assembly and shape.," *J. Cell Biol.*, vol. 198, no. 3, pp. 405–20, Aug. 2012, doi: 10.1083/jcb.201202097.

[470] J. E. Foderaro, L. M. Douglas, and J. B. Konopka, "MCC/Eisosomes Regulate Cell Wall Synthesis and Stress Responses in Fungi," *J. Fungi*, vol. 3, no. 61, pp. 1–18, 2017.

[471] H. X. Wang, L. M. Douglas, P. Veselá, R. Rachel, J. Malinsky, and J. B. Konopka, "Eisosomes promote the ability of Sur7 to regulate plasma membrane organization in *Candida albicans*," *Mol. Biol. Cell*, vol. 27, no. 10, pp. 1663–1675, May 2016, doi: 10.1091/mbc.E16-01-0065.

[472] L. M. Douglas, H. X. Wang, S. Keppler-ross, N. Dean, and J. B. Konopka, "Sur7 Promotes Plasma Membrane Organization and Is Needed for Resistance to Stressful Conditions and to the Invasive Growth and Virulence of *Candida albicans*," *MBio*, vol. 3, no. 1, pp. 1–12, 2012, doi: 10.1128/mBio.00254-11.Editor.

[473] K. Malinska, J. Malinsky, M. Opekarova, and W. Tanner, "Distribution of Can1p into stable domains reflects lateral protein segregation within the plasma membrane of living *S. cerevisiae* cells," *J. Cell Sci.*, vol. 117, no. 25, pp. 6031–6041, 2004, doi: 10.1242/jcs.01493.

[474] F. Fröhlich, R. Christiano, D. K. Olson, A. Alcazar-Roman, P. DeCamilli, and T. C. Walther, "A role for eisosomes in maintenance of plasma membrane phosphoinositide levels," *Mol. Biol. Cell*, vol. 25, no. 18, pp. 2797–2806, 2014, doi: 10.1091/mbc.E13-11-0639.

[475] R. Kabeche, A. Roguev, N. J. Krogan, and J. B. Moseley, "A Pil1-Sle1-Syj1-Tax4 functional pathway links eisosomes with PI(4,5)P2 regulation," *J. Cell Sci.*, vol. 127, no. 6, pp. 1318–1326, Mar. 2014, doi: 10.1242/jcs.143545.

[476] G. Grossmann, M. Opekarová, J. Malinsky, I. Weig-Meckl, and W. Tanner, "Membrane potential governs lateral segregation of plasma membrane proteins and lipids in yeast.," *EMBO J.*, vol. 26, no. 1, pp. 1–8, Jan. 2007, doi: 10.1038/sj.emboj.7601466.

[477] D. Berchtold *et al.*, “Plasma membrane stress induces relocalization of Slm proteins and activation of TORC2 to promote sphingolipid synthesis.,” *Nat. Cell Biol.*, vol. 14, no. 5, pp. 542–7, May 2012, doi: 10.1038/ncb2480.

[478] F. Fröhlich *et al.*, “A genome-wide screen for genes affecting eisosomes reveals Nce102 function in sphingolipid signaling.,” *J. Cell Biol.*, vol. 185, no. 7, pp. 1227–42, Jun. 2009, doi: 10.1083/jcb.200811081.

[479] M. Pasqua *et al.*, “The Varied Role of Efflux Pumps of the MFS Family in the Interplay of Bacteria with Animal and Plant Cells,” *Microorganisms*, vol. 7, no. 285, pp. 1–21, Aug. 2019, doi: 10.3390/microorganisms7090285.

[480] K. Van Dyck, P. Van Dijck, and G. Vande Velde, “Bioluminescence Imaging to Study Mature Biofilm Formation by *Candida* spp. and Antifungal Activity *In Vitro* and *In Vivo*,” in *Bioluminescent Imaging. Methods in Molecular Biology.*, 2020, pp. 127–143.

[481] A. Tyms, “Polyamines and the growth of bacteria and viruses,” in *The Physiology of Polyamines*, U. Bachrach and Y. Heime, Eds. Boca Raton, FL: CRC Press, 1989.

Appendix – Supplementary Data

Table SII.1. List of primers used in this study.

Name	Sequence (5'-3')
***CgEFG1* gene cloning**	
pGREG_CgEFG1_Fw	GAATTCGATATCAAGCTTATCGATACCGTCGACAATGTCTGAAAGAGAATTGCCTG
pGREG_CgEFG1_Rv	GCGTGACATAACTAATTACATGACTCGAGGTCGACTTACATGTGGTGATGTATTTGG
***CgTEC1* gene cloning**	
pGREG_CgTEC1_Fw	GAATTCGATATCAAGCTTATCGATACCGTCGACAATGACTGTCTCAAATGACAGCT
pGREG_CgTEC1_Rv	GCGTGACATAACTAATTACATGACTCGAGGTCGACTCAGTTGGACTGAATACCTTGC
pGREG576 GAL1-to-PDCl promoter replacement	
pGREG_PDC1_Fw	TTAACCCTCACTAAAGGGAACAAAAGCTGGAGCTAGCATTTTTATACACGTTTTAC
pGREG_PDC1_Rv	GAAAAGTTCTTCTCCTTTACTCATACTAGTGCGGCTGTTAATGTTTTTTGGCAATTG
pGREG576 GAL1-to-MT-I promoter replacement	
pGREG_MT-I_Fw	TTAACCCTCACTAAAGGGAACAAAAGCTGGAGCTCTGTACGACACGCATCATGTGGCAATC
pGREG_MT-I_Rv	GAAAAGTTCTTCTCCTTTACTCATACTAGTGCGGCTGTGTTTGTTTTTGTATGTGTTTGTTG
Deletion of *CgEFG1, CgTEC1*	
ΔCgEFG1_Fw	GGAGCAGGGAGTTACTGGTTAATGAGCGTAGACTTGAACTGAAAAGAAAATGTGCGGGCCGCTGATCACG
ΔCgEFG1_Rv	AACAATTCATTATGTTATACAATGGTACATAGCGATTCATTACGAATATTAAGTTACATCGTGAGGCTGG
ΔCgTEC1_Fw	AAGAGTACTAATACACATCGTACTCCCCCCCACAAATAACGCCCTCAATCTATATTGGCCGCTGATCACG
ΔCgTEC1_Rv	TCAGCAAAACATTTCTGCAGAAAAAATAAAAATGTAGCATTCCTACATCTCTCTCACATCGTGAGGCTGG
ΔCgEFG1_Fw_conf	GCCTGGATACACATACTTAC
ΔCgEFG1_Rv_conf	AACAGTAACTCCGTTGTG
ΔCgTEC1_Fw_conf	GACAGCTCGGTATCAGATAGGT
ΔCgTEC1_Rv_conf	GTGGAGATGATGCTTTCGAAGA
RT-PCR experiments	
CgACT1_Fw	AGAGCCGTCTTCCCTTCCAT
CgACT1_Rv	TTGACCCATACCGACCATGA
CgAWP13_Fw	TTAATATCTTGCTGGGCTTTTGG
CgAWP13_Rv	AGCGTAGCACTGTCTATGATTATTTCTT
CgPWP5_Fw	GGCTGGCTTTCGTGCAATA
CgPWP5_Rv	CGACGGACCCTTGTAAGATTGT
CgAED2_Fw	AAAGCCTCAATGGTATGACAGAAGAC
CgAED2_Rv	CAGATGAATTTTGGAATGGGAAA

Figure SII.1. Interaction of *C. glabrata* wild-type strain KUE100 with glass, polystyrene, silicone elastomer and polyvinyl chloride by SCFS, using different contact times: 0 s, 0.5 s, 1 s and 5 s. Characterization of these interactions is based on the maximal adhesion force, work of adhesion and rupture distance, with the representative force-distance curves for each material and for each contact time (the lighter the force curve, the higher the contact time). Horizontal lines indicate the average levels from at least 3 yeast cells, from at least 2 independent cell cultures, immobilized on the cantilever for the interaction with each material. 256, 100 and 25 force-distance curves were recorded for the interaction with the materials, with 0s, 0.5-1s and 5s, respectively. Error bars indicate standard deviations. *, P<0.05; **, P<0.01; ***, P<0.001; ****, P<0.0001.

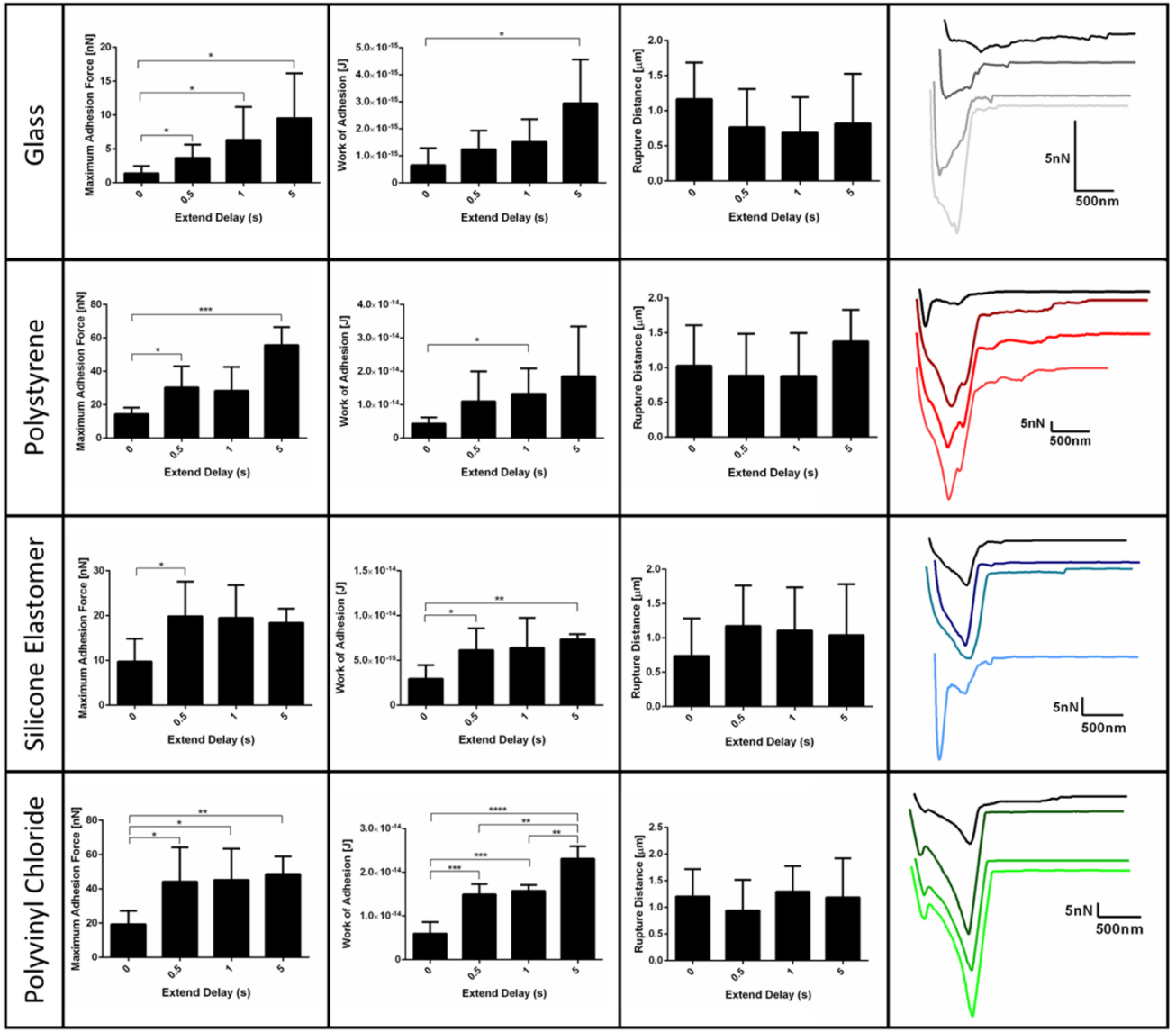

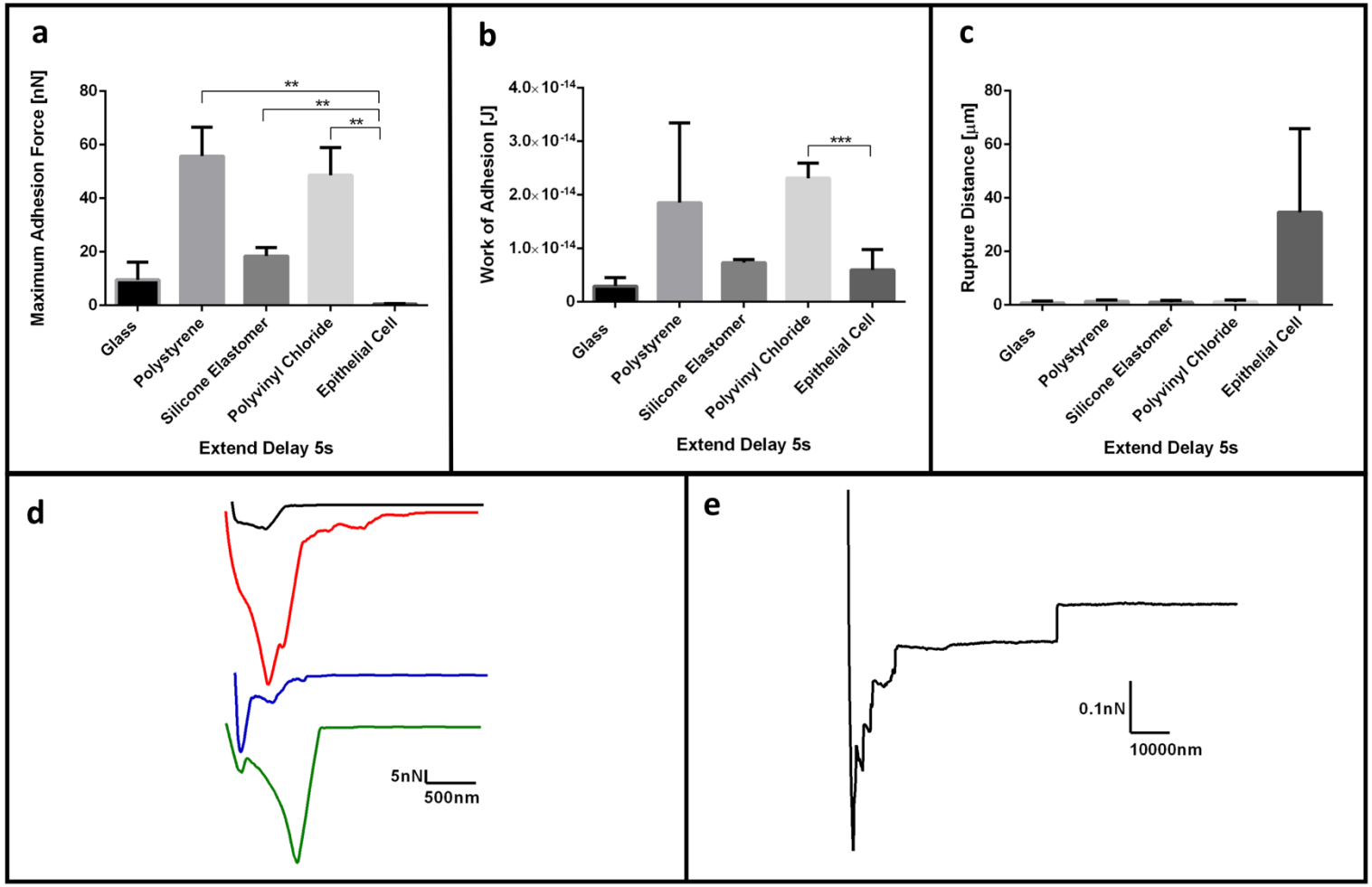

Figure SII.2. Comparison of *C. glabrata* wild-type KUE100 strain interaction with surface materials and human vaginal epithelial VK2/E6E7 cells, with 5 s of contact time. Average of the **a** maximal adhesion force, **b** work of adhesion and **c** rupture distance measured on each retraction curve. **d** Representative force-distance curves of the interaction with glass (black), polystyrene (red), silicone elastomer (blue) and polyvinyl chloride (green). **e** Representative force-distance curve of the interaction with epithelial cells. For every condition, at least 4 yeast cells, from at least 3 independent cell cultures, were immobilized on the cantilever for the interaction. Error bars indicate standard deviations. **, P<0.01; ***, P<0.001.

Table SII.2. Differently expressed genes upon *C. glabrata* 24 h biofilm formation on polystyrene comparatively to planktonic conditions, organized by GO term, with respective ID, log_2 fold-change, name, definition, and respective orthologs in *C. albicans* and *S. cerevisiae*. https://docs.google.com/spreadsheets/d/1buV_Ib31fLjc_mL9HWyo37gmdVlUp6UWHIr6OYmyqBg/edit?usp=sharing

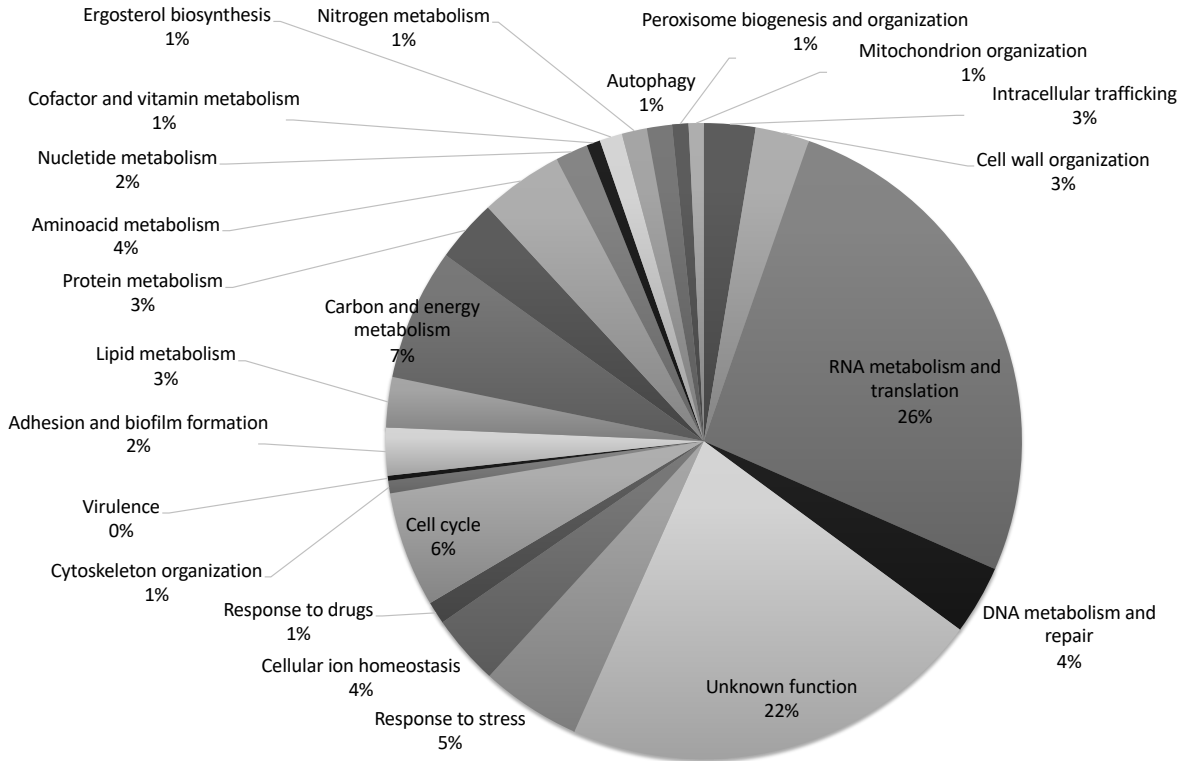

Figure SII.3. Categorization and frequency of the genes upregulated in *C. glabrata* cells upon 24 h of biofilm growth, given by the KUE100 wild-type cells grown in biofilm in relation to KUE100 wild-type cells grown in planktonic conditions, based on the biological process taxonomy of gene ontology (p value<0.05).

Table SII.3. Differently expressed genes in Δ*cgefg1* deletion mutant at 24 h biofilm formation on polystyrene, comparatively to the parental strain KUE100 in the same conditions, organized by GO term, with respective ID, log_2 fold-change, name, definition, and respective orthologs in *C. albicans* and *S. cerevisiae*. https://docs.google.com/spreadsheets/d/1ZvMSTQPeemm5JgRwjGlPkI_xevqcbwYhoPC4jJ2enII/edit?usp=sharing

Table SII.4. Differently expressed genes in Δ*cgtec1* deletion mutant at 24 h biofilm formation on polystyrene, comparatively to the parental strain KUE100 in the same conditions, organized by GO term, with respective ID, log_2 fold-change, name, definition, and respective orthologs in *C. albicans* and *S. cerevisiae*. https://docs.google.com/spreadsheets/d/1Y2yAIaWZSAodhopSBHYi1GNKTKuy3c1NiTjyL_gH3PM/edit?usp=sharing

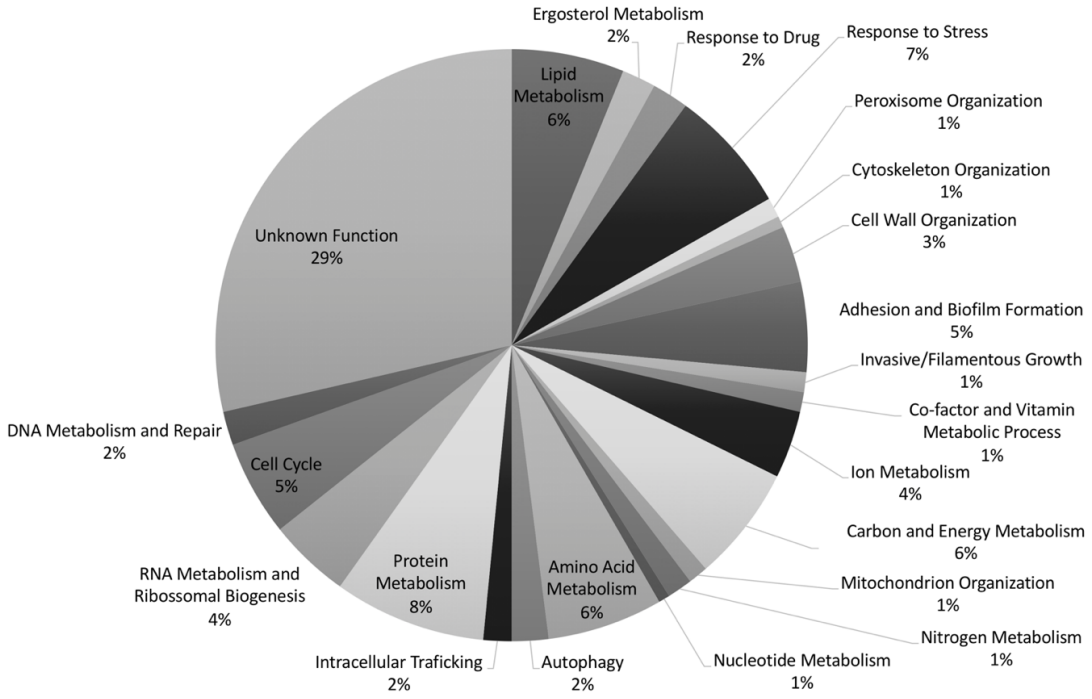

Figure SII.5. Categorization and frequency of the genes upregulated by CgEfg1 upon biofilm growth in *C. glabrata*, given by the *Δcgefg1* deletion mutant cells in relation to KUE100 wild-type cells grown in biofilm, based on the biological process taxonomy of gene ontology (p-value<0.05).

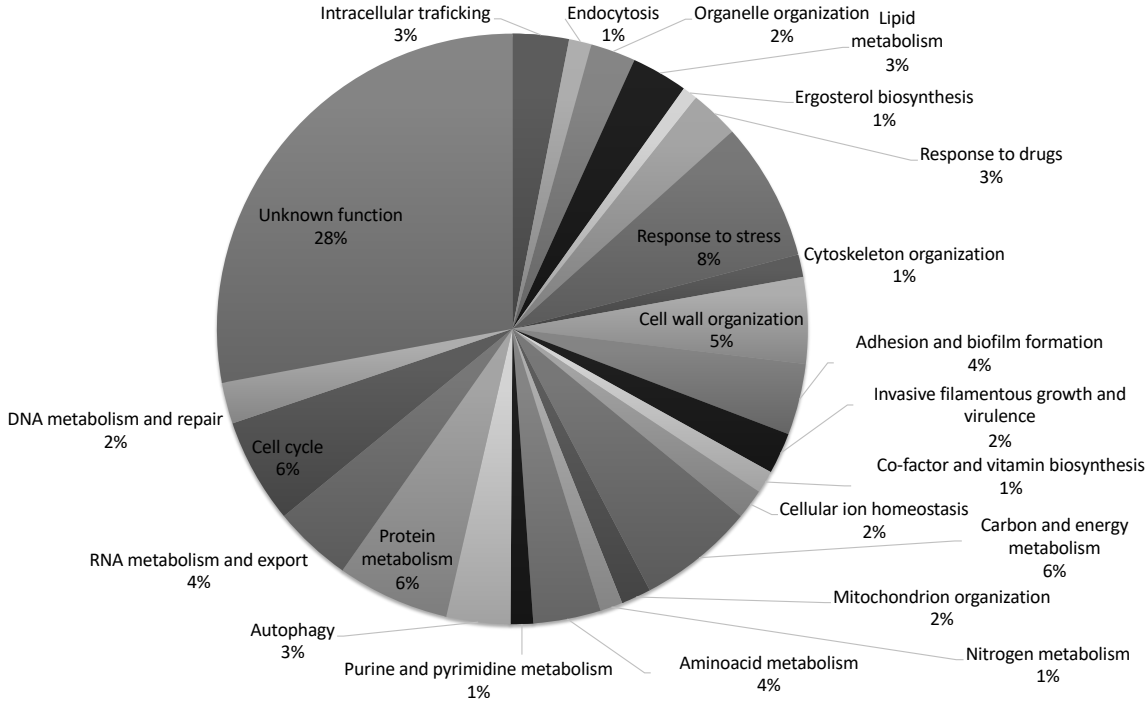

Figure SII.4. Categorization and frequency of the genes upregulated by CgTec1 upon biofilm growth in *C. glabrata*, given by the *Δcgtec1* deletion mutant cells in relation to KUE100 wild-type cells grown in biofilm, based on the biological process taxonomy of gene ontology (p-value<0.05).

Table SII.5. Adhesin-encoding genes activated upon *C. glabrata* KUE100 biofilm formation versus planktonic growth, repressed upon the absence of *CgEFG1* and *CgTEC1* genes upon *C. glabrata* planktonic growth and biofilm formation.
https://docs.google.com/spreadsheets/d/1riIrToyXrMRm_BCdaV0pyITfvj6VsY5yoGpciMJdB_k/edit?usp=sharing